Author:
Kandemir, Ali

Title:
Characterisation and Selection of Sustainable Discontinuous Natural Fibre Reinforced Polymer Constituents and Their Composites

Characterisation and Selection of Sustainable Discontinuous Natural Fibre Reinforced Polymer Constituents and Their Composites

By

ALI KANDEMIR

Department of Aerospace Engineering
UNIVERSITY OF BRISTOL

A dissertation submitted to the University of Bristol in accordance with the requirements of the degree of DOCTOR IN PHILOSOPHY in the Faculty of Engineering.

NOVEMBER 2023

Word count: 35000 (approx.)

Abstract

The increasing societal concern about the environment leads to a focus on sustainability in many engineering fields, including fibre reinforced polymer matrix composites (FRPs). Due to their non-environmentally friendly constituents, *i.e.* thermosets and synthetic fibres, this sector is committed to researching sustainable solutions. Two different approaches can be considered for possible solutions. The first approach is reducing the environmental impact of constituent materials by using sustainable raw materials, such as natural fibres and bio-based matrices. The second approach is reducing landfill waste by considering a "repair, reuse or recycle" approach for composites. Because the composite industry uses mostly thermoset matrices, which form irreversible bonding mechanisms when cured, it is difficult to apply the second approach. However, thermoplastic matrices or covalent adaptable network polymers can overcome this and make it easier to apply the second approach. Furthermore, changing the fibre reinforcement geometry from continuous to discontinuous promotes and facilitates the concept of repair and reuse, which are quite difficult to achieve with continuous FRPs. This is because after the possible repair or reuse process, factors such as manufacturing defects and flaws will be altered so that all performance predictions for the original product will become invalid; alternatively, those of discontinuous FRPs remain relatively the same. Moreover, highly aligned discontinuous FRPs produced with the High-Performance Discontinuous Fibre (HiPerDiF) method can show performance comparable to continuous FRPs. In this study, a number of plant-based natural fibres (curaua, flax, jute, kenaf) and potentially sustainable matrices (Elium®, Furacure, Vitrimax™) are investigated to be selected as sustainable and feasible constituents for a sustainable aligned discontinuous FRP produced with the novel HiPerDiF method. It is found that short flax fibres and a vitrimer resin are the best constituents for future sustainable aligned discontinuous FRPs studies due to promising mechanical performance and offering a circular economy via repair option in composite applications.

dedicated to my beloved father,
Erdinç Kandemir
(1964-2020)

Acknowledgements

Annem, Gönül Muşlu Kandemir, her şey sizin sayenizde, teşekkürler.

I would like to thank primary advisor, Prof. Steve Eichhorn, for his supervision, always on time support and guidance, and foremost, giving the importance on my mental health more than me, which a PhD student needs most.

I also would like to thank Prof. Ian Hamerton for his supervisory role, guidance and widening my perspective on relative fields to composites.

I thank Dr. Marco L. Longana, who never stopped acting like my main supervisor, and also a special thank for his constant, tenacious, and helpful guidance.

I want to thank also Dr. Thomas R. Pozegic for his advisory role during my first year, which was constructive and very supportive.

I cannot thank Prof. Paul Weaver enough. Thank you very much Paul for directing me to ACCIS-CDT programme while I was looking possible supervisors for a PhD project. Thanks to you Paul, I have been in one of the best post-graduate programmes in UK and gone through the best international experience.

Most importantly, I want to thank and acknowledge the Republic of Türkiye Ministry of National Education (Milli Eğitim Bakanlığı) for their YLSY grant and support during the difficult times.

The pillar of the BCI laboratories, Ian Chorley, thank you for all of your help and efforts to finish our experiments on time. Without you, none of the BCI students would graduate.

Another pillar but this time for the CDT programme or in general for admin stuff of PhD students, Dear Sarah Hallworth, thank you for all of your support, care, and attention. If it weren't for you, there would be a lot of struggling students around.

Dear ACCIS-CDT18 cohort, you are amazing! You guys made the horrid PhD journey bearable, especially during the Covid cr*p! For similar reasons, thanks BCI-SCR gang too.

Author's Declaration

I declare that the work in this dissertation was carried out in accordance with the requirements of the University's Regulations and Code of Practice for Research Degree Programmes and that it has not been submitted for any other academic award. Except where indicated by specific reference in the text, the work is the candidate's own work. Work done in collaboration with, or with the assistance of, others, is indicated as such. Any views expressed in the dissertation are those of the author.

SIGNED: ..... DATE: NOVEMBER 17, 2023

ALI KANDEMIR

List of Publications

The works presented in this thesis have been published in peer-reviewed journal papers and/or presented at international conferences.

Journal papers

[1] ***Ali Kandemir***; Thomas R. Pozegic; Ian Hamerton; Stephen J. Eichhorn; Marco L. Longana. Characterisation of Natural Fibres for Sustainable Discontinuous Fibre Composite Materials. *Materials* 2020, 13, 2129. DOI:10.3390/ma13092129

[2] Amy Fitzgerald*; Will Proud*; ***Ali Kandemir****; Richard J. Murphy; David A. Jesson; Richard S. Trask; Ian Hamerton; Marco L. Longana. A Life Cycle Engineering Perspective on Biocomposites as a Solution for a Sustainable Recovery. *Sustainability* 2020, 13, 2129. DOI:10.3390/su13031160
(*These authors contributed equally to this work.)

[3] ***Ali Kandemir***; Marco L. Longana; Tulio H. Panzera; Gilberto G. del Pino; Ian Hamerton; Stephen J. Eichhorn. Natural Fibres as a Sustainable Reinforcement Constituent in Aligned Discontinuous Polymer Composites Produced by the HiPerDiF Method. *Materials* 2021, 14, 1885. DOI:10.3390/ma14081885

[4] ***Ali Kandemir***; Marco L. Longana; Ian Hamerton; Stephen J. Eichhorn. Developing aligned discontinuous flax fibre composites: Sustainable matrix selection and repair performance of vitrimers. *Composites Part B: Engineering* 2022, 110139. DOI:10.1016/j.compositesb.2022.110139

Conference proceeding

[5] ***Ali Kandemir***; Marco L. Longana; Ian Hamerton; Stephen J. Eichhorn. Interfacial shear strength of flax fibre with sustainable matrices. ECCM20, June 2022, Lausanne, Switzerland. "Composites meet Sustainability – Proceedings of the 20th European Conference on Composite Materials" ISBN: 978-2-9701614-0-0

Use of published work in this thesis

This thesis is prepared by following the guidance on the integration of publications as chapters within the dissertation. Chapters 3, 4, and 5 are adapted from the publications [1], [3], and [4], respectively, and Chapter 2 is produced from the publication [2].

Table of Contents

List of Tables

List of Figures

Chapter 1

Introduction

This chapter introduces the fundamental concepts of the thesis to provide the reader with a comprehensive understanding of the context of the work carried out. Section 1.1 explains the basics of composite materials and provides an insight into the current industrial outlook with regards to fibre reinforced polymer composite manufacturing and their sustainability. Section 1.2 presents the aims and objectives of the research work, and establishes the novelty of the work. Section 1.3 outlines the structure of the thesis.

1.1 Background and Research Motivation

Material families are defined generally by their properties, or, their common reactions to stimuli. There are three common engineering material families - metals, ceramics, and polymers- that can be organised according to their properties. Figure 1.1(a) shows generalised stress-strain curves of these families, and there is a clear distinction between their failure behaviours, which can also be named brittle, ductile, and plastic. Figure 1.1(b) presents a comparison between the families in terms of properties. Composite materials consist of two or more materials coming from different families and have mechanical, physical, and chemical properties superior to those of the individual constituents [1]. Composites are typically produced to achieve the best performance in particular applications. For example, if high modulus and strength are required for an application, composites are the nearest to this performance criteria as seen in Fig. 1.1(a).

(a)

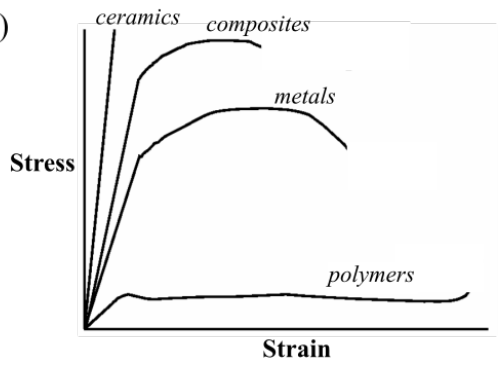

(b)

	Ceramic	Metal	Polymer
Hardness	⇧	⇩	⇩
Elastic modulus	⇧	⇧	⇩
High temperature strength	⇧	⇩	⇩
Thermal expansion	⇩	⇧	⇧
Ductility	⇩	⇧	⇧
Corrosion resistance	⇧	⇩	⇩
Resistance to wear	⇧	⇩	⇩
Electrical conductivity	⇕	⇧	⇩
Density	⇩	⇧	⇩
Thermal conductivity	⇕	⇧	⇩
⇧ Tendency to high values		⇩ Tendency to low values	

Figure 1.1: (a) Stress-strain curves and (b) property comparison of the material families [2].

Fibre reinforced polymer (FRP) composites are one of the important branches of composite materials, and they are attractive to many engineering applications owing to their low weight and high strength. Mechanically, FRPs are a combination of ceramic and polymer family members in which fibres behave like ceramics and reinforce the polymer matrices. Moreover, one of the most significant advantage of fibre-reinforced polymers is their versatility. They can be customised for high performance components or complex shapes by meeting specific requirements in terms of strength or stiffness through different lay-ups, orientations and material combinations. For this reason, FRPs are frequently used in the aerospace, automotive, civil, marine, sport, and wind energy industries [3–6].

Fundamental challenges with fibre-reinforced polymers are to combine the reinforcements with the polymer matrix while ensuring good consolidation, maximum control of fibre orientation, which determines the required mechanical performance, and above all, low cost [7]. There are a wide range of processes for the production of composites, such as injection moulding, vacuum-assisted resin transfer moulding, automated tape placement, and compression moulding [8]. Generally, FRPs are formed into the desired shape by lay-up of dry or pre-impregnated continuous fibres and consolidated with the matrix [8]. To achieve good consolidation, pressure must be applied over the entire surface of the part, which requires expensive equipment and increases manufacturing costs. Moreover, precuring and processability of dry or pre-impregnated continuous fibres in FRPs are also significant cost contributors since it requires orientation precision for mechanical performance and several manufacturing stages [9].

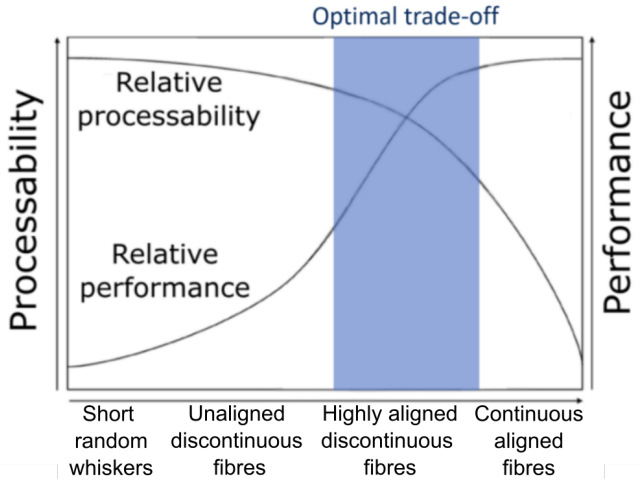

Figure 1.2: Relative processability* in terms of volume and part complexity versus potential best mechanical performance** of FRPs for different fibre architectures highlighting the optimal area (in blue) [7]. (*Processability is the ease with which a fibre-reinforced polymer composite can be manufactured, shaped, and assembled into a final product using various fabrication methods. **Performance refers to the ability of a fibre-reinforced polymer composite to meet or exceed the desired mechanical, thermal, and/or other functional requirements for a given application.)

As seen in Figure 1.2, aligned discontinuous fibre reinforced polymer composites (ADFRPs) offer the optimal trade-off between processibility and performance whilst keeping manufacturing

costs low. Moreover, ADFRP production methods provide an opportunity for hybridization (using more than one type of reinforcement material), which adds another layer to the versatility of FRPs, such as pseudo-ductile behaviour instead of brittle behaviour of FRPs or multifunctionality [10, 11]. Alignment and high aspect ratio of fibres are the key to achieving high performance in ADFRPs since alignment dictates fibre volume ratio and high aspect ratio affects stress transfer from the resin to the fibre [12].

Various methods are employed to align short fibres in the manufacturing of composites and can be categorised as dry and wet processes [7]. In dry processes, conventional techniques such as carding and combing are used but often result in mats lacking homogeneous packing and alignment [13]. To overcome these limitations, electrical and pneumatic methods offer higher production rates and improved alignment. Electrical alignment utilizes electric fields to align conductive fibres along the direction of the generated field [13]. Pneumatic alignment technology chops and sprays tows to create preforms and involves techniques like the glass-mat reinforced thermoplastic method [7].

Wet processes involve dispersing short fibres in liquid mediums, which are commonly ammonium alginate solution and glycerine. Ammonium alginate processing includes suspending fibres, extruding the mixture into a precipitate bath, and then drying the resulting gel filaments [14]. Glycerine processing, on the other hand, relies on dispersing fibres in the viscous medium and using fluid friction to align fibres and carrier fluid removal is crucial to prevent misalignment [7]. Centrifugal alignment methods also play a role in which aligned fibre mats are produced by discharging a fibre suspension onto a rotating cylinder, rapidly removing the fluid and retaining fibre alignment [15].

A recent technology, the HiPerDiF (*Hi*gh *Per*formance *Di*scontinuous *F*ibre) method, is a water-based process relying on a sudden momentum change of a fibre-water suspension. Compared to other methods, this method provides a higher degree of fibre alignment and property retention from recycled fibres [16, 17]. Figure 1.3 shows schematics of the overall ADFRP process and the novel HiPerDiF fibre head design and alignment method. *"Fibres, which can have a length between 1 and 12 mm, are suspended in water, accelerated through a nozzle, and directed in a gap between two parallel plates. The fibre alignment mechanism relies on a momentum change upon impact with the plate. The fibres then fall on a conveyor stainless mesh belt where the water is removed by suction. The aligned fibre preform are dried with infrared radiation to allow the resin impregnation process*" [11], which can be added at the end of the manufacturing stages. Remarkably, it has been shown that the mechanical performance of composites processed *via* HiPerDiF preforms is comparable to standard composite materials [18], since the length of the short discontinuous fibres exceeds the critical fibre length. It has also been demonstrated that the HiPerDiF method is a valid manufacturing method for the production and optimisation of high-performance hybrid composites with pseudo-ductile behaviour [19]. A very similar alignment technology, tailorable universal feedstock for forming (TUFF) method developed at the University

of Delaware funded by the Defense Advanced Research Projects Agency (DARPA), is also able to produce high performance highly aligned discontinuous carbon fibre preforms in a thin-ply format, which can be combined with thermoplastic or thermoset resins for prepreg, or used in a dry form for infusion based manufacturing processes [20].

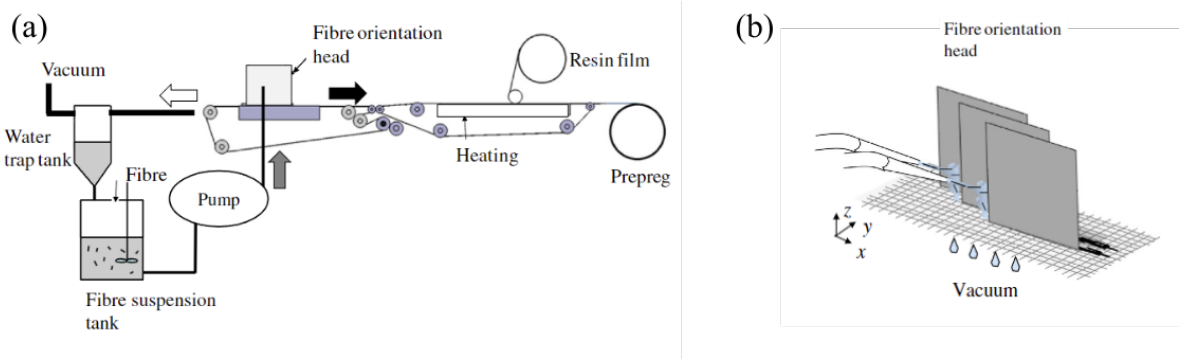

Figure 1.3: Schematics of (a) the HiPerDiF discontinuous fibre alignment process and (b) the HiPerDiF fibre alignment method in which fibres suspended in water are sprayed towards orientation plates with a vacuum under a pulled mesh belt [18].

High performance in conventional polymer matrix composites is defined as a material that provides high strength and stiffness combined with low density. A typical example is continuous carbon FRP. In discontinuous FRPs, high performance can be defined as a material that achieves similar mechanical performance to that of continuous FRPs. HiPerDiF is one of the few methods capable of demonstrating this potential to produce high-performance discontinuous FRPs, as shown in Fig. 1.4. Owing to this potential, this thesis assumes that composites produced by the HiPerDiF method are high-performance composites, especially when compared to composites produced using other discontinuous FRP production methods. However, it is worth noting that some of the non-optimized curing cycles during the manufacturing stages may result in poor performance and conflict with the term 'high performance'.

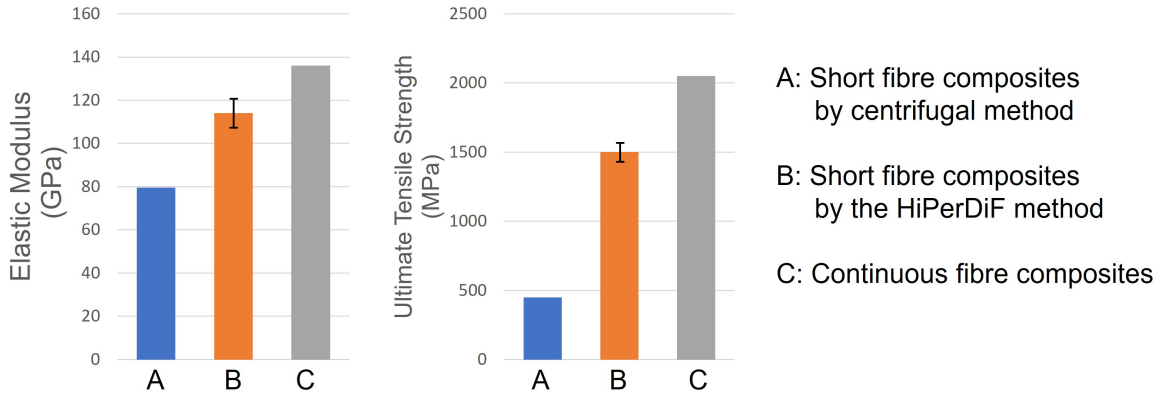

Figure 1.4: Mechanical performance of carbon FRPs produced using different methods [21].

In addition, the HiPerDiF method has a reduced environmental impact (EI) when compared to typical production of other discontinuous FRPs as the process uses water as an alignment medium unlike conventional glycerin-based processes [22, 23]. A recent EI analysis of the HiPerDiF technology, the first of its kind, has evidenced towards the reduction of EI for composite production [24]. Moreover, it has been demonstrated that the HiPerDiF method can use reclaimed synthetic fibres and natural fibres to produce high performance FRPs, which promises to address the sustainability in composite material and production industries [11, 25–30].

It has been shown that natural fibres, *e.g.* flax, requires more drying time under the drying stage to extract all the water absorbed by the fibres compared to synthetic fibres, *e.g.* carbon [11]. Moreover, it was concluded that a high content of water in the fibres prior to the drying stage or an excessive drying time do not have a substantial effect on the cured material's mechanical properties [11]. However, moisture retained within the preform or by the natural fibres could have induced porosity in resins during curing, and to prevent this, a careful selection of the fibres drying time must be considered. Apart from the hydrophilic concerns, using natural fibres in the HiPerDiF method may need an alteration related to the fibre diameter since they are significantly higher than most synthetic fibres and this can be overcome by modification of the plate distance in the alignment head.

1.2 Aim and Objectives

There is an expanding societal concern about the environment, which leads in turn to increased focus on sustainable practices in many engineering fields. FRPs are one of them and, they often include constituents in their manufacture, *e.g.* crosslinked polymers and synthetic fibres, that are not environmentally benign [31]. Consequently, the composites sector is becoming increasingly aware of its responsibility to conduct research into more sustainable solutions. Currently, two different approaches are receiving significant consideration: the first approach reduces the environmental impact of the constituent materials by using sustainable raw materials, such as natural fibres and bio-based matrices [32]. The second approach reduces the amount of manufacturing and postconsumer waste going to landfill by considering the "repair, reuse, or recycle" paradigm for composites [33]. As the composite industry currently relies more heavily on thermoset matrices, which undergo irreversible reaction when cured, it is difficult to apply the second approach widely. However, thermoplastic matrices or covalent adaptable network polymers offer the potential to overcome this issue, thereby making it easier to apply the second approach.

Furthermore, changing the fibre reinforcement geometry from a continuous to a discontinuous format promotes and facilitates the concept of repair and reuse, which are quite difficult to achieve with composites reinforced purely with continuous fibres; because, following potential repair or reuse processes, factors such as manufacturing defects, flaws, and bottlenecks become increasingly influential and assumptions about performance based on the virgin materials become invalid [7].

In contrast, when discontinuous fibre composites are considered, the influence of these factors remains similar before or after repair or in a second life cycle. Importantly, as mentioned before, highly aligned discontinuous fibre composites produced by the HiPerDiF method have been demonstrated to show practically the same performance as those produced from continuous fibres, allowing both mechanical properties and value to be recovered during remanufacture [18].

In addition, the increasing global demand for sustainable and environmentally friendly materials has led to a strong interest in exploring natural fibres as a viable alternative to synthetic fibres in composite materials [34]. With their renewable nature, biodegradability and lower carbon footprint, natural fibres offer significant advantages in terms of environmental sustainability [35]. In addition, their promising mechanical properties, abundance and potential cost effectiveness make them an attractive option for various applications [36]. In this work, the use of plant-based natural fibres in discontinuous fibre-reinforced composites is mostly examined, highlighting their potential for the development of sustainable and high-performance materials.

The aim of this thesis is to investigate the viability of using sustainable and biodegradable constituents within the HiPerDiF method to facilitate a circular economy. The objectives of this project are organised as follows:

- reviewing the current literature of fibre reinforced polymer composite constituents and singling sustainable candidates out owing to their availability, mechanical performance, and physical properties;
- identification of natural fibres that can be used for the HiPerDiF method in terms of their physical, mechanical and thermal properties;
- evaluating of natural fibres' interfacial performance with a common matrix in fibre reinforced polymer composites;
- testing the performance of ADFRPs delivered by the HiPerDiF method using the identified constituents, and selecting of the best candidate natural fibre according to its reinforcing performance in ADFRPs;
- identification and selection of sustainable matrices that can be used for the HiPerDiF method and can have harmony with the candidate natural fibre in terms of their physical, mechanical, interfacial, and thermal properties;
- investigation of mechanical and functional properties of sustainable aligned natural fibre reinforced polymer composites produced by the HiPerDiF method;
- examination of the reduce-waste concept by considering the repair option of sustainable composites;
- providing an example of a replacement of unsustainable composites with sustainable alternatives delivered by HiPerDiF in engineering applications.

Novelty statement

The present thesis provides a database of sustainable constituents for ADFRPs that offer several life cycles via repair ability and demonstrates that the use of the HiPerDiF method instead of typical (unsustainable) methodologies creates composites that performs anisotropic mechanical properties due to high alignment of short fibres.

1.3 Dissertation Outline

The present manuscript is produced by the publications given in *List of Publications* and structured according to the University of Bristol's guidance on the integration of publications as chapters within the dissertation. Chapter 2 is an extended literature review following this introduction and explores the major themes for the remainder of the work, *i.e.* available FRP composite constituents. Intrinsic properties of a number of the plant-based natural fibres are investigated for sustainable discontinuous fibre reinforced composites in Chapter 3, and their suitability with manufacturing methods is discussed. The candidate fibres found in Chapter 3 are used to make aligned discontinuous natural fibre reinforced composites in Chapter 4. Chapter 4 reports the mechanical and physical properties of these composites and allows reinforcing material and fibre length selection. Chapter 5 includes two parts, and the first part is a selection of sustainable matrices, in which commercially available and accessible potential sustainable matrices are used to carry out interfacial performance characterisation with the best candidate fibre, flax. After the matrix selection, the second part investigates the sustainability and repair performance of the matrix within flax FRP composites examining the solution of lengthening the circular economy of the natural fibre composite. Chapter 6 presents an overall discussion linking the publications and Chapter 7 concludes with a summary of findings and suggestions for future work. A Venn diagram presented in Figure 1.5 illustrates the relationship between the main topics and their related chapters.

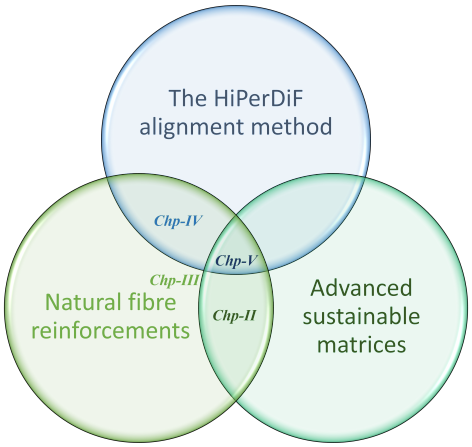

Figure 1.5: A Venn diagram that summarises the work presented in the thesis.

Chapter 2

Literature Review

Composite materials, such as carbon fibre reinforced epoxies, provide more efficient structures than conventional materials (*e.g.* metals, ceramics) through light-weighting, but the associated high energy demand during production can be extremely detrimental to the environment. Bio-based composites are an emerging class of material class with the potential to reduce a product's through-life environmental impact relative to wholly synthetic composites. As with most materials, there are challenges and opportunities with the adoption of biocomposites at the each stage of the life cycle. Life cycle assessment is an evaluation method for enabling the qualification of environmental impact, which can be incorporated in the conceptual development phase. Designers and engineers are beginning to actively include the environment cost of their products in their workflow, allowing them to play a significant role in future sustainability strategies. This chapter will introduce what potential sustainable constituents are, and outline how the concept can offer support in the selection and design for the environment, followed by a discussion of the advantages and disadvantages of biocomposites throughout their life cycle.

This chapter has been produced by using some parts of the published work listed below and updated with recent literature. Section 2.2 solely prepared by A.K. and amended by all authors. Others sections were constructed cooperatively between A.F., W.P., and A.K and rectified by all authors.

Amy Fitzgerald[†]; Will Proud[†]; ***Ali Kandemir***[†]; Richard J. Murphy; David A. Jesson; Richard S. Trask; Ian Hamerton; Marco L. Longana[*]. A Life Cycle Engineering Perspective on Biocomposites as a Solution for a Sustainable Recovery. *Sustainability* 2020, 13, 2129. DOI:10.3390/su13031160

[†]These authors contributed equally to this work.

[*]Corresponding author, who shaped and led the collaboration between A.F., W.P., and A.K. Author contribution is given by using the Contributor Roles Taxonomy: conceptualisation, A.F., W.P., A.K. and M.L.L.; supervision, R.J.M., D.A.J., R.S.T., I.H. and M.L.L.; visualization, A.F., W.P. and A.K.; writing—original draft preparation, A.F., W.P. and A.K.; writing—review and editing, all authors.

2.1 Synthetic and Bio-Based Composites

Fibre reinforced polymer composites have been pursued as light-weighting solutions for industries for decades, with their versatility and specific properties offering valuable technical advantages over traditional engineering materials, such as steel or aluminium. They allow for more freedom in design with complex geometries and can embed multi-functionality such as noise, vibration and harshness (NVH) damping, electromagnetic shielding and fire retardancy [37–40]. Whilst limited by current design criteria (see e.g., [41]), the high strength-to-weight ratio offered by composites gives the potential to reduce environmental impact (EI) significantly for applications such as transport, by enabling products with reduced weight, resulting in lower fuel consumption. Additional durability, achieved through environmental and corrosion resistance, provides extended use life for components [42]. In the UK alone, the composite market is expected to increase to around 10 billion GBP by 2030 (from just under 2.5 billion GBP in 2015), with the fastest growing industries being automotive, aerospace, renewable energy, and construction [43]. However, Composites Germany reported that the first half of 2020 saw a severe downturn in ratings due to the impact of the coronavirus pandemic on numerous business segments and areas of application [44]. Even so, an increase in the global production of composites is to be expected, especially with respect to the growing market in renewable energy.

Glass and carbon fibres are considered composites of "synthetic" origin (i.e., that both the fibre reinforcement and polymer matrix are manufactured and ultimately derived from mineral deposits or petroleum distillates). In terms of production weight, glass fibre is the most used synthetic reinforcement on the European market followed by carbon fibre [45, 46].Unfortunately, the embodied energy of mineral or petroleum based materials can be extremely high and recycling at end of life (EOL) is not straightforward [47]. As concerns over the changing natural environment due to anthropological climate change are becoming more urgent, producers and consumers have been moving towards composites produced from so-called "greener" materials [48]. The Sustainable Recovery plan has been devised by the International Energy Agency in response to the coronavirus pandemic crisis, proposing a "return to business" with sustainable development goals at the core, ensuring longer-term growth and future-proofing jobs [49]. The plan spans over six key areas including electricity, transport, industry, buildings, fuels and emerging low-carbon technologies-the transition of all of these could be facilitated by a greater integration of composite technology and, potentially, biocomposites.

For the purposes of this chapter, a clear distinction is made between composites of synthetic or bio-based materials:

- Biocomposites (BC) is the umbrella term for composites with either reinforcement or matrix derived from natural sources, or both of them (full BC) [50].
- Natural Fibre Reinforced Polymer (NFRP) composites use natural fibre reinforcements derived from plants, animals and geological processes paired with a synthetic matrix.

- Fibre Reinforced Bio-Polymer (FRBP) composites have a synthetic fibre reinforcement with a partially or fully bio-derived matrix.
- Fibre Reinforced Polymer (FRP) composites constitute a fully synthetic fibre reinforcement and matrix, and represent the most established composite combination currently available on the market.

The benefits of adopting BCs over FRP composites are evident within the academic literature. They are produced from naturally-renewable and abundant precursor feedstocks, and possess properties equivalent on a weight basis to their synthetic counterparts. Whilst they are potentially biodegradable at the end of their service lives, it is important to note that composites containing bio-based constituents will not guarantee biodegradability, a topic covered in more detail in the work of Sahari and Sapuann [51]. Despite this, their market uptake has been limited to date, and this review presents the challenges to commercialisation and explores promising opportunities for design with greener materials within the composites industry.

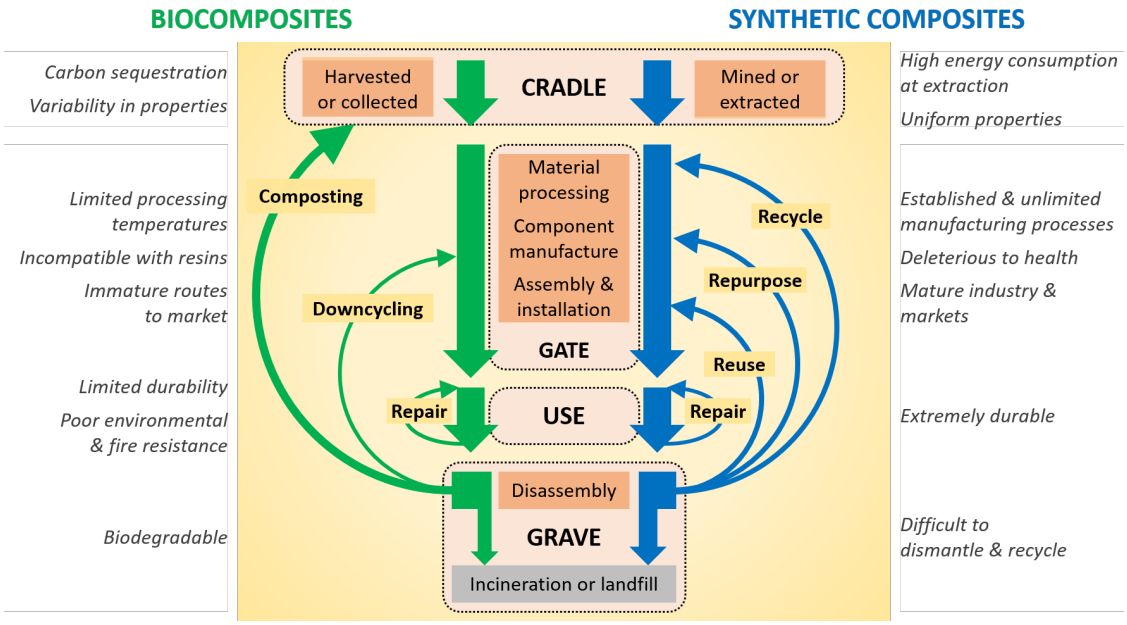

Figure 2.1: Mapping of design solutions within the life cycle framework of bio-based and synthetic composites to promote the adoption of the circular economy paradigm [52] for a sustainable recovery. The central flow diagram summarises the main processing steps from cradle to grave. The flow arrows indicate the paths material retention within the value chain. The notable characteristics at each life cycle stage of the two composite classes are listed on each respective side.

Engineers, designers, manufacturers and researchers are increasingly turning to Life Cycle Assessment (LCA) as an EI analysis method to clearly communicate the advantages of BCs over FRPs. This is a holistic approach that captures material input and waste output information along the whole life cycle of a product system. This inventory data is characterised through a

range of scientific techniques to determine the causal impact of that system on the environment and human health. Figure 2.1 shows the successive life cycles of a representative BC and FRP composite product within a Sustainable Recovery context.

Published LCAs available for BCs conclude that the addition of natural fibres to replace all or part of the synthetic fibres demonstrates a reduced EI for that component [53–59]. It has been reported that NFRPs consume around 63% less energy than glass fibre reinforced polymers (GFRPs) during their entire life cycle [59]. Whilst this provides a strong justification to consider selecting bio-based materials, there are other limitations that must be accounted for when replacing traditionally-used synthetic counterparts. Commercially, BCs are currently produced at a small scale, and therefore the process is not always fully optimised. Sometimes the EI of the BC can be higher than traditional composites.

2.2 Available Constituent Materials

Composites are produced by combining two or more constituent materials, with significantly different properties, to create a material of superior characteristics than the individual constituents. A typical FRP composite is made of two components: (i) fibres that are responsible for carrying the load and (ii) a matrix that binds the fibres together, distributing the load, providing a rigid shape and protecting the reinforcement from environmental effects. The interface between the fibre and matrix has an important role in the performance of the resultant composite [60]. The mechanical proprieties of the composite are estimated through the summation of constituent properties weighted according to their volume fractions. Failure behaviour is also influenced by the fibre-matrix bonding properties, quantified by the interfacial shear strength (IFSS). This section considers some of the options available for BC materials.

2.2.1 Natural Fibres

The term “natural fibres” include fibres of organic origin, i.e., plants and animals, or inorganic, i.e., minerals (Figure 2.4). Organic natural fibres are differentiated by their main unit, cellulose for plant fibres, and proteins for animal fibres. Plants represent the most diverse source of natural fibre: sources include the stems, leaves and fruits of most plants [61].

2.2.1.1 Plant Fibres

Plant fibres (including flax [62, 63], hemp [64, 65], jute [65, 66], curaua [67, 68], kenaf [69, 70] and sisal [65, 71]) have seen both increased research interest and commercial application in recent years [72, 73]. They display specific mechanical properties and added functionality comparable to traditionally-used synthetic fibres such as glass, as shown in Tables 2.1 and 2.2. The carbon sequestration at production and the potential for energy recovery properties at EOL and their potentially low cost contribute to their sustainability. Reduced dermal and respiratory irritation, together with reduced tool wear during processing can further drive down their EI [74, 75].

The mechanical properties of plant fibres are dictated by microfibril orientation, crystallinity and the microstructure (see Fig. 2.2 which is influenced by their composition i.e., the relative amounts of cellulose, hemicellulose, lignin, and sometimes pectin and wax [76]. As seen in Table 2.2, the range of tensile modulus and strength displayed by different plant fibre types is considerable. Additionally, the age of the plant, climatic conditions and fibre production processes may lead to variability in the properties between fibres of the same type [35]. Owing to the presence of multiple hydroxyl groups in the cellulose polymer, plant fibres are hydrophilic and can display significant moisture uptake, reducing most of the mechanical properties due to plasticisation of the chains and dimensional change within the fibre cell wall [77]. This can also present a problem with respect to the interface between fibre and matrix, and it is often necessary to introduce a compatibiliser in addition to pre-conditioning the fibres [78], discussed further in Section 2.2.3. The majority of plant fibres produced are relatively short but can be used in place of discontinuous reinforcements, and in combination with, for example, reclaimed carbon fibres to achieve specific functional properties [11]. Continuous fibres can be produced through traditional spinning techniques or more robust chemical dissolution techniques can be used to produce fibres such as viscose rayon, also a potential composite reinforcement [79]. The broad literature survey on mechanical properties of various plant fibre reinforced polymer composites has been given in

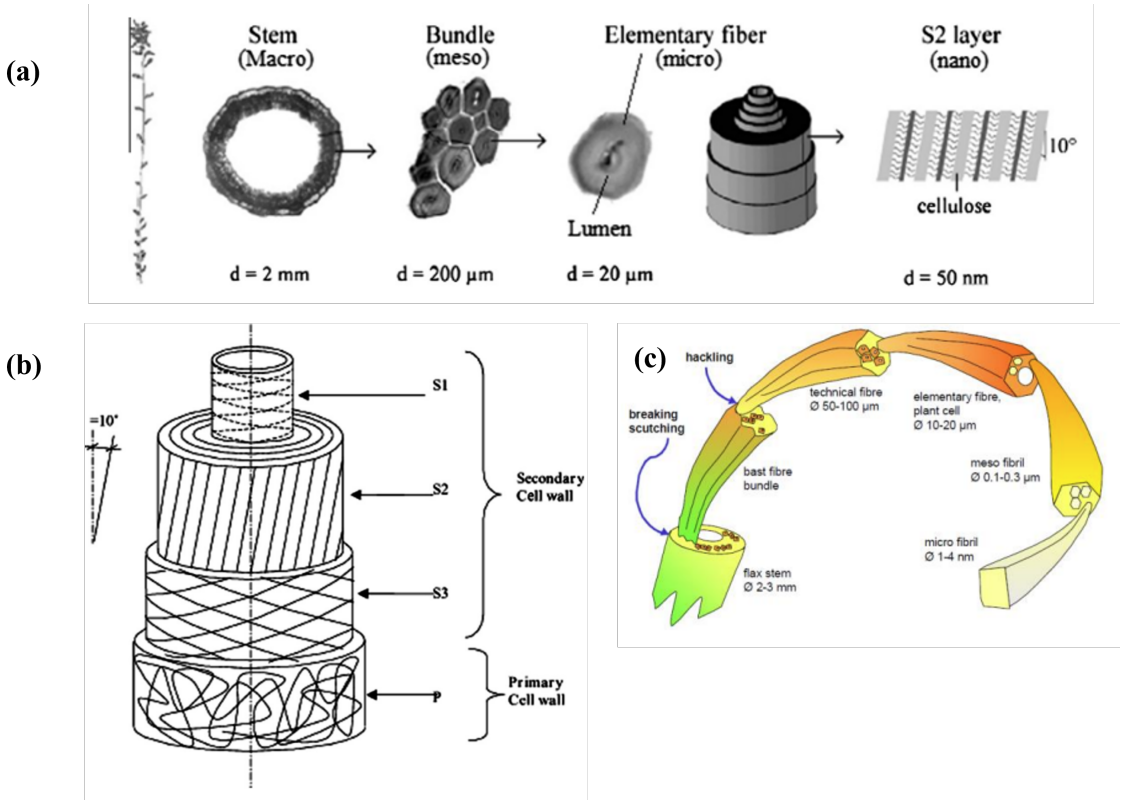

Figure 2.2: (a) Flax structure from the stem to the fibrillar level (b) the micro-structure of a plant fibre cell, and (c) a schematic representation of flax fibres at different levels of hierarchy. [80]

Ref. [81] and readers are directed towards Table 7 in this reference especially for the comparison with glass fibre reinforced polymers. The table gives a comprehensive comparison of matrix type, reinforcement form, manufacturing technique, and interface engineering on mechanical properties of various plant fibres in a composite form. An Ashby plot representation of the mentioned table is given in Figure 2.3, which shows the typical tensile properties of plant fibre reinforced polymers.

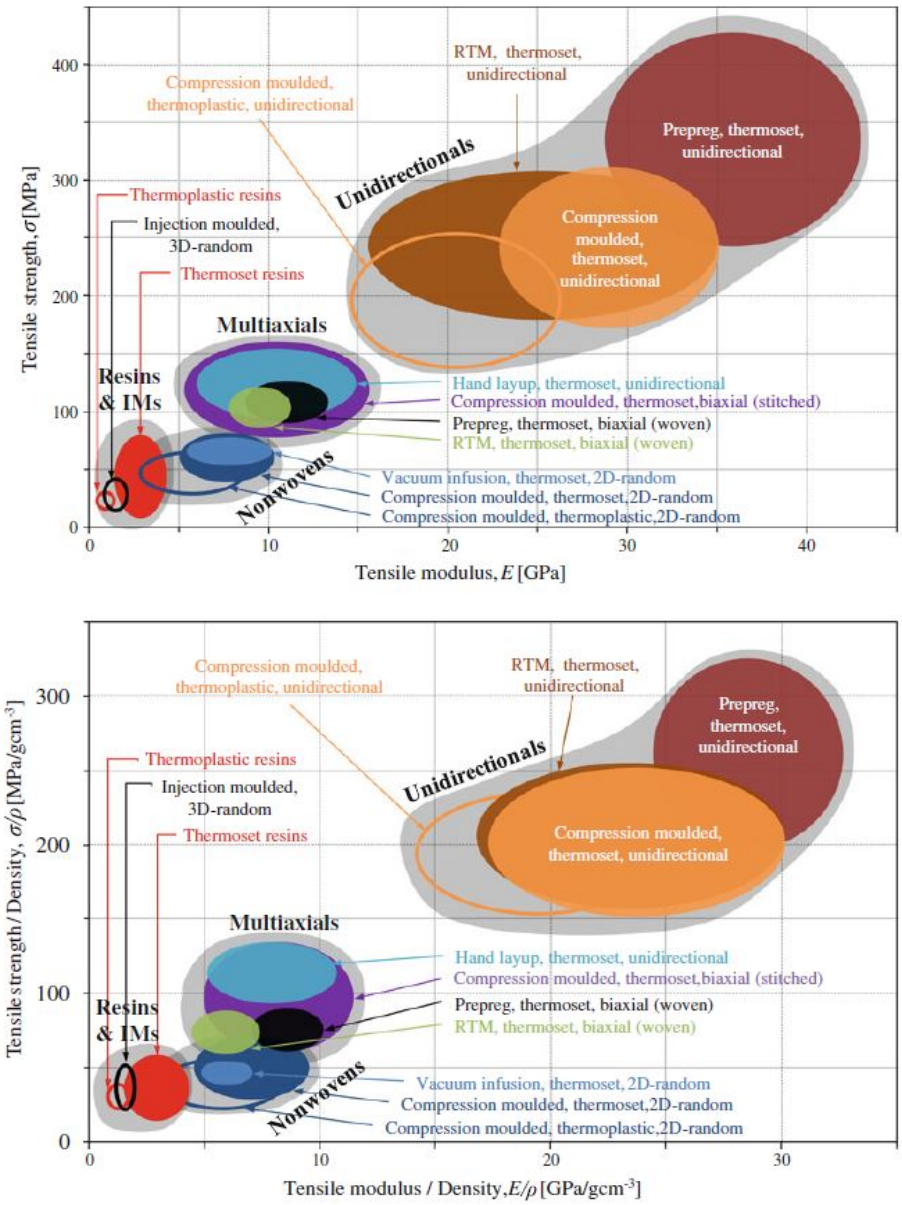

Figure 2.3: Common tensile mechanical properties (both absolute and specific) of plant based bast (*i.e.* flax, hemp, jute) fibre reinforced polymers produced using thermoplastics and thermosets, along with short-random/long-aligned fibre reinforcements processed by different manufacturing methods. The figure is taken from Ref. [81].

In this thesis, three specific plant fibres are focused on; flax, jute, and curaua due to promising mechanical properties, practical availability, and the micro-structural diversity inherent in fibres originating from different continents and climates. These fibres were explained in detail owing to their significant usage and relevance to the thesis work, aiming to gain insights into their unique characteristics.

Flax

The plant flax, *Linum usitatissimum*, is one of the most widely used to obtain natural fibres and one of the first to be extracted, spun and woven into textiles [80]. Use of flax in textiles dates back to 5000 BC [82] and there is also a disputable finding indicating that prehistoric hunter–gatherers used the fibrous form of flax in 30000 years ago [83]. As illustrated in Fig. 2.2, flax typically has a 64-71% cellulose content with up to 90% crystallinity, a microfibril angle of around 5-10°, and an aspect ratio of 1750 with 2-11% luminal porosity [81]. The European Confederation of Flax and Hemp have aimed to supply fully traceable and certified premium-quality flax fibres to composite manufacturers. These fibres are claimed to be sustainably grown in Western Europe and account for 80% of global production [84]. In recent years, the mentioned developments around Europe excite the flax based composite research and initiate the use of this fibre in industries for high performance FRP applications [85–89].

Jute

Jute or 'golden fibre' is obtained from the bark of the white jute, *Corchorus capsularis*, and occasionally from tossa jute, *Corchorus olitorius* [90]. As seen in Tab. 2.2, jute fibre has high mechanical properties similar to flax fibres; moreover, it is one of the most affordable fibres and it is second after cotton in terms of usage, global consumption, production, and availability [90]. Jute fibres are traditionally used for making hessian clothes, ropes, papers, shopping bags, floor mats [91], and their usage dates back to the 16th century [92]. Jute production is mainly populated in Asian countries (India, Bangladesh, China and Thailand), and from them India is responsible for half of global production [93]. Similarly to the structure of flax represented in Fig. 2.2, jute typically has a 61-72% cellulose content with up to 80% crystallinity, a microfibril angle of around 8°, and an aspect ratio of 100 with 10-16% luminal porosity [81]. Owing to economic and environmental benefits, this fibre has been used as a reinforcement in FRP applications [94, 95] and significant efforts have been performed to improve its performance by implementing nano-scale applications, i.e., use of graphene, which is the thinnest two-dimensional material [96].

Curaua

Curaua, *Ananas erectifolius* is relatively new and uncommon fibre type to the fibre literature compared to jute and flax and it is a hydrophilous species from the Amazon region [97, 98]. The plant was used in the pre-Columbian era for making hammocks and afterwards, traded by the local people to make string for their bows, fishing nets, or exchanged for cassava grown by other tribes [97, 99]. Curaua typically has a 71-74% cellulose content with up to 66% crystallinity, a

microfibril angle around 15°, and a 4-12% luminal porosity [97, 98]. Although curaua can be found in Guyana, Colombia, Venezuela and Surinam, Brazil (especially the state Pará) plays a significant role for fibre production especially for FPR composite applications [99, 100]. Moreover, Brazilian automotive industry invested to produce curaua fibre reinforced composites and with local research institutes, they carried out sustainability assessment, which revealed economic, environmental and social benefits of usage of curaua in composite car parts [101]. While Brazilian researchers lead the improvement of curaua in FRP applications[102–104], the collaborative works on curaua fibres have been started with European researchers to increase potential use in different continents [105].

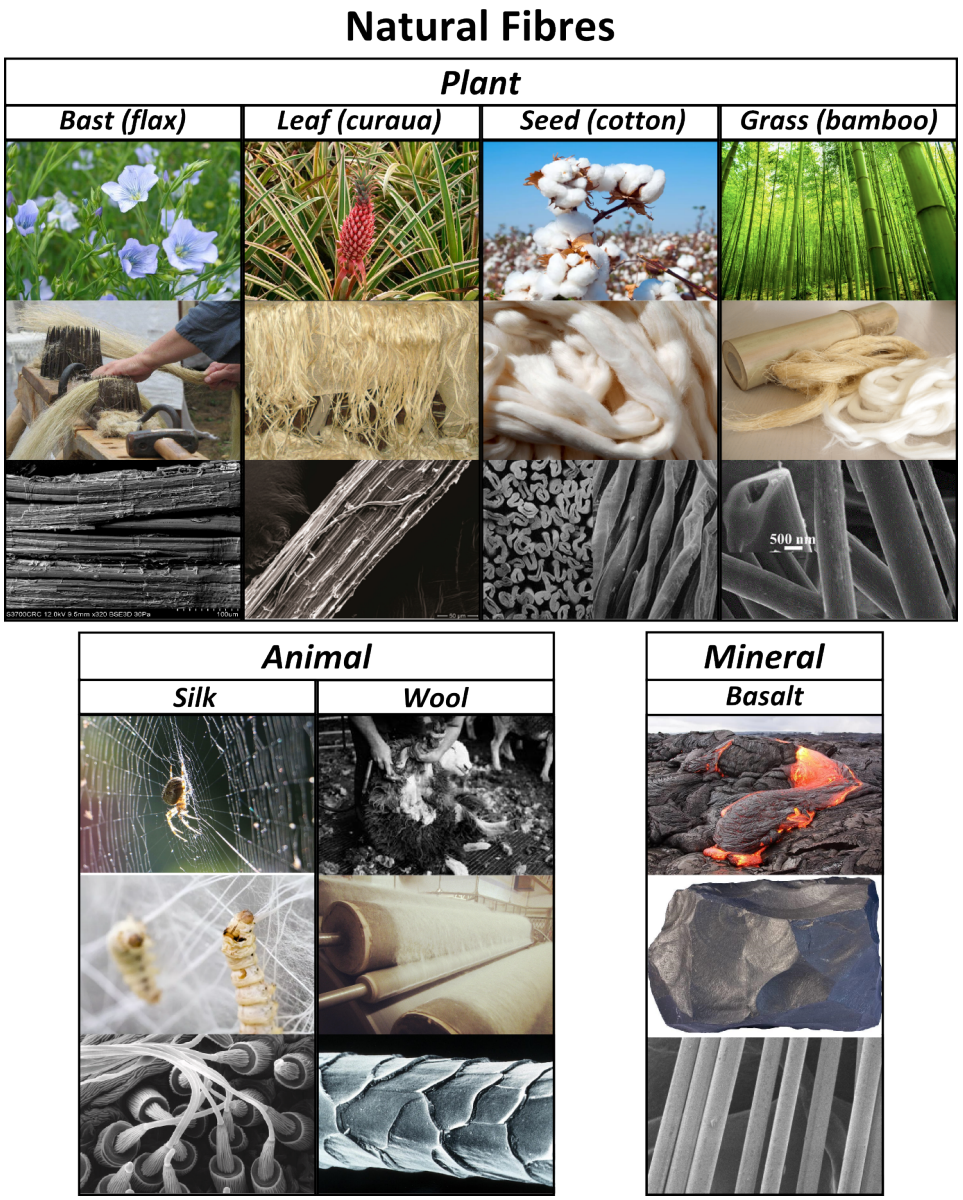

Figure 2.4: Classification of natural fibres through examples of sources, intermediate processes and end products. Image sources: ref. [106].

Table 2.1: Advantages and disadvantages of natural and glass fibres through life cycle stages: cradle, gate, use, grave.

	NATURAL FIBRES	**GLASS FIBRES**
STAGE	**ADVANTAGES**	
Cradle	High specific mechanical properties Abundant Potentially low cost Renewable Carbon sequestration Low energy consumption	High specific mechanical properties Abundant Low cost Non-corrosive
Gate	Low emission Low energy consumption Non-abrasive	Well-established industry Streamlined process
Use	Extremely lightweight Non-deleterious to health Good insulator	Durability Lightweight High operating temperatures
Grave	Low emission Low energy consumption Compostable Biodegradable	
STAGE	**DISADVANTAGES**	
Cradle	Immature supply chain Moisture absorption	Non renewable Deleterious to health
Gate	Moisture absorption Incompatibility with matrices Limited processing temperatures Abrasive	Deleterious to health High emissions High energy consumption
Use	Large variability of properties Moisture absorption Limited processing/service temperatures Durability Flame resistance	Deleterious to health Poor insulator
Grave		Difficult to recycle Non-biodegradable

2.2.1.2 Fibres of Animal Origin

Animal-derived fibres also come under the category of natural fibres and have the potential to contribute to the list of possible reinforcements. Processed animal fur and silk are biodegradable materials and are well-established, but production quantities are relatively limited: such

fibres are expensive and mainly directed at the textile industry for their comfort and thermal properties [107]. In an attempt to develop a more sustainable composite, a wool by-product from sheep farming was impregnated with a bio-derived resin, producing furniture and household items [108]. Certain spider draglines have a strength and stiffness comparable with carbon fibre, with an elongation to failure of up to 35%, which increases with strain rate, and a toughness higher than aramid fibre and steel [109, 110]. Even though these properties are well-known and suggest great engineering potential, the farming of spiders for in-vivo spinning is not currently feasible and farming for production of industrially significant quantities is logistically unrealistic. Despite the technical challenges in replicating the natural process [111] there has been extensive biomimetic research to produce engineered fibres either using spider silk protein [112] or non-protein sources [113]; however, these would be simply bio-inspired synthetic and not bio-derived fibres, and as such the environmental benefits may be compromised. In addition, scale up has been limited: a fundamental point with respect to the fibrisation of material is that it eliminates defects. It is still to be determined what would happen to the properties of spider silk if the fibres would be manufactured on the same scale as glass and carbon.

2.2.1.3 Mineral Fibres

Natural fibres can also be obtained from abundant minerals. Even though they are not regularly considered as bio-based, mineral fibres are the product of the direct transformation of a naturally-occurring resource without further chemicals or additives required to produce the final fibre product. For example, basalt fibres (BF) are drawn from molten igneous volcanic rocks through an energy-efficient process requiring lower labour input than the synthetic fibre material extraction processes [114]. Although glass fibre is also made from natural raw materials or minerals, the manufacturing process involves significant chemical alterations or synthetic additives, which means it is considered to be a synthetic fibre. On the other hand, BF are often considered natural fibres due to their simple manufacturing process which does not involve any chemical steps [114]. Despite a higher production cost per kg than glass fibre, BF exhibit enhanced specific mechanical and physical properties, such as fire resistance, chemical inertness, low humidity absorption, vibration and acoustic insulation [115]. BF are significantly lower cost than carbon fibres and have become a popular novel, lower impact material when used with glass fibres in hybrid composites [114]. They have also been used in hybrid basalt/jute BCs to improve mechanical, physical and thermal stability properties of the plant-based jute fibre BCs [116]. Owing to their thermal properties, BF reinforced thermoplastics have been patented as protective fire barrier materials [117]. Furthermore, BF composites rebars have been applied in civil engineering applications as a lower EI alternative to steel reinforcement for concrete [118]. Inman et al. have shown that BF composite rebar compared with conventional steel rebar in concrete beams are stronger and lighter with a better environmental profile, verified by LCA [119]. Kammeny Vek, a BF producer, compared basalt and glass fibres with woven fabrics through LCA

demonstrating the advantages of basalt fibres [120]. Whilst the incorporation of BF offers some environmental advantages, independent environmental assessments, i.e., LCA, with raw data collection is urgently needed to verify BF inclusion over synthetic counterparts and to contribute to the extremely limited pool of current environmental data available in the literature for BF.

Table 2.2: Mechanical and dimensional properties of natural and synthetic fibres.

	Stiffness (GPa)	**Tensile Strength (MPa)**	**Failure Strain (%)**	**Density (g cm^{-3})**	**Specific Stiffness (GPa cm^3 g^{-1})**	**Specific Strength (MPa cm^{3}g^{-1})**	**Fibre Length (cm)**	**Ref.**
Natural Fibres								
Plant Fibres								
Flax	40–105	370–1480	1.2–3.3	1.38–1.54	26–76	240–1070	10-100	[72, 121, 122]
Hemp	24–90	270–900	1.0–3.5	1.20	20–75	225–750	5-50	[73]
Sisal	10–40	540–720	2.2–3.3	1.30–1.60	6.3–31	340–550	1-15	[73]
Jute	12–60	610–780	1.0–1.9	1.30–1.50	8–46	410–600	12-90	[73]
Banana	12	500	4.5–6.5	1.00–1.50	8–12	330–500	30-90	[73]
Kenaf	15–53	223–930	9.1–12.3	1.20–1.40	11–44	160–775	15-70	[73]
Ramie	1–83	180–1630	1.6–14.5	1.00–1.55	0.6–83	115–1630	90-120	[73]
Curaua	12–50	540–1400	3.0–4.3	1.40–1.50	8.4–36	360–1000	-	[72, 121]
Animal Fibres								
Spider Silk	2–21	750–1840	17–52	1.32–1.35	1.5–16	550–1400	-	[123–125]
Silkworm Silk	1–16	175–1400	4–34	1.34	0.8–12	130–1050	3000-6000	[122, 123, 125]
Wool	0.5–2	170–200	5–35	1.30	0.4–1.5	130–155	5-12	[122, 123, 126]
Mineral Fibres								
Basalt fibres	93–110	3000–4840	3.1–6.0	2.63–2.80	33–42	1050–1850	0-∞	[115]
Synthetic Fibres								
Glass	72–76	3100–3800	4.7	2.54–2.57	28–30	1200–1500	0-∞	[115]
Aramid	70–140	2900–3450	2.8–3.6	1.45	48–97	2000–2400	0-∞	[115]
Carbon	230–600	3500–6000	1.5–2.0	1.78–1.95	120–340	1800–3400	0-∞	[115]

2.2.2 Matrices

Bio-based resins have been developed based on precursor materials of 100% biomass origin or, more commonly, a hybrid blend of synthetic and biomass material to tailor for specific characteristic requirements [127]. The mechanical properties of bio-based and synthetic polymers are summarised in Table 2.3. Of the bio-polymers discussed, most have a bio content below 50%, implying they are majority synthetic polymers and arguably could be classified as synthetic polymers. However, for the purposes of discussion, polymers with a non-zero bio-content will be classed as bio-based. Within the broad field of matrices, the three key sub-divisions are thermosets, thermoplastics and vitrimers, each with their own set of and disadvantages both technically and environmentally.

2.2.2.1 Thermosets

As a matrix, thermosets (such as epoxies, polyesters and vinyl esters) are often preferred in FRP composites due to their superior mechanical properties, durability and thermal stability. However most engineering thermosets are not biodegradable nor fully recyclable, which indicates a higher EI. Complete reviews of thermosetting resin composites recycling processes have been

presented by Pimenta et al. [128] and Oliveux et al. [129]: in general, the thermo-chemical processes required to reclaim the fibres for future use degrade the matrix, making its reuse challenging. Currently, the only way to fully reuse EoL thermosetting resin composites is to mechanically grind them and using them as filler [130], but this is often not convenient due to the low return value. The majority of all synthetic epoxy in the composite market (around 90%) is based on the diglycidyl ether of bisphenol A (DGEBA) derived from epichlorohydrin and bisphenol A [131]. The synthesis, properties and applications of thermoset resins derived from bio-based sources as alternative feedstocks to those derived from petroleum have been discussed [132], with matrices obtained from furans, plant oils and starch, and advances in cellulose and nanocellulose indicated as future matrix feedstocks [133]. Numerous approaches for synthesising bio-based epoxies with functional groups derived from natural sources such as tannins, cardanols, vegetable oils, woody biomass, lignin, terpenes, terpenoids and resin acids have demonstrated the ability of bio-based epoxy additives to enhance the toughness of polymer networks [134]. Bio-based thermosets derived from vegetable oil resources and terpenes have been studied to reduce the EI and their suitability for several applications have been demonstrated [135]. A bio-based epoxy resin, derived from vegetable oil and offering high fracture toughness, has been suggested to be the most appropriate in the current thermoset market [136]; other options include Ebecryl®, pine and vegetable oil-based SuperSap® epoxy, soy-based Envirez™ and linseed oil-based Vikoflex® [137]. Cardolite has recently introduced cashew nutshell liquid technology to produce bio-based epoxy curing agents, diluents and modifiers which, according to LCA results, releases less carbon dioxide equivalent per kg of resin relative to petroleum-based epoxies during production principally through carbon sequestration [138]. Bitrez has also announced a new generation of poly-furfural alcohol “PFA” resins named Furacure, which have a high degree of bio-based grade (up to 100%), compliant to REACH [139] and offers a high thermal performance [140]. However thermoset resins remain challenging to recycle at EOL since they can not be melted and reformed.

2.2.2.2 Thermoplastics

Traditional synthetic thermoplastics such as polypropylene (PP), polylactic acid (PLA), polyethylene (PE) and polystyrene (PS) are often touted as being recyclable at EOL [141] and they have been frequently paired with natural fibres to create NFRPs [142, 143]. They can be easily manufactured into complex parts and, more importantly, provide good impact resistance. However they do require high processing temperatures, which can limit some applications for NFRPs, since natural plant fibres physically degrade over 200 °C, making then unrecyclable [144]. Polyglycolic acid (PGA) is a bio-based polyester with desirable mechanical properties, but owing to its high melting temperature (220 °C) it is incompatible with NFRPs [145]. However, time dependent temperature characteristics can play an important role, and it should be noted that for some thermoplastics, i.e. PLA or PP, high processing temperatures up to 240°C with short cycle times

(*e.g.* 2-5 minutes) are adequate to produce NF reinforced thermoplastic composites [146, 147]. Polyhydroxyalkanoates (PHAs) represent a promising class of bio-based polyesters: a long but somewhat chequered history follows their initial development to pilot plant-scale by ICI in the late 1980s and subsequent commercialisation as BioPol, however interest faded at that time due to the relatively high cost. PHAs are naturally derived from microorganisms, and they exhibit a low density (~1.2 gcm^{-3} depending on crystallinity) and mechanical properties comparable to synthetic isotactic PP (with a highly regular distribution of methyl substituents on the polymer backbone) [148]. By adding hydroxy valerate to a PHA network, the resulting bio-based resin

Table 2.3: Properties of bio-based and synthetic resin systems, [1] Heat deflection temperature based on Envirez 70302 resin with 22% bio-based content, [2] Melting temperature of 100 wt.% bio-based HDPE Brasken SHA7260 min.94% bio content, interpreted from the differential scanning calorimeter cooling cycle and second heating cycle, [3] Vicat A softening temperature for Biotec Bioplast.

	Stiffness (GPa)	**Tensile Strength (MPa)**	**Density (kg m^{-3})**	**Maximum Service Temperature (°C)**	**Ref.**
Bio Resins					
Thermoset					
Bio-epoxy	3	69	1000	100	[149]
Unsaturated Polyester	2.5	73	-	90 [1]	[131]
Vitrimer	0.004-1.5	0.6-30	-	-20-150	[150]
Thermoplastic					
High Density Polyethylene	1.1–1.8	22–31.0	955	132 [2]	[1, 151]
Thermoplastic Starch	2.4	34	1350	58 [3]	[152]
olylactic acid	1.2-3.5	59-77	1070–1270	60-240	[153]
Polyglycolic Acid	6–7	60–99.7	1500–1710	225–230	[154]
Poly(3-hydroxybutyrate)	3.5–4	40	1200	175–180	[155, 156]
Synthetic Resins					
Thermoset					
Epoxy	2.41–4.5	27.6–130	1200	90–200	[1, 157]
Polyester	2.06–4.41	41.4–90	1200	60–200	[1, 157]
Vinylester	3.3–4.9	53–75	1150	>100	[157, 158]
Vitrimer	0.1-2.0	20-50	1050	20-240	[159]
Thermoplastic					
Polyproplene	1.14–1.55	31–41.4	900	70–140	[1, 157]
Polyphenylene Sulfide	3–4	65–110	1300	130–250	[157, 160]
Elium®	2.6	5.6	1036	107	[161]

demonstrates a melting temperature and mechanical properties equivalent to PE [145]. It has been demonstrated that a more sustainable and competitive BC is achievable by using bio-based high density PE (HDPE) resin with natural fibres or components such as wood flour, flax fibres and walnut shell flour [162]. Arkema has introduced a thermoplastic recyclable and reformable matrix series named Elium® resins, which are liquid resins for composite

applications and offer comparable performance to traditional epoxy resins [161, 163]. Owing to its low viscosity and high mechanical performance, the composite boat industry started to use these recyclable resin systems in their infusion processes to produce many parts of sailing boats, such as hull, deck, gangway, helm, mast, cockpit, deckhouse, etc., and a recyclable semi-rigid boat itself was made by using the Elium® resin system in 2019 [164]. Thermoplastic starch (TPS) is another biodegradable, renewable and low-cost bio-based resin, but has unsatisfactory mechanical properties and is subject to retrogradation [165]. A potential solution to this is to blend it with other bio-based or synthetic thermoplastics, increasing the renewable content and allowing for some biodegradation. Several TPS polymer blends are already commercially available [152] such as Bioplast®, Mater-Bi® and TPS/PCL, which have been successfully reinforced with various volume fractions of natural fibres, e.g., flax and ramie, obtaining tensile strengths in the range of 20 to 55 MPa [166]. Additionally, it was shown that blends of polysaccharides and starch appear to be compatible matrices with natural fibres [166]. LCA results have shown that whilst synthetic polymers are the best economic alternative, polymers with higher content of TPS exhibit increased environmental performance [167]. The biodegradability and potential for thermoplastics to be reformed means that they remain strong candidates for suitable NFRP pairing, but the low mechanical performance and creep drawback of bio-based thermoplastics are the main barriers to wider uptake [168].

2.2.2.3 Vitrimers

Vitrimers are a relatively new class of polymer [169], a branch of Covalent Adaptable Network (CAN) family, and can be synthesised from thermoset, thermoplastic or elastomer precursors. The term "vitrimers" is derived from "vitreous" and "polymer," indicating a material with a glassy or solid appearance. What sets vitrimers apart is their dynamic covalent bonds, which can exchange and rearrange while the material remains solid. This makes it possible for the polymer structure to switch by breaking or debonding and reforming the associations and bonds (without a net change in the number of bonds within the network, which makes it different than dissociative CANs where the decrease in crosslinking density is proportional to the loss in network connectivity, observed in step by step breaking and reformation of bonds [170]), under certain conditions, allowing the material to be reshaped and healed. The repairability, reformability and recyclability of vitrimers could make them more attractive compared to thermosets or thermoplastics in applications where high thermal or thermo-oxidative stability is not required [171]. Moreover, vitrimers mechanically behave like thermosets at operating temperatures meaning that structure relies on crosslinks rather than entanglement as seen in thermoplastics. This makes vitrimers more desirable compared to thermoplastics for repair/reform of the composites because (i) the dynamic bond exchange in vitrimers facilitates the rearrangement of polymer chains around the reinforcing fibres, promoting better adhesion and load transfer between the matrix and the fibres (ii) vitrimers can maintain or even enhance their mechanical properties

after multiple processing cycles. This contrasts with traditional thermoplastics, which may experience degradation in mechanical performance with repeated processing [168]. The combination of Bentonite particles with a vitrimer matrix synthesised from epoxidised natural rubber has been investigated for composite applications, demonstrating their heat-driven, self-healing recyclability [172]. A vanillin-based epoxy vitrimer matrix was used to produce a high-performance carbon fibre composite, and partial matrix degradation was achieved under mildly acidic conditions, resulting in high yields of composite recyclate [173]. The use of vitrimers could also compensate for the disadvantages of natural fibres, for example, nanocomposites produced by polydimethylsiloxane-based vitrimer exhibited high water resistance and strong overall adhesion, which is not typically awarded to NFRPs [174]. Other work in this field has produced a fully bio-based epoxy vitrimer from commercial epoxy soybean oil with fumaropimaric acid, exhibiting good shape memory, self-healing and reprocessing properties [175]. A fully bio-based polyimine vitrimer derived from fructose, was found to have a lower temperature requirement for synthesis and reuse than other vitrimers [176]. An imine-based hardener derived from a partially bio-based epoxy source was used to produce a vitrimer and paired with carbon fibre; closed-loop recycling of the composite was completed by removing the matrix in an amine solvent without degrading the carbon fibre or resin, which could then be used to produce recycled composites [177]. Furthermore, woven carbon fibre fabrics have been impregnated with powdered vitrimer matrices to fabricate composites rapidly; reshaping capability has also been demonstrated, suggesting the suitability of these materials for high volume production [178]. US-based company Mallinda has recently introduced vitrimer commercial products (Vitrimax™ T100 and Vitrimax™ T130) for the composite industry [179]. Their products are imine-linked polymer networks and offer proven reform, repair, and recycle abilities [180, 181], which makes them promising to lengthen the life cycle of composite products. In the EU, a recent VITRIMAT project (a consortium of a national centre, six academic, and seven industrial partners) focuses on vitrimers and industrial developments of daily life products, especially for adhesives, thermosets and composites for consumer goods, construction and automotive applications to answer the requisites of a circular economy [159]. As fibre reinforced vitrimer composites are a very recent addition to the designer's tool-kit, to date an LCA has not been performed: to establish the sustainability of this novel material class, LCA validation is urgently required.

2.2.3 Fibre-Matrix Interfaces

As a rule of thumb, unless a natural fibre has undergone additional processing, it has a rougher surface compared to a synthetic fibre. In principle, this can aid mechanical interlocking with the matrix, but the presence of hydrophilic hydroxyl groups may form hydrogen bonds with adventitious moisture, competing with those formed with a polar matrix resulting in poor mechanical performance as a composite [121]. Additionally, the reactive functional groups of the natural fibre may be covered by pectin and waxy substances that behave as a barrier, preventing

effective fibre-matrix bonding [171]. To overcome this issue, chemical treatments are applied to the fibre to provide increased wettability, water resistance, IFSS and compatibility with the matrix. Several chemical methods exist such as alkaline treatment, silane treatment, acetylation, benzoylation, peroxidation, sodium chlorite, isocyanate and fungal treatments [144]. The most common of these is the addition of sodium hydroxide, a highly alkaline species, which removes a portion of lignin, wax, pectin and oil from the system through a saponification mechanism, altering the crystallinity of the system. This increases the fibre-matrix bonding strength and the overall NFRP mechanic performance. However these treatments can be expensive, and release post-treatment chemicals and any byproducts as waste. Furthermore if the treatment yield is too low, then it can even limit the interfacial improvements [182]. Alternatively, fungal treatments have been demonstrated to be as effective as alkali treatments in terms of improving mechanical properties, yet are also potentially lower EI as they are based on the enhancement of a natural treatment process [183]. To provide NFRPs with further properties such as flame retardancy or water resistance, treatments will always be required and the EI of such treatments should be considered with LCA during the design phase.

As discussed, the interfacial properties between plant fibres and polymer matrices has been a subject of discussion in the literature, with arguments concluding that plant fibre composites often form poor interfaces with typical polymer matrices, especially compared to synthetic fibres. One of the reasons for this perception is the IFSS values, which are lower than those of synthetic fibres, or the critical fibre lengths measured, which are in the range of 0.2 - 3 mm [81]. These critical lengths are actually smaller than the typical fibre lengths of plant fibres such as jute and flax, which are at least 25 mm [81]. As a result, it is expected that most plant fibre composite manufacturing processes, except those involving compounded micro-scale fibres or fillers, would lead to a required embedded interface to allow better stress transfer and load distribution from matrix to fibres, particularly when aligned composites are produced.

2.3 Production

To employ a natural fibre in a composite application, it must undergo an extraction and preparation process. The quality of the fibre varies considerably due to this process, and it has a profound impact on the mechanical characteristics. The end product is tailored specifically for the intended application. The fibres can take various forms, such as mats, unidirectional prepregs, woven fabrics, and non-woven fabrics, among others. Retting is the initial step in extracting bast fibres from the woody substance and cellular tissues in which the fibres are situated within the plant stem. Scutching is a process used in fibre extraction to remove impurities and separate the valuable fibres from the non-fibre components. After that, there is hackling process used to further refine and separate the long fibres from short and coarse ones in plant materials like flax, hemp, and also for wool too. This process is commonly used in the production of high-quality textiles and other fibre products and after this the long fibres are ready for further processing, such as

spinning into yarn. The entire process is illustrated in Fig.2.5. Moreover, process parameters in these steps also have a significant influence on the mechanical properties of the final product. The overall objective of this procedure is to obtain uniform, lengthy, and intact fibre bundles that can be utilised in consolidated composite forms. While there might be some variations in the process between different producers, to ensure consistent quality, suppliers utilise batch mixing across multiple crops, harvests, and years. [184]

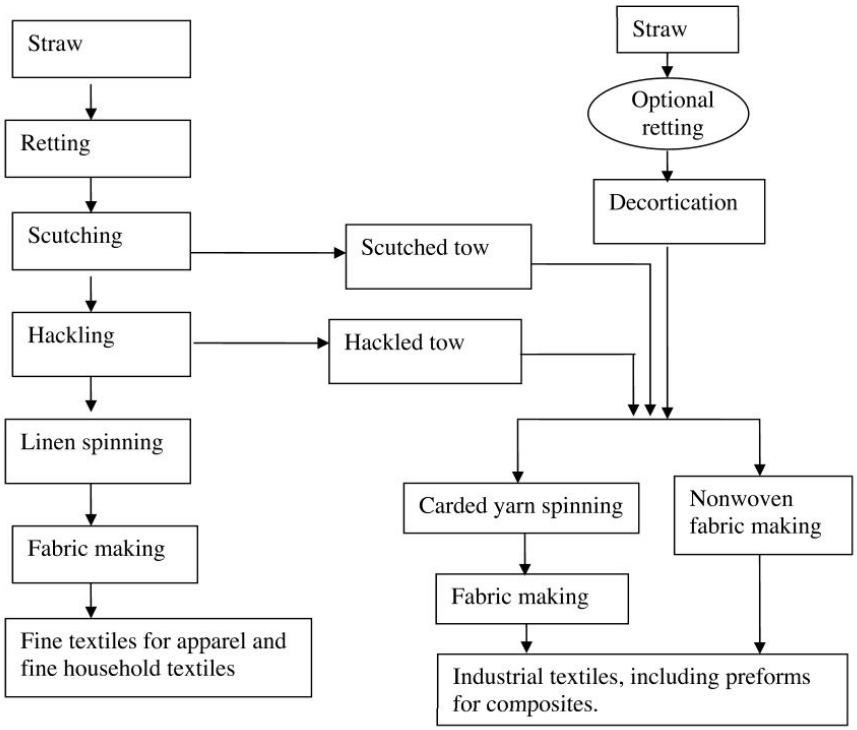

Figure 2.5: Production of bast fibres and their end uses [184].

Natural plant fibres and bio-based materials for BCs are cultivated on agricultural land and thus photosynthesise during production. This absorbs carbon dioxide from the atmosphere and locks it into the plant's molecular structure, storing the carbon and releasing oxygen as an output, i.e., carbon sequestration [185]. This is all powered by solar energy, an abundant and renewable energy source, and results in a reversal of GHG emissions, reducing harmful global warming. In stark contrast, the extraction of raw materials to produce glass or carbon fibres and synthetic polymers emits large amounts of excess carbon dioxide into the atmosphere; a significant contributor to climate change. It is by virtue of the lower carbon emissions and lower scores from other EI categories that bio-based materials have received such significant attention in recent years.

Unreliable harvest yields due to external factors, such as the microclimate, temperature and humidity, represent a significant challenge for BCs. Unsustainable farming practices are adopted to minimise the heterogeneity during cultivation, e.g., use of agrochemicals, the production and

application of which can grossly alter the energy use during plant growth. Other impacts can include land use change, water consumption, biodiversity loss, significantly reduced soil quality and increased stratospheric ozone depletion due to nitrogen dioxide emissions from fertiliser application [55, 186, 187].

Deng compared the EI of producing a GFRP (glass/epoxy) electrical circuit board component and an equivalent made from NFRP (flax/linseed oil) [55]. The use of the NFRP over GFRP significantly lowered the EI from GHG emissions associated with GF production but there was an increase in the marine ecotoxicity and eutrophication from surface fertiliser runoff, applied to the land for natural fibre growth. While the energy required for cultivating flax in the UK was low, the agrochemicals and retting processes increased energy consumption significantly [188]. Essentially, the environmental footprint of natural fibre or biomass production will come from: tillage, sowing, harvesting and fertilising processes, which depend on the particular fertilisers or agrochemicals used [187]. The cultivation process is a key area of BC material production which is limiting their environmental performance.

2.4 Processing

Once the cultivated natural plant fibres have grown, they need to be harvested and transformed into continuous fibres. Seasonal fluctuations of external factors affect the height of the plant and therefore strength and density of the fibres. For certain performance applications where designs must meet a given strength, additional processing stages may be required to ensure mechanical characteristics of the final composite are acceptable [189]. Fibre substructure processes, such as mat production, fibre yarns, granule production, fibre preparation and fibre treatment could represent a large proportion of the processing emissions [187].

In Europe, flax and hemp yarns are the most commonly used reinforcements for BCs. After harvest, they are both processed through different methods depending on their desired resulting properties. Extra treatments that give BCs the characteristics required of specific applications e.g., flame retardants, are incorporated at this stage. Since bio-based materials are hydrophilic in nature, they can be treated to prevent moisture absorption during their service life. Any treatments at this stage will increase the EI and economic cost, due to the production and application of these chemicals. However, LCAs demonstrate that no method is more efficient overall, and that any use of chemicals significantly negatively affects the EI score. It was also noted that, in particular, the lack of technological development in processing methods is seen as the decisively limiting factor for the natural fibre industry in Europe. The large labour input at the processing stage has limited hemp reinforcement production to Hungary and Romania where labour costs are low, and this blocks the wider spread of fibre production to Western Europe [190].

Due to the degradation of cellulose temperature, the processing temperature for natural fibres is limited to 200 °C which restricts the composite manufacturing options available and reduces the possible applications of NFRP [187]. The key limiting factor in selecting a processing

temperature is the influence that this has on resin viscosity. If a resin can only achieve permeation of a natural fibre fabric at a temperature greater than 200 °C, then its mechanical properties will be sub-optimal [191]. As such, either a greater mass of material would be required to achieve equivalent properties or the material would not be selected.

While the bio-based resins on the market are relatively new materials (approx. 10 years), fossil-based resins are more mature (50–60 years) and therefore an optimised product, in a heavily streamlined and competitive supply chain with access to stable markets and policy structure. Bio-based resins are by contrast produced in limited numbers of smaller-scale facilities, with emerging but fractious supply chains, and this affects the stability of pricing and access to assured markets [192].

By way of example, starch is relatively inexpensive in the UK as a bio-based resin feedstock, but prices can very considerably: starch from wheat is £263/tonne but starch from cassava can cost £986/tonne [193]. Cassava, being the superior starch feedstock is also grown in other countries around the world: in Ghana the cost is $1192/tonne, but in Thailand it is $275/tonne. There is also significant variability in the quality of the starch feedstock. When selecting these resin feedstocks, transport costs (economic and environmental) must be considered and incorporated into the LCA model at the design stage too. Whilst in theory these abundant and renewable bio-based feedstocks should be more economically and environmentally efficient than extraction and refining of synthetic fossil-based feedstock, this is often not yet the case.

Similar issues regarding quality variability and supply chain are present for some natural fibre reinforcements grown globally too. Whilst natural fibre alternatives to synthetic reinforcements are showing traction, more research on fibre processing, interfacial bonding and moisture sensitivity control is required in order to compete with glass fibre [59]. A promising first step has been the recommendation within a number of papers to use natural fibres in conjunction with synthetic fibres in a hybrid structure [11].

The HiPerDiF approach is a novel method for manufacturing fibre reinforced composites that aims to improve production and processing compared to traditional methods, which provides hybridization options to the composite processing especially to intermingled and intraply samples [17]. It also offers the advantage of producing highly aligned short fibre preforms, which can achieve high performance levels similar to continuous fibre composites [18]. This method stands out among other approaches due to its use of highly aligned discontinuous fibres, which not only enhance manufacturability but also provide the opportunity to create a ductile or a pseudo-ductile response under loading [17]. Traditional composites rely on continuous fibres embedded in a polymer matrix, which can have high specific stiffness and strength but are prone to catastrophic failure. HiPerDiF, on the other hand, can utilize highly aligned discontinuous fibres, improving the manufacturing of complex structural parts and enabling better load distribution within the composite with the option of providing a ductile or pseudo-ductile response [10, 17].

The length and orientation of fibres are crucial factors that influence the properties of

composites. HiPerDiF takes into account the critical length of fibres to maximize fibre breakage during loading rather than slip between the fibres and matrix. This unique approach maintains a high degree of fibre alignment throughout the manufacturing process, resulting in aligned short fibre preforms with excellent mechanical performance [16]. However, it is important to note that post-processing steps, such as impregnation and curing, may introduce slight misalignment or variations in fibre orientations, which can affect the final properties of the composite. Other common methods for producing fibre-reinforced composites include Resin Transfer Moulding (RTM), Vacuum Assisted Resin Infusion (VARI), Sheet Moulding Compound (SMC), and Hand Lay-up (HL). Each method has its own advantages and limitations in terms of fibre arrangement, impregnation techniques, or shape production complexity [8].

RTM is a common method for producing natural fibre-reinforced composites. It offers the advantage of creating complex shapes with good surface finish and allows for good control over fibre orientation arrangement. This method is well-suited for producing large and structurally complex parts. However, it does have some limitations. RTM requires expensive tooling and equipment, and the cycle times can be longer compared to other methods. Additionally, it is limited to low-viscosity resins, which may restrict the choice of matrix materials [76].

The VARI technique enables the production of large, high-quality parts with good fibre arrangement and low void content. VARI offers flexibility in terms of using different reinforcement fabrics and resin systems. It is suitable for complex shapes and relatively low-cost tooling. However, VARI requires a vacuum bagging setup and careful control of resin flow, which can increase cycle times. Achieving high fibre volume fractions can be more challenging compared to other methods [8].

SMCs are another example for commonly used composites for high-volume production of fibre-reinforced composites. It is well-suited for parts with complex shapes and excellent dimensional stability. SMC allows for good control over fibre arrangement and the integration of multiple components into a single part. However, it is limited to flat or moderately curved shapes and requires specific machinery and tooling, resulting in higher costs compared to some other methods [8, 76].

Lastly, HL of continuous fibre prepregs (mainly for carbon or glass fibres) is a low-cost method suitable for small-scale or custom production. It offers flexibility in fibre arrangement and can accommodate various reinforcement fabrics. HL is commonly used for producing large parts or prototypes with relatively simple shapes. However, it is a labour-intensive process, leading to longer production times. HL may introduce variability in fibre content and arrangements, and the surface finish quality may not be as high as with other methods [8].

The HiPerDiF method is relatively new method compared to the ones mentioned above. The recent developments on the HiPerDiF machines made method to be able to produce dry and pre-impregnated materials that can be used for composite production. However, due to the low fibre volume fraction content, pre-impregnated HiPerDiF materials are still significantly resin

rich compared to the available pre-pregs. The reason is behind this fibre preform areal density is lower but this is sometimes advantageous. For example, additive manufacturing methods, such as 3D printing, may prefer low fibre volume fraction for the pre-impregnated feedstocks. Another recent development activity focuses on how to use dry fibre preform in resin infusion techniques. There is no official results on this yet, but fibre misalignment and lower areal weight of dry fibre preform are disadvantages for production and performance of composites produced by these techniques compared to other methods.

2.5 Application

The additional upstream environmental burden of producing FRPs over traditional materials such as steel and aluminium has been justified downstream during the use phase by offering longer service lives with lower maintenance impacts, contributing to the sustainable solution that composites can offer. Currently, information regarding the maintenance, durability and service efficiency parameters of BCs is incomplete, and these are critical to ensure that BC components will have the same use life length as their synthetic FRP counterparts [56]. The intended application of the composite will have significant influence over the EI and the economic cost. Whilst BCs have the advantageous light-weighting properties for transportation applications, issues regarding their durability mean they are unsuitable for applications under the hood of vehicles and are limited to decorative or cosmetic interior applications; the same is true for aircraft applications [194].

On a more positive note, the automotive industry has already established a strong demand for NFRP during the last decade: even in 2012 over 95% of NFRPs commercially produced in the EU were used for non-structural automotive components, manufactured predominantly by compression moulding [81]. Natural fibres such as ramie, flax and jute have significantly superior sound dampening capabilities over their synthetic competitors that is attractive for automotive interior applications, such as door panels, dashboards, roof liners and seat shells [29, 195]. Additionally, components made from hemp composites do not splinter or leave sharp edges when cut, an important feature for the automotive sector when considering collisions [196].

There are several niche areas where the multifunctionality of NFRPs have the potential to be explored. Conductivity (i.e., dielectric performance) of natural fibre composites was discussed in a review by Al-Oqla et al. [197]. Dielectric constant is the measure of a material's ability to store energy from an incident electric field, and a high dielectric constant implies the material can absorb electromagnetic radiation. A composite of this kind could be classed as multi-functional, absorbing radiation whilst supporting a system structurally, although it should be noted that the absorption of moisture would raise the dielectric constant. In this context, sisal/polyester and jute/polypropylene have undergone testing and indicated promising performance [198, 199]. Feng et al. demonstrated a bio-based benzoxazine resin had encouraging dielectric properties and an area for future work could be its coupling with a natural fibre to produce dielectric BCs. [200].

Cured polybenzoxazines are traditionally quite brittle in engineering applications and the composites would require significant toughening before use. Yang et al. studied cotton, wool and flax fibre yarns applied to an artificial muscle actuator to produce high-performance sportswear [201]. The yarns were twisted into artificial muscles by a motor as a smart fabric concept. To mimic perspiration stress from physical activity on the fabric, moisture was added causing the yarns to contract and a flap to open, releasing heat and cooling the user. Additionally, flax and hemp fibres have high damping and absorption capacity relative to synthetic fibres, resulting in their use in automotive, sporting goods and musical instruments [202, 203]. Bio-based resins have also found novel application as hygienic interior decorative coatings: a bio-based acrylic chitosan-nano silica hybrid resin, with anti-bacterial properties and hydrophobicity, minimises the risk to human health by reducing exposure to harmful synthetic resin irritants [204].

The inherent flammability of BCs means they are wholly inadequate for application in high-rise construction, which have stringent fire safety regulations [205]. Additionally, since bio-based materials are naturally hydrophilic, if left untreated over their service life they will be prone to fungal and bacterial growth, resulting in higher maintenance impact and costs. However when BF/epoxy composites were exposed to seawater ageing at different temperatures, their mechanical performance was found to be similar to that of GFRP with the same epoxy matrix after sea water saturation, which suggests potential use for BF composites in marine structures [206].

As more companies face pressure and international target commitments to reduce their carbon dioxide emissions, other industries are turning towards natural or bio-based products. The fashion industry, in particular, has seen a marked increase in demand for fibres like flax and hemp, generating more competition for the dwindling amounts of land available, which may result in a price hike [207]. The automotive industry is heavily price-dependent and may not be able to compete with these industries for bio-based materials [189]. This has also stimulated comment within the BC sector that their limited uptake to date has been contributed to by a lack of "political will", including policy instruments, tax relief or stimulation packages that may incentivise investment, and this could be due to the deeply rooted global market dominance of fossil material companies [208]. However this setback is driving innovation within the BC field, and as they become more mainstream it is hoped they will experience wider acceptance by the markets. For example, fibre precursors and resin feedstocks are now being developed from algal blooms, reducing the dependence on scarce land resources for material production as well as addressing the eutrophication that has caused the exponential growth in toxic blooms all over the world [209–213].

2.5.1 Reuse and Repair

With the recent advancements in self-healing technology and the nature of thermoplastics [33], it is possible to reuse composite parts in the manufacturing stages and possible to repair them while in use or reuse and after the components' end of life. There are several approaches to

the concept of reuse or repair in fibre reinforced composites; however, most repair methods involve joining methods such as adhesive bonding, patching or welding [214–218]. In addition, reconsolidation is another common technique for thermoplastic composites and thermosets, which contain reversible bond formation [171] for reuse and repair. The concept of reconsolidation can be used as a patch repair, especially for vitrimer composites. Lorwanishpaisarn *et al.* [219] have shown that carbon fibre composites produced using a novel bio-based vitrimer are able to deliver a full mechanical strength recovery after a one-step single patch repair technique as illustrated in Fig. 2.6. Therefore, patch repair techniques can be used as a new viable method to extend the service life of structural materials and reduce the waste during the manufacturing stages.

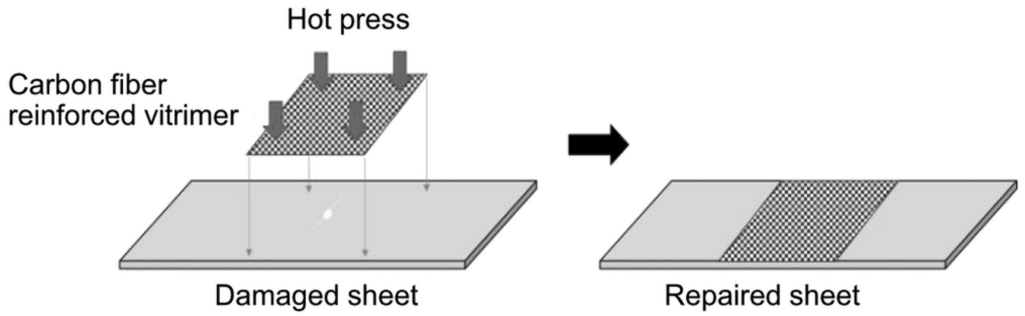

Figure 2.6: The illustration of one-step patch repair using the carbon fibre-reinforced vitrimer [219].

Moreover, hollow fibres and microencapsulation approaches are based on releasing healing chemicals by using fibres filled with or particles filled with healing agents, which flow to the crack area when damage is induced and solidifies [220]. These methods have been extensively studied in the last decades for the repair of FRPs, and the best efficiencies have been reported up to 93% [33]. Additionally, using embedded adhesive particles that can be activated via heating system (such as lasers) were proposed as another self-repair systems in FRP applications and full mechanical recovery was reported for both tensile strength and flexural strength [221]. These repair methods can allow components to be in use at least for another cycle and provide service life extension of structural materials.

2.6 End of Life

Owing to the environmentally damaging nature of material extraction and production, the overarching aim of the circular economy model is to keep resources within the industrial system loop in a sustainable way, to prevent the unnecessary production of virgin materials [222]. As a result, composite waste landfilling has recently been prohibited in an increasing number of European countries, for example Germany [223, 224] and EU law now requires 95% by weight of all automotive vehicles produced in the EU to be re-used, recovered or recycled at the end of their life [225]. Unfortunately for BCs, any form of reclamation technology is not currently possible due to operating temperatures of more than 200 °C, e.g., pyrolysis requires temperatures between

450 °C–700 °C that would completely burn bio-based materials [226]. Chemical processes such as solvolysis would also damage bio-based materials beyond repair. Vitrimer resin technology may offer low temperature or low energy repair-reuse-recycle options based on the Waste Hierarchy preference, but this has not yet been qualified by an LCA.

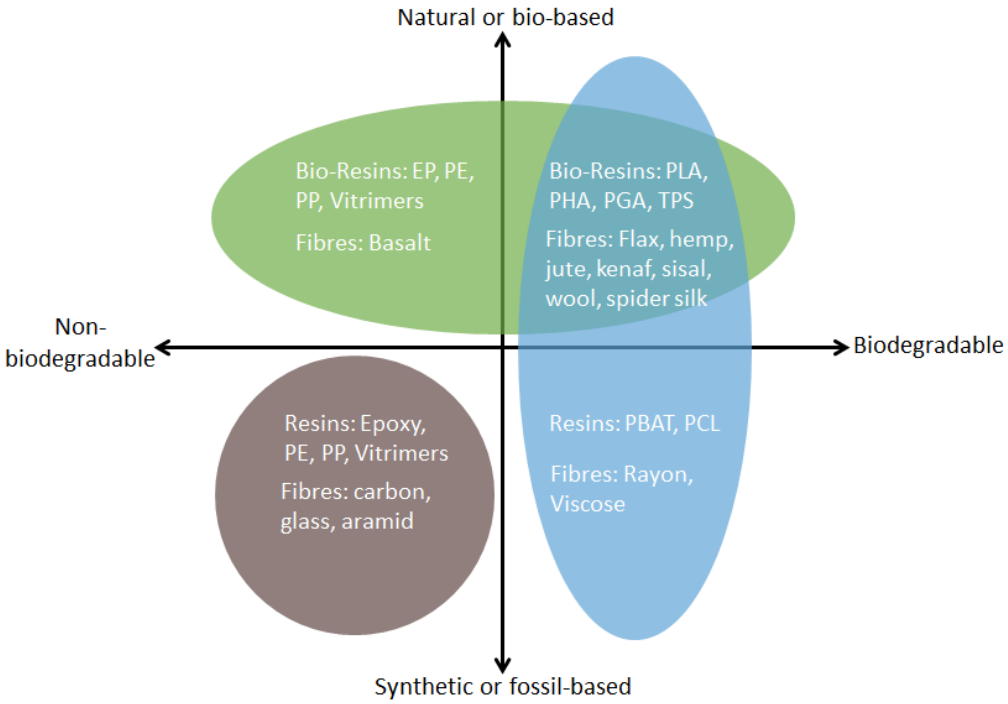

Figure 2.7: Biodegradability of the most common bio-based and synthetic composite fibre reinforcements and resin matrix systems. The data is taken from references in Section 2.2 and [192, 227, 228].

Biodegradability refers to the ability of organic material to break-down with the help of microorganisms, such as bacteria and fungi, within a certain time frame. These microorganisms change the materials' molecular structure to give base substances such as water, carbon dioxide, methane, basic elements and biomass [229]. If biodegradable fibres were combined with a biodegradable resin this would produce a biodegradable composite. Under the correct conditions, biodegradable materials can be degraded relatively quickly by microbes and natural processes, returning nutrients back to the biological system to prepare for the next material cycle. When managed correctly, the environmental benefits are numerous: improvements in soil quality, increased biodiversity and a reduction of waste going to landfill. Fully biodegradable composites, although extremely rare for structural applications, are not recyclable in the traditional sense of keeping materials as-manufactured. Figure 2.7 shows the biodegradability of the main fibres and resins discussed within this chapter in their purest form, i.e., of 100% synthetic or 100% bio-based origin. It is anticipated that some bio-resin blends that include some non-biodegradable constituents could exhibit a certain amount of biodegradability depending on the respective

amounts, however there have been limited studies into this as yet.

The risk of contamination from synthetic composite wastes has subsequently meant that industrial composting facilities for biodegradable BCs are underdeveloped [230]. Conversely, if synthetic composite constituents are contaminated with bio-based materials (for example, blended bio-resins), the longer-term durability of reusing composite structures cannot be guaranteed. Some studies have examined the mechanical recycling of BCs as a recycling route, possible through grinding down the composite to the desirable size for filler material [230, 231]. Whilst the EI of the recycling process must remain extremely low in order to be environmentally and economically feasible, this could become an attractive option for the automotive sector which have a legal obligation to recycle/reuse 95% of EOL vehicles. Unfortunately, this may compromise the onward application of the recyclate due to the decrease in resulting properties, such as tensile stress, impact strength and E-modulus of fibres, as well as decrease in the molar mass of the resin.

The only other option available for EOL of BCs within the traditional Waste Hierarchy framework is incineration, with the possibility of heat recovery, which will release the sequestered carbon back into the atmosphere as carbon dioxide, along with the release of other potentially harmful off-gases. Combustion of bio-based materials, such as sisal or kenaf fibre, has a significantly lower gross calorific value than for glass or carbon fibres, and would result in a comparatively lower EI than the incineration of purely synthetic FRP composites [222].

One of the leading challenges for waste BCs is that the disposal options available are not considered during the early product design stage. The focus has traditionally been on the performance and durability. Whilst the hybridisation of natural fibres with synthetic and blends of bio-resins do appear to offer environmental benefits at the production and use stages, they can cause more complications at the EOL stage. This furthermore highlights the importance of adopting an LCA approach at the design stage of composite product.

2.7 Conclusions

BCs can form part of the circular solution for the Sustainable Recovery plan, allowing carbon sequestration at production and biodegradability at end of life, and enabling the manufacture of high value products. However, composites with materials of mixed origin (bio-based and synthetic) present technical and environmental challenges different to those of purely synthetic composites during the life cycle.

For natural fibres, comparable with glass fibre, the use of pesticides and unsustainable farming methods cause the largest EI during their production. They are also competing with other industries, such as fashion, biofuels and agriculture, for a dwindling amount of land, the supply and demand of which can lead to significant price instability. Extra treatments of natural fibres after harvest are a way to improve IFSS with matrices and overall mechanical performance of BC during use. However, there is no consensus about the efficiency of treatments

and they increase the EI of the processing phase of their life cycle. Furthermore, popular synthetic composite manufacturing methods are not suitable for BCs which would degrade at processing temperatures over 200 °C degrees.

BCs have been available on the composite market for some time now, yet their widespread uptake has been limited, and the academic literature still focuses on their potential, instead of actual, applications. Despite the environmental advantages over their synthetic counterparts, there are issues over compatibility with traditional applications, such as their hydrophilic nature, low thermal resistance, flammability and variation across fibres. The geographical locations of certain bio-based feedstocks means establishing pathways to manufacture or market can also be a challenge when compared to the streamlined synthetic material route. Competition from other industries, such as agriculture, fashion or even land for human settlement remains a growing issue, and as a result is driving innovation in other bio-based feedstocks, for example, fibres from algal blooms.

Progress has been observed regarding matrices made from bio-based materials: renewable thermosets, recyclable thermoplastics, biodegradable blends and the innovation of a new polymer class, vitrimers. These can be considered as strong candidates to address EOL issues associated with FRPs in lower temperature applications, since they have wide range of greener solutions (such as reuse-repair-recycle) as well as being derived from renewable bio-based materials.

At the end of its use, a BC has the potential to return to earth to biodegrade and replenish the soil for new material growth. It is important to acknowledge that biodegradation results in the release of sequestered carbon back into the atmosphere. Additionally, it is worth highlighting certain drawbacks, such as the limited availability of industrial composting facilities. This limitation is particularly significant for most biodegradable polymers used in conjunction with plant fibres, as they typically necessitate such facilities. Moreover, due to their processing and resin pairing, biodegradability could be compromised. Legal frameworks also block the landfilling of composites within Europe now, and the recycling options for BCs remain limited due to the high temperatures required. Currently the only option available is incineration with heat recovery. More research is urgently needed on the EOL handling data for BCs, which can be used to implement legal and fiscal mechanisms to encourage the adoption of greener solution for a sustainable recovery, e.g., industrial composting facilities or focusing on several life cycles that enables a circular economy.

2.8 Outcomes

In this thesis, an intense characterisation campaign has been planned to carry out on fibre reinforced composite constituents to assist in material selection for high performance sustainable composites, while aiming to achieve circular economy using reuse-repair-recycle options. Natural fibres were foreseen to be the best reinforcing agent to obtain high performance sustainable FRPs according to their mechanical properties, renewability, and biodegradability, hence lower impact

on environment. Next step, a number of natural fibres will be investigated to understand their compability with sustainable FRP processing methods and to compare their intrinsic properties for material selection. Furthermore, matrix in FRPs play an important role and they have a major environmental impact. As mentioned in this section, there has been new candidates for advanced matrices to offer sustainable solutions and high performance. Following steps will include exploring the harmony of candidate matrices with the natural fibres and discussing their circular economy options whether they promote reuse-repair-recycle. As a final step, a sustainable NFRP will be produced with the selected constituents, will be investigated mechanically and physically, will be assessed in terms of sustainability.

Chapter 3

Identification of Sustainable Discontinuous Fibre Reinforcements for Composites

In this chapter, four types of abundant natural fibres (jute, kenaf, curaua, and flax) are investigated as naturally-derived constituents for high performance composites. Physical, thermal, and mechanical properties of the natural fibres are examined to evaluate their suitability as discontinuous reinforcements whilst also generating a database for material selection. Single fibre tensile and microbond tests were performed to obtain stiffness, strength, elongation, and interfacial shear strength of the fibres with an epoxy resin. Moreover, the critical fibre lengths of the natural fibres, which are important for defining the mechanical performances of discontinuous and short fibre composites, were calculated for the purpose of possible processing of highly aligned discontinuous fibres. This chapter is informative regarding the selection of the type and length of natural fibres for the subsequent production of discontinuous fibre composites.

This chapter has been adapted from the following published work:
Ali Kandemir[*]; Thomas R. Pozegic; Ian Hamerton; Stephen J. Eichhorn; Marco L. Longana. Characterisation of Natural Fibres for Sustainable Discontinuous Fibre Composite Materials. *Materials* 2020, 13, 2129. DOI:10.3390/ma13092129

[*]Corresponding author. Author contribution is given by using the Contributor Roles Taxonomy: conceptualisation T.R.P. and M.L.L.; data curation A.K.; formal analysis A.K.; funding acquisition I.H., S.J.E., and M.L.L.; investigation A.K. and T.R.P.; methodology A.K., T.R.P., and M.L.L.; supervision T.R.P., I.H., S.J.E., and M.L.L.; visualisation A.K.; writing—original draft A.K.; writing—review and editing all authors.

3.1 Introduction

Owing to their light weight, superior specific strength, and stiffness, composite materials play a vital role in engineering applications and are continually replacing conventional monolithic materials. However, sustained growth in the composite industry can only be achieved if components and methodologies are sustainable, with the additional considerations of economic and environmental factors. Consequently, the composites industry is becoming increasingly aware of the importance of materials selection, manufacturing, end-of-life waste management strategies, and the life cycle assessment (LCA), a fundamental tool for the design phase [232, 233].

Natural fibre reinforcements have attracted considerable attention in the composite industry owing to their specific mechanical properties and environmental advantages [35, 234]. Natural fibres are an abundantly available, sustainable, biodegradable, and economically viable alternative to synthetic fibres, such as carbon, glass, and aramid, which share none of these characteristics [36]. Although natural fibres have begun to replace synthetic fibres in several applications [34], their use needs to be validated through comparison of their mechanical properties against those of reinforcements commonly used in industry. One of the drawbacks is the low thermal stability of natural fibres. This limits the possibility to couple them with high temperature processing polymeric matrices [234]. Another limiting factor that needs to be accounted for during the design and manufacturing is their hydrophilic nature; this is especially critical for applications wherein these materials are exposed to humid conditions [235].

Discontinuous fibres are easier to procure than continuous fibres, and their composites are able to exhibit high mechanical performances, comparable with those of continuous fibre counterparts if high levels of alignment and optimum critical fibre lengths are attained [12, 236]. Moreover, highly aligned discontinuous fibre composites (ADFRC) have been considered as the best compromise where processability and performance requirements intersect [7]. The sustainability of composite materials in terms of manufacturing and recycling can be addressed by discontinuous fibre composite processing methods, such as the HiPerDiF method [18]. It has been shown that natural fibres can be manufactured by the HiPerDiF method, and hybrid flax/reclaimed carbon composites have exhibited significant cost reduction and increase in functional properties, i.e., damping, for the applications wherein a reduction in mechanical properties is an acceptable trade-off [11]. It is therefore possible to obtain a sustainable and reliable solution for high performance composites that use natural fibres in a discontinuous fibre composite processing method.

For obtaining high mechanical performances in discontinuous short fibre composites, one of the key parameters is the critical fibre length, which is highly dependent on the interfacial bonding between a matrix and a fibre. The interfacial shear strength (IFSS) is a measure of this interfacial bonding. By using values of the IFSS, it is possible to calculate the critical fibre length. There are several methods with which to obtain IFSS [237]; the most common methods are fibre pull-out [238–240] and fibre fragmentation tests [241–244]. However, these methods have their

own limitations. For instance, for the fibre fragmentation tests a transparent matrix is required and also the strain to failure of the matrix should be at least 3 times of that of fibre since a state of saturation where the fragmentation lengths stabilize must be reached and it may not happen if matrix fails at low strains. On the contrary for pull-out tests, the brittle fibre systems are difficult to perform the tests. The success of test is governed by the critical fibre length and maximum and most importantly, the pull-out test is prone to end effects, where stress concentrations occur near the edges of the specimen [237]. A third, the discrete approach, is the microbond test, which allows the direct and reproducible measurement of the single fibre-matrix interface strength, eliminating any meniscus effects [245, 246], and has been widely preferred for evaluating the IFSS for different fibre/resin systems [247, 248].

In this chapter, natural fibres, jute, kenaf, curaua, and flax were characterised to determine their physical, thermal, and mechanical properties, and these were compared with conventional synthetic fibres. The thermal stability of the fibres was determined using non-isothermal and isothermal thermogravimetric analysis (TGA) to ensure the operating temperature limit of the fibres. The tensile properties of the fibres were determined through single fibre tensile tests and the IFSS of the fibres with epoxy resin was obtained using the microbond test. The critical fibre length and aspect ratio of the fibres were calculated. These results are useful in informing the choices for fibre type and lengths that would be suitable for sustainable, high performance, discontinuous fibre composites.

3.2 Materials

Four promising natural fibres from different continents and climates—jute, kenaf, curaua, and flax, were used in this work. The jute fibres, provided from Shams UK Ltd., were Bangla Tossa fibres collected in Bangladeshi jute cultivation areas. The fibres were processed by the company by batching, carding, and drawing the filaments. The kenaf fibres, processed by a decorticator, were collected at Malang, East Java, Indonesia. The curaua fibres were collected at Santarem, Para, Brazil by conventional methods (hand crafted). The flax fibres, sourced from Eco-Technilin (Flaxtape™, Normandy, North of France) were produced using a proprietary process. All the fibres were off-the-shelf products and used as received; no sizing was present or applied to the fibres. Prior to testing, all fibres were dried in a vacuum oven at 70 °C, overnight, and samples were then stored in a desiccator to prevent further moisture uptake. In this work, the usage of the term *fibre* represents a bundle of ultimate fibres; i.e., fibrils, [249].

In this work, a commercially available epoxy resin, commonly used in industry to produce high performance composites, was selected. PRIME™20LV (*ex* Gurit) diamine-cured difunctional resin was used in combination with a PRIME™20 hardener with a weight ratio of 100:26. With a curing cycle of 7 h at 65 °C recommended by the manufacturer [250], this resin allows sufficient working time at room temperature to prepare the microbond test specimens.

3.3 Experimental Work

3.3.1 Physical Characterisation

3.3.1.1 Visual Characterisation

Cold mounting was used to prepare the specimens for fibre cross-section examination under an optical microscope (Zeiss Axio Imager M2). The matrix used for cold mounting was PRIME™20LV resin. Standard wet grinding and polishing for polymer matrix composites were used for each specimen. Figure 3.1 shows the optical microscopy images of the cross-sections of the natural fibres. As seen in Figure 3.1, the cross-section of the kenaf fibres was found to be circular. For jute, the cross-sections were found to be more rectangular, and for flax more elliptical. Curaua fibres were found to have a circular cross-section with ragged edges. As also seen in Figure 3.1, kenaf fibres have considerably larger diameters than the other fibres, whereas the rest are of the same order of magnitude in terms of size. The diameter of each individual fibre bundle was determined using an optical microscope, taking an average at three points along the fibre; the measurements were performed on fifty specimens for each fibre type. For the post-processing of data in mechanical characterisation, fibres were assumed to be circular in their cross-sections. The diameters of the fibre bundles used in mechanical tests were measured to be 64.05 ± 5.93, 208.34 ± 12.08, 86.86 ± 2.39, and 63.76 ± 5.06 μm for jute, kenaf, curaua, and flax fibres, respectively.

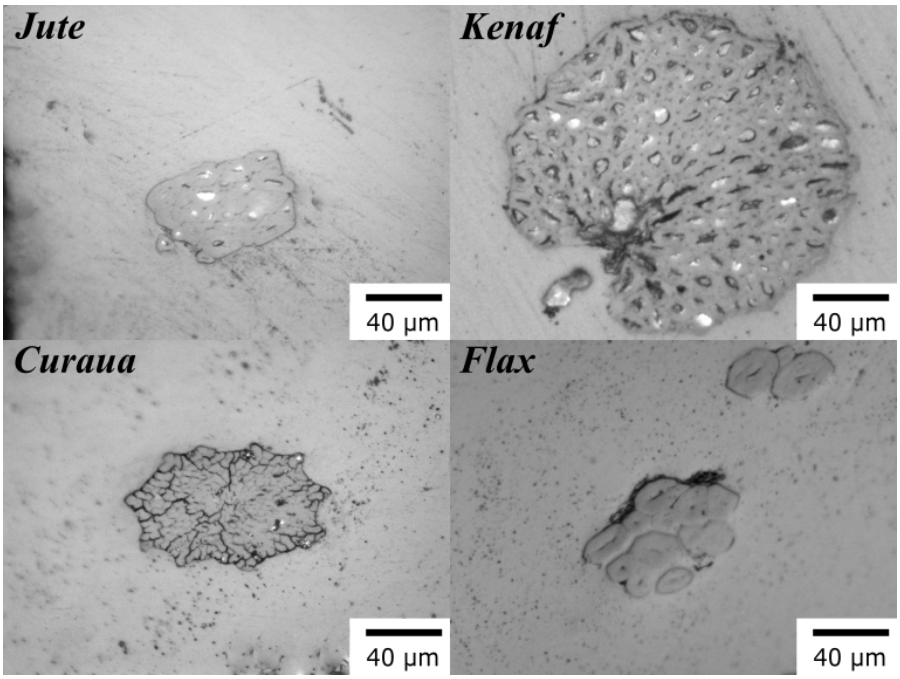

Figure 3.1: Cross-sectional optical microscopy images of jute, kenaf, curaua, and flax fibres.

3.3.1.2 Density Characterisation

The apparent density, bulk density, apparent porosity, and water absorption of the natural fibres were obtained by following Archimedes principle (the buoyancy method) and recommendations of ASTM C830-00 using a precision balance (sensitivity 0.1 mg) [251]. Initially, each fibre was dried in a vacuum oven overnight and the dried fibre mass, D, was weighed immediately after removing from the oven. Each fibre was then immersed in water in a vacuum chamber, overnight, and the saturated weight of fibre, W, weighed in air afterwards. As a last step, the suspended weight of fibre, S, was measured while immersing the fibre in water.

Apparent (AD) and bulk density (BD) were calculated by using Equations (3.1) and (3.2), respectively:

$$AD\,(g\,cm^{-3}) = \frac{D}{D-S} \times \rho_{\text{medium}} \tag{3.1}$$

where ρ_{medium} denotes density of displacement medium.

$$BD\,(g\,cm^{-3}) = \frac{D}{W-S} \tag{3.2}$$

Apparent porosity (AP) that describes open pores (which are pores within a material that is interconnected with the surrounding void space or external environment and are accessible and allow fluids, gases, or other substances to freely pass through or interact with the material) in terms of volume were calculated by Equation (3.3) as follows:

$$AP\,(\%) = \frac{W-D}{W-S} \times 100 \tag{3.3}$$

Water absorption (WA), which expresses the percentage of water absorbed by the dry fibre, was calculated by using Equation (3.4).

$$WA\,(\%) = \frac{W-D}{D} \times 100 \tag{3.4}$$

The buoyancy method is relatively cost-effective and easy to perform, but its accuracy depends on the choice of immersion fluid for natural fibres. On the other hand, the helium pycnometry method provides the most accurate and highly repeatable measurements due to its accessibility of pores. However, this method requires specialized equipment designed specifically for density testing, which can be more expensive compared to apparatuses used in other tests [252]. According to the literature, the buoyancy method using canola oil and soybean oil yields similar results to those obtained by pycnometry. Moreover, the use of a vacuum also aids in the immersion of the liquid and the removal of microbubbles, leading to better results with the buoyancy method [253]. When conducted carefully, the buoyancy method using water can provide similar results, otherwise uncertain results can be found. And it is important to mention that the standard deviation is much higher compared to other oil mediums and the pycnometry method [252].

Table 3.1 shows the physical properties of the natural fibres. It was found that kenaf has the highest density (1.57 g cm^{-3}) among them. The densities of jute, curaua, and flax were

calculated to be 1.51, 1.50, and 1.54 g cm^{-3}, respectively. The calculated density value for flax is in agreement with the literature values (1.54 [254] and 1.40–1.55 g cm^{-3} [255]), which were obtained from different methods, such as helium pycnometer (1.54 g cm^{-3} [256]), gas pycnometer (1.49–1.52 g cm^{-3} [253]), and immersion in water (1.54 g cm^{-3} [257]). The calculated densities for jute and curaua were found to be in close agreement with literature values (1.30–1.50 g cm^{-3} [254, 255] for jute; 1.52–1.56 g cm^{-3} [255] for curaua), whereas kenaf fibres (1.22–1.45 g cm^{-3} [255, 258]) were found to be slightly higher. The bulk densities of the fibres were calculated to be 0.68, 0.78, 0.68, and 0.74 g cm^{-3} for jute, kenaf, curaua, and flax, respectively, displaying a correlation between apparent and bulk density. Moreover, it was seen that all fibres have the same significant amount of porosity within the range 50%–55%. On the contrary, the calculated water absorption values differ significantly. Curaua (~82%) and jute (~81%) fibres tend to absorb more water content compared to kenaf (~65%) and flax (~70%) fibres. It was concluded that the penetration of water into the natural fibres is considerable.

Table 3.1: Physical properties of jute, kenaf, curaua, and flax fibres. Errors represent standard errors of means.

Fibre	**Apparent Density (g cm^{-3})**	**Apparent Porosity (%)**	**Water Absorption (%)**	**Bulk Density (g cm^{-3})**
Jute	1.51 ± 0.01	54.86 ± 2.20	81.08 ± 7.75	0.68 ± 0.04
Kenaf	1.57 ± 0.02	50.53 ± 1.20	65.21 ± 3.76	0.78 ± 0.03
Curaua	1.50 ± 0.01	54.58 ± 5.61	81.98 ± 17.57	0.68 ± 0.08
Flax	1.54 ± 0.01	51.72 ± 0.15	69.60 ± 0.19	0.74 ± 0.00

3.3.1.3 Surface Analysis

Furthermore, Brunauer–Emmett–Teller (BET) surface area analysis of the natural fibre samples was performed in a static volumetric adsorption system (Micromeritics 3-Flex) using ultra-high pure N_2 (Air Products. 99.9999%) up to 1 bar pressure. Before adsorption measurements, ~150 g of chopped loose fibres were heated up to 373 K under vacuum for 12 h to remove moisture and pre-adsorbed gases. The BET surface area was obtained within the relative pressure range of 0.05–0.25 at a temperature of 77 K.

Table 3.2 shows BET surface area measurements (S_{BET}) and calculated geometric surface area (S_{geo}), surface roughness (SR), and specific surface area (SSA) values of the fibres. Jute, which is processed by carding and drawing, showed the highest BET surface area, 2.28 m^2g^{-1}. It was found that kenaf and curaua have similar BET surface areas, 1.17 and 1.32 m^2g^{-1}, respectively. On the contrary, flax showed the lowest BET surface area, which is 0.37 m^2g^{-1}, similar to previously reported values (0.31–0.51 m^2g^{-1} [259]). Additionally, BET surface areas of jute and curaua have been reported as 2.01 and 0.87 m^2g^{-1} [67], which are consistent with the measured values.

Table 3.2: Surface area properties of jute, kenaf, curaua, and flax fibres. S_{BET}, S_{geo}, SR, and SSA denote BET surface area, geometric surface area, surface roughness, and specific surface area, respectively. Errors represent standard errors of means. ($S_{geo} = 4(\rho d)^{-1}$, $SR = S_{BET}/S_{geo}$, $SSA = \rho S_{BET}$.)

Fibre	$\mathbf{S_{BET}}$ **($m^2\ g^{-1}$)**	$\mathbf{S_{geo}}$ **($10^{-2}\ m^2\ g^{-1}$)**	**SR**	**SSA** **(μm^{-1})**
Jute	2.28 ± 1.07	4.14 ± 0.38	55.11 ± 26.35	3.44 ± 1.61
Kenaf	1.17 ± 0.12	1.22 ± 0.07	96.04 ± 11.36	1.84 ± 0.19
Curaua	1.32 ± 0.61	3.07 ± 0.09	43.02 ± 19.97	1.98 ± 0.92
Flax	0.37 ± 0.18	4.07 ± 0.32	9.05 ± 4.37	0.57 ± 0.27

To obtain better understanding about surface roughness, SR and SSA values (dependent and independent on diameter, respectively) were calculated. As seen in Table 3.2, it was found that flax fibres have a higher surface roughness (9.05 ± 4.37) than glass fibres (~1–1.7) [260]. However, jute, kenaf, and curaua fibres have nearly one order of magnitude higher surface roughness compared to flax fibres. The same trend was also observed in SSA values; flax fibres have the lowest SSA, while the other fibres have higher SSA values.

3.3.2 Thermal Analysis

The non-isothermal and isothermal decompositions were carried out in a simultaneous thermal analysis (STA) instrument (Netzsch STA 449 F1 Jupiter [Netzsch-Gerätebau GmbH, Wolverhampton, UK]) under flowing nitrogen. The dynamic TGA data for the fibres were obtained between 40 and 800 °C at a heating rate of 10 °C min^{-1} and a nitrogen flow rate of 50 mL min^{-1}. Two different temperatures, 175 °C and 225 °C, were maintained for 1 h to study the isothermal decomposition of the fibres under a nitrogen atmosphere with the same flow rate in the non-isothermal runs. Each sample weighed between 5 and 12 mg for each run of the decomposition tests and alumina crucibles were used as sample holders.

The dynamic TGA curves for natural fibres are shown in Figure 3.2. After initial weight loss caused by the vaporisation of absorbed moisture in the fibre, the first decomposition started at ~220–230 °C and the onset temperature for the maximum decomposition, which is attributed to cellulose degradation in the structure [261], was found to be within 320–335 °C. Following the maximum decomposition, there is a gradual weight decrease related to lignin degradation, which requires higher condensation temperature [262]. Moreover, ~80% weight loss was observed between the temperatures 150 and 700 °C for jute, kenaf, and curaua, whereas flax showed a lower mass loss (72%). Residual masses were ~11.5%–13.5% for jute, kenaf, and curaua and ~21% for flax at 800 °C.

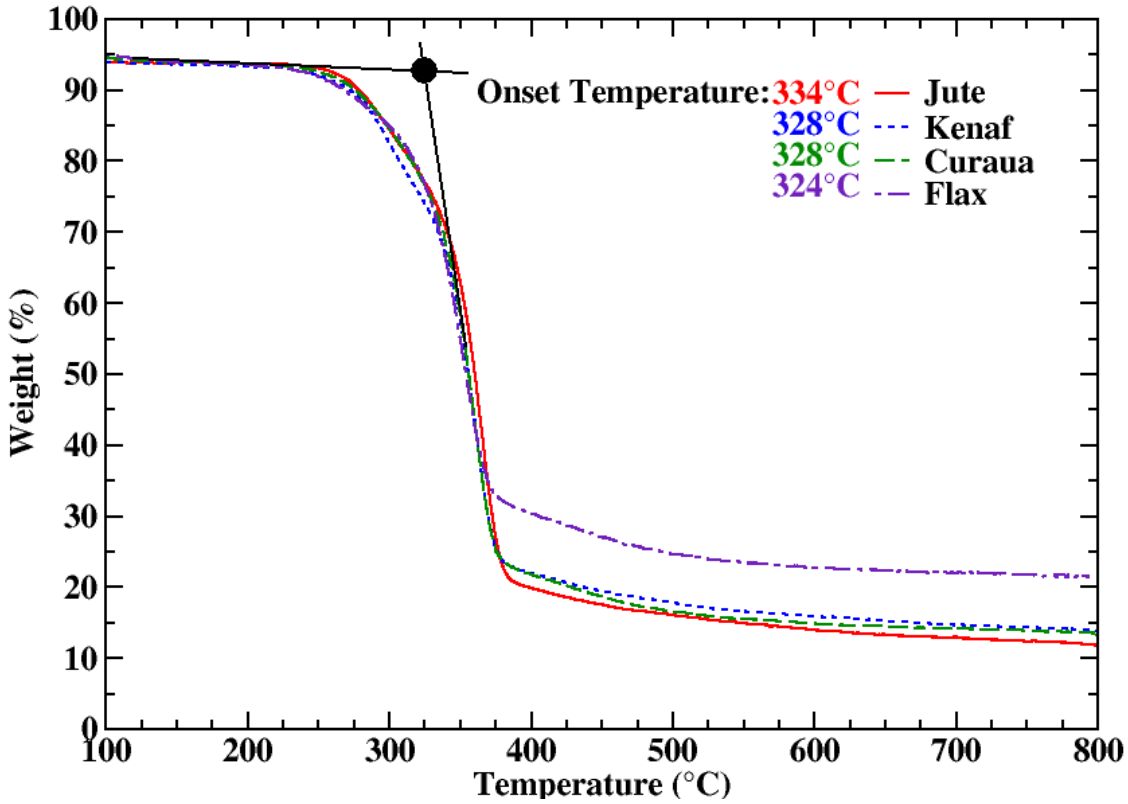

Figure 3.2: Dynamic TGA curves of jute, kenaf, curaua, and flax fibres as a function of temperature. Onset temperatures of the fibres are shown as insets.

The dynamic TGA curves showed that significant decomposition starts at ~220–230 °C for the fibres and as indicated for natural fibres [234]; they degrade after ~200 °C. Therefore, isothermal TGA tests were carried out at 175 °C and at 225 °C; the isothermal TGA curves of the fibres are shown in Figure 3.3. Temperature profiles during tests as a function of time are also shown in Fig. 3.4. As seen in Fig. 3.4, +10°C temperature differences happened during the tests compared to the target temperatures and the fibres were exposed to over temperature until the last 30 minutes of the tests. The first mass loss, amounting to ~7%, corresponding to water release from the fibres [261], occurring within 10 minutes during an isothermal analysis, was also observed in the dynamic TGA data (Figure 3.2). For 175 °C isothermal heating, no significant weight loss was observed for all fibres; gradual decrease in the weight of the fibres was seen during 225 °C isothermal heating. Thus, it was concluded that the fibres are thermally stable up to 175 °C. It is important to mention that this conclusion stands for the longer processing times, as seen in the figure, the mass loss is identical for the first 10 minutes, which means that the fibres can be processed up to 10 minutes for higher temperatures.

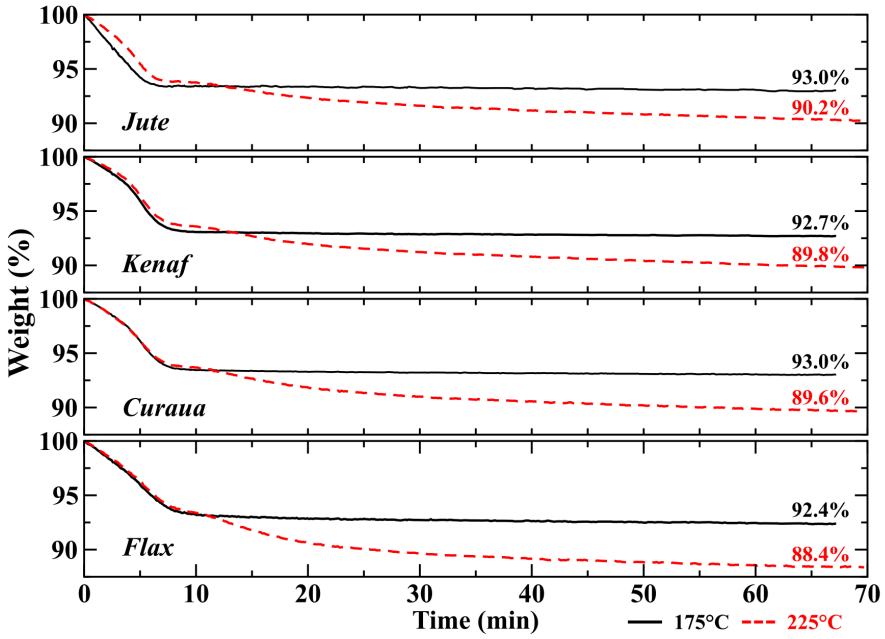

Figure 3.3: The isothermal TGA of jute, kenaf, curaua, and flax fibres during isothermal heating at 175 °C (black lines) and 225 °C (red dashed lines). Weights (%) after 1 h isothermal TGA run of the fibres are highlighted inside plots.

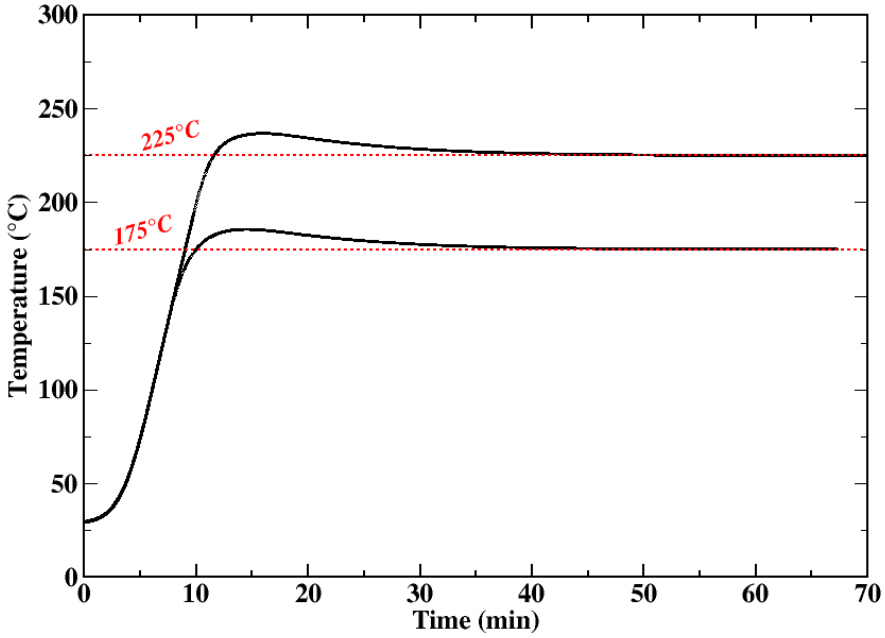

Figure 3.4: Temperature profile as a function of time during isothermal heating at 175°C and 225 °C.

3.3.3 Mechanical Characterisation

3.3.3.1 Single Fibre Tensile Test

The mechanical properties of the natural fibres were determined by using a single fibre tensile test method (SFTT) [263]. The fibres were attached to plastic tabs that were arranged in a silicone holder to maintain a gauge length of 40 mm. Due to the larger gauge length, it is expected to underestimate the fibre strength due to the population of defects in longer fibres compared to smaller fibres. Dynamax 3139 adhesive was used to attach the fibres to plastic tabs, which were subsequently cured under UV light for at least 2 h. Fibres underwent quasi-static tensile loading using a Dia-stron LEX820 Extensometer machine (Dia-Stron Limited, Andover, UK) using a 20 N load cell and with a strain rate of 0.02 mm/sec. For each fibre type, more than ten single fibres were successfully tested. Each of the tested single fibres' diameter was measured using optical microscopy by taking an average of 5 measurements from the fibre. These fibre diameters were used in the stress calculation, assuming a circular cross-section. The representative stress and strain curves for the natural fibre types are shown in Figure 3.5. As seen in the figure, plant fibres show non-linear stress-strain behaviour mainly due to the microfibril angle and it was seen in the stress-strain curves a low microfibril angle non-linearity is observed in the results (especially for Curaua and Flax fibres which may have up to 10-15° microfibril angle), which will induce non-linear behaviour also in the composite form [264].

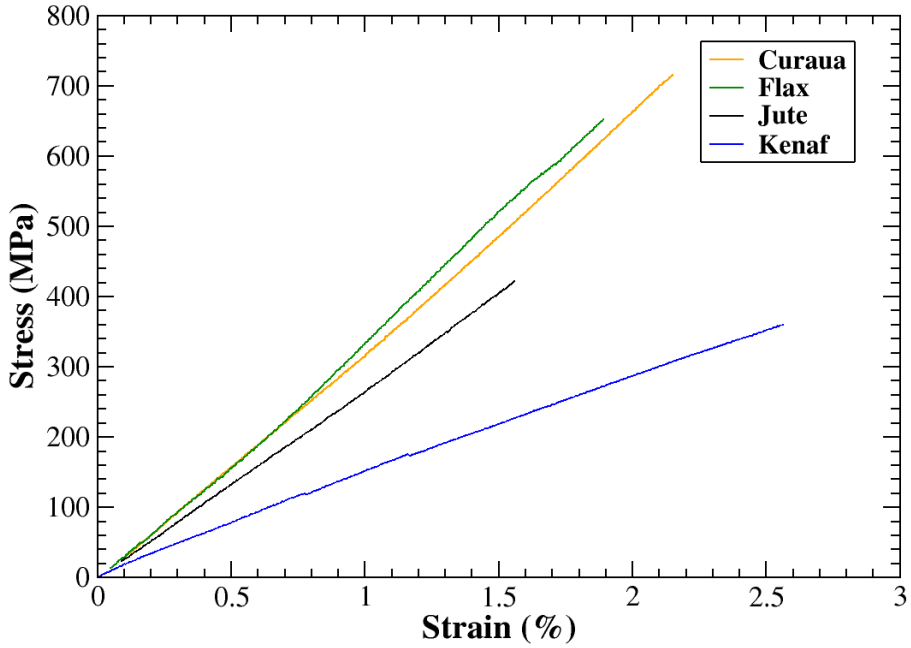

Figure 3.5: Representative stress strain curves for curaua, flax, jute, and kenaf fibres.

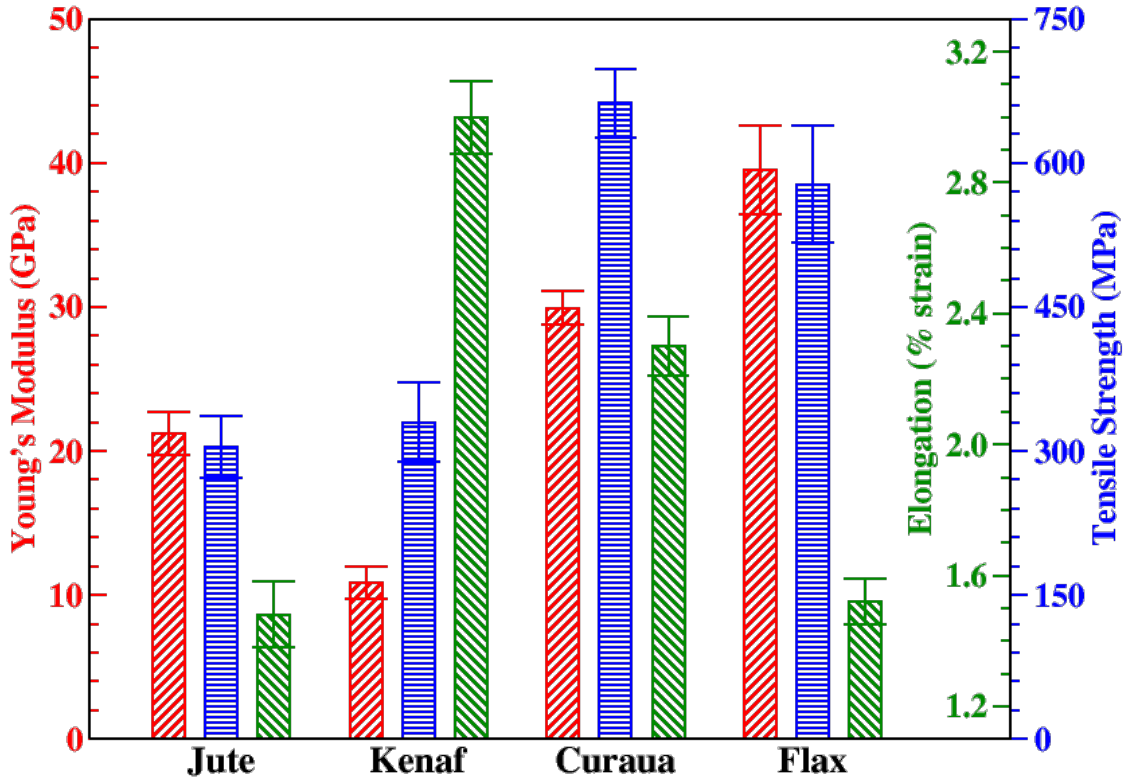

Figure 3.6: Young's modulus (red /), tensile strength (blue −), and elongation to break (green \) values of jute, kenaf, curaua, and flax fibres.

Young's moduli, tensile strength, and elongation at break of the fibres, which were assumed to have circular cross section, are shown in Figure 3.6. It is important to say that by using this assumption it is likely to underestimate or overestimate the mechanical properties of the fibres depending on their aspect ratio [265]. Moreover, Young's moduli of the fibres were determined between the strain range of 0.05-0.15% to eliminate the effect from the nonlinear stress–strain curves on linear fitting. It was found that flax has the highest Young's modulus (~40 GPa) and curaua is the second highest (~30 GPa) among the four fibres. Young's modulus values for kenaf and jute were found to be ~11 and 21 GPa, respectively. Moreover, curaua showed the highest tensile strength (~660 MPa) and flax showed the second highest value (~580 MPa). On the contrary, jute and kenaf showed similar lower tensile strength values, which are ~300 and 330 MPa, respectively. In terms of stiffness and strength, the mechanical performances of curaua and flax fibres are better than those of jute and kenaf fibres. As expected, the stiffest fibre, i.e., flax, showed low elongation at break of 1.52 ± 0.07%; however, the lowest elongation at break was observed in jute—1.48 ± 0.10%, and could be related to the high content of cellulose compared to lignin in jute's structure [266]. Kenaf fibres have significantly high lignin content [267] and their elongation at failure was found to be 3.00 ± 0.11%, which is the highest amongst the other fibres. Curaua fibre has a moderate lignin content but also moderate hemicellulose and high cellulose

contents in its structure [268], which might result high stiffness and moderate elongation at break (2.30 ± 0.09%). In addition, it should be noted that each fibre type has different fibre characteristics such as microfibril angle, crystallinity, and lumen size, which plays a significant role on their mechanical properties.

Moreover, Weibull analysis was applied to the strength values of the fibres. Weibull analysis is a probabilistic approach and has been widely used to determine the statistical behaviour of the strengths of single fibres [269]. The Weibull shape (m) and scale parameter (σ_0) represent scatter of the data and the Weibull strength, respectively. The Weibull parameters for the natural fibres were calculated and σ_0 values of the fibres were found to be 341, 373, 717, and 646 MPa for jute, kenaf, curaua, and flax, respectively. It was seen that the Weibull strength values of the fibres are slightly higher than the mean strength values. m for jute, kenaf, curaua, and flax were calculated to be 2.98, 2.81, 5.88, and 3.06, respectively. Higher m means the low dispersion of Weibull strength, or in other words, fracture stress. It was seen that curaua has the highest m value, ~6, and the other fibres show nearly same m value, ~3.

3.3.3.2 Microbond Test

The microbond test, commonly used to evaluate interfacial bond strength in composite materials, is subject to several assumptions and limitations [237, 245, 246]. Firstly, the test assumes a constant droplet shape throughout the experiment, although in practice, factors such as fibre surface roughness and wetting behaviour can influence the droplet shape. Secondly, the test results are operator and test-setup dependent, as variations in fibre alignment, droplet application, and loading conditions can introduce inconsistencies. Thirdly, the test assumes no stress concentration at the blade tip, although stress concentrations can occur and affect the failure mechanism and bond strength measurements. Moreover, it assumes a constant shear stress along the interface, which is not the case, and it also assumes the gap between the blades does not make a difference to interfacial shear strength, which actually does as shown in the literature [270]. Lastly, achieving shear debonding failure can be challenging, as weak bonding may result in droplet slippage, while strong bonding can lead to fibre breakage. Controlling the droplet size and achieving a suitable embedded length range become important challenges in promoting shear debonding. Considering these limitations, comparing microdroplet test data between different studies, particularly when using bundles instead of individual fibres, is difficult due to the influence of droplet shape, operator variability, stress concentration effects, and the complexity of achieving the desired failure mode.

To determine the IFSS of the natural fibres with an epoxy matrix, a microbond method [245] was used. The microbond methodology followed the same methodology as the fibre tensile test preparation, initially; the fibres were attached to plastic tabs that were arranged in a silicone holder to maintain a gauge length of 40 mm. Dynamax 3139 adhesive was used to attach fibres to plastic tabs, which were subsequently cured at ambient temperature (ca. 20 °C) under UV

light for at least 2 h. After this point, the epoxy resin droplets were applied to the fibres and cured in an oven following the manufacturer's recommended procedure. An optical microscope was used to measure the droplet position on the fibre, the droplet size, and droplet embedded area for each microbond test. A Dia-stron LEX820 Extensometer was used with the microbond module which comprises a thin metallic plate (microvice) with a narrow cut in the middle to accommodate the fibre but prevent the microdroplet from passing through. A schematic of the microbond test setup is illustrated in Figure 3.7. Appropriate microvice gap separation (gap sizes; 50, 80, 150, 180, 225, 275, and 330 μm) was used depending on the size of the droplet to achieve a pure shear stress distribution. To determine the failure type, each fibre was observed using an optical microscope after the test. Different types of failure mechanisms, successful shear failure (IFSS), fibrillation of fibres within the droplet (fibrillation), fibre failure in the vicinity of the droplet (FFD), fibre failure (FF), and broken matrix (MB), were observed during the microbond tests. Following figures (Fig. 3.8-3.12) show examples of the failure types (IFSS, Fibrillation, FFD, FF, and MB) observed in IFSS tests. It is important to check the droplet positions before and after the tests to ascertain failure type, especially for IFSS since it may be deceptive to check only test data.

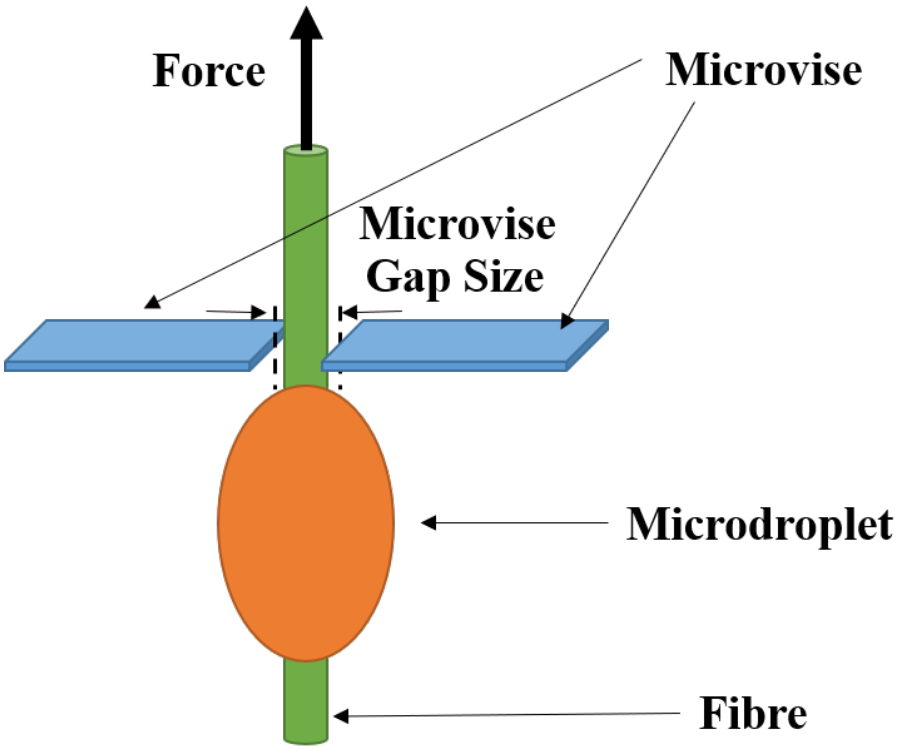

Figure 3.7: A schematic of the setup of the microbond test.

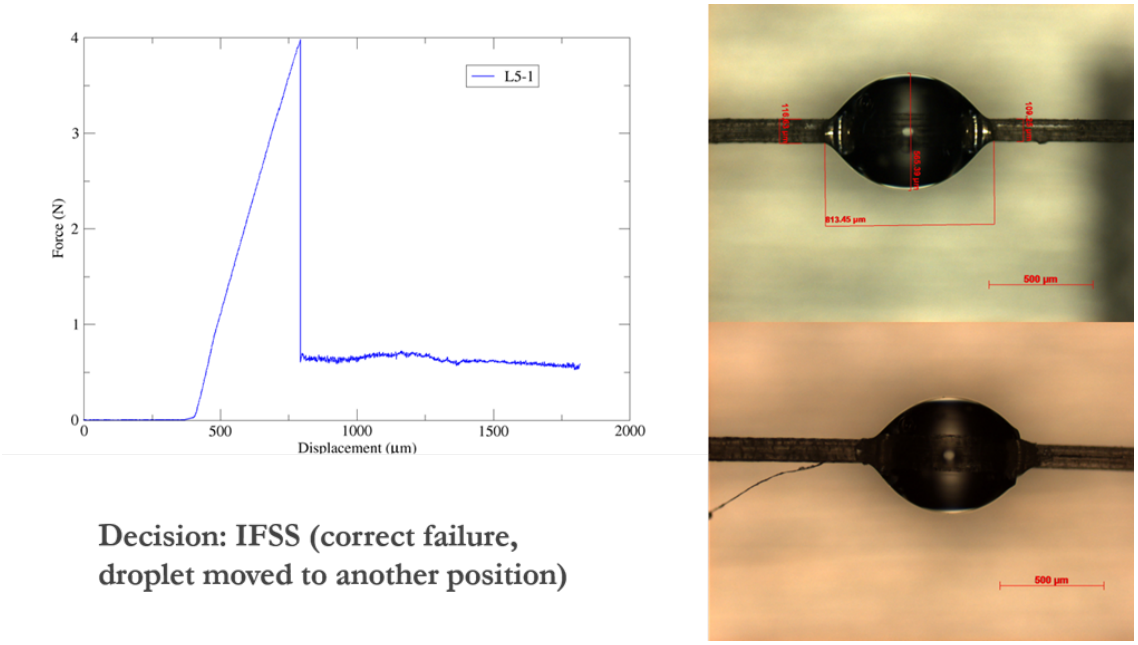

Figure 3.8: An example of IFSS failure.

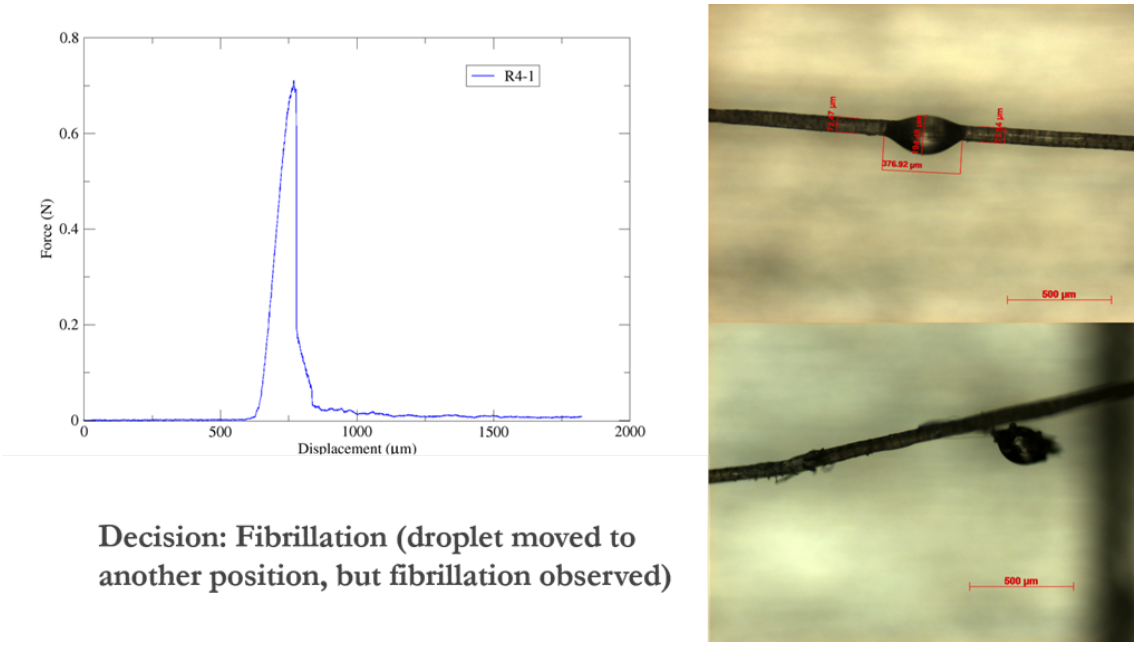

Figure 3.9: An example of fibrillation failure.

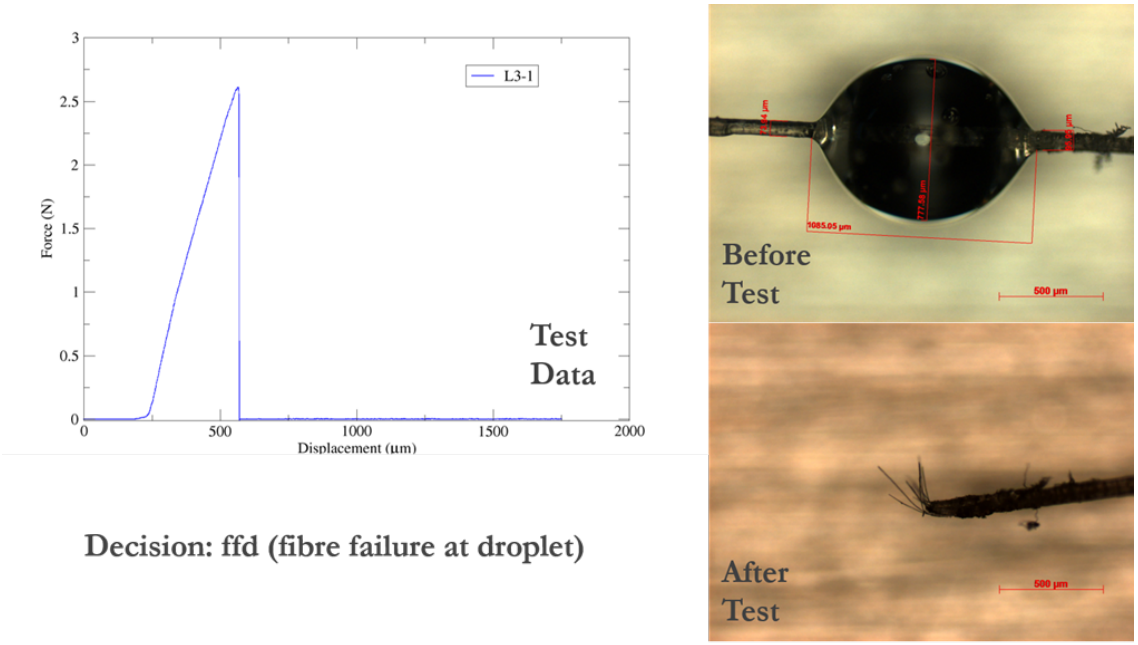

Figure 3.10: An example of FFD failure.

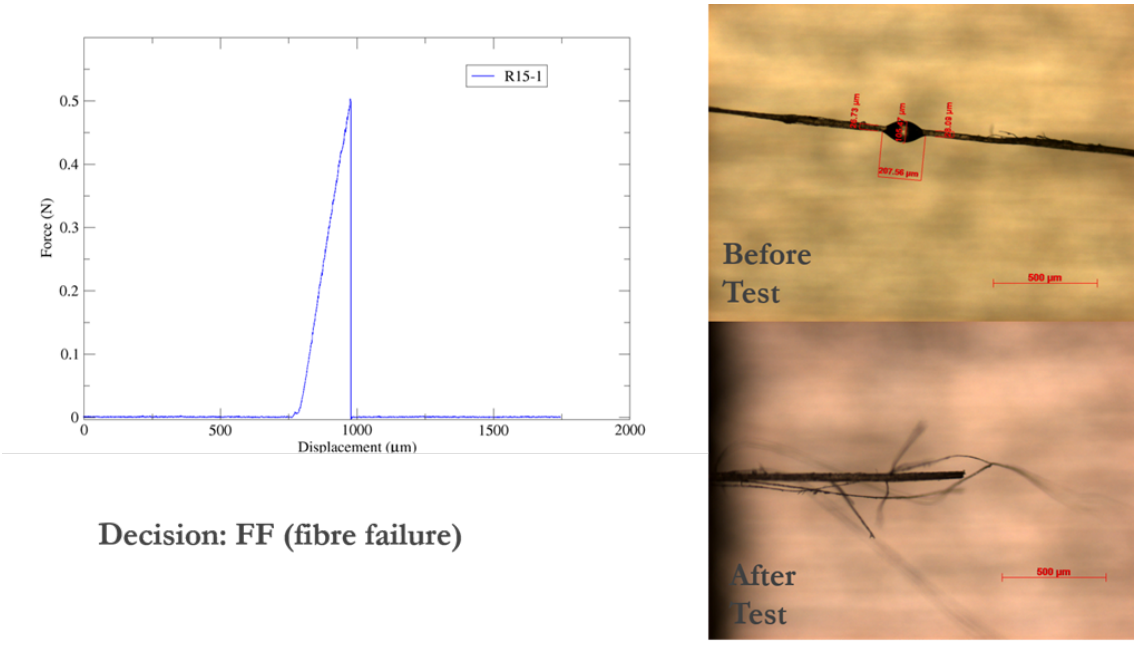

Figure 3.11: An example of FF failure.

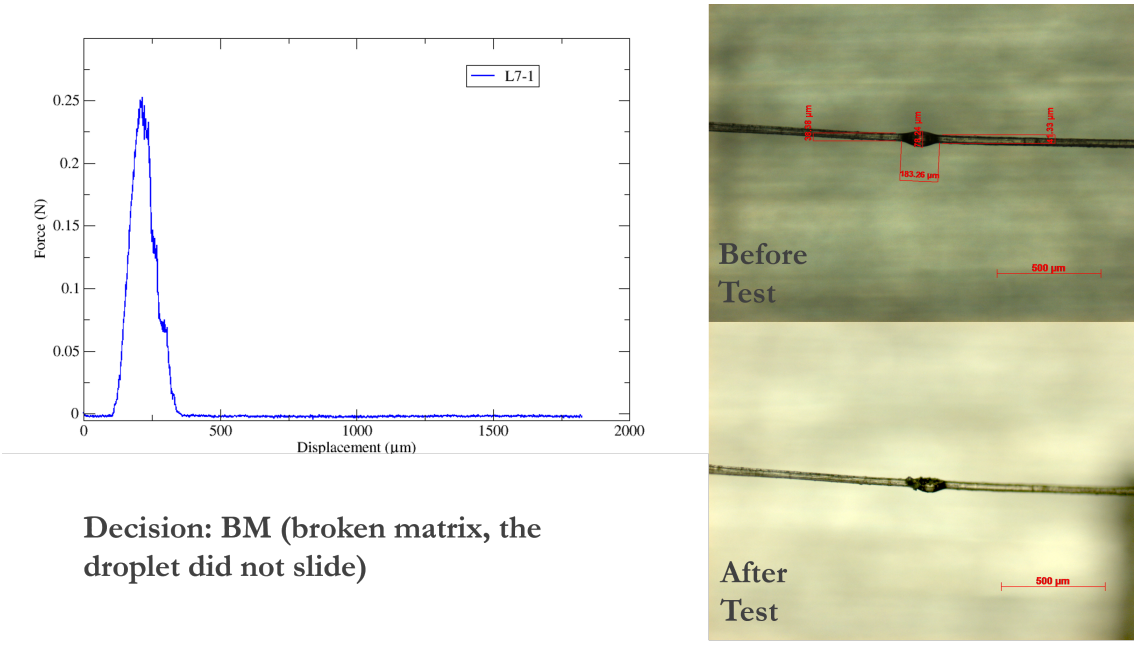

Figure 3.12: An example of MB failure.

Figure 3.13 shows the microbond test results for the fibres as a function of debonding force and fibre embedded area. As seen in the figure, fibrillation failure takes place at low forces compared to other failure types for all fibres due to local weak interactions of ultimate fibres in a fibre bundle. No clear trend was seen for other failure types for jute and kenaf fibres. On the contrary, for curaua and flax fibres it was seen that IFSS failure requires more force compared to other failure types, especially FFD and MB. The reason for this trend is related to the strengths of curaua and flax fibres, which are stronger than jute and kenaf fibres. It was also noted that mechanically stronger fibres are less likely to show fibre failure. For example, no fibre failure was observed for flax fibres and fewer fibre failures were observed for curaua fibres. Besides, it was seen that the shear distribution across the droplet, when it is contacted with the microvice, dictates the failure type. Visual inspection during the tests revealed that if the shear distribution is not equal at both sides of the droplet, generally, the failure tends to be FFD failure.

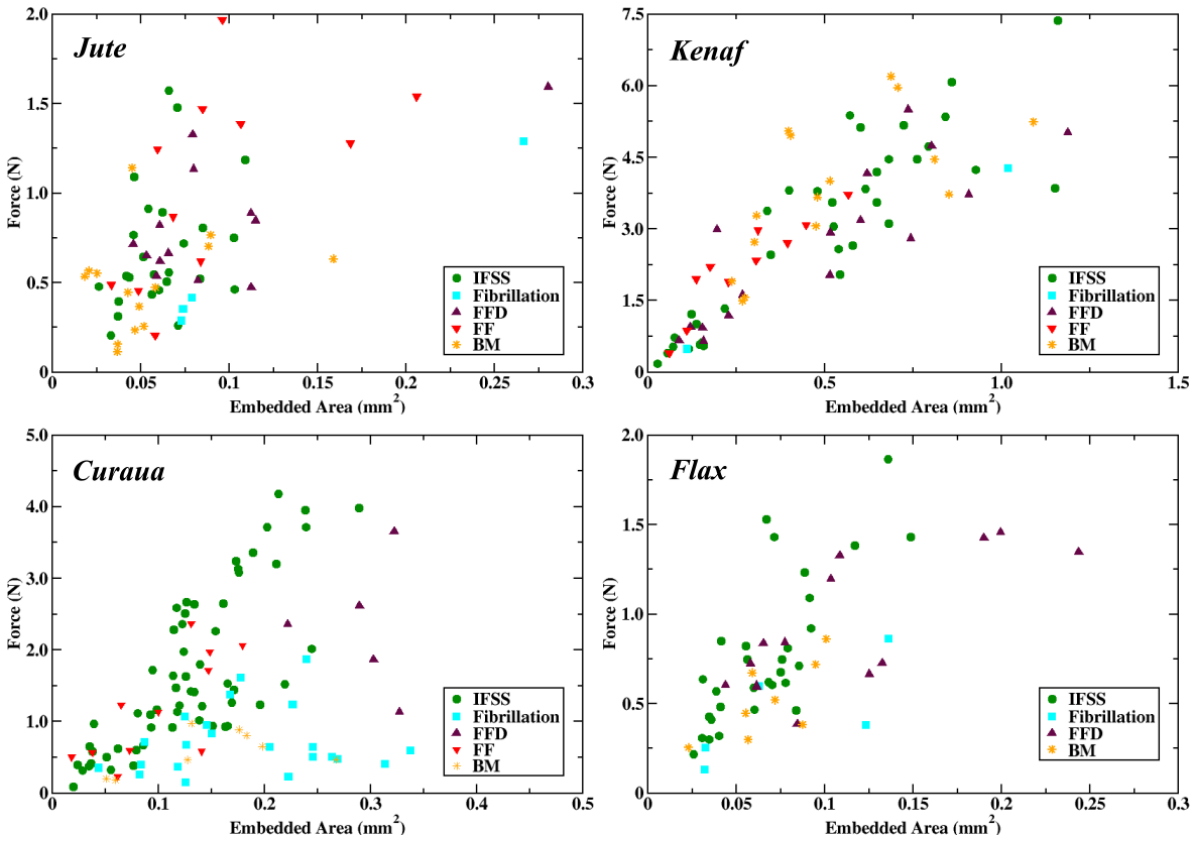

Figure 3.13: Microbond test results of jute, kenaf, curaua, and flax fibres in terms of debonding force versus embedded area. Green circle, turquoise rectangular, maroon up-triangle, red down-triangle and orange stars refer to failure methods, IFSS, fibrillation, fibre failure at droplet position (FFD), fibre failure (FF) and broken matrix (MB), respectively.

The IFSS between fibre and matrix is calculated using Equation (3.5):

$$IFSS_{(MPa)} = \frac{F_{d(N)}}{A_{e(mm^2)}} = \frac{F_{d(N)}}{\pi l_e d_{(mm^2)}} \tag{3.5}$$

where F_d and A_e (l_e and d) denote debonding force and embedded area (embedded length and fibre diameter), respectively. Applying a boundary condition $Force(l_e = 0) = 0N$, a linear fit was applied to get an IFSS value for the fibres by considering only the successful shear failure samples, as shown in Figure 3.14. IFSS values obtained from linear fits are 10.37, 5.94, 13.17, and 11.38 MPa for jute, kenaf, curaua, and flax fibres, respectively. The mean and standard error of IFSS values were calculated to be 11.64 ± 1.13, 6.41 ± 0.32, 12.93 ± 0.67, and 11.83 ± 0.79 MPa for jute, kenaf, curaua, and flax fibres, respectively (Figure 3.15). As seen in Figure 3.14, IFSS values obtained from linear fits are within the range of upper and lower bounds of 95% confidence, and in fairly good agreement with the mean IFSS values.

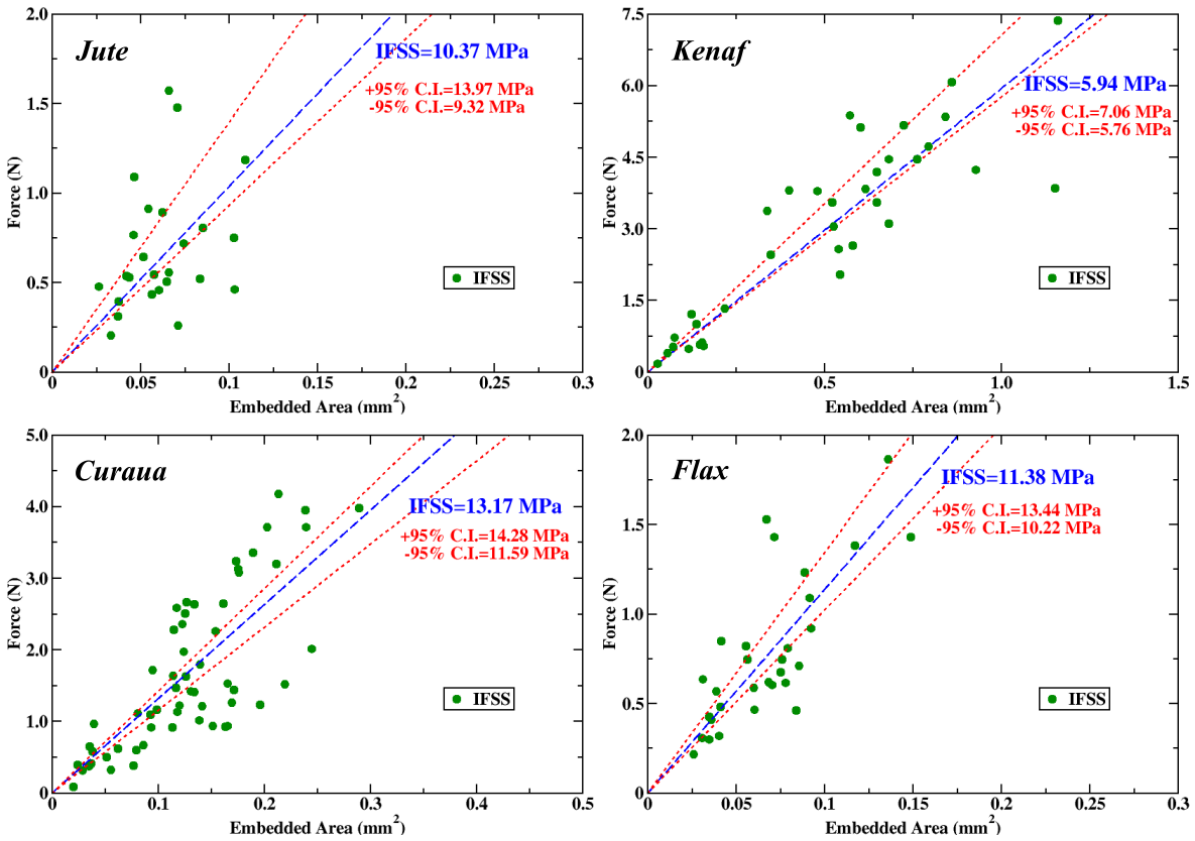

Figure 3.14: Microbond test results of jute, kenaf, curaua, and flax fibres in terms of debonding force versus embedded area with data only from samples that displayed a successful interfacial failure, IFSS. Linear fit (blue dashed lines) was applied to the data, and results are shown in the figure with the upper and lower 95% confidence intervals (red dotted lines).

To get effective reinforcement from ADFRC, the fibres must be longer than the critical fibre length, because this allows maximum load transfer amongst fibres/matrix and the failure of the composite material to be initiated by the fibres rather than fibre-matrix debonding. The critical fibre aspect ratio is calculated from following Equation (3.6) below.

$$\frac{l_c}{d} = \frac{\sigma_f}{2 \times IFSS} \tag{3.6}$$

where l_c, d, and σ_f denote the critical fibre length, diameter (at the droplet), and tensile strength of a fibre, respectively. Figure 3.15 shows the mean IFSS, l_c, and l_c/d ratio values of the fibres. Besides the mechanical properties such as σ_f and IFSS, l_c depends on the fibre diameter, d, as seen in Equation (3.6). In this work, l_c values of the fibres were found to be 0.84 ± 0.14, 5.37 ± 0.79, 2.22 ± 0.18, and 1.56 ± 0.23 mm for jute, kenaf, curaua, and flax, respectively. Since the diameters of the different fibres vary, it is worth reporting the ratio of l_c to d, owing to the fact that it allows us to predict l_c from the diameter. As seen in Figure 3.15, l_c/d is similar (~25) for kenaf, curaua, and flax; conversely, it is half of the value of those for jute, which shows the lowest l_c.

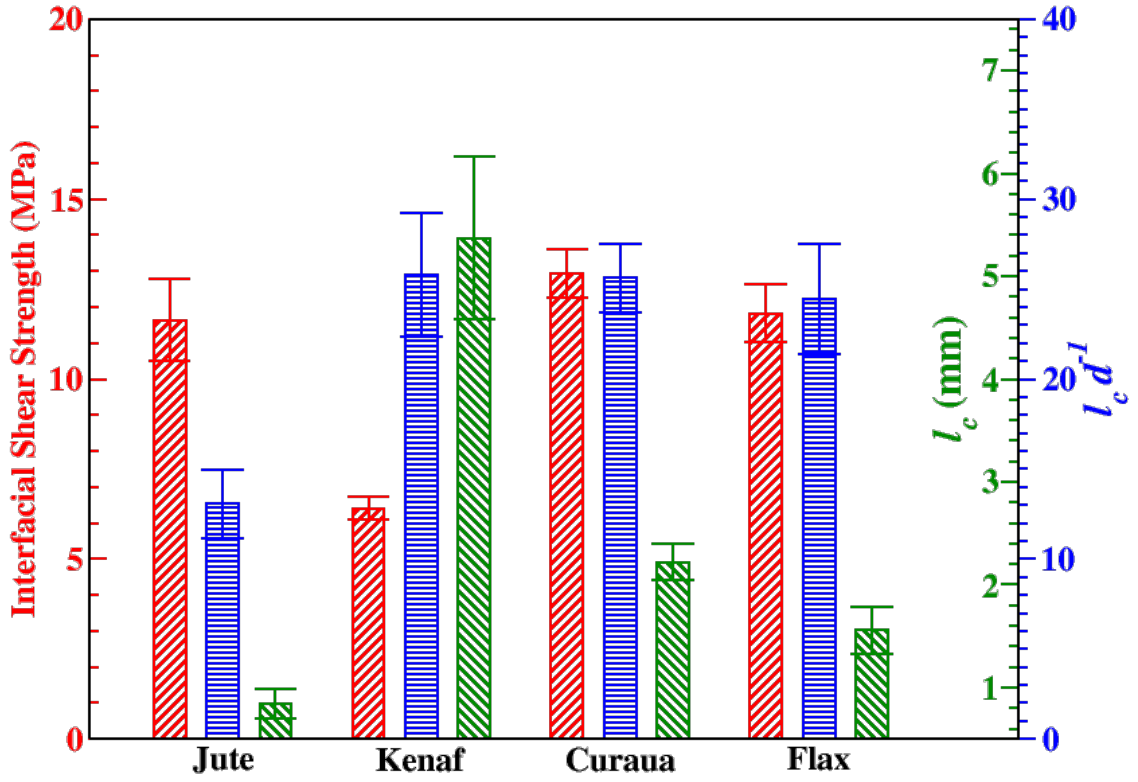

Figure 3.15: Interfacial shear strengths, IFSS (red /) and the critical fibre lengths, l_c (green \), of jute, kenaf, curaua, and flax fibres; and l_c/d (blue −) ratio values.

3.4 Discussion

For composite manufacturing, the range over which the material is thermally stable defines the process parameters and the choice of matrix system. Having confirmed the necessity to pre-dry the fibres prior to processing, it was concluded that the natural fibres are stable up to ~175 °C. This is a safe processing temperature for natural fibres since no significant decomposition was observed. It is also worth mentioning the fact that the drying processes are required to be able to process natural fibres with water-sensitive polymers and methods.

The IFSSs of jute, curaua, and flax fibres, were found to be approximately 11–14 MPa. Seghini et al., who used a similar epoxy (Prime 27 resin–Prime 20 hardener), calculated the IFSS with flax fibre through the single yarn fragmentation test, obtaining values between 16 and 24 MPa [242]. Furthermore, the IFSSs for flax with different epoxy systems have been reported as 33 MPa (24 MPa with Maleic anhydride sizing) [243] by using single fibre fragmentation tests, 23 MPa [271], and 13–17 MPa [238] by pull-out tests. It was noted that the obtained IFSS for flax fibre with our epoxy system is consistent with the lower bound of IFSS obtained by other research. On the other hand, there has been a large range of results for jute/epoxy from 4 MPa [272] obtained by using a single fibre microbond test to 34–52 MPa [273] obtained by using

single fibre pull-out tests. It is worth mentioning that the round-robin study has also shown that pull-out tests give a higher IFSS value than the microbond tests [274]. To the best of the authors' knowledge, there are no IFSS data for kenaf and curaua fibres with epoxy matrices available.

While the use of different epoxy systems prevents a direct comparison between the natural fibres and synthetic fibres, the natural fibres may show comparable IFSS values to those of glass fibres; however, the IFSS of glass fibres can be enhanced significantly by sizing. For instance, by using microbond tests, Baley et al. [247] showed that untreated flax/epoxy has an IFSS of 22.7 MPa, whereas glass with a textiloplastic sizing had a value of 29.3 MPa. Moreover, glass fibres that have different sizings, as coupling agents have exhibited IFSS values in the range 38–53 MPa with an epoxy matrix by using the microbond test [275]. Besides, it was found that carbon/epoxy has an IFSS value of 55–58 MPa with the microbond methodology [276], higher than the obtained IFSS values in this work and most of the reported values for natural fibres. There is no consensus for the effect of sizing on natural fibres to enhance or reduce IFSS due to the studies showing either enhancement or diminution [239, 240, 244]. However, it is also worth noting that natural fibres have a rougher surface, which enhances good mechanical interlocking with the matrix.

The interface between the fibre and the polymer matrix in fibre-reinforced polymer composites plays a crucial role in determining the overall performance and mechanical properties of the material. When the critical length of the fibre is small and discontinuous fibre reinforced polymers are used, the interface has a significant influence on the stress transfer mechanism between the fibre and the matrix. A strong interface facilitates efficient stress transfer between the fibre and the matrix, enabling the applied load to be carried by the fibres. In addition to load transfer, a strong interface indicates also important for achieving good bonding and interfacial adhesion between the fibre and the matrix. Strong interfacial adhesion happens when there is sufficient bonding between the two components, which prevents debonding, delamination, and fibre pull-out during loading. These failure mechanisms can significantly reduce the mechanical properties of the composite. The length efficiency factor is a way to understand the contribution of the fibre in reinforcing the composites, determined by the ratio of the critical fibre length to the actual length of the fibre. Of note is the relationship between the critical fibre length and the ratio between the fibre tensile strength and the IFSS between fibre and matrix. Assuming that a natural fibre has the same diameter as glass fibre and that both a NFRP and a glass fibre reinforced polymer (GFRP) are made with the same fibre length, the critical fibre length and the length efficiency factor must be the same in both composites for the ratio of fibre tensile strength to IFSS to be the same. This means that NFRP, which has a lower tensile strength than glass fibre, requires a proportionally lower IFSS compared to GFRPs. Therefore, the general perception that NFRP has poor IFSS compared to GFRPs is superficial since they do not require better IFSS [81].

SR and SSA values revealed that jute, curaua, and flax fibres have different surface roughness characteristics that can be associated with IFSS values. As seen in Table 3.2, flax fibres have

high IFSS values without significantly high SR and SSA values, whereas jute and curaua fibres have higher SR and SSA values which result in high IFSS values. SSA values of jute and curaua also show that jute fibres have more mechanical interlocking with the matrix per unit length compared to curaua. Since IFSS is a function of surface roughness, it can be concluded that flax has the highest performance with an epoxy matrix in terms of IFSS; however, jute and curaua fibres display good mechanical interlocking, which could be an important factor with other resin systems.

Since some of the most important advantages of natural fibres are their specific mechanical properties, specific stiffnesses and strengths of the fibres were calculated by using measured density values. In addition to that, specific mechanical properties of the fibres are compared with conventional glass, carbon fibres, and other work in the literature, as shown in Table 3.3. The mechanical properties of natural fibres vary over a wide range; nevertheless, most of the obtained specific mechanical properties of the fibres are consistent with the literature. As seen in Table 3.3, the properties of flax fibres obtained in this work and the literature values of curaua and flax fibres are comparable with glass fibres.

Table 3.3: Specific mechanical properties of jute, kenaf, curaua, and flax fibres compared with literature values of natural and synthetic fibres. Errors represent SEMs.

This work	**Specific Young's Modulus (GPa cm^3 g^{-1})**	**Specific Strength (MPa cm^3 g^{-1})**	**Failure Strain (%)**
Jute	14.04 ± 1.00	201.36 ± 21.52	1.48 ± 0.10
Kenaf	6.93 ± 0.71	210.52 ± 26.45	3.00 ± 0.11
Curaua	19.96 ± 0.77	441.53 ± 24.07	2.30 ± 0.09
Flax	25.64 ± 2.01	375.36 ± 39.72	1.52 ± 0.07
Glass [72]	28–30	940–1350	2.5–3.4
Jute [72]	7–39	270–650	1.2–2.0
Kenaf [72]	12–42	538	3.0
Curaua [72]	8.4–36	360–1000	3.0–4.3
Flax [72]	26–76	240–1070	1.2–3.3
Carbon [277]	128–130	1900–2700	1.5–2.1

In addition to that, there can be several advantages of using natural fibre reinforced composites. For example, some composite structural applications require high buckling performance, which is mainly related to the thickness of structures, and natural fibres have the advantage of being low density materials. Instead of using over-dimensioned conventional composite structures, natural fibre reinforced composite structures can provide high buckling performance without weight penalty. Additionally, it has been concluded that natural fibre reinforcements are preferable to glass reinforcements due to both the specific mechanical properties [278] and the environmental friendliness, as evidenced by LCA [187]. Furthermore, it is worth mentioning that the research performed by five different laboratories about the stiffness values of natural

fibres has reported that Young's modulus at low strain is 30% higher than the values obtained by SFTT [279]. Therefore, it can be concluded that natural fibres show higher Young's moduli, and methods (such as SFTT) underestimate this property.

3.4.1 Natural Fibres as Alternatives to Glass Fibres in ADFRCs

By using the obtained data, it is possible to evaluate, in a hypothetical scenario, the effect of substituting glass with natural fibre in discontinuous fibre composites. A modified rule of mixtures, Equation (3.7), is used to compare the specific Young's moduli of natural and glass fibre based ADFRCs:

$$\frac{E_c}{\rho_c} = \eta_0 \eta_1 V_f \frac{E_f}{\rho_f} + V_m \frac{E_m}{\rho_m} \tag{3.7}$$

where E_c is the highly aligned discontinuous fibre composite Young's modulus in the fibre direction, ρ_c is the density of the composite material, η_0 is a modulus reduction factor dependent on fibre orientation, η_1 is the fibre length efficiency factor, E_f and E_m are Young's moduli of the fibre and matrix, and ρ_f and ρ_m are the densities of the fibre and matrix, respectively. For ADFRCs with high levels of fibre alignment, η_0 can be assumed to be ~0.9, as shown by Yu et al. in [18]. η_1 can be calculated from the shear lag theory [280] with Equation (3.8),

$$\eta_1 = 1 - \frac{tanh(al/d)}{al/d} \qquad where \quad a = \sqrt{\frac{-3E_m}{2E_f \ln V_f}} \tag{3.8}$$

where l is the fibre length.

Owing to the superior mechanical properties compared to the natural fibres tested, flax and curaua fibres were selected for the case studies based on the hypothetical scenario of substituting glass with natural fibre in ADFRCs. Table 3.4 introduces the properties of fibres and matrices used in Equations (3.7) and (3.8) to obtain the mechanical properties of resultant ADFRCs. The properties of flax and curaua fibres are the ones obtained in this work corrected for SFTT underestimation [279].

Table 3.4: Material properties used in the case studies.

Parameters	**Natural Fibres**		**Glass Fibre**	**Matrix**
	Flax	**Curaua**	**C100, Vetrotex** [19]	**PRIME™20LV** [250]
E (GPa)	52	39	73	3.50
ρ (g cm^{-3})	1.54	1.50	2.60	1.15
d (mm)	64	87	7	-

Figure 3.16 shows the contour plot of the increase in specific Young's modulus (IiSYM), which is a percentage change when flax fibre substitutes glass fibre in ADFRCs as a function of fibre length, l, and fibre volume fraction, v_f. In Figure 3.16, IiSYM increases from the dark blue to dark red regions and white lines evince the transition lines, which reveal the influence of l clearly.

As seen in Figure 3.16, there is more than 15% and up to 20% IiSYM in ADFRCs when glass fibres are substituted for flax fibres for every l and v_f higher than 0.3. The effect of v_f on IiSYM is constant and it leads to increase in IiSYM. On the contrary, l has two different effects on the IiSYM. From micron level to 1–10 mm, l leads to a dramatic decrease for IiSYM. After that, there is a gradual rise for IiSYM and for higher v_f; these trends get more clear. As an example, the black star in Figure 3.16 shows the condition of v_f = 0.7 and l = 3 mm, which is higher than the l_c of flax fibre, and it is the point at which 18% performance enhancement is seen. At that point, the effect of increasing l clearly shows two different trends, a significant decrease or a gradual increase.

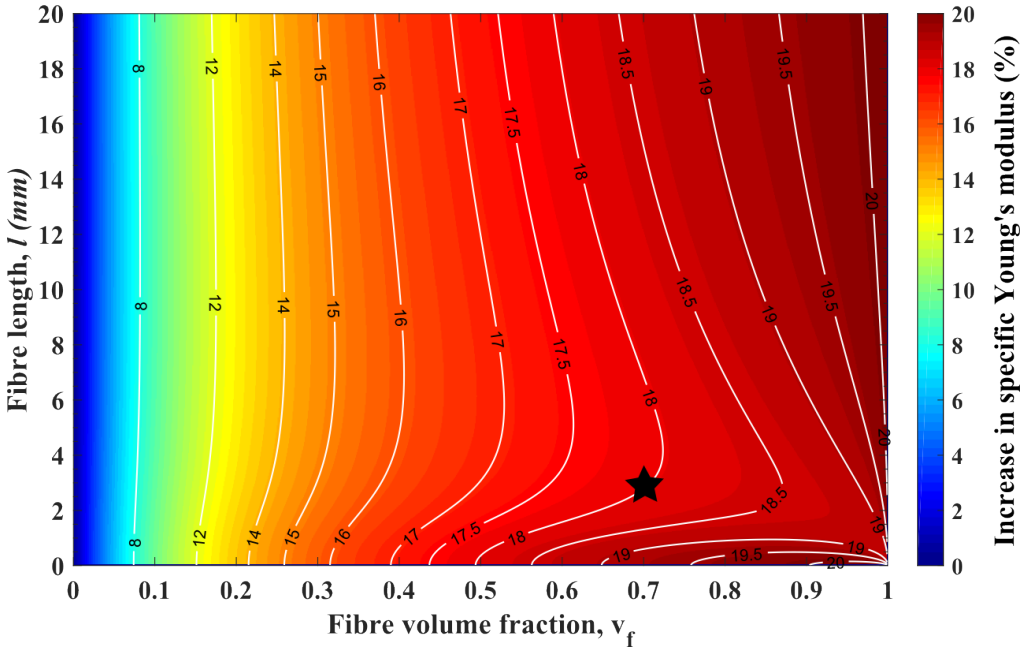

Figure 3.16: Contour plot of the increase in specific Young's modulus, when highly aligned discontinuous glass fibre composites switched to highly aligned discontinuous flax fibre composites, in terms of fibre volume fraction and fibre length. White isolines are scaled by the right hand colour axis.

Moreover, the same hypothetical scenario was repeated for another promising fibre, curaua. Figure 3.17 shows the contour plot of the IiSYM when curaua fibre substitutes glass fibre in ADFRCs as a function of fibre length, and fibre volume fraction. It was seen that there is a ~4.5%–6.5% decrease in specific Young's modulus when v_f is between 0.3 and 0.7 in the curaua fibre case. The same trend mentioned in the first case study about the IiSYM function of l was also seen clearly, especially at the bottom right corner of the plot; (i) first, IiSYM decreases when l increases from micron level to 1–2 mm; (ii) then IiSYM increases gradually. Even though curaua fibres in ADFRCs cause a decrease in mechanical properties when replacing glass fibres, advantages in environmental friendliness and sustainability remain and make the 5%–6% reduction in specific Young's modulus an acceptable trade-off.

As expected, the stiffer flax fibre shows positive and better performance than curaua fibre in the hypothetical scenario of substituting glass with natural fibre in ADFRCs. However, curaua fibre shows agreeable reduction and may become more favourable than glass fibre if the sustainability aspects are taken into account through LCA as well.

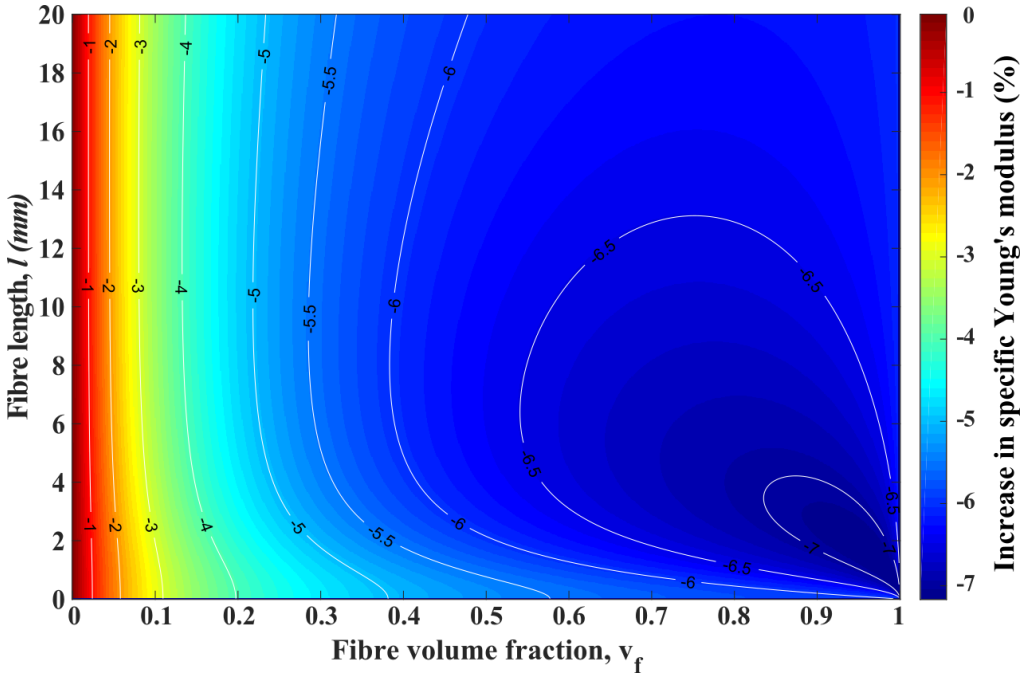

Figure 3.17: Contour plot of the increase in specific Young's modulus, when highly aligned discontinuous glass fibre composites are switched to highly aligned discontinuous curaua fibre composites, in terms of fibre volume fraction and fibre length. White isolines are scaled by the right hand colour axis.

3.5 Conclusions

- Thermogravimetric analysis based on the isothermal and non-isothermal TGA curves of the fibres revealed that the ideal processing temperature, where no significant degradation was observed, is ~175 °C for the fibres. It was seen that the pre-dried fibres have moisture uptake approximately 6.5–7 wt% from the environment, and during the heating period, the fibres lose all of the moisture uptake before the targeted temperature is reached.

- Jute has the lowest critical fibre length value and the lowest critical aspect ratio among those tested. However, jute shows moderate mechanical properties compared to curaua and flax. On the other hand, kenaf fibres showed the poorest interfacial performance and mechanical properties compared to other fibres.

- In terms of mechanical and interfacial properties, curaua and flax were found to be promising natural fibre reinforcements to obtain high performance. It is foreseen that it will

be possible to obtain more sustainable composites with specific mechanical properties comparable with those of glass fibre reinforced plastic.

- This chapter allows sustainable material selection as reinforcement for ADFRC, and the prime candidates were determined to be curaua and flax fibres. It was also demonstrated that flax fibres perform better mechanically compared to glass fibres in ADFRCs.

- The prime candidates, flax and curaua, and also jute, will be selected to reinforce common matrices to produce ADFRC in the following work. It is important mention that the properties of fibres obtained in this chapter are prior to being subject to an ADFRC production method, the HiPerDiF process, which may affect the properties of the fibres after processed. As mentioned in Chapter 1.1, the natural fibres processed through the HiPerDiF method needs additional waiting time during the drying stage to retain prior properties, which will be in consideration.

- The data obtained, especially the critical fibre lengths, in this chapter will assist manufacturing and understanding of mechanical and physical behaviour of ADFRCs produced with these fibres. The epoxy resin used in this study will be assumed to represent the epoxy resin family so that the critical fibre length can be decided based on the data obtained in this study. It should be noted that, ideally, each matrix/fibre system will be investigated by performing microbond tests to calculate IFSS and hence critical fibre length. However, due to the experimental difficulties regrading to the microbond tests, especially with the thermoplastic and high viscosity thermoset resins, the fibre lengths used in the HiPerDiF method were decided on the assumption above and for thermoplastic resins the critical fibre length should be higher since expected IFSS value is significantly smaller than the thermoset resins.

Chapter 4

Selection of a Discontinuous Natural Fibre Reinforcement for Sustainable Composites

In this chapter, a number of plant based natural fibres -curaua, flax, and jute fibres- are used to reinforce epoxy, poly(lactic acid) (PLA), and polypropylene (PP) matrices to form aligned discontinuous natural fibre reinforced composites (ADNFRC). These matrices were chosen because they are widely used polymers in composite applications and also due to the factors such as cost, availability, processability, environmental impact, mechanical performance, and potential compatibility with the fibres. The novel HiPerDiF method is used to produce high performance ADNFRC. The tensile mechanical, fracture, and physical (density, porosity, water absorption, and fibre volume fraction) properties of these composites are reported. In terms of stiffness, epoxy and PP ADNFRC exhibit similar properties, but epoxy ADNFRC shows increased strength compared to PP ADNFRC. It was found that PLA ADNFRC had the poorest mechanical performance of the composites tested, due principally to the limits of the polymer matrix. Moreover, curaua, flax (French origin), and jute fibres are found to be promising reinforcements owing to their mechanical performance in epoxy and PP ADNFRC. However, only flax fibre with desirable fibre length is considered to be a suitable reinforcement constituent for future sustainable ADNFRC studies in terms of mechanical performance and current availability on the market, particularly for the UK and EU. This chapter is decisive regarding the selection of the type and length of fibres for the subsequent production of sustainable discontinuous natural fibre composites.

This chapter has been adapted from the following published work:
Ali Kandemir[*]; Marco L. Longana; Tulio H. Panzera; Gilberto G. del Pino; Ian Hamerton; Stephen J. Eichhorn. Natural Fibres as a Sustainable Reinforcement Constituent in Aligned Discontinuous Polymer Composites Produced by the HiPerDiF Method. *Materials* 2021, 14, 1885. DOI:10.3390/ma14081885

[*]Corresponding author. Author contribution is given by using the Contributor Roles Taxonomy: conceptualization all authors; data curation A.K.; formal analysis A.K.; funding acquisition M.L.L., I.H. and S.J.E.; investigation A.K. and M.L.L.; methodology A.K. and M.L.L.; resources; T.H.P. and G.G.d.P.; supervision M.L.L., I.H. and S.J.E.; visualization A.K.; writing—original draft A.K.; writing—review and editing all authors.

4.1 Introduction

Fibre reinforced polymer matrix composites (FRP) are a vital class of lightweight engineering materials that display high specific stiffness and strength. Since they are lightweight, FRP are key materials for most engineering applications, e.g., aerospace, automotive, marine and wind energy [3–6]. However, the main constituents of FRP, the matrix and fibres, are difficult to recycle at end-of-life, and since they are predominantly petroleum-based non-renewable materials this prevents them being truly sustainable [32]. Therefore, the use of sustainably derived FRP is becoming an unavoidable option for petroleum-based components in structural engineering applications, due to growing public and industrial environmental awareness [31].

Most of the widely used synthetic reinforcements for FRP, such as carbon and glass fibres, are not renewable and the processes available to recycle them are not economically feasible [130, 281]. The production of these fibres, especially carbon fibre, relies on limited sources, whereas natural fibres (NF) are abundantly available around the world in various forms [36]. NF are an ideal reinforcement constituent as being not only renewable and relatively cheap, they are also recyclable materials; in addition, NF can be produced sustainably and can simplify waste management processes [282]. Their wear performances in FRP, which can trigger energy efficiency and cost effectiveness during the processing stages, are better than those of their synthetic counterparts [283]. Even though NF have some drawbacks, such as low thermal stability and hydrophilic character, they have the potential to exhibit high performance in FRP. They are key alternatives to synthetic fibres (e.g., aramid, carbon, and glass) that do not share the mentioned sustainable features of NF [34].

Most synthetic fibres can be produced in a well-aligned continuous format able to achieve high performance in FRP for engineering applications. NF are however limited by the characteristic dimensions of their source and can only be processed into relatively long, aligned, discontinuous fibres. However, to employ aligned continuous fibres in the manufacture of composites is labour intensive, and incurs high environmental impact and cost during production [284, 285]. On the other hand, composites produced in this manner may exhibit high mechanical performance, even comparable to continuous fibre composites, when a high degree of alignment is achieved with fibres of lengths greater than the critical fibre length [18]. The discontinuities in the reinforcement improve their formability, facilitating defect-free manufacturing of structural parts with complex shapes [7]. Consequently, the cost and environmental impact of production can be reduced significantly. As mentioned before, The HiPerDiF (high performance discontinuous fibre) method is a discontinuous FRP production technology, invented at the University of Bristol [16], that has been shown to manufacture FRP materials rapidly with high levels of alignment from discontinuous fibres [286]. The elastic modulus, strength, and failure strain of aligned discontinuous fibre reinforced composites (ADFRC) manufactured with the HiPerDiF method have been found to be similar to those of continuous FRP analogues [18].

Building upon a previous chapter that presents a selection of reinforcement materials for

aligned discontinuous natural fibre reinforced polymer composites (ADNFRC), four different types of natural fibres, curaua (Brazilian origin), flax (Polish origin), flax (French origin), and jute (Indian origin), were used in this research work as raw reinforcement materials for the HiPerDiF method to form highly aligned discontinuous fibre preforms. Epoxy, poly(lactic acid) (PLA), and polypropylene (PP) matrices were reinforced with aligned discontinuous natural fibre (ADN) preforms to obtain ADNFRC. ADNFRC were mechanically characterised by using standard tensile test methods. The mechanical and physical properties of the natural fibres were compared within the same and different polymer matrices to reveal their reinforcement performance in ADNFRC. The promising sustainable reinforcement agents for ADNFRC were determined owing to their mechanical performance and physical sufficiency with the production method; hence, the obtained broad results in this work improve the reinforcement selection of materials for high performance and sustainable discontinuous FRP for future studies and industrial applications.

4.2 Materials and Methodology

4.2.1 Fibres

Curaua fibres were collected in Brazil (Santarem, Para) using hand-crafted conventional methods. The jute fibres were Bangla Tossa fibres sourced by and they were collected in jute cultivation areas in Bangladesh processed by batching, carding, and drawing the filaments. The two flax fibres, sourced from Eco-Technilin-Flaxtape™ (Normandy, Northern France) and flax fibres Ekotex (Namysłów, Poland) were produced via the use of a proprietary process. Since there are two different types of flax fibre, the flax from Poland is referred to as 'flax-cu' because it is used for construction (cu), while the flax from France is referred to as 'flax-ft' owing to the product name Flaxtape™ (ft). All the fibres were used in the condition they were received. Table 4.1 demonstrates the properties of the natural fibres.

Table 4.1: Constituent properties.

Constutient	**Density ($g\ cm^{-3}$)**	**Elastic Modulus (GPa)**	**Tensile Strength (MPa)**	**Critical Length (mm)**	**Ref.**
Fibres					
curaua	1.50	39	660	2.22	Chp. 3.3
flax-ft	1.54	52	580	1.56	Chp. 3.3
flax-cu	1.40	-	-	-	[11]
jute	1.51	27	300	0.84	Chp 3.3
Matrices					
epoxy	1.20	-	-	-	[287]
PLA	1.24	-	45	-	[288]
PP	0.92	1.5	-	-	[10]

No data sheets were given by the providers and flax-cu fibres were too short to perform any mechanical or interfacial tests.

The investigated length of the discontinuous NF was determined according to previous chapters on interfacial properties of NF with epoxy resin 3. For curaua and flax-ft, two different cut lengths were used; (i) the first selected cut length was 2 mm, which is close to their critical fibre length (l_c), which were found to be 2.22 and 1.56 mm, respectively, (ii) the second cut length was 6 mm, which is significantly higher than the l_cs. As seen in Table 4.1, the l_c of jute is less than 1 mm. Practically the HiPerDiF method works with fibre lengths above 1 mm and below 12 mm. Because of that, the cut length was determined as 4 mm, which is significantly higher than the l_c of jute and this allows a comparison with 6 mm curaua and flax-ft cut lengths. Flax-cu fibres were sourced already cut from the company as 4 mm and used to compare with jute 4 mm fibre lengths.

4.2.2 ADN Preforms

The HiPerDiF method was used to produce 150 × 5 mm^2 ADN preforms that were laid-up to obtain the ADNFRC used in this work. *A schematic of the HiPerDiF discontinuous fibre alignment machine is shown in Figure 4.1a. Fibres, which can have a length between 1 and 12 mm, were suspended in water, accelerated through a nozzle, and directed in a gap between two parallel plates. The fibre alignment mechanism relies on a sudden momentum change of the fibre-water suspension upon impact with the plate. The fibres then fall on a conveyor stainless mesh belt where the water is removed by suction, stage (1) in Figure 4.1. The aligned fibre preform was dried with infrared radiation (stage 2) to allow the resin impregnation process* [11], which is the built-in option (stage 3). In this work, stage 3 was not used to impregnate resin to produce ADN prepregs due to the necessity of the hot press for better impregnation. An image of the HiPerDiF machine is shown in Figure 4.1b.

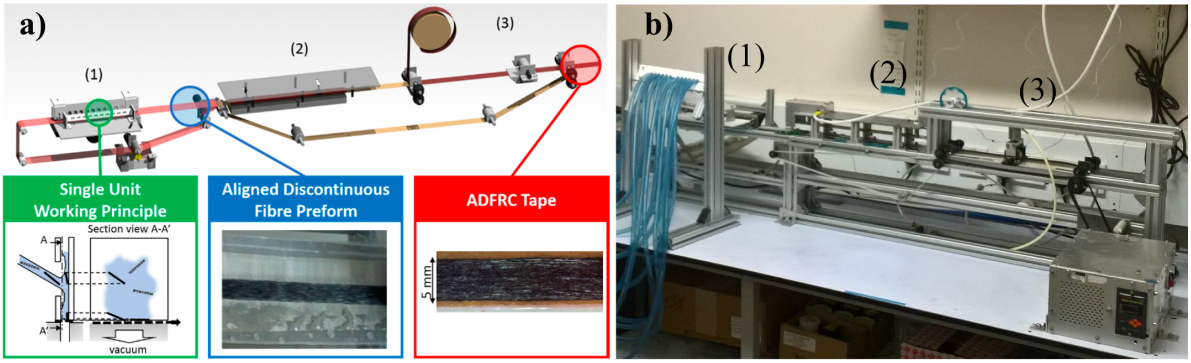

Figure 4.1: (a) The HiPerDiF fibre alignment method principles and dry carbon fibre preform output (stage 2) [11, 289], (b) an image of the second generation HiPerDiF machine (Bristol Composite Institute, Bristol, UK) highlighted with stages mentioned in Sec. 4.2.2.

Fibre volume concentration in the water suspensions was set 0.001 wt% and the suspension used to inject the water fibre mixture through twelve nozzles into an alignment head at a flow rate of 4-6 litres per minute. The meshed belt was operating at a speed of 1.5-2.5 mm

s^{-1}. Natural fibre preforms were partially dried after the infrared heater stage. As mentioned in previous chapters, the HiPerDiF method does not affect the natural fibre properties when longer drying stage is applied and because of that fibres were left for drying at least 48 hours in room temperature. However, it is important to mention that this is an assumption based on the previous study which showed (i) no significant change on mass of the fibres before and after the HiPerDiF process, and (ii) no statistically significant difference on mechanical properties of composite specimens made with dried fibres when compared. Due to rapid drying stage that causes shrinkage, there may be physical or chemical changes in natural fibres, and this can be investigated in micro level in future studies.

4.2.3 Matrices and Prepregging

Three widely available polymers were used as matrices for the ADNFRC; epoxy, PLA, and PP acquired in film form; their properties are shown in Table 4.1. For an epoxy matrix, Skyflex K51 (SKChemicals, Seoul, Korea) resin films were procured. PLA was sourced from 3D4Makers (Haarlem, The Netherlands) as a 3D printing filament and PLA films were produced by using a 3D printer with a roughly 0.1 mm thickness for the impregnation. PP films were acquired from Propex Fabrics GmbH (Gronau, Germany). For epoxy ADNFRC, a single-ply prepreg was prepared using the consolidation process illustrated in Figure 4.2 by placing an ADN preform between two epoxy matrix films. A 5 bar pressure was applied for a minute at 60 °C on a slowly moving consolidation belt to obtain an epoxy ADNFRC prepreg. For PLA ADNFRC prepregs, the same process was used but with a different temperature; 210 °C under 5 bar pressure for a minute, to achieve better impregnation. To be sure about impregnation of the PP film into the bed of natural fibres, a different method was applied for prepregging. The PP sandwiched ADN preforms were placed in a semi-closed mould and the mould was placed in an oven under vacuum for 3 h at 165 °C. It has been shown that for long term heat treatment, temperatures up to 175 °C may be used without degrading natural fibres [121]. As such, the temperature used in this work, should produce no adverse effects, such as thermal degradation of the fibres.

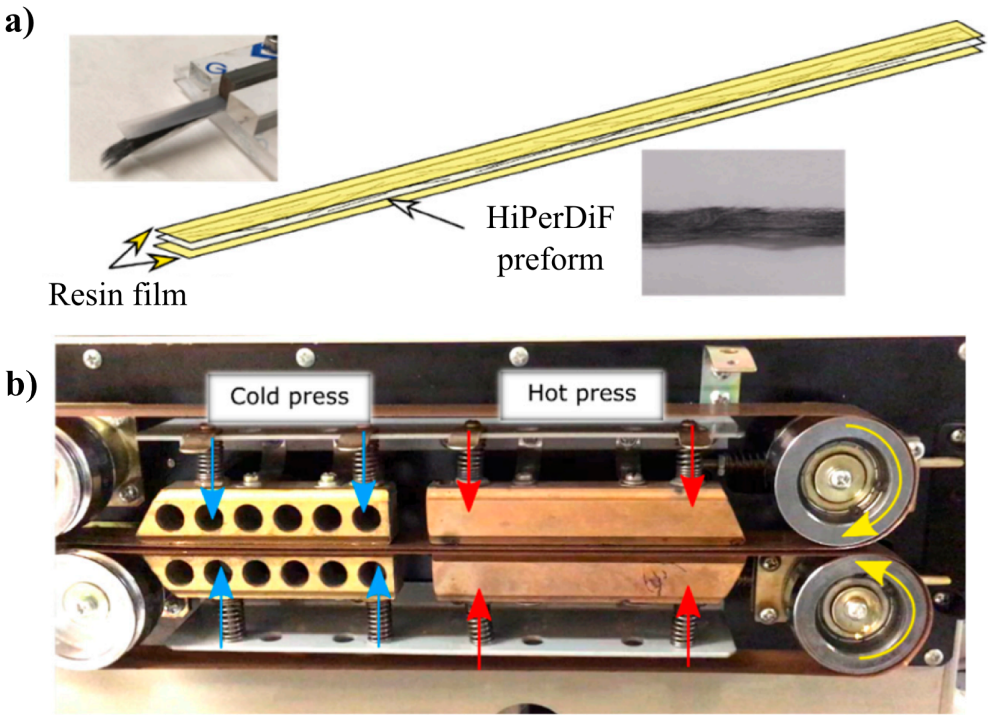

Figure 4.2: (a) An example of the HiPerDiF (carbon fibre) preform sandwiched between two polymeric films before consolidation process (b) Prepregging process. Figures were taken from [290].

4.2.4 ADNFRC Manufacture

To manufacture composite specimens four layers of ADN prepregs were stacked in a semi-closed mould and cured by vacuum bag moulding in an autoclave at ~6.9 bar pressure. The epoxy ADNFRC specimens were cured at 125 °C for 135 min, whereas the PLA and PP samples were cured at 170 °C for 150 min.

4.2.5 Mechanical Testing

Referring to ASTM D3039/D3039M-17 [291], the ADNFRC specimens were tensile tested on an electro-mechanical testing machine at a test speed of 2 mm/min. The strain was measured by a video extensometer (IMETRUM, Bristol, UK). A 10 kN load cell (Shimadzu, Kyoto, Japan) was used to record the load. The gauge length of the specimens was 50 mm and all specimens were protected against any adverse effects from gripping pressure by attaching glass fibre/epoxy end tabs. Figure 4.3 shows examples of the top view geometry of ADNFRC and the details of the tensile test. As seen in the figure, the nominal ADNFRC specimen sizes for width and length were 5 and 150 mm, respectively; specimen thicknesses where within the approximate ranges 0.39–0.74, 0.14–0.33, 0.36–0.51, and 0.30–0.43 mm for curaua, flax-cu, flax-ft, and jute ADNFRC specimens, respectively.

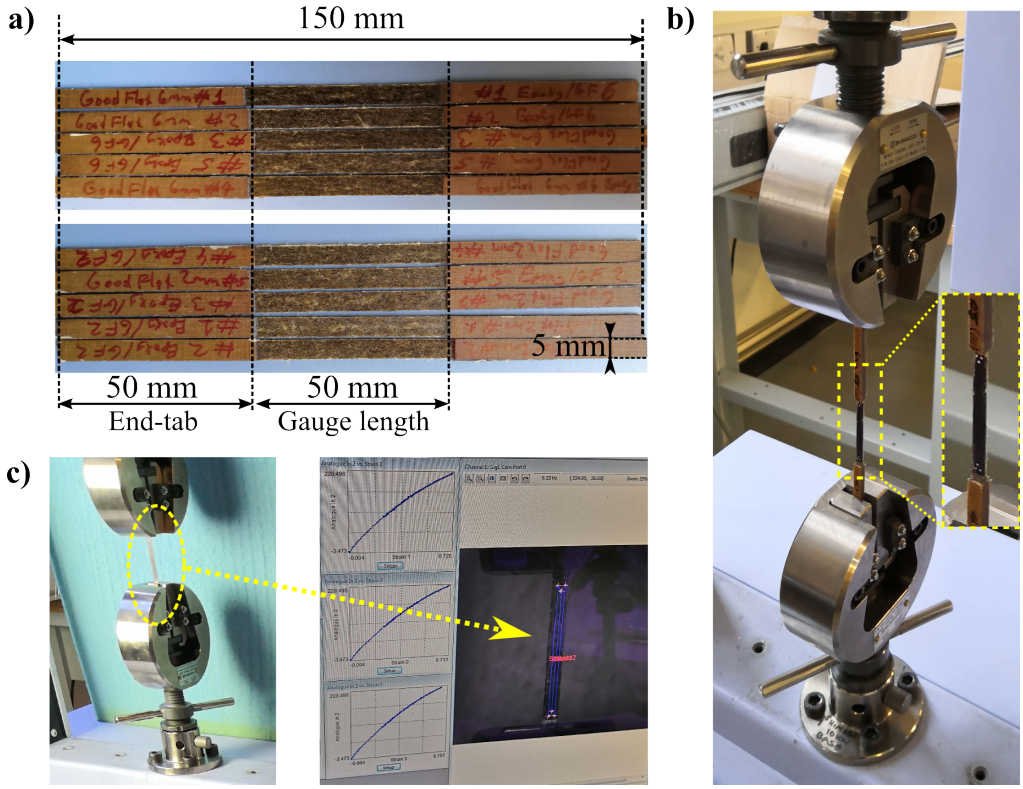

Figure 4.3: (a) Top view of ADNFRC specimens (2 mm and 6 mm flax-ft epoxy composites) and their geometry, (b) the tensile test rig with specimen magnified, (c) the specimen during measurement and the resulting image on video gauge.

4.2.6 Visual Characterisation

A high resolution scanner (Epson Expression 11000XL, Epson, Shinjuku, Tokyo) was used to acquire high resolution images of the ADN preforms. An optical microscope (Zeiss Axio Imager M2, Carl Zeiss AG, Oberkochen, Germany) and a scanning electron microscope (Hitachi TM3030Plus, Hitachi, Ltd., Tokyo, Japan) were used to analyse fibre length distributions, cross-sections, and fracture surfaces of the ADNFRC. Cold mounting followed by standard wet grinding and polishing for polymer matrix composites was applied to make the specimens, for cross-section analysis of each ADNFRC under the microscope. The figures of the specimens are shown in Sections 4.3.1 and 4.3.2.

4.2.7 Density, Porosity, and Water Absorption of ADNFRC

Initially, each ADNFRC specimen was dried overnight, and the dried mass (D) was weighed immediately upon its removal from the vacuum oven used for the drying process. Subsequently, each specimen was immersed in water in a vacuum chamber, again overnight, and the saturated masses (W) of the specimens were weighed in air after its removal. Finally, the suspended weights (S) of specimens were measured while they were immersed in water. Figure 4.4 shows the experi-

mental procedure schematically. These weights were then used to calculate the apparent density (AD), bulk density (BD), apparent porosity (AP), and water absorption (WA) of the ADNFRC specimens following the ASTM standard C830-00 (Equations (4.1)–(4.4), respectively) [251] and Archimedes principle (the buoyancy method) using a precision balance (sensitivity 0.1 mg).

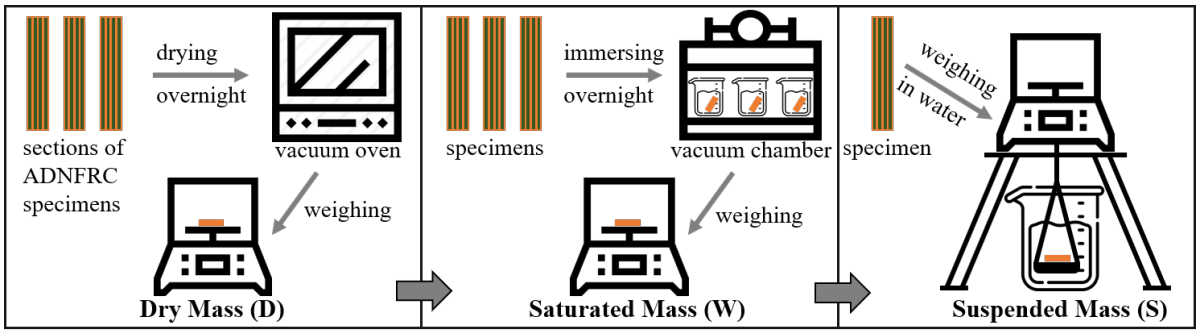

Figure 4.4: A schematic representation of steps and measurements for density, apparent porosity and water absorption of the composite specimens.

$$AD\,(g\,cm^{-3}) = \frac{D}{D-S} \times \rho_{\text{medium}} \tag{4.1}$$

$$BD\,(g\,cm^{-3}) = \frac{D}{W-S} \tag{4.2}$$

$$AP\,(\%) = \frac{W-D}{W-S} \times 100 \tag{4.3}$$

$$WA\,(\%) = \frac{W-D}{D} \times 100 \tag{4.4}$$

where ρ_{medium} is density of displacement medium.

4.3 Results

4.3.1 Properties of ADN Preforms

Figure 4.5 shows the fibre length distribution of NF that are used to produce ADN preforms. The fibre length distributions of NF were obtained by measuring more than 100 fibre lengths in each group type using an optical microscope.

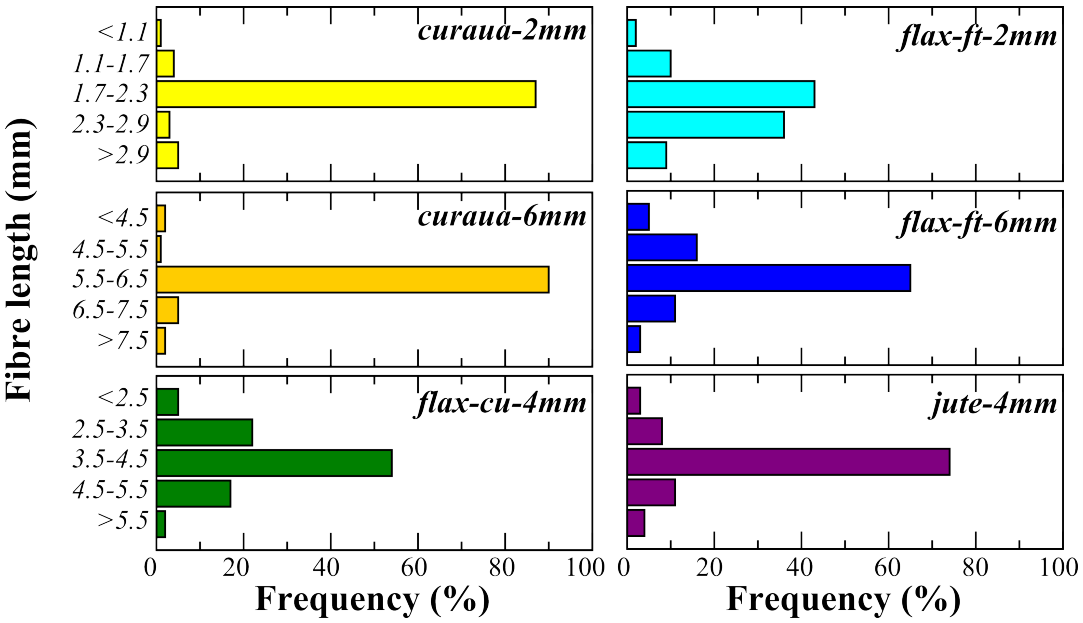

Figure 4.5: Fibre length distributions of the selected groups of natural fibres.

As seen Figure 4.5, the average length of all groups of NF corresponds to the nominal value with a narrow distribution around it, except flax-ft-2m, which has a wide distribution centered above the nominal value. Curaua fibre type has nearly 90% selected fibre length frequencies for both 2 mm and 6 mm. Likewise, it was found that the selected fibre length frequency is significantly high ~75% for jute-4mm fibre type and also for flax-ft-6mm, which is ~65%. The lowest selected fibre length frequency, ~43%, was seen in flax-ft-2mm. The fibre length distribution and also fibre length orientation may affect the mechanical properties of the overall composite, and this can be estimated by using fibre misalignment and fibre length factors in the rule of mixture equations. These factors were previously examined, and it was found that the HiPerDiF alignment process has a 10% knockdown effect on mechanical properties on the overall composite [18], therefore it is expected that the highly ADN preform composites can achieve 90% of the continuous form of those composites.

With the discontinuous natural fibres, ADN preforms were produced using the HiPerDiF method. The aerial weight of ADN preforms was determined by dividing the mass of a preform section, measured using a precision balance (sensitivity 0.1 mg), by the area measured using high resolution scans (resolution 3200 dpi) with the ImageJ software. Table 4.2 shows the aerial weight of ADN preforms and Figure 4.6 shows the sections of ADN preforms.

Table 4.2: Aerial weight of ADN preforms.

ADN Preforms	***Curaua* (2 and 6 mm)**	***Flax-cu* (4 mm)**	***Flax-ft* (2 and 6 mm)**	***Jute* (4 mm)**
Aerial Weight (g/m^2)	116.21	33.53	79.17	65.38
SD (g/m^2)	5.64	9.09	5.46	6.01

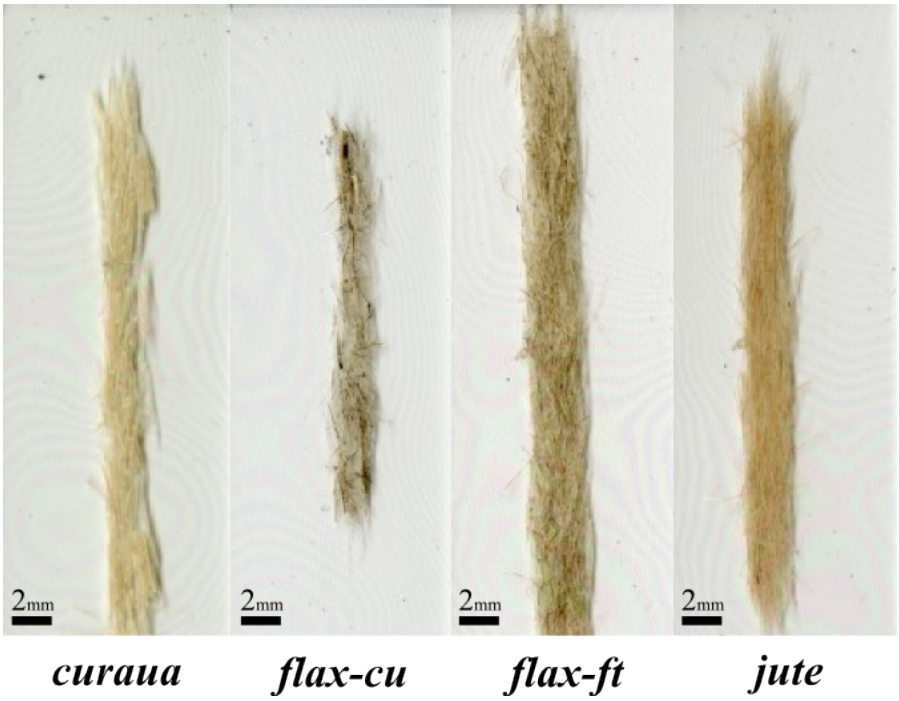

Figure 4.6: Top view of ADN preforms.

The aerial weight of curaua preforms was found be the highest, 116 g/m^2, among all other fibre types. Flax-ft and jute preforms have aerial weights of 79 and 65 g/m^2, respectively, with a standard deviation ~6 g/m^2. However, it was found that flax-cu preforms exhibit the lowest aerial weight, which is 34 g/m^2 with a standard deviation ~9 g/m^2. The reason for these differences is thought to be the considerable amount of debris and the quality of the flax-cu fibre batch sourced from the provider. It is worth mentioning that the preforms of each fibre produced with the HiPerDiF method will lead to have different thicknesses, fibre volume fractions, and fibre orientations because of these the mechanical comparison of these fibre preform composites may not be totally satisfactory but it is adequate to comprehend which fibre has the best potential with the HiPerDiF method.

4.3.2 Physical Properties of ADNFRC

The cross sections and fracture areas of ADNFRC samples were examined using optical and scanning electron microscopy. Figures 4.7-4.12 shows micrographs of all ADNFRC. However, only

the 6 mm flax-ft ones are highlighted and discussed in this section because they showed the best mechanical reinforcement performance among all fibres. Table 4.3 shows the physical properties of 6 mm flax-ft aligned discontinuous natural fibre reinforced composites and Figure 4.12 shows the cross sectional optical and the fracture area scanning electron micrographs of 6 mm flax-ft reinforced epoxy, PLA and PP ADNFRC.

Table 4.3: Physical properties of 6 mm flax-ft aligned discontinuous natural fibre reinforced composites (F6). Errors represent SD.

ADNFRC	**Apparent Density (g cm^{-3})**	**Apparent Porosity (%)**	**Water Absorption (%)**	**Bulk Density (g cm^{-3})**
F6/Epoxy	1.35 ± 0.04	37.15 ± 2.12	44.02 ± 3.43	0.85 ± 0.03
F6/PLA	1.26 ± 0.04	38.52 ± 2.45	49.68 ± 3.48	0.78 ± 0.01
F6/PP	1.24 ± 0.01	20.00 ± 2.89	20.23 ± 3.49	0.99 ± 0.03

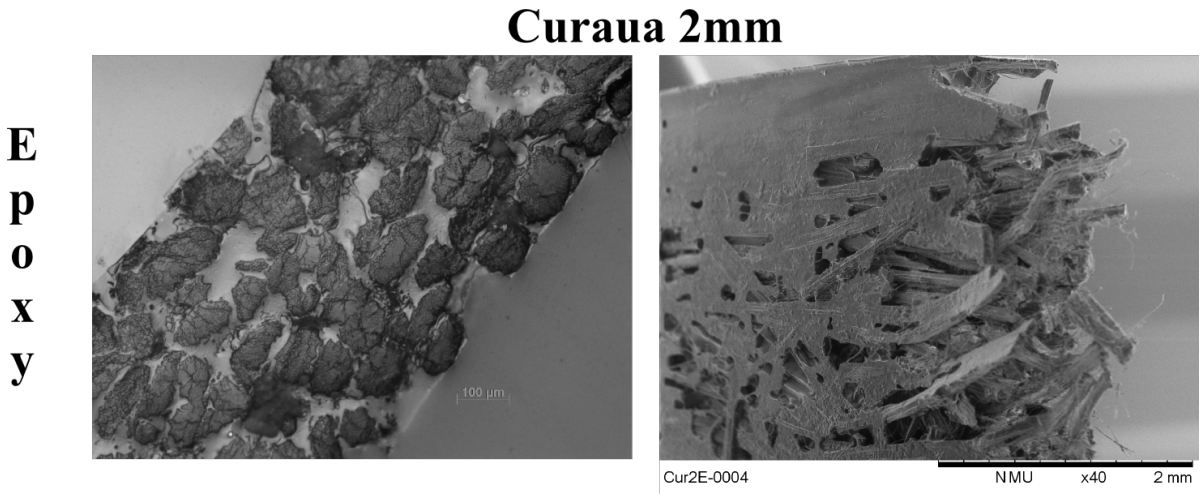

Figure 4.7: The cross sectional optical images (left column) and the fractured area imaged in scanning electron micrographs (right column) of 2 mm curaua aligned discontinuous natural fibre composites.

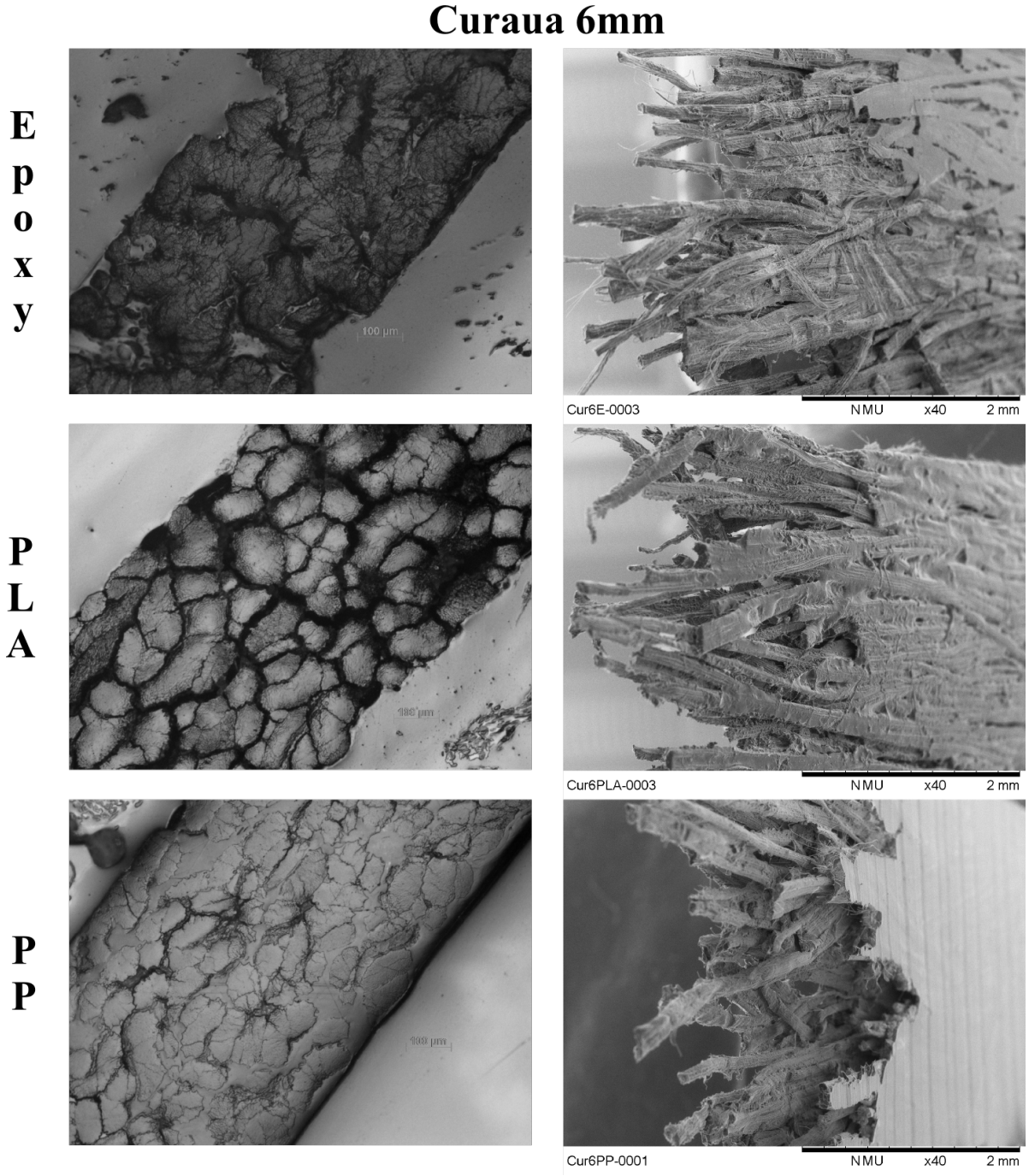

Figure 4.8: The cross sectional optical images (left column) and the fractured area imaged in scanning electron micrographs (right column) of 6 mm curaua aligned discontinuous natural fibre composites.

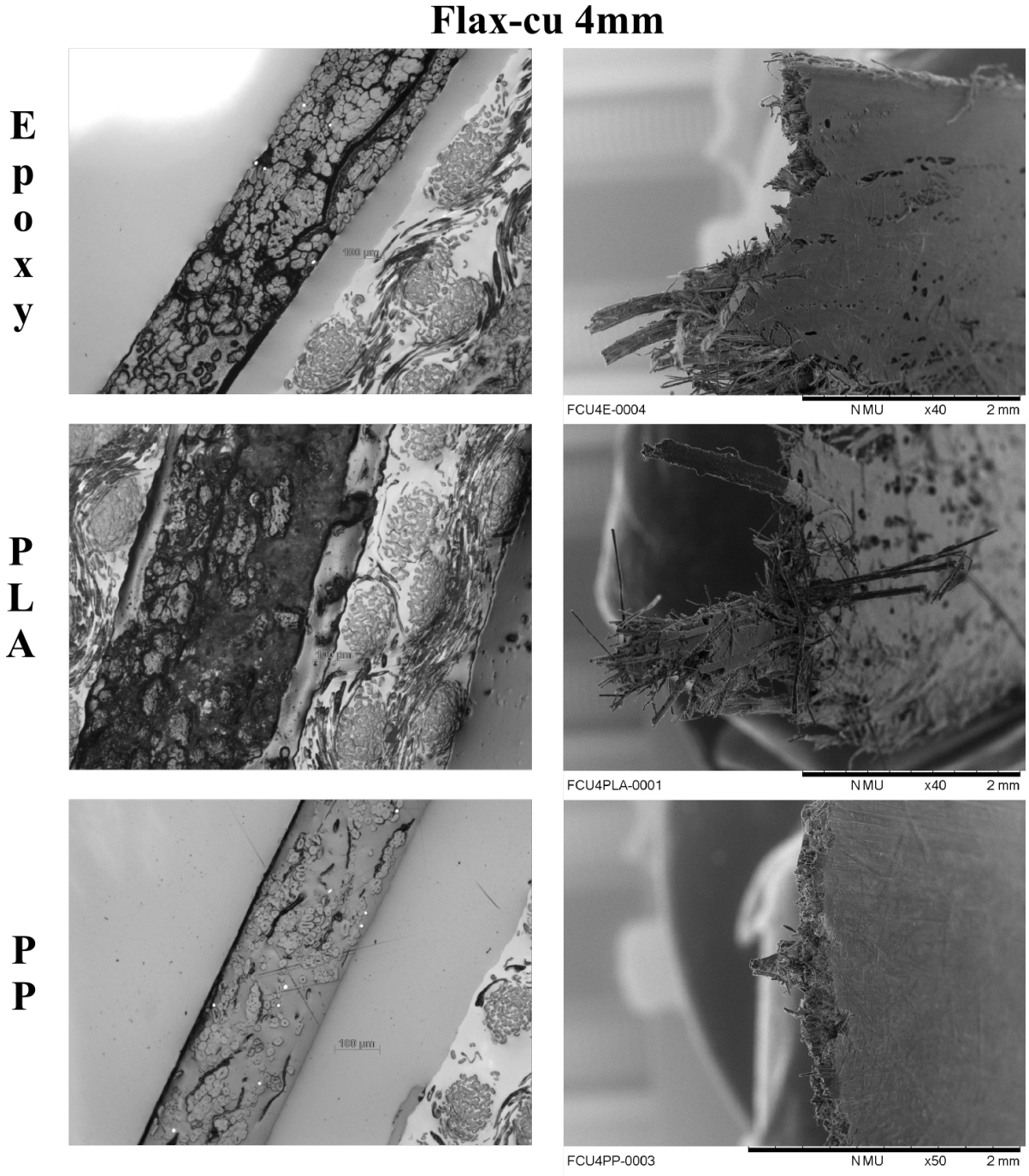

Figure 4.9: The cross sectional optical images (left column) and the fractured area imaged in scanning electron micrographs (right column) of 4 mm flax-cu aligned discontinuous natural fibre composites.

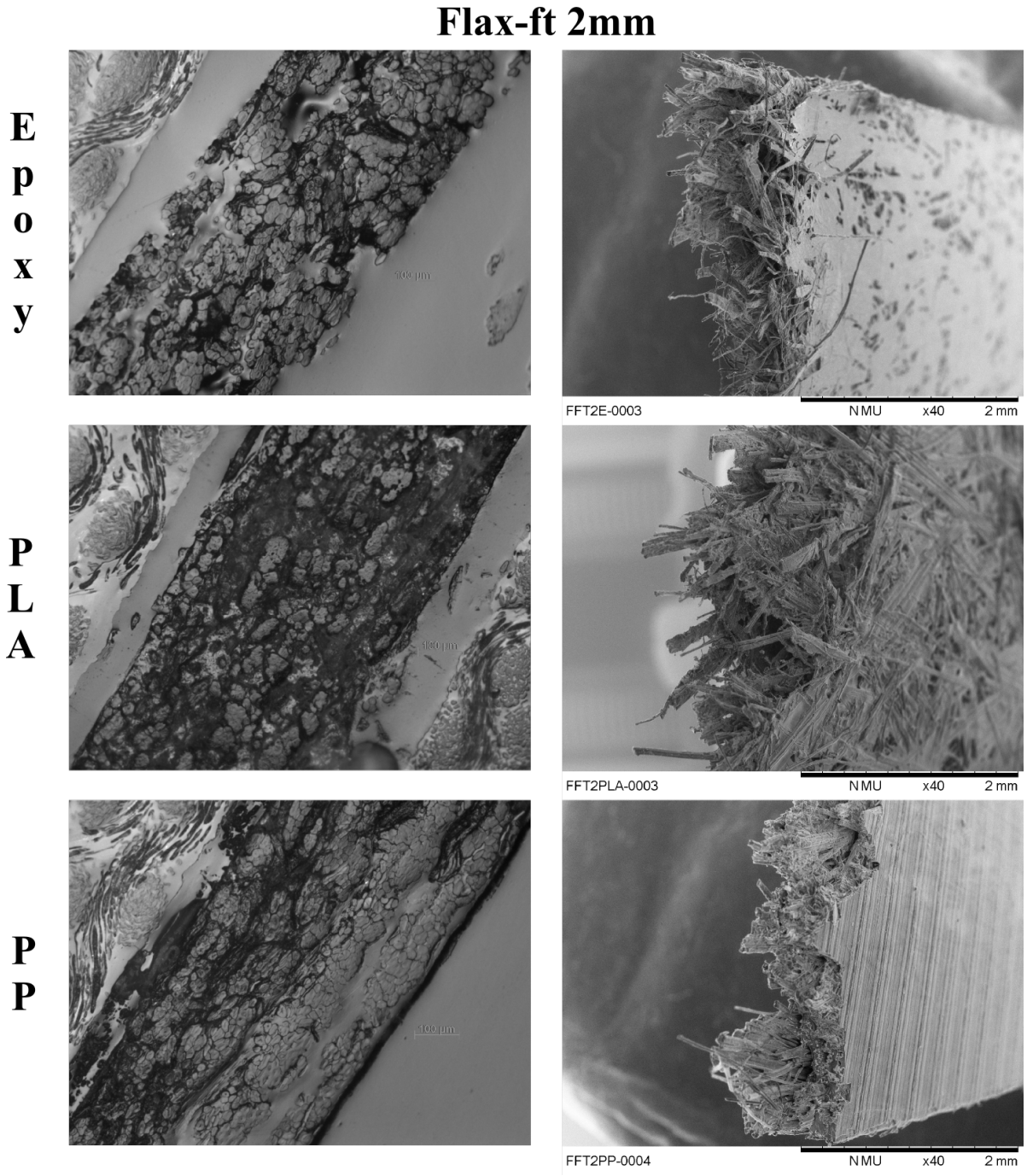

Figure 4.10: The cross sectional optical images (left column) and the fractured area imaged in scanning electron micrographs (right column) of 2 mm flax-ft aligned discontinuous natural fibre composites.

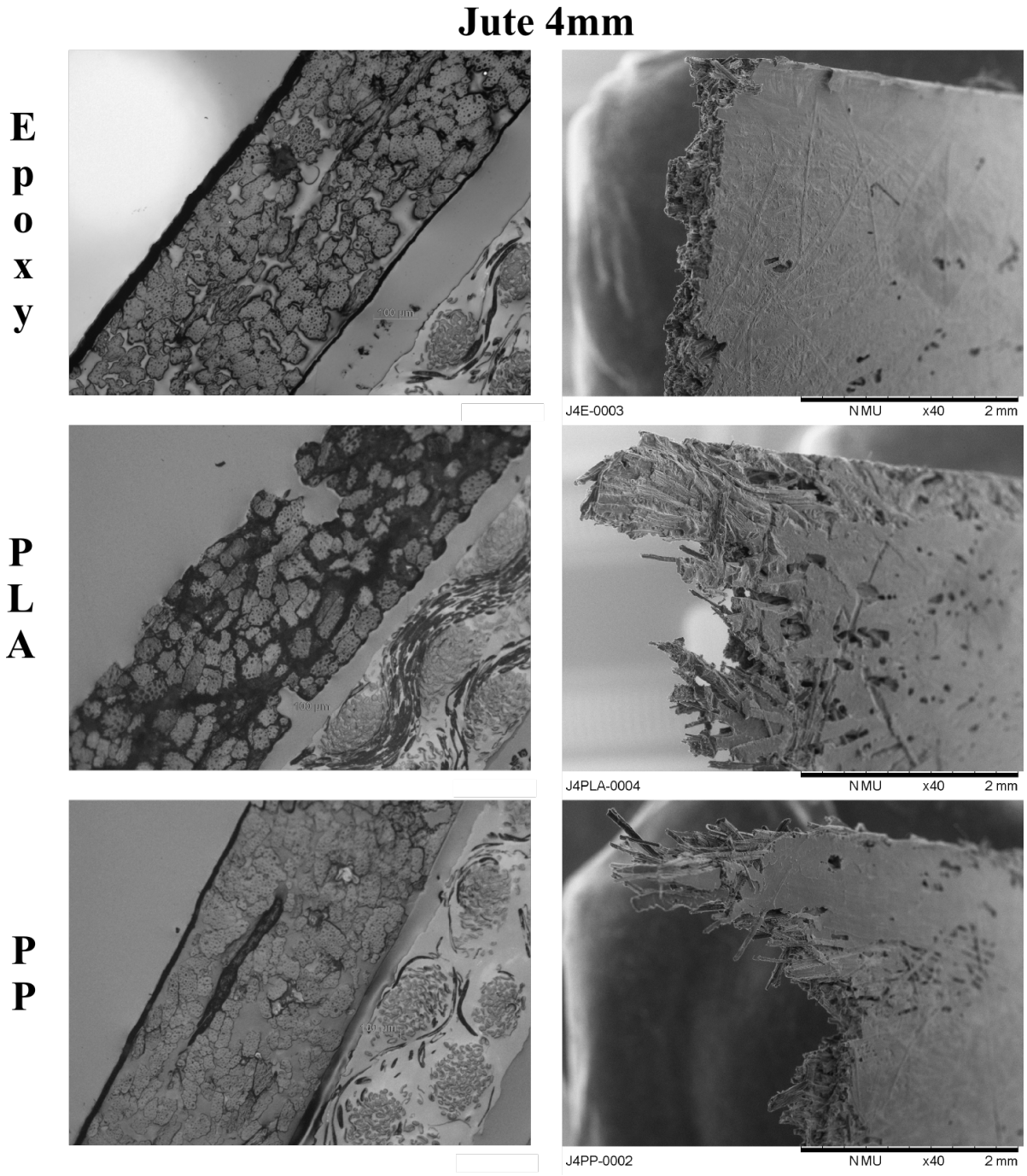

Figure 4.11: The cross sectional optical images (left column) and the fractured area imaged in scanning electron micrographs (right column) of 4 mm jute aligned discontinuous natural fibre composites.

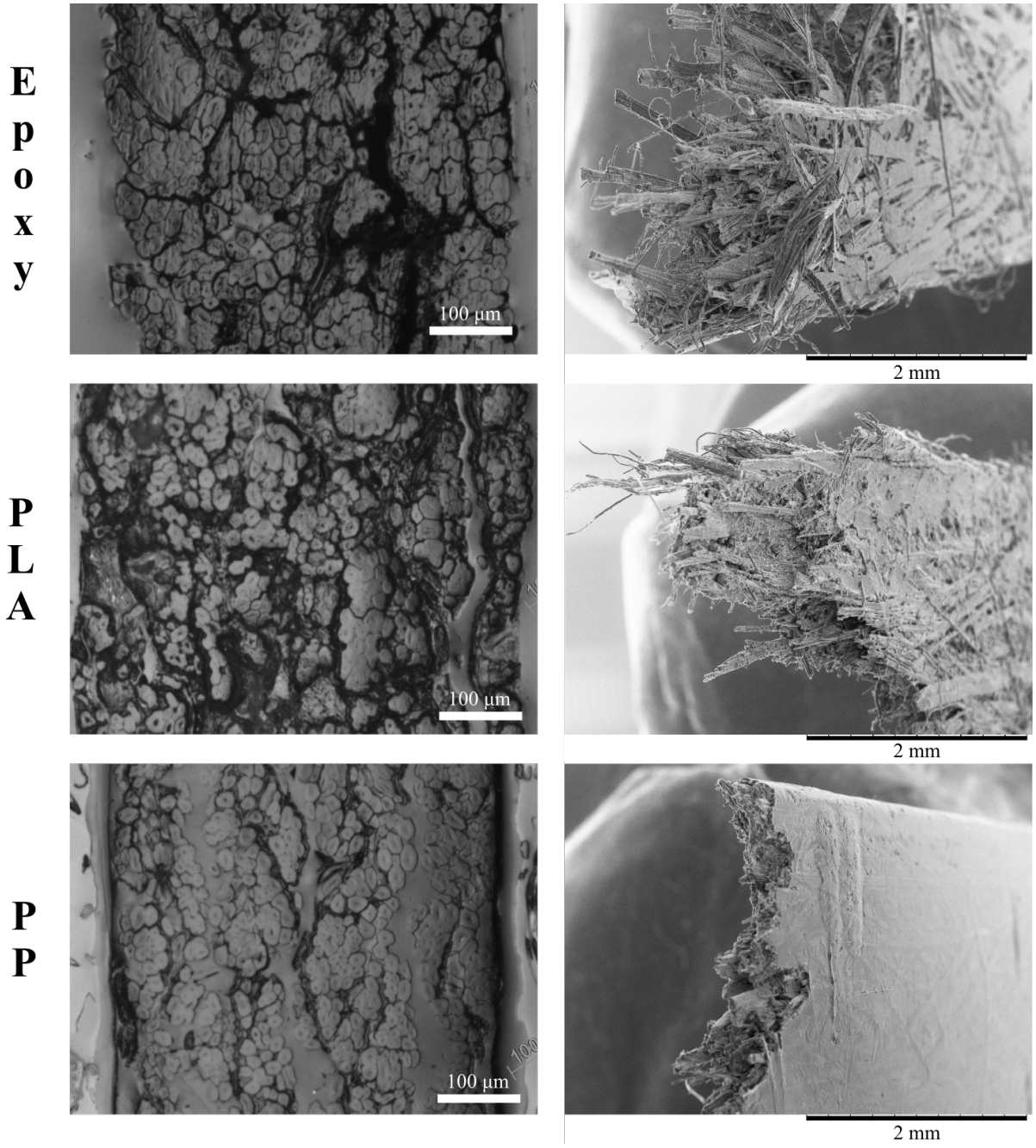

Figure 4.12: The cross sectional optical images (left column) and the fractured area imaged in scanning electron micrographs (right column) of 6 mm flax-ft aligned discontinuous natural fibre composites.

The cross-sectional area images shown in Figure 4.12 (left column) reveal adhesive flaws between the layers of the prepreg, mainly for PLA and epoxy ADNFRC. In contrast, for PP ADNFRC, greater uniformity is noted. In the process of manufacturing PP and PLA ADNFRC, the consolidation of the four prepreg layers is carried out at a temperature of 170 °C. This

manufacturing temperature is higher than the melting point of PP (130 °C), which facilitates the reduction of the polymer's viscosity, providing greater homogenization and adhesion of the layers of the prepreg. However, a temperature of 170 °C is in range of the melting point of PLA (170 °C to 220 °C), giving a viscosity of 10^5 cps [292], which is probably the main reason for not obtaining adhesion between the layers. Likewise, the epoxy film during the curing cycle to reach 125 °C present a viscosity between 5000 and 70,000 cps [287], leading to a similar behaviour to the PLA composite during consolidation. Besides, the thickness of the film used affects the conditions for obtaining good adhesion of the layers.

The fracture images shown in Figure 4.12 on the right reveal that both PLA and epoxy ADNFRC have fibre pull-out, suggesting a low interfacial adhesion between the matrix and the fibres. On the other hand, the images of PP ADNFRC show evidence of a perfect wrapping of PP surrounding the natural fibers that also indicates a good fibre/matrix adhesion. This is evidenced by a clean fracture surface with simultaneous rupture of matrix and the fibres, without the presence of significant pull-out effect. This failure mechanism is inherent to the prepreg manufacturing process, where interfacial bonding between the fibre and the matrix is formed. PP ADNFRC had special treatments where the prepreg was subjected to heating in an oven for 3 h at 165 °C, which probably promoted a better homogeneity of the polymer.

Density, porosity and water absorption are some of the most important properties for FRP in engineering applications. This is especially true for natural FRP due to the adverse effects on their properties and thus their long-term performance [235, 293]. The physical properties of 6 mm flax-ft ADNFRC was investigated and Table 4.3 shows the apparent density, porosity, water absorption, and bulk density of 6 mm flax-ft ADNFRC (F6).

It was seen that F6/Epoxy has the highest density, 1.35 g cm^{-3}, among all F6 ADNFRC. The densities of F6/PLA, and F6/PP were found to be 1.26 and 1.24 g cm^{-3}, respectively. The calculated bulk densities of the fibres are 0.85, 0.78, and 0.99 g cm^{-3} for F6/epoxy, F6/PLA, and F6/PP, respectively, displaying a different trend compared to apparent densities. Furthermore, it was found that the apparent porosity of F6/epoxy and F6/PLA are nearly twice (~38%) as high as F6/PP (20%). The same trend is also seen in water absorption values where F6/PP had a 20% water absorption, less than half that of F6/Epoxy and F6/PLA, which are almost similar, 44% and 50%, respectively. It was concluded that the porosity and the water intake of the F6/epoxy and F6/PLA composites significantly higher than F6/PP composites.

By using a simple rule of mixtures approximation, fibre and matrix volume ratio can be roughly estimated for ADNFRC. The density of a composite is determined by the summation of constituent densities weighted according to their volume fractions as shown in the following Equation 4.5 (neglecting the contribution of voids):

$$\rho_{ADNFRC} = \rho_{NF} \times v_{NF} + \rho_{resin} \times (1 - v_{NF}) \tag{4.5}$$

where ρ_{ADNFRC}, ρ_{NF}, and ρ_{resin} are the density of ADNFRC, natural fibre, and polymer, respectively. v_{NF} represents the fibre volume fraction of the composite. Therefore, the density values

of F6 ADNFRC (Table 4.3) were used to calculate v_{NF} of 6 mm flax-ft in ADNFRC by applying Equation 4.5. Table 4.4 shows v_{NF} the calculated values for 6 mm flax-ft (F6) fibres in epoxy, PLA, and PP ADNFRC (see Table 4.1 for the parameters used to calculate v_{NF}).

Table 4.4: Fibre volume fraction, v_{NF}, of 6 mm flax-ft (F6) in the ADNFRC.

ADNFRC	**F6/Epoxy**	**F6/PLA**	**F6/PP**
v_{NF}	0.427	Na (0.074*)	0.516

*the calculated result is not acceptable due to the significant degradation of PLA in water.

As seen in Table 4.4, it was calculated that v_{NF} of F6 in PP ADNFRC is the highest fraction among all ADNFRC and more than half, ~0.52. Figure 4.12 displays similar high v_{NF} with good adhesion and negligible amount of voids for PP ADNFRC. In addition, the relatively high v_{NF} is also visible for F6/epoxy ADNFRC with the existence of a few voids (Figure 4.12). For epoxy ADNFRC, v_{NF} of F6 was calculated ~0.43. Moreover, it is known that moisture significantly degrades PLA depending on the temperature or pressure [294]. The existence of a significant amount of voids, the presence of the natural fibres, and poor adhesion render PLA ADNFRC degradable in water during the physical property measurements; because of that, the approximation used to calculate the volume fractions cannot be reliable for v_{NF} of F6 in PLA ADNFRC, which was calculated as ~0.074. Therefore, the anticipated density and v_{NF} for F6/PLA are higher than those obtained in this work. Moreover, it must be noted that Eq. 4.5 is not suitable for these composites since high porosity is expected, however it is used because it is a good assumption to understand impregnation quality between the resin types. For different fibre types, similar physical properties and trends are foreseen on the grounds that curaua, flax-ft, and jute fibres have similar densities, porosities and water absorption properties [121].

4.3.3 Mechanical Properties of ADNFRC

Tensile tests were performed to obtain the mechanical properties of epoxy, PLA, and PP ADNFRC. In total, five specimens were tested for each ADNFRC type, except for jute epoxy and flax-cu PP where four specimens were tested. Only one specimen was usable for tensile testing after curing the specimens for flax-cu PLA ADNFRC due to the low packing density of the ADN preform and the low adhesion between PLA and flax-cu. In total, 27 measurements were taken for both the thickness and width of ADNFRC specimens by using a precise micrometer and caliper for converting force to stress. Figure 4.13 shows the representative stress–strain curves of ADNFRC.

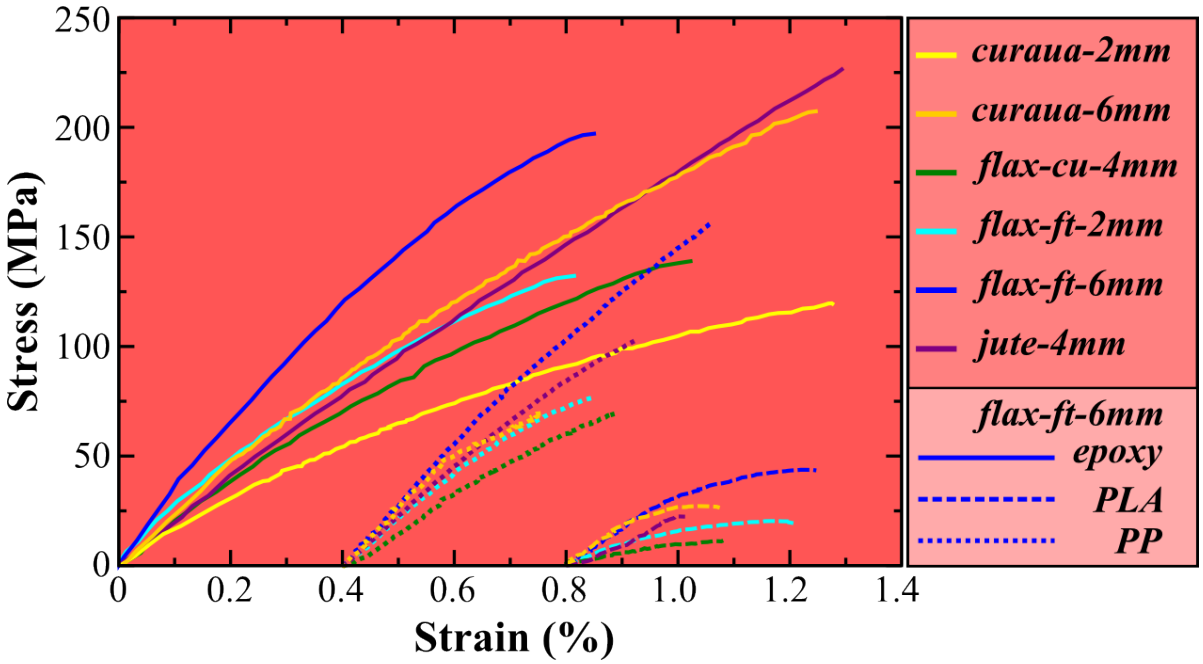

Figure 4.13: Representative stress–strain curves for the tensile tested aligned discontinuous natural fibre composites specimens and the colour/line code. For PLA and PP curves, 0.8 and 0.4 strain reference points are the starting points, respectively.

As seen in Figure 4.13, all PLA ADNFRC exhibit a significant amount of non-linear deformation and they have a smaller linear elastic region compared to epoxy and PP ADNFRC. The general stress–strain behaviour of PP ADNFRC appears to be linear elastic. The linear elastic region of this sample is comparable in strain to epoxy ADNFRC. Most of the epoxy ADNFRC shows what is thought to be non-linear deformation up to fracture. Moreover, it was seen that 2 mm curaua epoxy ADNFRC undergoes non-linear deformation earlier than 6 mm curaua epoxy ADNFRC and shows more non-linear deformation in comparison. Similar trends were observed for 6 mm and 2 mm flax-ft ADNFRC. For epoxy and PLA ADNFRC, 2 mm flax-ft starts showing non-linear deformation earlier than for the 6 mm flax-ft specimen, whereas in PP ADNFRC both of them undergo non-linear deformation at a similar strain. From the stress–strain curves, the elastic modulus of ADNFRC were calculated by calculating the slope of the linear elastic region between 0.05% and 0.015% strain values. Figure 4.14 shows the elastic moduli, tensile strength (σ_t) and strain at σ_t of ADNFRC.

The highest elastic modulus values are seen for epoxy ADNFRC, which are between ~21 and 32 GPa. On the other hand, PLA ADNFRC exhibit the lowest elastic modulus values (between ~8 and 17 GPa), which are significantly lower compared to epoxy and PP ADNFRC. PP ADNFRC shows similar elastic modulus values (between ~18 and 31 GPa) compared to those of epoxy ADNFRC. Moreover, the epoxy ADNFRC have the highest σ_t (between ~140 and 206 MPa) among all resin types. PLA ADNFRC also show the lowest σ_t values (<50 MPa), which are lower than those of PP ADNFRC and significantly (statistically significant difference was determined by

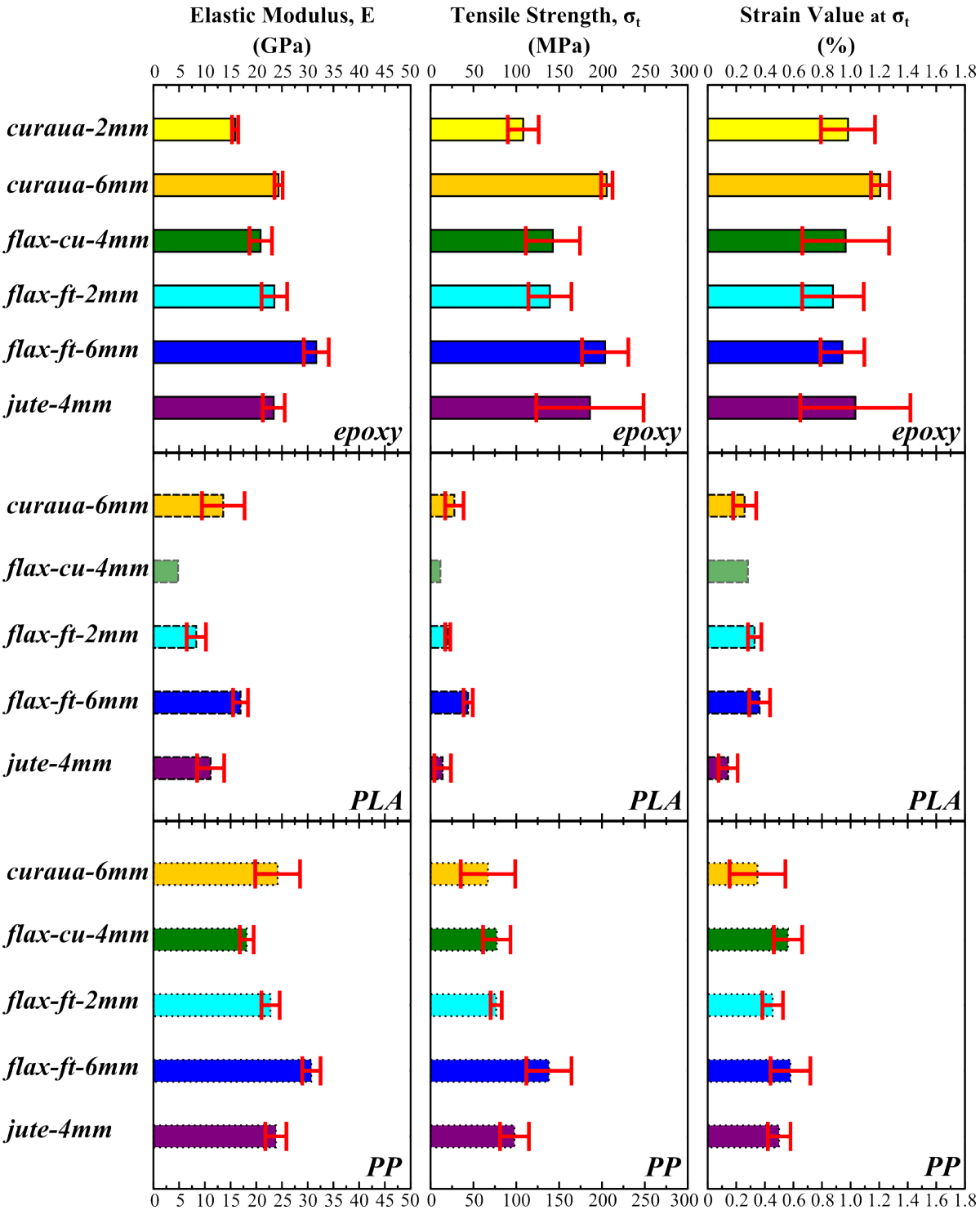

Figure 4.14: The mechanical properties of aligned discontinuous natural fibre composites, elastic moduli, tensile strength (σ_t) and strain at σ_t, respectively, from left to right. Top to bottom: epoxy (solid line), PLA (dashed line), and PP (dotted line). Error bars indicate standard deviation (SD).

t-test where $p < 0.01$ between all groups) lower than those of epoxy ADNFRC. The PP ADNFRC show moderate σ_t values (between ~67 and 138 MPa) and they are significantly lower than those of epoxy ADNFRC. The strain values at σ_t for epoxy ADNFRC reside between ~0.9–1.2%. PLA and PP ADNFRC exhibit lower strain values at σ_t compared to epoxy-based samples, with values residing between ~0.14–0.36% and ~0.35–0.58%, respectively. The main reason of PLA and PP ADNFRC exhibited lower strain values was considered to be a poor impregnation compared to epoxy, therefore, optimised processing parameters like temperature, pressure and time needs to be investigated to obtain better impregnation.

As seen in Figure 4.14, 6 mm flax-ft epoxy ADNFRC have the highest elastic modulus values (~32 GPa) among the four types of fibres followed by 6 mm curaua, 2 mm flax-ft, 4 mm jute, and 4 mm flax-cu epoxy ADNFRC in which the elastic modulus values range between ~21 and 24 GPa. In total, 2 mm curaua ADNFRC exhibit the lowest elastic modulus values among all epoxy ADNFRC as ~16 GPa. The obtained stiffness values are comparable with the reported values for continuous unidirectional flax/epoxy (~32-40 GPa) and E-glass epoxy (~31-39 GPa) systems produced by RTM or prepregging manufacturing methods [81]. For σ_t, 6 mm curaua and 6 mm flax-ft epoxy ADNFRC have the highest values, ~206 and 204 MPa, respectively. Besides, 4 mm jute epoxy ADNFRC exhibit comparably high σ_t, ~186 MPa with a high standard deviation. The σ_t values of 4 mm flax-cu and 2 mm flax-ft were found to be ~143 and 139 MPa, respectively. On the other hand, 2mm curaua epoxy ADNFRC show the lowest σ_t, ~108 MPa, among all epoxy ADNFRC, similar to the elastic moduli. The obtained strength values are slightly lower than the reported values for continuous unidirectional flax/epoxy (~260-380 MPa) and lower than E-glass epoxy (~800-1100 MPa) systems produced by RTM or prepregging manufacturing method [81].

Furthermore, the 6 mm flax-ft fibre type also exhibits the highest elastic modulus value (~17 GPa) among all PLA ADNFRC types. In total, 6 mm curaua PLA ADNFRC have the second highest elastic modulus, ~14 GPa, and 4 mm jute 4-mm PLA ADNFRC the third highest, ~11 GPa. The lowest elastic modulus values were found for 2 mm flax-ft and 4 mm flax-cu PLA ADNFRC, ~8 and 5 GPa, respectively. However, since, as explained above, only one sample has been tested, the results for 4 mm flax-cu PLA ADNFRC cannot be considered representative of the material behaviour. The lowest σ_t value was found for 4 mm flax-cu PLA ADNFRC as ~12 MPa, however 4 mm jute PLA ADNFRC show low σ_t value (~12 MPa) compared to other fibre types with a high standard deviation, which indicates it could be much weaker. In total, 6 mm curaua and 2 mm flax-ft PLA ADNFRC have moderate σ_t compared to other PLA ADNFRC, ~28 and 20 MPa, respectively. Among all PLA ADNFRC, it was found that 6 mm flax-ft PLA ADNFRC are the strongest (~44 MPa). Even though the obtained stiffness and strength values are significantly low due to bad impregnation, they are in the same range with the reported values of flax/PLA systems in the literature, which are 3-25 GPa for stiffness and 35-151 MPa for strength or the reported values of jute/PLA systems in the literature, which are 2-12 GPa for stiffness and 32-91 MPa for strength [295].

Moreover, 6 mm flax-ft PP ADNFRC show the highest elastic modulus value in composites with the same resin type and also comparable values (~31 GPa) with epoxy ADNFRC, which is also better than the reported stiffness value of unidirectional continuous flax/PP composites produced by compression moulding (~27 GPa) and a hand layup continuous E-glass/PP system (~26 GPa) [81]. The same comparable trends are found for 6 mm curaua, 2 mm flax-ft, and 4 mm jute PP ADNFRC where the elastic modulus values reside between ~23 and 24 GPa. The lowest elastic modulus value was found for 4 mm flax-cu PP ADNFRC as ~18 GPa, which is lower than that of the epoxy counterpart. In total, 6 mm flax-ft PP ADNFRC was found to be the strongest again within the same resin type with a ~138 MPa tensile strength. However, this value is not comparable with the reported strength value of unidirectional continuous flax/PP composites produced by compression moulding (~251 MPa) and hand layup continuous E-glass/PP system (~700 MPa) [81], which may be overcome with better impregnation. The second highest value for σ_t was observed for the 4 mm jute PP ADNFRC that is close to 100 MPa. In total, 4 mm flax-cu and 2 mm flax-ft exhibit similar σ_t values-~77MPa. It was found that the weakest PP ADNFRC is the 6 mm curaua sample—namely a value of ~67 MPa with a high standard deviation.

4.4 Discussion

As seen in Figure 4.6 and Table 4.2, for flax-ft and jute ADN preforms, acceptable aerial weight and distribution of fibres through the width were obtained, and with these features it is expected to have a high and well distributed fibre volume fraction in ADNFRC, and therefore higher mechanical properties. In contrast, those features of curaua or flax-cu ADN preforms were found to be insufficient. One reason for this is thought to be the fibre size (e.g., diameter and thereby aspect ratio) which leads to change of feed rate in the HiPerDiF method. The fibre size for curaua is higher than the other fibre types (as seen Figures 4.7 and 4.8), and this affected the process method to produce curaua ADN preform as a slow feed rate, i.e., low water flow to the HiPerDiF alignment head and low conveyor belt speed (Figure 4.1a), was used to have sufficient aerial weight and better distribution of fibres through the width. Another reason was found in the quality of the source material. There were considerable amounts of debris in the source materials, particularly for flax-cu, but also for curaua in small quantities. The source materials of flax-ft and jute fibres have negligible amounts of impurities.

The alignment of fibres in ADFRC can be examined by analysing fibre orientation using optical microscopy and ellipse fitting of the cross-sections of fibres in ADFRC [290]. However, because of the inherent characteristics of natural fibres, i.e., non-perfectly circular cross-sections, their alignment in ADNFRC cannot be determined by using basic characterisation techniques. It is known that the HiPerDiF method, which has a increased fibre alignment compared to other methods, provides 80% and 65% of fibre distribution in the range of $\pm 3^{\circ}$ for a preform and composite form, respectively [16]. Therefore, only a 10% decrease in mechanical performance of ADNFRC is expected due to the fibre misalignment factor, as has been previously demonstrated

[18].

A previous study [121] revealed that flax is the stiffest fibre, followed by curaua and jute fibres, respectively. As seen in Figure 4.14, for fibre lengths higher than the critical fibre length, the stiffness trend of curaua, flax-ft, and jute ADNFRC is in agreement with the intrinsic stiffness trends of the fibres. Furthermore, similar trends can be observed for tensile strength, especially for epoxy ADNFRC, since intrinsically flax and curaua fibres are stronger than jute fibres. However, flax-ft and jute fibres were more compatible with the HiPerDiF method to produce ADN preforms. Therefore, flax-ft ADNFRC show better tensile strength in all polymer ADNFRC compared to the other ADNFRC. Even though curaua fibres are stronger than jute fibres, tensile strength of jute ADNFRC is similar to that of curaua ADNFRC.

The presence of fibres that are shorter than the critical length increases the non-linear behaviour of the ADNFRC. As seen in Figure 4.13, 2 mm fibre length curaua shows more non-linear behaviour than 6 mm fibre length curaua for epoxy ADNFRC. Similar trend was also observed in 2 mm and 6 mm fibre length flax-ft ADNFRC. In addition, the presence of fibres that are shorter than the critical length reduces the mechanical performance of the ADNFRC drastically. In total, 2 mm curaua epoxy ADNFRC showed the lowest strength and stiffness among those tested, which was expected since critical lengths for curaua have reported to be higher than 2 mm. It was found that there are, respectively, ~35% and ~50% reductions in stiffness and tensile strength of curaua epoxy ADNFRC between 2 mm and 6 mm fibre lengths. Since the most of the fibre lengths in the distribution for 2 mm curaua are equal to or less than the critical length (as seen in Figure 4.5), a significant reduction is seen. Because of the significant amount of mechanical performance loss observed in epoxy ADNFRC and the limited source of curaua fibre, we decided not to proceed with the 2 mm curaua fibre for other polymer ADNFRC. For 2 mm flax-ft, there is less but still a considerable amount of fibre length distribution that is equal to or less than the critical length. Therefore, the noticeable reduction in mechanical properties was expected and observed in all flax-ft ADNFRC. For epoxy ADNFRC, they are ~25% and ~32% reductions for stiffness and tensile strength, respectively, between 2 mm and 6 mm flax-ft epoxy ADNFRC. For other flax-ft polymer ADNFRC, it was found that stiffness reduction was ~52% and ~25% for PLA and PP ADNFRC, respectively. For tensile strength, the reductions due to fibre length were found to be ~55% and ~44% for flax-ft PLA and PP ADNFRC, respectively. Furthermore, the 6 mm flax-ft fibre type showed the best mechanical performance in all polymer ADNFRC compared to other fibre types.

The high homogenization both in the manufacture of PP prepregs and in the consolidation of the final composites are factors that determine the low values of water absorption and porosity of these materials in comparison to others (PLA and epoxy ADNFRC). It is noted from microscopy images (Figure 4.12), that the PLA and epoxy ADNFRC allow greater water diffusion between the layers due to the lack of full adhesion. Although PP and PLA ADNFRC are manufactured using equal times and temperatures, the PP film benefits from the fact that it can be processed

at a lower temperature than PLA. In addition, fibres are limiting factors in the use of high manufacturing temperatures; thus, PLA could not be worked at higher temperature levels, facilitating a greater homogenization of the matrix, as occurred with the PP film.

4.5 Conclusions

- Epoxy ADNFRC and PP ADNFRC were found to be the stiffest materials; however, epoxy ADNFRC are stronger than PP ADNFRC. It was found that PLA ADNFRC shows poor mechanical properties and the reason is considered as the lack of good adhesion and homogenization around the fibres due to limited processing temperature of natural fibres that is less than melting point of PLA.

- Among all fibre types and fibre lengths, 6 mm flax-ft ADNFRC displayed the best performance in terms of mechanical properties in each ADNFRC polymer group. On the other hand, 6 mm curaua ADNFRC and 4 mm jute ADNFRC showed good mechanical performance either being the second or the third in terms of mechanical properties.

- PP ADNFRC exhibited significantly lower porosity and water absorption capacity compared to other polymer types and also PP ADNFRC has the lowest density. It was found that the adhesion between PP and the natural fibres is better than epoxy and PLA ADNFRC.

- It was found that flax-ft and jute fibres can be processed with the HiPerDiF method since the ADN preforms of flax-ft and jute have acceptable aerial weight and fibre distribution through the width. Jute fibres exhibit good mechanical performance in ADNFRC and suitability with the HiPerDiF method, but flax-ft has also the advantage of having a low environmental impact as a constituent material for ADNFRC because the current market status of the fibres. In addition the location of the production method makes flax fibre more sustainable than other fibre types for the EU and UK [190, 296].

- Flax-ft fibre type was found to be the most promising candidate for these composites. Moreover, it was revealed that 6 mm fibre length for flax is acceptable to achieve high performance in ADNFRC since it is considerably higher than the critical length. On the other hand, jute and curaua fibre types remain as good candidates for future studies when the above mentioned features are satisfied.

- The result of a fibre selection, 6 mm fibre length flax-ft, will be used to reinforce a potential sustainable matrix in the following work, which includes also the selection of a sustainable matrix from potential advanced matrices. The interfacial shear strength of the potential sustainable matrix and flax fibre will be a key selection feature for high performance ADNFRC. Moreover, the properties and sustainability of sustainable ADNFRC produced with selected constituents will be analysed.

Chapter 5

Sustainable Matrix Selection and Properties of Aligned Discontinuous Flax Fibre Reinforced Vitrimers

In this chapter, the interfacial properties of flax fibres, which proved to be the best candidate in previous chapters, with three potentially sustainable advanced matrices are reported. These matrices are a vitrimer that combines the beneficial properties of both thermosets and thermoplastics, an entirely bio-based thermoset, and an advanced thermoplastic resin. Each of the selected matrices offers the potential for either recyclability, repairability, reusability, or the use of renewable sources and a reduction in the emissions of volatile organic compounds. Microbond tests were used to evaluate the interfacial shear strength and critical fibre length. It was found that the vitrimer and the bio-based thermoset matrices had a higher level of adhesion with flax fibres compared to a traditional epoxy matrix; the advanced thermoplastic resin shows the poorest adhesion. The vitrimer matrix was selected as a candidate for a sustainable and repairable discontinuous flax fibre reinforced composite. Mechanical and low-temperature rapid repair performance of an aligned discontinuous flax fibre composite, produced using the HiPerDiF method, were investigated. End-to-end and single patch repair methods were performed: vitrimer matrix composites show the potential for a mechanical strength recovery that would allow them to be reused over several life cycles, enabling a circular economy. This chapter provides information on the selection of the sustainable matrix and the best sustainable path for discontinuous natural fibre composites.

This chapter has been adapted from the following published work:
Ali Kandemir[*]; Marco L. Longana; Ian Hamerton; Stephen J. Eichhorn. Developing aligned discontinuous flax fibre composites: Sustainable matrix selection and repair performance of vitrimers. *Composites Part B: Engineering* 2022, 110139. DOI:10.1016/j.compositesb.2022.110139

[*]Corresponding author. Author contribution is given by using the Contributor Roles Taxonomy: conceptualization all authors; data curation A.K.; formal analysis A.K.; funding acquisition all authors; investigation A.K.; methodology A.K.; supervision M.L.L., I.H. and S.J.E.; visualization A.K.; writing—original draft A.K.; writing—review and editing all authors.

5.1 Introduction

Aligned discontinuous FRP (ADFRP) composites are one of the most important categories of these materials, offering good processability, *i.e.*, the capability to be formed into complex shapes with limited defects [297]. They also offer mechanical performance similar to those of continuous FRP if high levels of alignment and optimum critical fibre length are attained [7, 236]. Moreover, the production of continuous FRP structures is labour intensive and produces a significant amount of manufacturing waste, which leads to high environmental impact and costs [284, 285, 298]. In contrast, manufacturing with ADFRP is potentially more sustainable as the discontinuities in the reinforcement improve their formability, facilitating defect-free manufacturing of structural parts [7, 299].

As explained before, to achieve high mechanical performances in ADFRP, one of the crucial parameters is the critical fibre length, which is highly dependent on the interfacial bonding between a matrix and a fibre [237]. Following the fibre selection, the fibre-matrix interface is an essential selection criterion for the sustainable matrix to develop a high-performance ADFRP. Interfacial shear strength (IFSS) is a measure of the bonding, adhesion, or the interaction between a fibre and a matrix material. By using values of the IFSS, the critical fibre length, where the fibre acts as effective reinforcement, can be calculated. The most common methods to obtain IFSS for flax fibres with different matrix systems are fibre pull-out [238–240, 300], fibre fragmentation [241–244] and microbond tests [121, 246, 247].

In this study, the interfacial properties flax fibre/sustainable matrices for high-performance ADFRPs were examined. The interfacial performance of flax fibres was investigated using the microbond test method [245] when coupled with three potentially sustainable advanced matrices:

- an advanced thermoplastic resin, which offers recyclability and reformability,
- an entirely bio-based thermoset, which offers the use of renewable sources and a reduction in volatile organic compounds emissions,
- a vitrimer, a new class of polymer materials that shows reversible chemical cross-links and combines the beneficial properties of both thermosets and thermoplastics [170, 171]; offering recyclability, repairability and reusability.

For sustainable ADFRPs, vitrimers outweigh other matrices, due to their remarkable potential for use in the circular economy [301]. It is also possible to derive them entirely from renewable sources [150]. It has been shown that a glass fibre reinforced vitrimer can be repaired by applying heat and pressure due to exchangeable disulphide crosslinks [302]. It has also been demonstrated that composite specimens can be reshaped in a hot press machine and can be recycled *via* mechanical or chemical recycling methods. Furthermore, Tanyton *et al.* [181] have reported an energy-neutral closed-loop recycling process for a malleable polyimine networked vitrimer resin/carbon fibre composite in which it was possible to completely recover and reuse both

components. In addition, it was shown that delamination damage on carbon fibre reinforced vitrimers can be perfectly repaired through simple heat-pressing. Therefore, a vitrimer was selected as a sustainable matrix for flax fibre reinforced composites since it satisfies the principles of a zero waste hierarchy [303]. Aligned flax fibre reinforced vitrimer (ADFFRV) specimens were produced using the HiPerDiF method and investigated mechanically and physically. Two strategies were applied to repair ADFFRV, and the mechanical recovery performances were reported for the ADDFRV and vitrimer specimens.

5.2 Sustainable Matrix Selection

This part of the paper presents the interfacial characterisation and analysis of flax fibres with three potentially sustainable advanced matrices; an advanced thermoplastic, a bio-based thermoset, and a vitrimer. A promising matrix is selected for flax composites by considering the interfacial shear strengths and its possible contribution to the sustainability of FRPs.

5.2.1 Materials

The flax fibres were grown and processed by Eco-Technilin-Flaxtape™ (Normandy, France) using a proprietary approach and were used as received. The tensile strength and diameter of the flax fibres were reported in a previous study [121], they were namely ~580 MPa and ~64 μm, respectively.

Arkema Elium®150 was selected as the advanced thermoplastic resin due to its properties such as post-thermoformability, recyclability, and mechanical properties similar to epoxy [163]. To prepare the material, a blend of resin and hardener, was mixed manually with a 100:2 ratio, heated in an air oven at 40 °C for 20 min, and then held at room temperature overnight.

Furacure, a poly(furfural alcohol)(PFA)-based developmental resin, provided from Bitrez Ltd., was chosen as a bio-based resin, being a REACH compliant polymer [139], of high bio-based grade with fire resistance, which is advantageous in natural fibre composites [140]. The resin was prepared using a 24:1 resin to hardener ratio, manually mixed, and cured at 160 °C for 120 min in an air oven according to recommendations by the manufacturer.

Vitrimax™T100, imine-linked vitrimer procured from Mallinda Inc., was selected as a dynamically exchangeable covalent polymer network, offering both thermoplastic and thermoset features. Commercial vitrimers are comparative newcomers to the field of matrix chemistry, although the concept was first observed in a laboratory scale over a decade ago [169]. Vitrimax™ resins offer remouldability, reshaping, covalent welding, recyclability, reusability, and high mechanical performance [179, 180]. To prepare the resin blend, the hardener and resin were blended in the ratio (2.5:1), then carefully mixed manually, and cured in an air circulating oven at 135 °C for 60 min.

5.2.2 Microbond Tests

The microbond method [245] was applied to determine the interfacial shear strength (IFSS) of flax fibres with each of the selected matrices. A schematic and a picture of the experimental test setups for the microbond tests are shown in Figure 5.1.

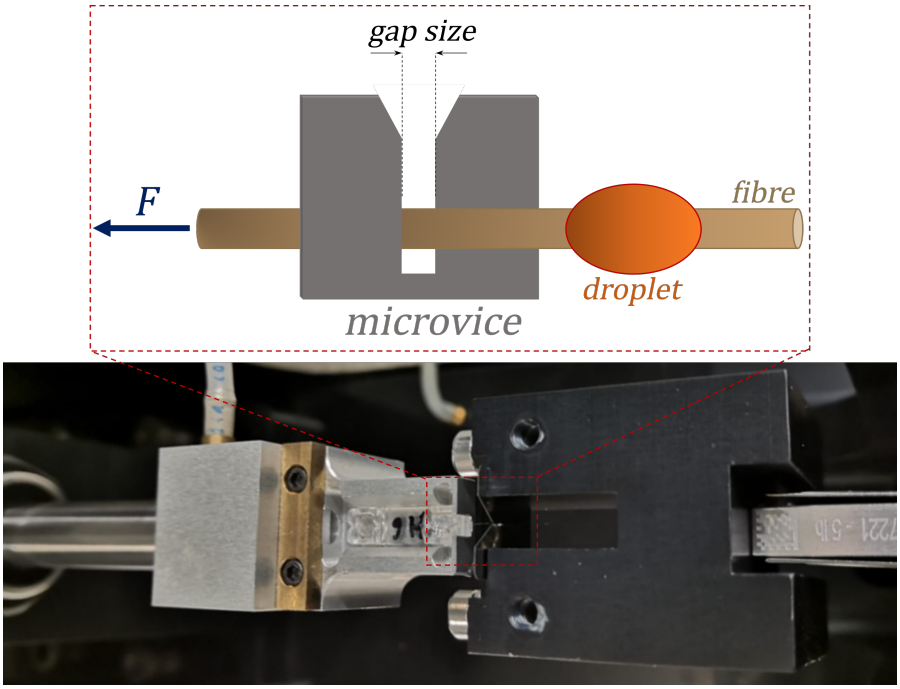

Figure 5.1: A schematic of the microbond test (above) and a photograph of the experimental setup (below).

The fibres were mounted between plastic end-tabs arranged in a silicone holder to maintain a gauge length of 40 mm. Dynamax 3139 adhesive was used to bond the fibres to the end-tabs, and this was cured at ambient temperature (~20 °C) under UV light (λ = 368 nm) for at least 2 h. Resin droplets were then applied to the fibres and cured following the procedures outlined in Section 5.2.1. An optical microscope, Zeiss Axio Imager M2 (Carl Zeiss AG, Oberkochen, Germany), was used to measure the droplet position on the fibre, its size, and the embedded area for each microbond test specimen. For the microbond test, a Dia-stron LEX820 Extensometer (Dia-Stron Ltd., Andover, UK) was used to deform the samples with a microbond apparatus, which comprises of a microvice, *i.e.*, a thin metallic plate with a narrow cut in the middle to accommodate the fibre but to prevent the microdroplet from passing through (Fig. 5.1). Microvice gap separation was varied (gap sizes; 50, 80, 150, and 180 μm) depending on the diameter of the droplet, which ranged from ~ 70 up to 1000 μm, to achieve an ideal contact for force distribution. More than 150 droplets were prepared for each matrix system. However, the number of droplets produced and successfully tested for each flax/matrix combination were 62, 57, 66, and 73 for Elium®, epoxy, Furacure, and Vitrimax™ resins, respectively. Moreover, droplet embedded length

varied between 260–1200, 180–900, 150–650, and 170–1300 μm for Elium®, epoxy, Furacure, and Vitrimax™, respectively. Droplet diameter varied between 80–900, 70–210, 70–430, and 85–1000 μm for Elium®, epoxy, Furacure, and Vitrimax™, respectively. Because of non-constant droplet embedded length against droplet diameter ratio, comparison of the data with the literature may be difficult and this may affect the deviation in the results. Similarly, the droplet distance from the microvice was not kept constant due to experimental setup limitations however it was between 200-400 μm. After each test the fibre was observed using an optical microscope to determine if debonding had occurred. Specimens that showed debonding failure mechanisms were deemed admissible for the calculation of IFSS. The IFSS between fibre and matrix was calculated using Eq. 5.1:

$$\tau = \frac{F_d}{\pi d l_e} \tag{5.1}$$

where τ, F_d, d, and l_e denote IFSS, debonding force, fibre diameter and embedded length, respectively. In Eq. 5.1, the denominator represents the embedded area. It is worth mentioning that the high surface roughness of flax fibres, 10 times higher than glass fibres [121], and their elliptical cross-section [121] may have an effect on the calculated IFSS value. However, to a first approximation, a circular cross section was assumed since only a single fibre type is studied here for comparison purposes.

For efficient reinforcement in short or discontinuous fibre reinforced composites, the filaments must have lengths exceeding the critical fibre length. This then maximises stress transfer between the constituents, and the failure of the composite material is likely to be initiated by the fibres rather than fibre-matrix debonding. The critical fibre length is calculated using the following Eq. 5.2:

$$l_c = \frac{d\sigma_f}{2\tau} \tag{5.2}$$

where l_c, d, and σ_f represent the critical fibre length, diameter (within the droplet), and fibre tensile strength, respectively.

5.2.3 Results and Discussion

Figure 5.2 shows the microbond test results for the sustainable matrices coupled with flax fibre as a function of force and embedded area. As reported before, fibres, exhibit several failure mechanisms during a microbond test. These include shear failure (debonding), fibrillation of fibres within the droplet (fibrillation), fibre failure in the vicinity of the droplet (FFD), fibre failure (FF), and broken matrix (BM); a summary of these has been previously published by Kandemir *et al.* [121]. Examples of debonding failure, the mechanism experimentally admissible for the calculation of IFSS, from the performed microbond tests for all samples are shown in Figure 5.3-5.5. To better understand the interfacial performance of potential sustainable resins, flax-epoxy (PRIME™20LV) system data from a previous study [121], which was obtained with the same experimental methodology, were included in this study for comparison.

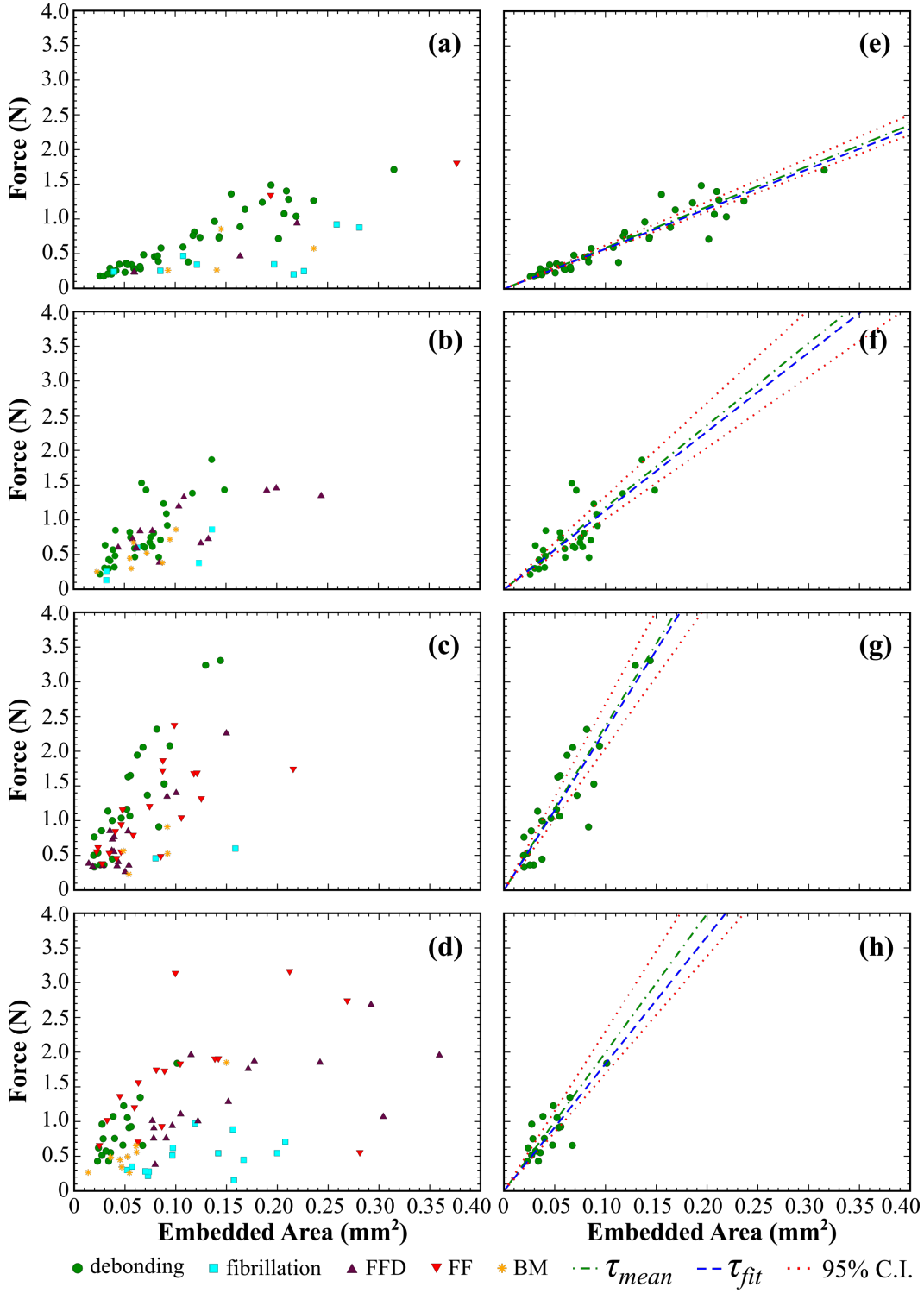

Figure 5.2: Microbond test results of flax fibres with the (a,e) Elium®, (b,f) epoxy, (c,g) Furacure, and (d,h) Vitrimax™ matrices in terms of force versus embedded area. (a–d) shows all data obtained from the test consisting of different failure mechanisms, (e–h) panel shows data only for debonding failure (green dots). Green dotted and blue dashed lines represent τ_{mean} and τ_{fit}, respectively. Red dotted lines show the upper and lower 95% confidence intervals (C.I.).

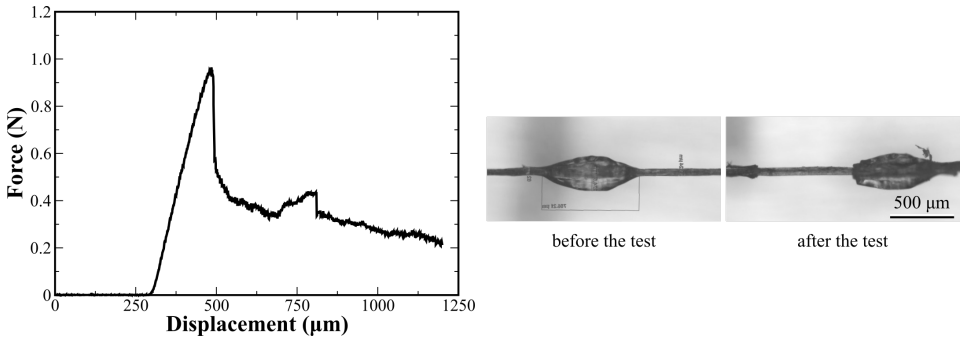

Figure 5.3: An example of the microbond test: test data, droplet positions before and after the test, respectively, for Arkema Elium®150 - flax fibre system.

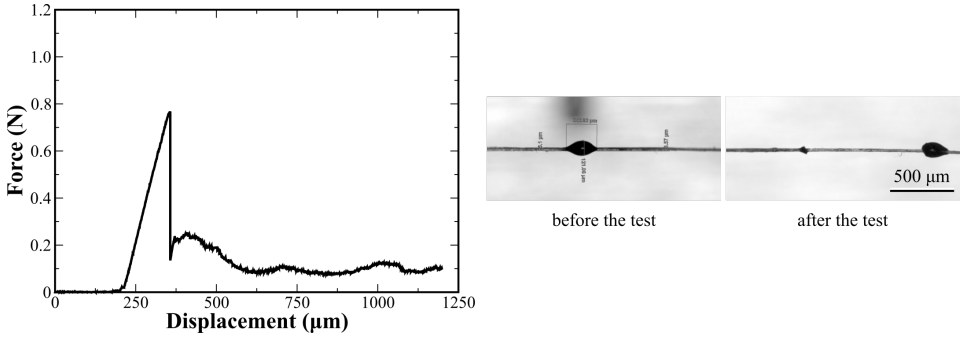

Figure 5.4: An example of the microbond test: test data, droplet positions before and after the test, respectively, for Furacure (PFA) - flax fibre system system.

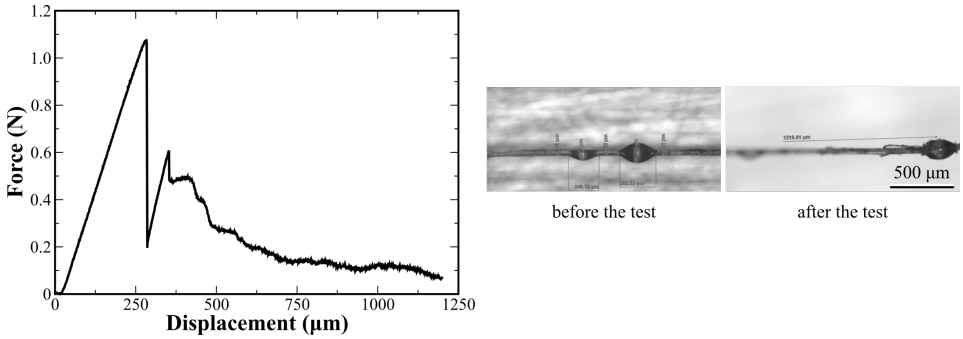

Figure 5.5: An example of the microbond test: test data, droplet positions before and after the test, respectively, for Vitrimax™T100 flax - fibre system system.

A linear fit that passes through the origin was applied to the debonding data to get the IFSS value, τ_{fit}, for the investigated fibre/resin combinations. τ_{fit} and τ_{mean}, which is the average IFSS values calculated for each debonding data using Eq. 5.1, are given in Table 5.1. A good consistency was found between τ_{fit} and τ_{mean}. Moreover, τ_{fit} lines were in good agreement by being within the range of upper and lower bounds of 95% confidence intervals, as highlighted in Fig. 5.2.

Table 5.1: Interfacial shear strength values obtained by linear fitting (τ_{fit}) and the mean of interfacial shear strength values (τ_{mean}), critical fibre length (l_c), and critical aspect ratio (AR_c) of Elium®, epoxy, Furacure and Vitrimax™ matrices coupled with flax fibres. ρ and errors, ±, represent the correlation coefficient, and standard errors of the mean, respectively.

Flax Fibre coupled with	τ_{fit} **(MPa)**	τ_{mean} **(MPa)**	l_c **(mm)**	AR_c **(mm/mm)**
Elium®150	5.9 (ρ:0.96)	5.9 ± 0.2	3.1 ± 0.7	48.9 ± 6.6
epoxy	11.4 (ρ:0.77)	11.8 ± 0.8	1.6 ± 0.4	24.4 ± 4.2
Furacure	23.1 (ρ:0.90)	23.7 ± 1.5	0.8 ± 0.2	12.2 ± 2.1
Vitrimax™T100	18.3 (ρ:0.78)	20.0 ± 1.5	0.9 ± 0.2	14.5 ± 2.6

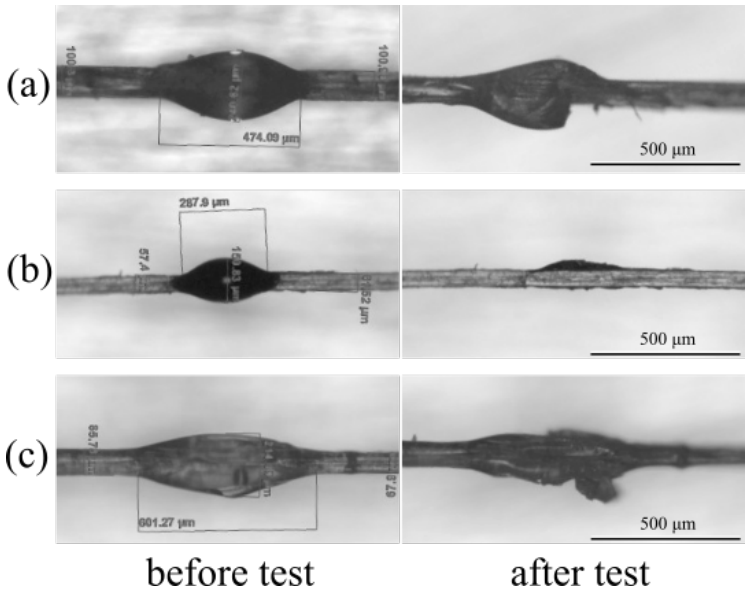

Figure 5.6: Examples of BM failures; microscope images of the droplet before and after the test for (a) Vitrimax™T100 (b) Furacure, and (c) Elium® - flax fibre systems.

Different behaviours were observed in failure types of flax fibres with the advanced matrices. Fibre failures (FF and FFD) are less frequently observed for Elium® and epoxy matrices as compared to Furacure and Vitrimax™ matrices. These data indicate that matrices with stronger IFSS tend to cause more fibre failure when coupled with natural fibres. It is noted also that fibrillation failure occurs before the applied force reaches the point of debonding, indicating that the fibres have weaker interactions between the fibrils than the bond with the resin. Moreover, a BM type failure was observed for small embedded areas (up to 0.10 mm^2) for thermoset based matrices, whereas the thermoplastic-based matrix (Elium®) exhibited the same failure type to 0.25 mm^2. This may imply that BM type failure is expected for smaller thermoset droplets in which the microvice damages the matrix, or for thermoplastic droplets where there is an insufficient degree of bonding within the microdroplet (see Fig. 5.6). Moreover, the residual stresses developed during the specimen manufacturing stage, caused by the different curing

or heat treatment required by each polymer, may influence the results of the microbond test; however, their effect is intrinsic to a particular fibre polymer combination.

To compare IFSS values of the microbond test data, statistical analysis was carried out using analysis of variance evaluated at a 95% level of significance and a p-value <0.05. Figure 5.7 presents this analysis, showing the variance of IFSS values of Elium®, epoxy, Furacure and Vitrimax™ matrices with flax fibres.

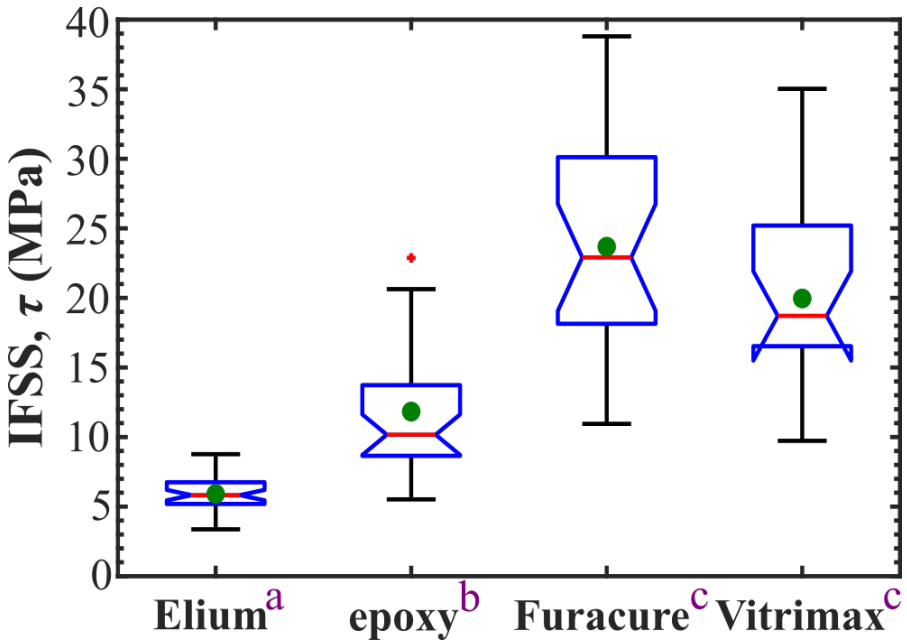

Figure 5.7: Analysis of variance of interfacial shear strength data of Elium®, epoxy, Furacure and Vitrimax™ matrices with flax fibres. Green dot, red line, black lines, and blue lines show mean, median, maximum and minimum values, and quarter percentiles and control limit values, respectively. Unique letters a, b, and c represent where there is a statistical difference ($p < 0.05$, N = 132), or not (c, $p > 0.05$), for resins.

This analysis demonstrates that Elium® has a significantly lower IFSS than epoxy resin. In addition, these are both significantly different to Furacure and Vitrimax™, which were found to have no statistically significant difference. It was found that Elium® shows the lowest adhesion performance with flax fibres. On the other hand, the Furacure and Vitrimax™ resins showed the highest level of adhesion, and they have a higher level of adhesion with flax fibres than the standard Prime20LV epoxy system. Moreover, the IFSS values for flax with different epoxy systems have been reported variously as 13–17 MPa [238], 23 MPa [271] by pull-out tests, 16–24 MPa (Prime20LV system) [242] by single yarn fragmentation test, and 33 MPa (24 MPa with maleic anhydride sizing) [243] by using single fibre fragmentation tests. It is noted here that the 'round-robin' test programme has also shown that pull-out tests give a higher IFSS value than the microbond tests [274]. Therefore, Furacure and Vitrimax™ are expected to have a higher IFSS, given that pull-out or fibre fragmentation tests have typically been carried out on these

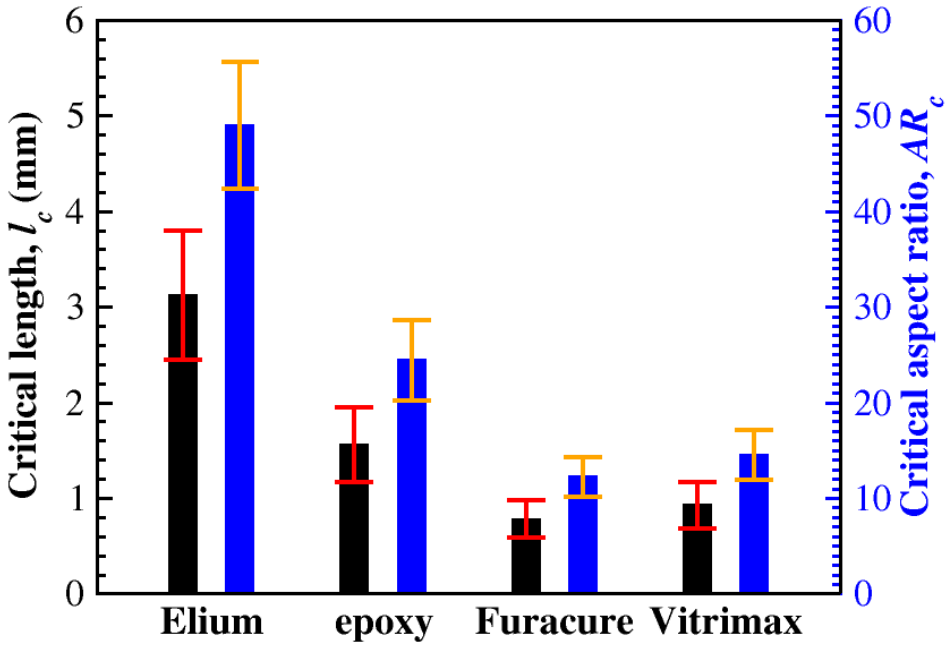

Figure 5.8: The critical fibre lengths, l_c (black), and the critical aspect ratio values, AR_c (blue) of Elium®, Furacure and Vitrimax™ with flax fibres. Error bars represent the standard errors of the mean.

resin systems. Although there is no consensus on which tests are the most reliable, it is expected that the IFSS values of both resin systems will be noticeably higher than the reported values in this study, hence also reflecting higher tensile strength values for FRPs [304].

Figure 5.8 reports both the critical fibre length and the critical aspect ratio (AR_c) values of the all matrix — flax fibre systems. The data are also summarised in Table 5.1. Increased reinforcement in discontinuous flax FRP can be obtained when fibres with longer lengths than the reported critical length values are used in the manufacturing stages. Moreover, the critical aspect ratio concept may be of more technical relevance than the critical fibre length [305], because different manufacturing processes may deliver fibres with different diameters but similar mechanical properties [306].

5.2.4 Sustainable Matrix Selection

In the first part of this chapter, the interfacial properties of flax fibres with three potentially sustainable advanced matrices were investigated and were compared with a commonly used commercial epoxy. It was found that Furacure and Vitrimax™ matrices are good candidates for making sustainable composites with flax fibres thanks to high interfacial shear strength. Since reuse, repair, and recycling options fit with end-of-life goals and provide more use of the already made-material, the Vitrimax™ matrix was selected for further mechanical and physical examination within discontinuous flax fibre composites.

5.3 Repair Performance of Vitrimer

This part of the chapter presents the manufacturing, mechanical and physical characterisation of short flax fibre reinforced vitrimers. In addition, the rapid low-temperature repair performance of aligned discontinuous flax fibre reinforced vitrimers (ADFFRVs) is uncovered.

5.3.1 Materials and Manufacture

To manufacture composite specimens, four layers of aligned 6-mm long flax fibre preforms (75–85 gsm) produced *via* the water based HiPerDiF fibre alignment method were sandwiched between five layers of Vitrimax™T100 resin film (150–250 gsm) sourced from Mallinda Inc. Figure 5.9 shows fibre volume fraction and estimated mechanical properties calculations for the manufactured composite. Further information about the use of the HiPerDiF technology to align natural fibres can be found in [11, 307]. The composite stack was then cured by vacuum bag moulding in an autoclave at 135 °C at 1 bar pressure for 30 min followed by another 30 min at ~6.5 bar pressure. Pure vitrimer resin specimens were prepared using the same semi-closed mould and cured at 135 °C at 1 bar for 30 min followed by another 5 min at 3 bar. The glass transition temperature, T_g, of Vitrimax™T100 is 100 °C and the theoretical topology freezing temperature, T_v, has not been disclosed. Since T_v is governed by T_g in polyimine vitrimer systems, it can be assumed that T_v is lower than or equal to the T_g value and can be determined by dynamic mechanical analysis [176].

Material	Aerial Weight (gm^{-2})	Density (gcm^{-3})	Aerial Volume (cm^3m^{-2})
Flax fibre	~ 80 (75-85)	1.54	~52
VitrimaxT100	~ 200 (150-250)	1.05	~191

Equation for fibre volume fraction (v_f) = Aerial volume of flax / Aerial volume of the composite

$$v_f = 4\times\text{flax} / (4\times\text{flax} + 5\times\text{vitrimax}) = 4\times52 / (4\times52 + 191\times5) = 208 / 1163 = \sim 0.179 = 17.9\% \quad \textbf{(S1)}$$

Material	Tensile Strength (MPa)	Elastic Modulus (GPa)
Flax fibre	~ 580	~ 52
VitrimaxT100	~ 34	~ 2.7

Equation for simple rule of mixtures for elastic modulus (E) = $E_{composite} = E_f v_f + E_m(1-v_f)$

$$E_{composite} = 52\times0.179 + 2.7\times0.821 = 11.53 \text{ GPa} \quad \textbf{(S2)}$$

Equation for simple rule of mixtures for tensile strength (TS) = $TS_{composite} = TS_f v_f + TS_m(1-v_f)$

$$TS_{composite} = 580\times0.179 + 34\times0.821 = 131.7 \text{ MPa} \quad \textbf{(S3)}$$

Figure 5.9: Fibre volume fraction and estimated mechanical properties calculations of the composite made of four layers of aligned 6-mm long flax fibre preforms that are sandwiched between five layers of Vitrimax™T100 and properties of the constituents.

5.3.2 Testing Methodology

5.3.2.1 Tensile Test

Referring to ASTM D3039/D3039M-17 [291], the ADFFRV and vitrimer specimens were tensile tested on an electro-mechanical testing machine at a test speed of 1 mm min^{-1}. Extension was measured using a video extensometer (IMETRUM, Bristol, UK) and converted to strain. A 10 kN load cell (Shimadzu, Kyoto, Japan) was used to record the load. The nominal sizes for specimens' widths and lengths were 5 and 150 mm, respectively; no end-tabs were used, and the specimens were gripped with hand-screwed clamps leaving a 50 mm gauge length. The specimen thicknesses were between 1.1–1.4 mm for the ADFFRV specimens and between 0.6–0.7 mm for the vitrimer specimens.

5.3.2.2 Visual Characterisation

A high-resolution scanner (Epson Expression 11000XL, Epson, Shinjuku, Tokyo) was used to acquire high-resolution images of the fractured regions of the composite specimens. An optical microscope (Zeiss Axio Imager M2, Carl Zeiss AG, Oberkochen, Germany) was used to analyse cross-sections of the composite specimens. Cold mounting followed by standard wet grinding and polishing for polymer matrix composites was applied to make the specimens for cross-section analysis. A scanning electron microscope (Hitachi TM3030Plus, Hitachi, Ltd., Tokyo, Japan) was used to analyse the fracture surfaces of the composite specimens.

5.3.2.3 Repair Strategy

A low-temperature and rapid technique was devised in order to assess the repair performance of aligned discontinuous flax fibre vitrimers. Broken samples were placed in a semi-closed mould that was then located between heated plates in a 50 kN load cell (Instron, Buckinghamshire, UK). Then a 0.69 MPa pressure was applied for 5 min at 120 °C to repair the samples. The broken ends of the samples were placed in contact with one another, and two repair strategies were tested; (i) unpatched and (ii) single-patched on samples that had already been broken and repaired using method (i). Methods (i), (ii), and the repair process are represented schematically in Figure 5.10. Patches were obtained from a spare specimen and assumed to be identical to the original specimen in terms of fibre volume fraction and alignment. For comparison, vitrimer specimens also were repaired using method (i). However, during repair, the pressure was applied for only 3 min, again at 120 °C to prevent resin leaking at the edges of the sample and drastic dimensional changes.

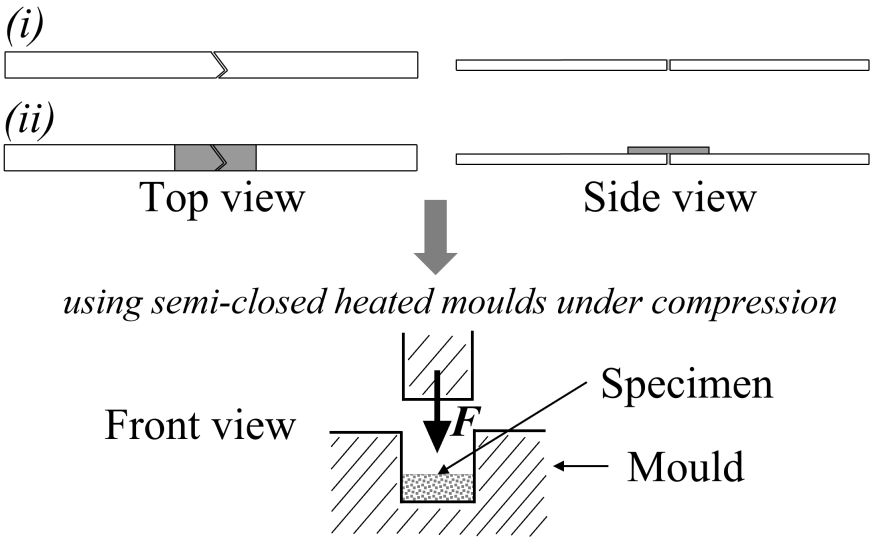

Figure 5.10: Schematics of two composite repair strategies taken from a top view and a side view of the specimens; (i) end-to-end repair and (ii) single-patched on samples that are pre-fractured and repaired using (ii), and a schematic representation of the repair process. White filled shapes and grey filled rectangular regions represent the fractured specimen pieces and a patch, respectively. The patch is identical to the original specimen.

5.3.3 Results and Discussion

5.3.3.1 Mechanical Properties of Original and Repaired Vitrimer

Tensile tests were performed to obtain the mechanical properties of the vitrimer. In total, six pure vitrimer specimens were tested: four successfully broke within the gauge length, and were used to calculate the mechanical properties of the as-manufactured specimens. Those specimens were then repaired, once, twice, and three times. Figure 5.11 reports representative stress–strain curves, typical high-resolution images and the mechanical properties of as-manufactured (original) and repaired vitrimer specimens.

Table 5.2: Mechanical properties of as-manufactured (original) and repaired vitrimers (Vitrimax™T100). Errors represent SD from the mean.

	Elastic Modulus (GPa)	**Tensile Strength (MPa)**	**Strain to Failure (%)**
Original	2.1 ± 0.1	34.1 ± 0.8	2.1 ± 0.3
1st repair	2.7 ± 0.2	34.5 ± 5.6	1.6 ± 0.4
2nd repair	2.7 ± 0.2	38.4 ± 5.2	1.7 ± 0.3
3rd repair	2.6 ± 0.2	34.5 ± 4.5	1.6 ± 0.3

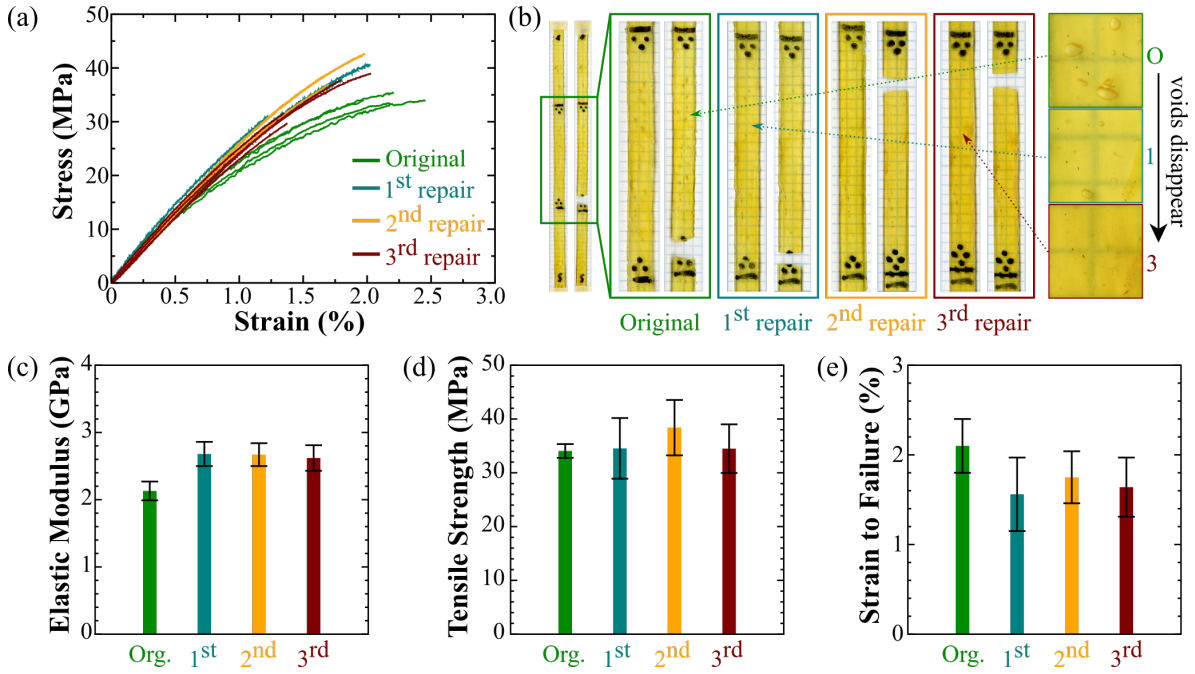

Figure 5.11: (a) Representative stress–strain curves, (b) high resolution images, (c) elastic modulus, (d) tensile strength, and (e) strain to failure of the original (Org.) and repaired (1st, 2nd, 3rd repairs) vitrimer specimens. Errors represent standard deviations (SD) from the mean.

As seen in Figure 5.11a, the stress–strain curves of the repaired specimens show similar trends and comparable values of failure strain and strength. There is however a noticeable difference from the original curves, where the data deviate more markedly from linearity compared to the repaired specimens. Figure 5.11c, d, and e show elastic modulus, tensile strength, and strain to failure of the vitrimer specimens, respectively. In addition, the mechanical properties are summarised in Table 5.2. A statistically significant increase was observed in elastic modulus values from the original to a first time repaired vitrimer specimen, after which a plateau was reached for further repairs. The reason for the modulus increase was thought to be the extraction of air (see Fig. 5.11b) from trapped voids between the vitrimer film layers during the manufacturing process, and caused by the high-pressure applied during the first repair step in which a temperature above T_g~T_v was applied. The failure regions of specimens were inspected and found to be far from the location where there are visible voids. No significant change was observed between the original and repaired vitrimer specimens in terms of tensile strength. Tensile strength values were found to be consistent with the stress at break of a crosslinked polyimine network, which has been reported to be ~40 MPa [180] and 10–60 MPa [181] from two independent studies. Furthermore, a slight decrease was seen for the strain to failure from the original to repaired vitrimer specimens.

5.3.3.2 Mechanical Properties of Original and Repaired Flax Fibre Reinforced Vitrimers

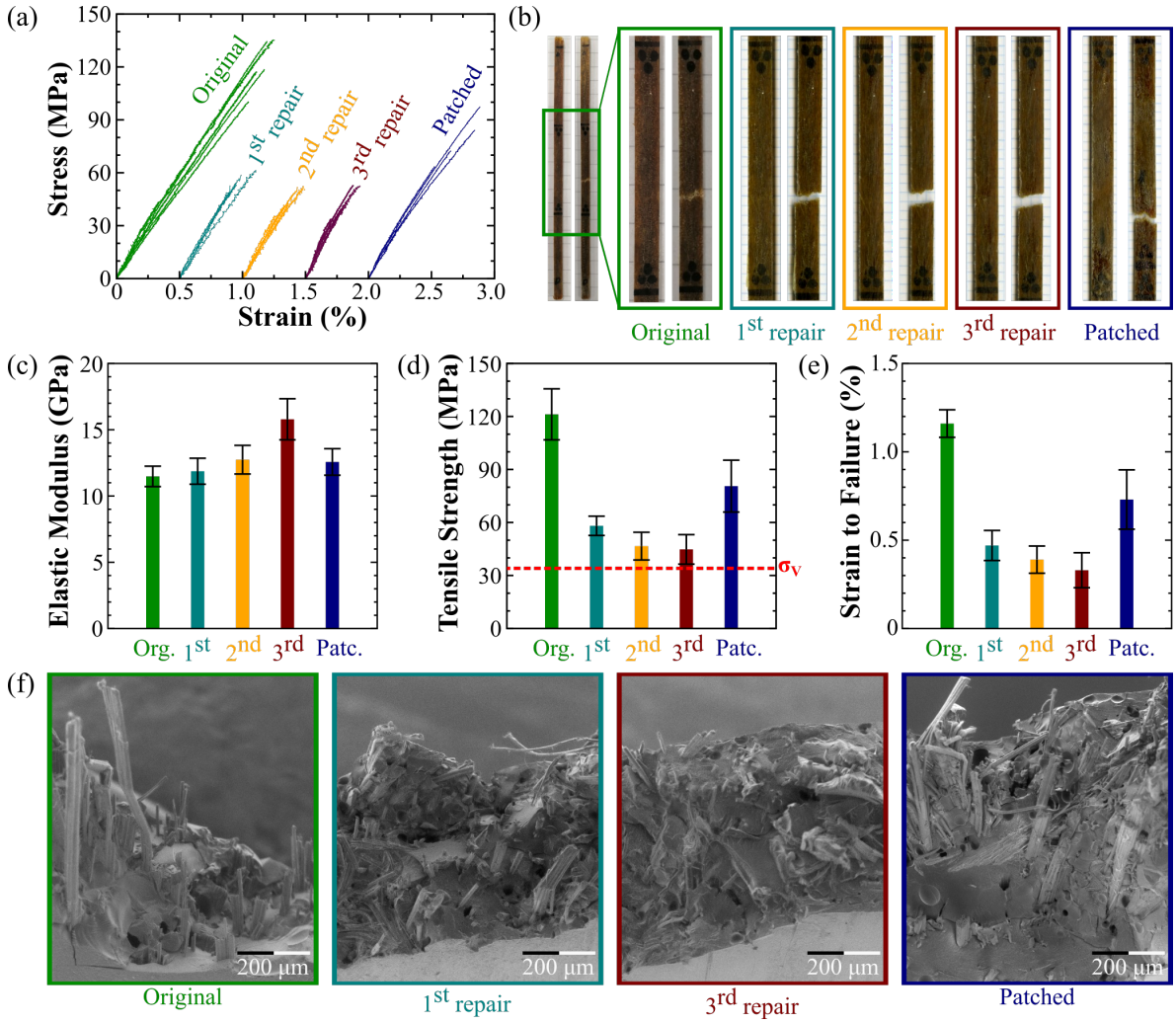

Figure 5.12: (a) Representative stress–strain curves, (b) high resolution images, (c) elastic modulus, (d) tensile strength (red line represents tensile strength of the vitrimer), (e) strain to failure for original (Org.) and repaired (1st, 2nd, 3rd repairs) and patched (Patc.) specimens, (f) typical scanning electron micrographs of the original and repaired ADFFRV specimens. Errors represent SD from the mean. In (a), 0.5, 1.0, 1.5, and 2.0% strain reference points are the starting points, respectively, for the 1st, 2nd, 3rd, and patched repairs.

The mechanical properties of the ADFFRVs were determined, both on original and repaired specimens. In total, six specimens were tested, of which five (four for single side patched ADFFRV) successfully broke within the gauge length and were used to calculate the mechanical properties. Figure 5.12 reports representative stress–strain curves, high-resolution images, mechanical properties, and scanning electron micrographs of original, repaired, and patched ADFFRV specimens. The expected fibre volume fraction calculated using the average areal weights and

Table 5.3: Mechanical properties of as-manufactured (original) and repaired aligned flax fibre reinforced vitrimers. Rule of mixtures (RoM) is calculated for v_f = 17.9%. Errors represent SD from the mean.

	Elastic Modulus (GPa)	**Tensile Strength (MPa)**	**Strain to Failure (%)**
RoM	11.5 ± 0.7	131.7 ± 4.9	-
Original	11.5 ± 0.8	121.2 ± 14.4	1.2 ± 0.1
1st repair	11.9 ± 1.0	58.1 ± 5.5	0.5 ± 0.1
2nd repair	12.7 ± 1.1	46.6 ± 7.8	0.4 ± 0.1
3rd repair	15.8 ± 1.5	44.1 ± 8.4	0.3 ± 0.1
Patched	12.6 ± 1.0	80.6 ± 14.7	0.7 ± 0.2

densities of the constituents was found to be 17.9% (see Fig. 5.9 Equation S1). The mechanical properties of fractured and repaired ADFFRVs are summarised in Table 5.3.

As seen in Figure 5.12a, there are decreasing trends in the stress–strain curves of the ADFFRV specimens in terms of their slope, and the strain and stress values at failure for each end-to-end repair stage. In contrast, the patched repair specimens showed a moderate increase in properties. Figure 5.12c shows the elastic modulus of the ADFFRV specimens; agreement was found between the expected elastic modulus calculated using the RoM (see Fig. 5.9 Equation S2) and the experimentally determined values of the as-manufactured ADFFRV, 11.5 ±0.7 GPa and 11.5±0.8 GPa, respectively. The match between oversimplified RoM is coincidental since it is expected that the RoM result is overestimated due to that fact that porosity in the system will decrease the mechanical performance. This coincidental match may indicate that the tensile strength of the flax fibre was under-calculated since it was done with 40mm gauge length because longer length fibres give lower strengths. It may also indicate that fibre length distribution and effect plays negligible role since it was greater than the l_c (1 mm).

In addition, a dramatic increase was seen in elastic modulus values of end-to-end repair stages. After the patched repair method, a decrease in the elastic modulus value towards the original value was observed. The elastic modulus increase trend for end-to-end repair stages and a decrease after the patched repair is needed to be investigated in detail for future. There is no literature knowledge on this behaviour; however, there is a stiffening effect for fibres gone through heat treatment cycles, which may be related to this behaviour [308].

Figure 5.12d shows the tensile strength of the ADFFRV specimens. A good correspondence was also found between the expected tensile strength estimated using the simple rule of mixtures, which is 131.7±4.9 MPa (see Fig. 5.9 Equation S3), and the tensile strength of the original ADFFRV, which is 121.2±14.4 MPa. Moreover, it was seen that there is a negative exponential saturation trend towards the tensile strength of the vitrimer in end-to-end repair cycles of ADFFRV specimens. As seen in the high resolution scans of tensile tested ADFFRV specimens (Fig. 5.12b), the failure points occurred in the same locations as the original materials for all the

end-to-end repaired samples. Wu *et al.* [309] have seen similar behaviour where repaired vitrimer specimens were broken in the same location as the original material failure region after re-joining broken pieces in the mould with a small overlap in the fractured area and hot-pressing them at 190°C for 2h with a pressure of 0.5 MPa. The strength recovery of carbon/vitrimer systems was ~%67, which is better than that observed in ADFFRV 1st repair (~%50) that is significantly shorter than their method with respect to time. The elastic modulus remained the same in their study similar to in this study after 1st repair cycle. Additionally, the failure regions became less rough, indicating a lower presence of fibres and a more resin dominated healing. When the patching repair method was applied to the three times repaired ADFFRV, the failure region became more jagged. In addition, the fibres became noticeable on the failure surface, which is in a slightly different location compared to the previous failures.

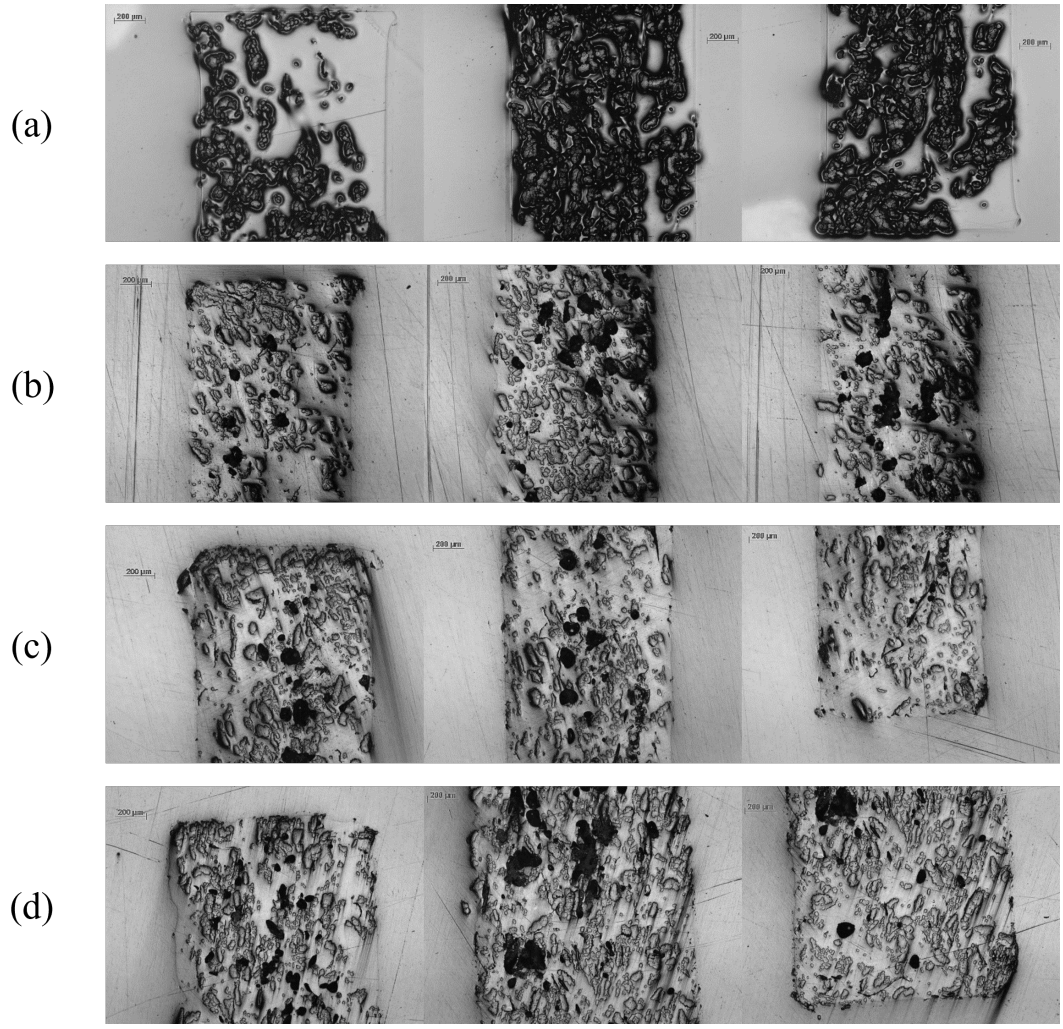

Figure 5.13: The cross section images of (a) original (b) first time end-to-end repaired (c) three times end-to-end repaired and (d) single-patched repaired aligned discontinuous flax fibre reinforced vitrimers.

As seen in table 5.3, an almost doubling of tensile strength was seen for the patched repaired ADFFRV samples compared to the three times repaired materials; this in turn is nearly two-thirds of the original samples. To reveal the reason behind the change in mechanical performances in repaired ADFFRV, scanning electron microscopy analysis was carried out for the failure region of ADFFRV specimens, as shown in Figure 5.12f. It can be seen that there are aligned fibres in the failure region of the original ADFFRV. There are however fewer aligned or distorted fibres, and in some regions no fibres at all, in the end-to-end repaired ADFFRVs. Zhao *et al.* [310] reported similar electron microscopy analysis on healed vitrimer composite specimens after the tests, which showed the broken fibres embedded in the vitrimer matrix and residual cylindrical grooves caused by the broken fibres being pulled out. The fracture surface of secondly healed specimen was rougher in comparison to the one of firstly healed specimen since there were more broken fibres and grooves. Additionally, the broken fibres had no better load-bearing capacity than the long fibres, and the recovery of mechanical properties was limited due to this [310], which was also seen in end-to-end repaired ADFFRV specimens in this study. As observed in high resolution scans of tensile tested ADFFRV, the presence and condition of fibres were changed after repair and affected the mechanical performance of the composites. After the patch repair, the number of aligned fibres increased, which could explain the increase in tensile strength, and some distorted fibres were observed. In the images of the cross-sections of the patched and original specimens, no significant differences were observed (see Fig. 5.13). Moreover, a significant decrease was observed for the strain to failure values in the end-to-end repair specimens. An increase in the strain to failure value towards the value of the original composites was seen in the patched specimens after three times of repairing ADFFRV.

5.4 Conclusion

- The bio-based (PFA) and vitrimer (imine-linked) resins were observed to be good candidates for producing sustainable composites with flax fibres due to high IFSS values. On the other hand, the advanced thermoplastic resin, Elium®, showed the poorest adhesion with flax fibre.
- Owing to its reversible covalent network feature and high IFSS, a vitrimer resin was selected as a promising candidate for sustainable discontinuous flax fibre composites, and its repair performance was examined.
- End-to-end and single patch repair methods were used as a repair strategy to investigate the repair capabilities of the vitrimer resin in flax fibre reinforced composites. It was found that a rapid and low-temperature end-to-end repair strategy is able to recover half of the strength of the as-manufactured composites.
- The single patch repair method showed better recovery (~67%) than end-to-end repair. The single patch repair method might show better mechanical recovery when applied as first

repair strategy. The patch method can be suitable by applying heat, pressure, and vacuum on a crack region for reinforcing the area where cracks happened on the composite product. But it is important to mention a simple repair technique, which can be obtained by heat, pressure, and time on vitrimer composite products in industry, can be used for prevention of crack propagation or extending fatigue life of composite product if the material is not fractured aggressively for example for creep or impact damage.

- It was foreseen that time, temperature, and pressure must be optimised to identify the maximum repair performance of fibre-reinforced vitrimer composites. In conclusion, aligned natural fibre reinforced vitrimers can be reused, repaired, and recycled: this represents a step towards a circular economy and sustainability in fibre reinforced composites.

Chapter 6

Overall Discussion

This chapter revisits the key findings of the research topics, identifies their connections and comments on limitations. Based on results and limitations, future perspectives on sustainable discontinuous fibre reinforced polymers and methods to examine their properties are also presented in this chapter.

6.1 Overarching Remarks

In Chapter 3, abundant plant-based natural fibres were investigated intrinsically in terms of physical, thermal, and mechanical properties to assess their suitability for aligned discontinuous fibre reinforced polymer (ADFRP) manufacturing methods. Moreover, micromechanical tests were carried out to determine the stiffness, strength, elongation and interfacial shear strength of the fibres with epoxy resin to provide a database for sustainable reinforcement material selection. In addition, the critical lengths of the natural fibres, which are important for defining the mechanical performance of short fibre composites, were calculated for processing ADFRPs. The critical fibre length and micromechanical test results supported the following chapter.

In Chapter 4, candidate fibres, which are curaua, flax, and jute fibres, were used to reinforce epoxy, PLA, and PP matrices to produce the HiPerDiF ADFRPs. These composites' mechanical and fracture properties were investigated as well as their physical properties (density, porosity, water absorption, and fibre volume fraction). This investigation presented another extensive database and allowed a material selection by considering their mechanical and processing performance in ADFRPs, mainly focusing on the HiPerDiF process. As a result, flax fibre with a desirable fibre length (6 mm or more) was found as a promising sustainable reinforcement material for ADFRPs in terms of mechanical performance and current market availability, especially for the UK and EU.

Chapter 5 presented a further database for the candidate flax fibre, which shows the interfacial shear strength of flax fibre when coupled with sustainable polymers to allow matrix selection. The considered sustainable polymers were a vitrimer that combines the advantageous

properties of thermosets and thermoplastics, a fully bio-based thermoset and an advanced thermoplastic because each of them offers the potential for recyclability, repairability, reusability, use of renewable sources or reduced emissions of volatile organic compounds. The vitrimer and bio-based thermoset matrix were found to have higher adhesion to the flax fibres compared to a conventional epoxy matrix; the advanced thermoplastic resin had the lowest adhesion. The vitrimer matrix was selected as a candidate for recyclable and repairable; hence sustainable flax fibre reinforced composites. The mechanical and low-temperature rapid repair performance of a composite made from aligned flax fibres produced using the HiPerDiF method was investigated. End-to-end and single patch repair methods were performed: vitrimer matrix composites showed a potential for strength recovery that would allow reuse over multiple life cycles, consistent with the circular economy goals in FRPs.

In the individual chapters of this thesis, plant-based natural fibres to produce ADFRPs were investigated in detail. First, a foundation was laid by evaluating the physical and mechanical properties of numerous natural fibres in order to create a database for the selection of sustainable reinforcement materials. Building on this, the fibres and matrices were examined and from this study flax was identified as a promising sustainable material for ADFRP. Finally, the focus shifted to matrix selection, demonstrating the excellent adhesion of the Vitrimer matrix to flax fibres and its potential for recyclable and repairable composites. These results are in line with the goals of the circular economy and highlight the feasibility of sustainable solutions for FRP. This research contributes to this field by creating comprehensive databases, providing insights into material and matrix selection, and demonstrating the potential for sustainable processes in the manufacture of ADFRP.

Furthermore, the mechanical properties and fibre volume fractions of investigated aligned flax fibre reinforced composites in this study are given in Table 6.1, and they are compared with the literature on similar flax fibre systems and common synthetic FRPs in aligned or continuous fibre form. Table 6.1 visualises important results in the presented thesis and includes the results of the high fibre volume fraction trial on aligned discontinuous flax fibre reinforced vitrimers (ADFFRVs) from the following section.

It is well known that the best competitive advantage of natural fibre-based composites is their specific mechanical properties against synthetic FRPs, but this does not work against carbon FRP due to extraordinary carbon fibres' intrinsic mechanical properties and density. Generally, high carbon fibre volume fraction FRPs have a density around 1.5-1.6 gcm^{-3}, and high glass fibre volume fraction FRPs have a density around 1.9-2.2 gcm^{-3}. As seen in this work, moderate or high natural fibre volume fraction FRPs have a density around 1.2-1.4 gcm^{-3}, which shows a slight difference between carbon FRPs to compare specific mechanical properties. Conversely, the difference in densities makes natural FRPs comparable to glass FRPs in terms of specific mechanical properties. If we take the case of discontinuous flax/Vitrimax™ and continuous glass/epoxy FRP systems, specific elastic modulus values can become similar, as predicted before

Table 6.1: Mechanical properties and fibre volume fractions of investigated aligned flax fibre reinforced composites and comparison with unidirectional and random aligned flax, glass, and carbon FRP literature values [18, 26, 81, 86, 159, 311]. HiPerDiF-aligned discontinuous (H-AD) FRP, aligned discontinuous FRP (AD), continuous(C) FRP, random aligned (R) and normalised results (N) are the types mentioned in the table. All flax fibres represent the same type of flax obtained from Ecotechnilin but carbon and glass fibres may represent different types of their classes. Some of flax/Vitrimax™T100 results were taken from Section 6.2.

	Type	**Elastic modulus (GPa)**	**Tensile strength (MPa)**	**Fibre volume fraction**
flax/epoxy	H-AD	32	204	0.43
flax/PLA	H-AD	17	44	-(<0.3)
flax/PP	H-AD	31	138	0.52
flax/Vitrimax™T100	H-AD	12	121	0.18
flax/Vitrimax™T100	H-AD	18	175	0.27
flax/Vitrimax™T100	N	30	294	0.50
flax/epoxy	C	35	280	0.42
flax/epoxy	C	32	268	0.48
flax/epoxy	C	40	378	0.42
flax/MAPP	C	18	151	0.33
flax/PBS	C	17	184	0.33
flax/PHA	C	20	182	0.33
flax/PLA	C	20	216	0.34
flax/PP	C	18	133	0.32
flax/PP	C	26.9	251	0.43
flax/epoxy	R	9.2	60	0.22
flax/PP	R	8.8	57	0.40
flax/PP+3.5wt%MAPP	R	8.6	68	0.40
glass/epoxy	C	53	1252	0.60
glass/epoxy	C	39	1080	0.55
glass/epoxy	C	31	817	0.48
glass/PP	C	43	720	0.58
glass/PP	C	26.5	700	0.35
glass/PP	R	6.2	89	0.22
glass/PP	R	2.2	49	0.15
carbon/epoxy	C	136	2048	0.60
carbon/epoxy	H-AD	80.6	816	0.41
carbon/epoxy	H-AD	115	1509	0.55
carbon/epoxy	AD	60	650	0.35
carbon/epoxy	AD	119	1211	0.55
carbon/Vitrimax™T100	C	69	900	0.62
carbon/Vitrimax™T130	C	114	1723	0.62

in Chapter 3. However, specific tensile strength values are still better for glass/epoxy systems. This may be improved with sizing or initial fibre quality, as mentioned in Chapter 2. As seen in Table 6.1, there is a significant change in the mechanical properties of Vitrimax™T100 and Vitrimax™T130 for carbon FRPs. Therefore, changing the Vitrimax™ type proposes a better performance for flax fibre FRPs. In addition to sustainability and specific elastic modulus, improved tensile strength can make the flax/Vitrimax™T130 system completely competitive with continuous glass FRPs.

It was also seen in Table 6.1 that ADFRPs produced with the HiPerDiF method show similar performance to the literature values of continuous or aligned FRPs. For example, the mechanical properties of flax/Vitrimax™T100 composite are comparable to those of biodegradable flax/MAPP, PBS, PHA, PLA, and PP composites, even with a smaller fibre volume fraction. Moreover, it was reported in Chapter 5 vitrimers and biobased thermosets have IFSS values between 20-24 MPa, which are higher than those of biodegradable polymers, which are 5-16 MPa [86]. This difference promises better performance and dictates a different sustainable route that does not include the biodegradability that MAPP, PBS, PHA, and PLA resins provide. It was expected that aligned fibre-reinforced biobased thermosets, which have slightly higher IFSS values than vitrimers, have the better or similar mechanical performance to vitrimer composites.

Moreover, Table 6.1 also visualises the advantages of aligned FRPs over randomly aligned FRPs. Randomly aligned flax and glass FRPs have maximum 10 GPa tensile modulus and less than 100 MPa tensile strength. H-AD type flax FRPs shows much better mechanical performance (except PLA in terms of tensile strength) for equivalent or lower fibre volume fractions (*i.e.* flax/vitrimax systems). It should be noted that normalised result of flax/Vitrimax has comparable mechanical properties to those of flax/epoxy continuous FRPs, flax/PP continuous FRPs, glass/PP continuous FRPs (only tensile modulus) and glass/epoxy continuous FRPs (only tensile modulus) for similar fibre volume fraction values.

6.2 ADFFRV: higher fibre volume fraction results

Additional work was carried out to assess mechanical and repair properties for higher flax fibre volume fraction in ADFFRVs. To manufacture composite specimens, four layers of aligned 6-mm long flax fibre preforms were sandwiched between 3 layers of Vitrimax™T100 resin film, with which one layer of resin film was in the middle. The lay-up has a nominal fibre volume fraction of 0.266 calculated by using the methodology in Fig. 5.9, and the manufactured composites were expected to have 179 MPa of tensile strength and 16 GPa of elastic modulus. Six specimens were tensile tested to failure, and their stress-strain curves are given in Fig. 6.1.

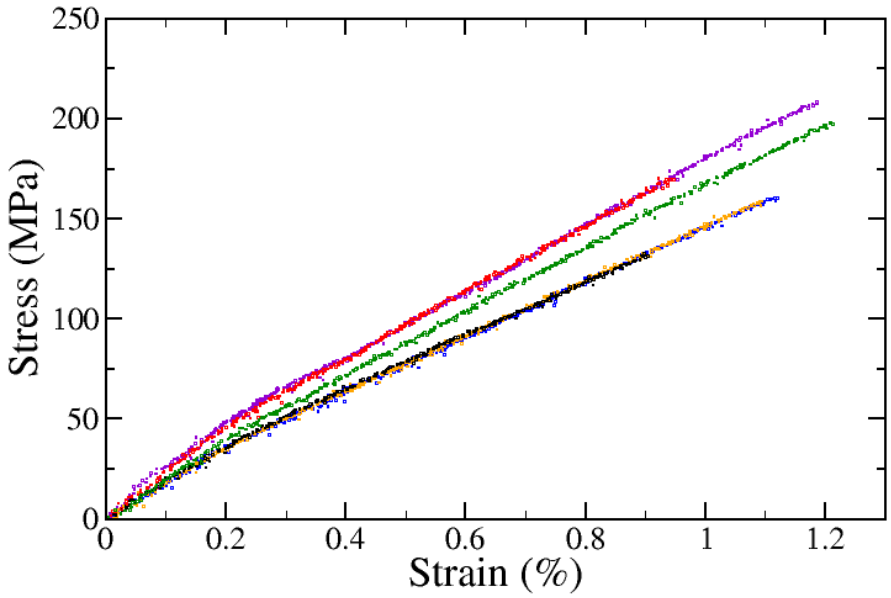

Figure 6.1: Stress-strain curves of higher discontinuous flax fibre volume fraction vitrimer composites.

As seen in Fig. 6.1, the stress-strain curves of this batch have a similar behaviour compared to as-manufactured flax fibre reinforced vitrimers given in Fig. 5.12. Under load, natural fibres can undergo reorientation, especially in unidirectional or highly aligned discontinuous FRPs and this reorientation may result in changes to the stress distribution and consequently affect the overall stress-strain behaviour [312]. As the natural fibres reorient, the composite's stiffness and strength could change and leads to nonlinearity.However, the nonlinearity is observed in the stress-strain curves is not considered to be a strain hardening, and it is considered to be matrix yielding, which shows decreasing gradient. The composite specimens showed similar brittle failure. Stress at the failure of the specimens relies on between 136-211 MPa, and strain at failure values are between 0.9-1.2%. Elastic modulus was calculated to be between 16-20 GPa. The obtained mechanical properties and expected mechanical properties according to the nominal fibre volume fraction were found to be in agreement. Figure 6.2 shows the mechanical properties of the composites in terms of fibre volume fraction with the comparison of a simple rule of mixtures (RoM) line and expected value at 0.5 fibre volume fraction after normalisation by using the experimental values.

As seen in Fig. 6.2, the elastic modulus values obtained from experiments follow the RoM trend, especially the lower volume fraction value at the RoM line. On the other hand, the higher volume fraction value is slightly above the RoM values line. Because of that, the normalised value (30 GPa) at 0.5 fibre volume fraction, which is calculated by using two experimental values and the elastic modulus of the vitrimer (2.7 GPa), is higher than the expected value (27 GPa) of the RoM line. Furthermore, the experimental tensile strength values also follow the RoM trend and are slightly under the values line. The normalised value (294 MPa) at 0.5 fibre volume fraction that is obtained by using two experimental values and the tensile strength of the vitrimer (34

MPa) is very close to the expected value (307 MPa) of the RoM line.

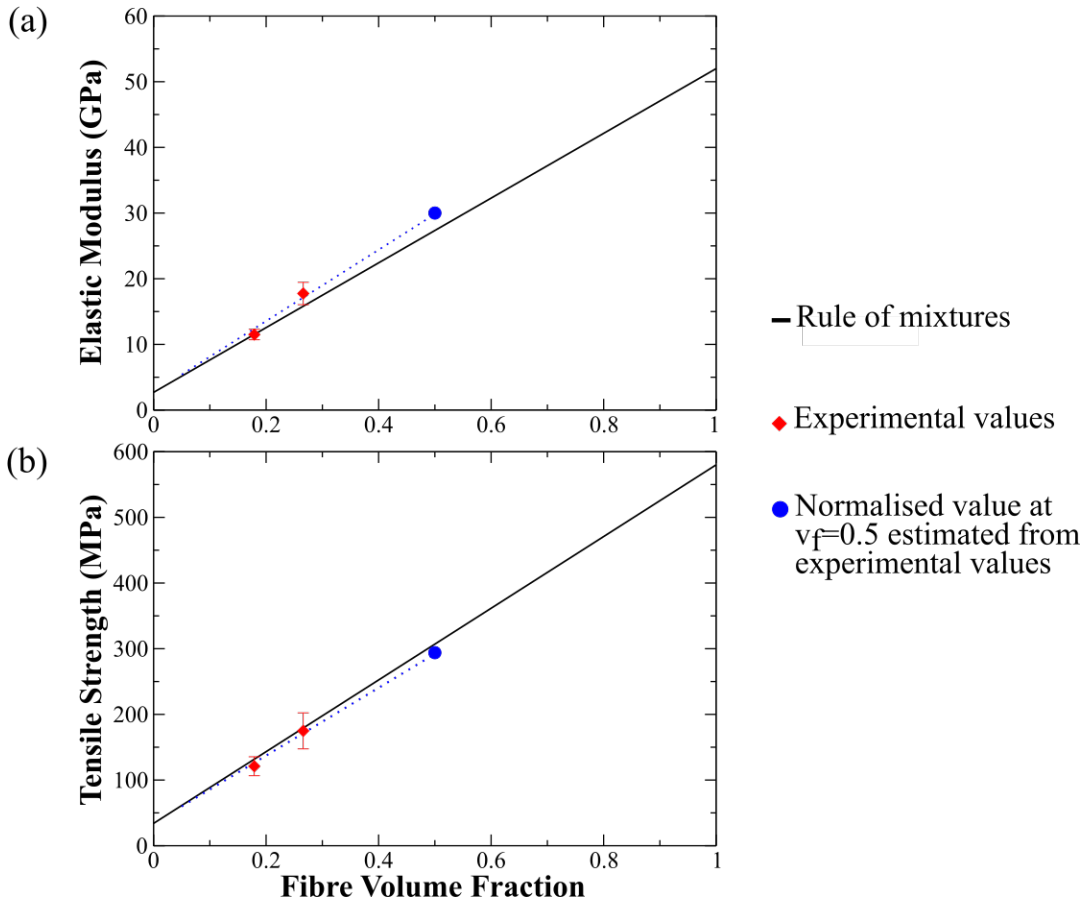

Figure 6.2: (a) Elastic modulus and (b) tensile strength of aligned discontinuous natural fibre reinforced vitrimers in terms of fibre volume fraction. A rule of mixtures (which assumes zero porosity, perfect load transfer, perfect interface between resin and fibre, and no misaligned fibres) was used to draw the linear line. Error bars indicate standard deviation.

The repair work done in Chapter 5 was applied to the composite specimens that have higher volume fractions as well. After a visual examination, it was found that the repaired samples were poorly healed after a tensile failure, and only two of them were repaired. Owing to time constraints, material, and Covid-19 restrictions, further investigations on why this happened were cancelled. However, this experience hints at and supports several ideas and experimental plans that can be valuable for future works, which will be mentioned later in the following chapter.

In Table 6.1, it can be clearly seen that flax/Vitrimax™ ADFRPs are promising in terms of their mechanical properties when compared with flax/epoxy or other flax/systems. Potential very high fibre volume fraction flax/Vitrimax™ ADFRPs can be in the position of the best mechanical properties in natural fibre composites. To expand this potential, a similar analysis done in Sec.3.4.1 was applied to compare aligned discontinuous glass fibre reinforced vitrimers and ADFFRV. This is a hypothetical scenario to evaluate the effect of substituting glass with flax

fibre in vitrimer composites. Table 6.2 shows the parameters used in Eqs. 3.7 and 3.8 to produce the counterplots, which displays the change increase in specific Young's modulus (IiSYM) of the vitrimer composites. Figure 6.3 shows the contour plot of IiSYM, which is a percentage change when flax fibre substitutes glass fibre in vitrimer composites as a function of fibre length, l, and fibre volume fraction, v_f. In Figure 6.3, IiSYM increases from the dark blue to dark red regions and white lines evince the transition lines, which reveal the influence of l clearly.

Table 6.2: Material properties used for contour plots produced by using Eqs. 3.7 and 3.8.

Parameters	**Flax Fibres EcoTechnilin** [this study]	**Glass Fibre C100, Vetrotex** [19]	**Matrix Vitrimax™T100** [179]
E (GPa)	52	73	2.70
ρ (g cm^{-3})	1.54	2.60	1.05
d (mm)	64	7	-

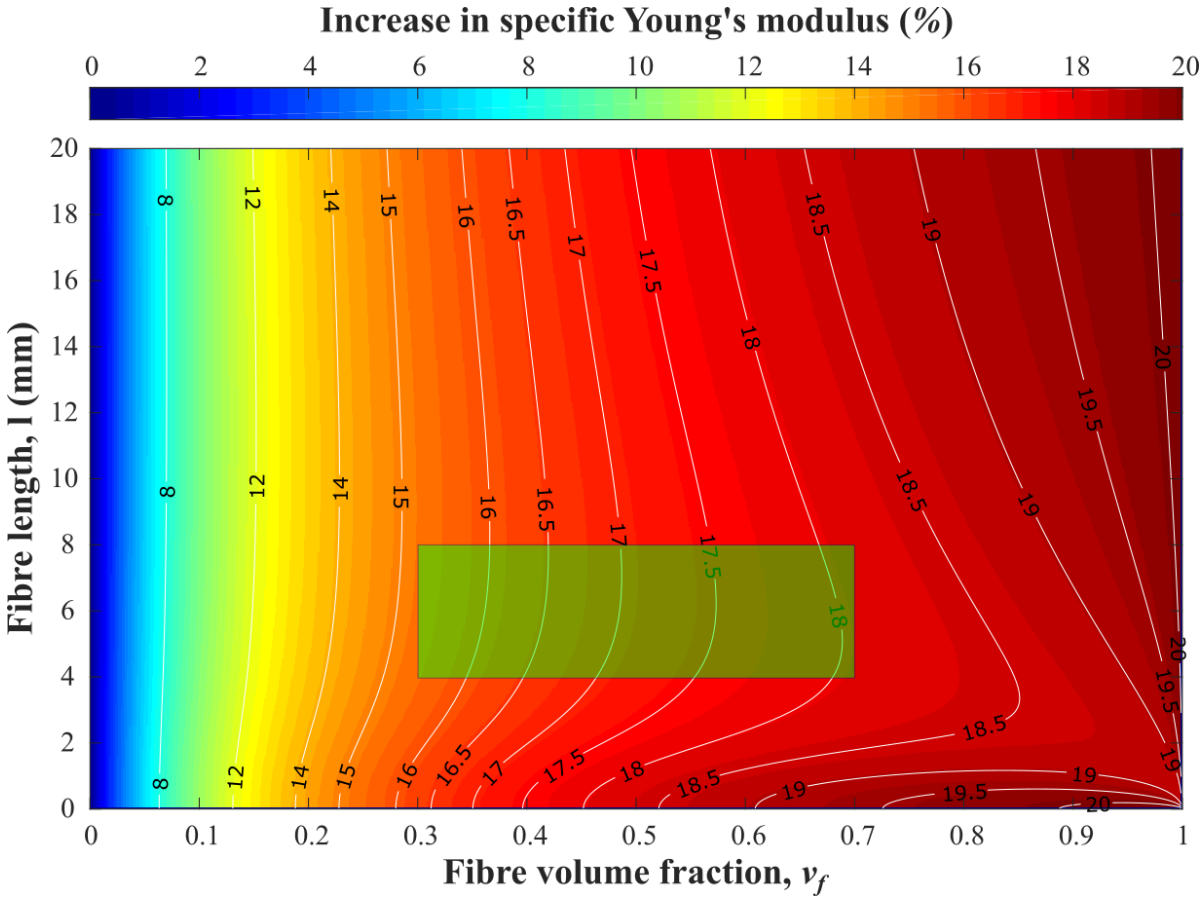

Figure 6.3: (a) Contour plot of the increase in specific Young's modulus, when glass fibre is replaced by flax fibre in aligned discontinuous fibre reinforced vitrimers, in terms of fibre volume fraction and fibre length. White isolines are scaled by the top colour axis.

Similar to Figure 3.16, Figure 6.3 shows more than 10% and up to 20% IiSYM in aligned discontinuous fibre reinforced vitrimers (ADFRVs) when glass fibres are substituted for flax fibres for every l and v_f higher than 0.1. The advantage of using flax fibre instead of glass fibres in ADFRVs strengthens in terms of IiSYM when v_f increases. On the other hand, the effect of l on IiSYM is not straightforward, as explained in Sec. 3.4.1. From the micron level to a few mm, l leads to a dramatic decrease and, after that, a gradual rise for IiSYM.

Since the present thesis showed that 6 mm flax fibre is a good fibre length for reinforcing polymers and the current version of the HiPerDiF machine works well with fibres that have 2-10 mm fibre length, it can be assumed that 4-8 mm l is an optimum flax fibre length for future works. If it is assumed that a region between 0.3-0.7 of v_f is an optimum v_f for future studies, a green box in Fig. 6.3 highlights the influence of using flax fibres in ADFRVs compared to glass fibres. As seen in the figure, 17% performance enhancement is the average gain when glass fibres are substituted for flax fibres in ADFRVs.

Recently, Summerscales *et al.* [265] provided the extended rule of mixtures to predict the mechanical properties of natural FRPs considering natural fibres' irregularity on area calculation. They have introduced fibre area correction factors for the rule of mixtures. As shown in Chapter 3, flax fibres have elliptical areas rather than circular areas. However, for simplicity, the mechanical properties of natural FRPs are calculated by using apparent diameter to determine the cross-sectional area of the polygonal natural fibres. Summerscales *et al.* showed that it is common to predict the mechanical properties (such as stiffness and strength) of natural FRPs low according to the scientific literature. Their proposed equation can produce improved predictions of the moduli and strengths of natural FRPs. By using their proposed equation, Eq. 3.7 is updated and shown in Eq. 6.1 below;

$$\frac{E_c}{\rho_c} = \kappa \eta_d \eta_0 \eta_1 V_f \frac{E_f}{\rho_f} + V_m \frac{E_m}{\rho_m} \tag{6.1}$$

where κ is the fibre area correction factor (FACF) and η_d is the fibre diameter distribution factor, which is 1 for fibres, which does not show variety in modulus according to the diameter. FACF is calculated as the mean circular cross-sectional area that is derived from the apparent diameter and divided by the mean true cross-sectional area for a statistically significant number of the fibres [265]. For flax fibres, FACF factors have been calculated as 1.06, 1.12, 1.39, 2.55, and 2.70 in the literature [265]. By considering the lowest values for flax fibres and the discrepancy in Fig. 6.2(a) (between the normalised value at $v_f = 0.5$ and rule of mixtures line), FACF of flax fibres are taken to be 1.1 in the calculations performed in this thesis. Figure 6.4 shows the contour plot of IiSYM with the effect of FACF when flax fibre substitutes glass fibre in vitrimer composites as a function of l and v_f.

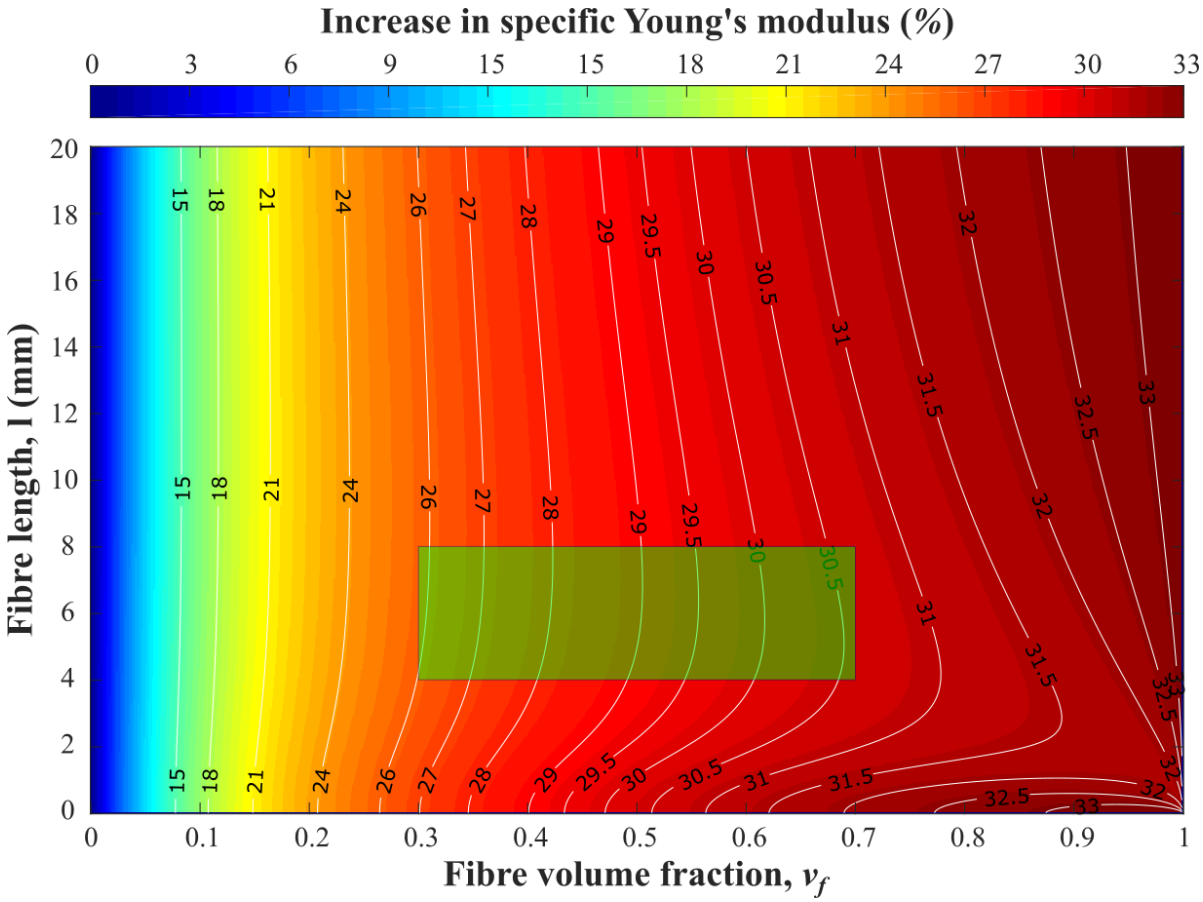

Figure 6.4: Contour plot of the effect of fibre area correction factor on the increase in specific Young's modulus with, when glass fibre is replaced by flax fibre in aligned discontinuous fibre reinforced vitrimers, in terms of fibre volume fraction and fibre length. White isolines are scaled by the top colour axis.

As seen in Fig. 6.4, if one considers the condition for every l and v_f higher than 0.15, there is more than 20% and up to 32% IiSYM in ADFRVs when the effect of FACF is considered. With the effect of FACF, it is seen that natural fibres can be predicted to be more effective in terms of specific mechanical properties. A green box highlights that up to 30% performance enhancement can be easily obtained by using 6mm flax fibres instead of 6mm glass fibres in ADFRVs. This analysis, with the correction of FACF, shows that significant weight saving can be achieved if natural FRPs take the place of glass FRPs in applications such as sporting goods, transport, and automobile industries.

Moreover, Marie [313] recently presented a life cycle analysis (LCA) on glass and flax fibre production from cradle to gate by using the MarineShift 360 software, which is an LCA tool designed specifically for the marine composite industry. By using the cumulative energy demand (CED) method, which includes all primary energy input to a material and the energy stored within the material itself, the overview of energy impact was demonstrated, and some of the

findings are given in Table 6.3. Table 6.3 shows the energy consumption results of flax and glass fibre products obtained by LCA using the MarineShift360 software, including renewable and non-renewable breakdown categories.

Table 6.3: Energy consumption of flax and glass fibre products.

Energy category	**Unit**	**Flax fibre**	**Glass fibre**
Non-renewable (biomass, fossil, nuclear)	MJ	12.9	35.5
Renewable (biomass, geothermal, solar, water, wind)	MJ	127.1	2.3
Total	MJ	140.0	37.8
Renewable percentage	%	90.8	<0.1

As seen in Table 6.3, the total energy consumption for flax fibres is more than that of glass fibres. However, as mentioned before, the CED method calculation includes renewable biomass energy (*i.e.* from the sun) absorbed by the flax fibres during growth and has a major contribution to the value. Clearly, this imposes no additional burden on global energy generation. The main burden on global energy generation is the energy coming from non-renewable sources. In this category, flax fibre needs 12.9 MJ, whereas glass fibre needs 35.5 MJ, which is nearly three times more than that of flax fibre.

Moreover, the total energy consumption of producing flax fibres is 140 MJ and most of it (127.1 MJ) is obtained from renewable energy, which is nearly 91%. On the contrary, the renewable energy percentage over total energy consumption of producing glass fibres is less than %0.1, which is a significant indication of unsustainability. Therefore, it is clear that the replacement of natural FRPs over glass FRPs is favourable not only for weight saving in engineering applications but also for providing sustainability during manufacturing stages in the composites industry.

However, it is important to say that including this embodied solar energy may not be a standard practice and an adequate analysis when calculating flax fibre energy consumption. Dissanayake et al. performed a standard LCA and reported that flax fibre produced through no-till cultivation and warm water retting exhibits an embodied energy of 59 GJ/tonne compared to 55 GJ/tonne for a glass mat. But the spinning process further increases the embodied energy for flax yarn to 86 GJ/tonne while it is 26 GJ/tonne for continuous glass fibre [314]. Therefore, replacing glass fibres with natural fibres may depend on the specific reinforcement form and associated processes chosen to obtain greener approaches in terms of energy consumption.

Chapter 7

Conclusions

The present thesis has aimed to investigate sustainable material selection for high performance short fibre reinforced composites produced by a novel alignment technology, the HiPerDiF method. Focusing on plant-derived natural fibres, an intensive characterization of composite constituents was conducted to contribute data to the literature on sustainable constituents. It has been also shown that aligned discontinuous fibre reinforced polymers are effective in tackling the environmental concerns in composite field. The work concluded with the promotion of a reuse/repair strategy that either can extend lifetime or enable the circular economy. This chapter highlights the main conclusions and provides recommendations for future work.

7.1 Highlights

In this thesis, the aim was investigating the viability of using sustainable and biodegradable constituents within the HiPerDiF method to facilitate a circular economy, and the aim is achieved by defining the combination of short flax fibres and a vitrimer matrix as sustainable composite constituents, which are capable of facilitating circular economy, offering high performance and decreasing the environmental impact with features of the constituents (renewable, biodegradable, reusable and recyclable). In line with the objectives, the important outcomes of this thesis were highlighted as follows:

- Plant based natural fibres were chosen as an available sustainable candidate family in fibre reinforced polymer composites alongside mineral based natural fibres. Some advanced matrices such as (vitrimers, high performance thermoplastics, and bio-based thermosets) were also selected as available sustainable polymers.

- Several abundant natural fibres (jute, kenaf, curaua, and flax) were investigated physically, mechanically, and thermally to identify their suitability for the HiPerDiF method. Flax and curaua fibres were found to be the strongest and stiffest of the fibres tested, with jute exhibiting moderate stiffness and strength. Kenaf fibres were found to be the poorest in terms of mechanical performance.

- Thermogravimetric analysis showed that the ideal processing temperature of the natural fibres is up to ~175 °C, where no significant degradation was observed in the fibres. The fibres used in this study have moisture uptake of approximately 6.5–7 wt% from the environment, and the fibres can lose most of the moisture uptake during the potential heating period of composite production.
- The interfacial shear strength of the natural fibres with a commercial epoxy matrix were evaluated and it was found that the interfacial strength values of curaua, flax, and jute fibres are similar and between 12-13 MPa, whereas kenaf has a value of 6 MPa. It was shown that natural fibres have significantly higher surface roughness than synthetic fibres, which can help for mechanical interlocking and offer more surface area interactions.
- Jute, curaua and flax fibres were used to reinforce common polymers -epoxy, PLA, and PP - to produce aligned natural fibre discontinuous composites delivered by the HiPerDiF method. The reinforcement performance and suitability of the fibres with the method were examined and flax fibres with 6 mm length was found to be the best reinforcing candidate for aligned natural fibre discontinuous composites.
- After selecting the best candidate for reinforcement, a selection of sustainable matrices that is compatible with the candidate reinforcement fibre was next step. The interfacial shear strength and critical lengths of flax fibres with three potentially sustainable advanced matrices (Elium®, Furacure, and Vitrimax™T100) were examined for the selection of sustainable matrix. Advanced thermoplastic, Elium®, showed the poorest interfacial shear strength compared to a commercial epoxy, Furacure, and Vitrimax™T100. Conversely, Furacure and Vitrimax™T100 showed a higher level of adhesion with flax fibres. It was found that both Furacure and Vitrimax™T100 have a critical flax fibre length of less than a millimetre.
- The vitrimer matrix, Vitrimax™T100, was selected as a candidate for a sustainable, reusable, and repairable discontinuous flax fibre reinforced composite. Using the HiPerDiF method, discontinuous flax fibre reinforced vitrimers were produced and their physical, mechanical, and functional properties were investigated. Different repair techniques applied to vitrimer matrix composite specimens following tensile testing showed the potential for a mechanical strength recovery that would allow them to be reused over several life cycles, enabling a circular economy.
- It was demonstrated that the candidate natural fibres, especially flax fibres, perform better mechanically compared to glass fibres in ADFRCs in which sustainable matrices are reinforced with them. It was suggested that the potential applications are the replacement of unsustainable composites with sustainable ADFRCs in engineering applications, such as sporting goods, transport, and automobile industries in which weight reduction and sustainability are of paramount importance.

7.2 Suggestions for Future Work

The results and conclusions of this thesis propose clear research directions for future work; therefore, the present section aims to guide PhD/MSc project proposals to those interested in researching the sustainability of FRPs.

The present thesis has demonstrated that short natural fibres can be used to create high performance composites that are sustainable. It was shown that other natural fibres could also be used; some can try other plant-based, animal-based or mineral-based fibres. Already commercialised flax fibres from Eco-Technilin (France) and the water-based HiPerDiF method already promise low environmental impact and sustainability in ADFRPs. Therefore, by making the flax fibres and the HiPerDiF method pillars of future research, the following variables should be investigated to achieve a better understanding of ADFRP in terms of mechanical performance, manufacturing, repair/recycle/reuse options and environmental impact (EI).

A new family of polymers, vitrimers, offer many great properties such as high mechanical performance, recycling, reuse and repair options for FRPs. There are intensive research and commercialisation efforts around the EU in the vitrimer field, and in the US, there is the Mallinda company, which provides two commercialised Vitrimax™ resin types. However, obtaining the best from vitrimer properties in sustainable FRPs needs to be analysed. Even though the curing cycles are provided, optimisation of the manufacturing stages, especially for the HiPerDiF method, should be analysed for better fibre volume fraction and impregnation. It was observed in this study that the repair technique or strategies may be parameters to be examined according to the fibre volume fraction or impregnation quality. Therefore, starting from time, temperature, and pressure, some parameters need to be investigated. Another parameter worth investigating is the repair technique, and as mentioned in the literature review, patch techniques are able to recover and sometimes reinforce broken or damaged composite products. Therefore, the dimensions, lay-up and choice of patch side (single or double) are parameters that need to be studied and a relationship to repair quality quantified. *In-situ* imaging or scanning techniques during manufacturing, curing and repair stages of the vitrimer composites would help the investigations significantly, but designing and building rigs or systems for this purpose may be worth considering. However, using post-production or post-repair imaging and scanning techniques, especially CT scanning, could provide a good level of understanding of flax fibre ADFRP in terms of mechanical performance, manufacturing, repair/recycle/reuse options. In addition, an EI analysis, *i.e.* cradle to grave life cycle analysis including potential several use cycles of flax/vitrimer ADFRPs, could be valuable to widen the outcomes of the project. A number of suggested tests could be carried out as follows:

- Optimising composite manufacturing stages: analysing the curing cycles of the matrices and densities of the HiPerDiF preforms to optimize the fibre volume fraction and impregnation quality.

- Assessing repair techniques for aligned discontinuous flax fibre reinforced vitrimers (ADFFRVs): investigating different repair techniques for ADFFRVs, focusing on their effectiveness in recovering and reinforcing damaged composite products. Studying the influence of three main parameters repair time, temperature, pressure, and optimising these parameters. Moreover, performing a further study on the choice of patch side (single or double) and patch size on the quality of repairs.
- Developing in-situ imaging or scanning techniques: designing and building rigs or systems to enable real-time imaging or during repair stages of ADFFRVs composites. This will provide valuable insights into the process dynamics and help understand the influence of various parameters on the repaired composite properties.
- Conducting cradle-to-grave life cycle analysis: performing a comprehensive life cycle assessment of flax/vitrimer ADFRPs, considering multiple use cycles and potential environmental impacts. Quantifying the energy consumption, greenhouse gas emissions, and other relevant factors to assess the sustainability and overall environmental performance of the composite.

References

[1] W. Callister and D. Rethwisch, *Materials Science and Engineering 8th Edition SI Version*. John Wiley & Sons, Inc., 2010.

[2] A. Kalemtas, "Composite materials course notes," Mugla Sitki Kocaman University, Tech. Rep., 2015.

[3] C. Soutis, "Fibre reinforced composites in aircraft construction," *Progress in Aerospace Sciences*, vol. 41, no. 2, pp. 143 – 151, 2005.

[4] H. Adam, "Carbon fibre in automotive applications," *Materials & Design*, vol. 18, no. 4, pp. 349 – 355, 1997.

[5] F. Rubino, A. Nisticò, F. Tucci, and P. Carlone, "Marine application of fiber reinforced composites: a review," *Journal of Marine Science and Engineering*, vol. 8, no. 1, p. 26, Jan 2020.

[6] L. Mishnaevsky, K. Branner, H. Petersen, J. Beauson, M. McGugan, and B. Sørensen, "Materials for wind turbine blades: an overview," *Materials*, vol. 10, no. 11, p. 1285, Nov 2017.

[7] C. W. Matthew Such and K. Potter, "Aligned discontinuous fibre composites: A short history," *Journal of Multifunctional Composites*, vol. 2, no. 3, pp. 155 – 168, 2014.

[8] D. K. Rajak, D. D. Pagar, P. L. Menezes, and E. Linul, "Fiber-reinforced polymer composites: Manufacturing, properties, and applications," *Polymers*, vol. 11, no. 10, 2019.

[9] A. Hartmann, A. Wöginger, and M. Neitzel, "Cost effective processing of continuous fiber reinforced thermoplastics," *Materials Technology*, vol. 13, no. 4, pp. 160–165, 1998.

[10] J. Tang, Y. Swolfs, M. L. Longana, H. Yu, M. R. Wisnom, S. V. Lomov, and L. Gorbatikh, "Hybrid composites of aligned discontinuous carbon fibers and self-reinforced polypropylene under tensile loading," *Composites Part A: Applied Science and Manufacturing*, vol. 123, pp. 97–107, 2019.

[11] M. L. Longana, V. Ondra, H. Yu, K. D. Potter, and I. Hamerton, "Reclaimed carbon and flax fibre composites: Manufacturing and mechanical properties," *Recycling*, vol. 3, no. 4, pp. 52–0, 2018.

[12] H. Fukuda and T.-W. Chou, "A probabilistic theory of the strength of short-fibre composites with variable fibre length and orientation," *Journal of Materials Science*, vol. 17, no. 4, pp. 1003–1011, 1982.

[13] T. Sunny, K. L. Pickering, and S. H. Lim, "Alignment of short fibres: an overview," *Processing and Fabrication of Advanced Materials-XXV*, pp. 616–625, 2017.

[14] N. Parratt, "Whisker alignment by the alginate process," *Composites*, vol. 1, no. 1, pp. 25–27, 1969. [Online]. Available: https://www.sciencedirect.com/science/article/pii/S001043616980008X

[15] Z. Liu, T. A. Turner, K. H. Wong, and S. J. Pickering, "Development of high performance recycled carbon fibre composites with an advanced hydrodynamic fibre alignment process," *Journal of Cleaner Production*, vol. 278, p. 123785, 2021.

[16] H. Yu and K. Potter, "Method and apparatus for aligning discontinuous fibres," *UK patent, Patent application*, no. 1306762.4, filed: 2013-04-15, application granted: 2017-07-19.

[17] M. L. Longana, H. Yu, J. Lee, T. R. Pozegic, S. Huntley, T. Rendall, K. D. Potter, and I. Hamerton, "Quasi-isotropic and pseudo-ductile highly aligned discontinuous fibre composites manufactured with the hiperdif (high performance discontinuous fibre) technology," *Materials*, vol. 12, no. 11, 2019.

[18] H. Yu, K. Potter, and M. Wisnom, "A novel manufacturing method for aligned discontinuous fibre composites (high performance-discontinuous fibre method)," *Composites Part A: Applied Science and Manufacturing*, vol. 65, pp. 175 – 185, 2014.

[19] H. Yu, M. L. Longana, M. Jalalvand, M. R. Wisnom, and K. D. Potter, "Hierarchical pseudo-ductile hybrid composites combining continuous and highly aligned discontinuous fibres," *Composites Part A: Applied Science and Manufacturing*, vol. 105, pp. 40 – 56, 2018.

[20] S. Yarlagadda, J. Deitzel, D. Heider, J. Tierney, and J. W. Gillespie Jr, "Tailorable universal feedstock for forming (tuff): overview and performance," *SAMPE 2019-Charlotte, NC, May 2019*, 2019.

[21] H. Group, "A novel method of dfrps," in *XXX*, 2018.

[22] G. Bagg, M. Evans, and A. Pryde, "The glycerine process for the alignment of fibres and whiskers," *Composites*, vol. 1, no. 2, pp. 97–100, 1969.

[23] G. E. G. Bagg, H. Edwards, M. E. N. Evans, J. A. Lewis, and H. Ziebland, "Aligning fibres," Mar. 30 1976, uS Patent 3,947,535.

[24] A. M. Fitzgerald, N. Wong, A. V. L. Fitzgerald, D. A. Jesson, F. Martin, R. J. Murphy, T. Young, I. Hamerton, and M. L. Longana, "Life cycle assessment of the high performance discontinuous fibre (hiperdif) technology and its operation in various countries," *Sustainability*, vol. 14, no. 3, 2022.

[25] M. L. Longana, N. Ong, H. Yu, and K. D. Potter, "Multiple closed loop recycling of carbon fibre composites with the hiperdif (high performance discontinuous fibre) method," *Composite Structures*, vol. 153, pp. 271 – 277, 2016.

[26] M. L. Longana, H. Yu, M. Jalavand, M. R. Wisnom, and K. D. Potter, "Aligned discontinuous intermingled reclaimed/virgin carbon fibre composites for high performance and pseudo-ductile behaviour in interlaminated carbon-glass hybrids," *Composites Science and Technology*, vol. 143, pp. 13–21, 2017.

[27] R. J. Tapper, M. L. Longana, H. Yu, I. Hamerton, and K. D. Potter, "Development of a closed-loop recycling process for discontinuous carbon fibre polypropylene composites," *Composites Part B: Engineering*, vol. 146, pp. 222–231, 2018.

[28] M. L. Longana, H. Yu, I. Hamerton, and K. D. Potter, "Development and application of a quality control and property assurance methodology for reclaimed carbon fibers based on the hiperdif (high performance discontinuous fibre) method and interlaminated hybrid specimens," *Advanced Manufacturing: Polymer & Composites Science*, vol. 4, no. 2, pp. 48–55, 2018.

[29] R. J. Tapper, M. L. Longana, I. Hamerton, and K. D. Potter, "A closed-loop recycling process for discontinuous carbon fibre polyamide 6 composites," *Composites Part B: Engineering*, vol. 179, p. 107418, 2019.

[30] P. Aravindan, F. Becagli, M. L. Longana, L. G. Blok, T. R. Pozegic, S. J. Huntley, T. Rendall, and I. Hamerton, "Remanufacturing of woven carbon fibre fabric production waste into high performance aligned discontinuous fibre composites," *Journal of Composites Science*, vol. 4, no. 2, 2020.

[31] M. Jawaid and M. Thariq, *Sustainable Composites for Aerospace Applications*, ser. Woodhead Publishing Series in Composites Science and Engineering. Elsevier Science, 2018.

[32] A. K. Mohanty, S. Vivekanandhan, J.-M. Pin, and M. Misra, "Composites from renewable and sustainable resources: Challenges and innovations," *Science*, vol. 362, no. 6414, pp. 536–542, 2018.

[33] D. Y. Wu, S. Meure, and D. Solomon, "Self-healing polymeric materials: A review of recent developments," *Progress in Polymer Science*, vol. 33, no. 5, pp. 479–522, 2008.

[34] R. Fangueiro and S. Rana, *Natural Fibres: Advances in Science and Technology Towards Industrial Applications From Science to Market*. Springer, Dordrecht, 2016.

[35] K. Pickering, M. A. Efendy, and T. Le, "A review of recent developments in natural fibre composites and their mechanical performance," *Composites Part A: Applied Science and Manufacturing*, vol. 83, pp. 98 – 112, 2016, special Issue on Biocomposites.

[36] D. N. Saheb and J. P. Jog, "Natural fiber polymer composites: A review," *Advances in Polymer Technology*, vol. 18, no. 4, pp. 351–363, 1999.

[37] S. Das and T. Yokozeki, "A brief review of modified conductive carbon/glass fibre reinforced composites for structural applications: Lightning strike protection, electromagnetic shielding, and strain sensing," *Composites Part C: Open Access*, vol. 5, p. 100162, 2021.

[38] J. Plocher, L. Mencattelli, F. Narducci, and S. Pinho, "Learning from nature: Bio-inspiration for damage-tolerant high-performance fibre-reinforced composites," *Composites Science and Technology*, vol. 208, p. 108669, 2021.

[39] D. May, C. Goergen, and K. Friedrich, "Multifunctionality of polymer composites based on recycled carbon fibers: A review," *Advanced Industrial and Engineering Polymer Research*, vol. 4, no. 2, pp. 70–81, 2021, recycling of Polymer Blends and Composites.

[40] Ákos Pomázi and A. Toldy, "Development of fire retardant epoxy-based gelcoats for carbon fibre reinforced epoxy resin composites," *Progress in Organic Coatings*, vol. 151, p. 106015, 2021.

[41] P. R. Spendley, S. L. Ogin, P. A. Smith, and A. B. Clarke, "Design allowables for notched and unnotched cfrp in tension and compression under differing ambient conditions," *Plastics, Rubber and Composites*, vol. 38, no. 2-4, pp. 80–86, 2009.

[42] D. Hull and T. Clyne, *An Introduction to Composite Materials*, D. Hull and T. Clyne, Eds. Cambridge University Press, 1996.

[43] "Composite materials market forecast for the united kingdom (uk) from 2015 to 2030, by industrial sector," https://www.statista.com/statistics/624539/composite-market-industry-sector-uk/, accessed: 2022-08-08.

[44] "Composites germany - results of the 15th composites market survey," https://www.composites-germany.org/images/PR_03-2020_market_survey_01_2020.pdf.

[45] E. Gutierrez and F. Bono, “Review of industrial manufacturing capacity for fibre-reinforced polymers as prospective structural components in shipping containers,” European Commission - JRC Scientific and Policy Reports, Tech. Rep., 2013.

[46] M. Sauer, M. Kunhel, and W. Elmar, “Composites market report 2018 - market developments, trends, outlook and challenges,” Carbon Composites, Tech. Rep., 2018.

[47] S. Kara and S. Manmke, “Composites: Calculating their embodied energy,” The University of New South Wales, Tech. Rep., 2009.

[48] J. Chard, L. Basson, G. Creech, D. Jesson, and P. Smith, “Shades of green: Life cycle assessment of a urethane methacrylate/unsaturated polyester resin system for composite materials,” *Sustainable Biobased Composites Materials*, vol. 11, no. 4, 2019.

[49] “Iea (2020), sustainable recovery, iea, paris,” https://www.iea.org/reports/sustainable-recovery.

[50] J. Carruthers and R. Quarshie, “Technology overview biocomposites,” NetComposites, Tech. Rep., 2014.

[51] J. Sahari and S. Sapuan, “Natural fibre reinforced biodegradable polymer composites,” *Reviews on advanced materials science*, vol. 30, no. 2, 2012.

[52] “Towards a circular economy: Business rationale for an accelerated transition (2015),” https://www.ellenmacarthurfoundation.org/.

[53] C. Boland, R. De Kleine, G. Keoleian, E. Lee, H. Kim, and T. Wallington, “Life cycle impacts of natural fiber composites for automotive applications: Effects of renewable energy content and lightweighting,” *Journal of Industrial Ecology*, vol. 20, no. 1, 2015.

[54] T. Corbière-Nicollier, B. Gfeller Laban, L. Lundquist, Y. Leterrier, J.-A. Månson, and O. Jolliet", “Life cycle assessment of biofibres replacing glass fibres as reinforcement in plastics,” *Resources, Conservation and Recycling*, vol. 33, no. 4, pp. 267 – 287, 2001.

[55] Y. Deng, D. Paraskevas, Y. Tian, K. Van Acker, W. Dewulf, and J. R. Duflou, “Life cycle assessment of flax-fibre reinforced epoxidized linseed oil composite with a flame retardant for electronic applications,” *Journal of Cleaner Production*, vol. 133, pp. 427 – 438, 2016.

[56] S. Joshi, L. Drzal, A. Mohanty, and S. Arora, “Are natural fiber composites environmentally superior to glass fiber reinforced composites?” *Composites Part A: Applied Science and Manufacturing*, vol. 35, no. 3, pp. 371 – 376, 2004, aIChE 2002.

[57] A. La Rosa, G. Cozzo, A. Latteri, A. Recca, A. BjÃ¶rklund, E. Parrinello, and G. Cicala, "Life cycle assessment of a novel hybrid glass-hemp/thermoset composite," *Journal of Cleaner Production*, vol. 44, pp. 69 – 76, 2013.

[58] A. D. La Rosa, G. Recca, J. Summerscales, A. Latteri, G. Cozzo, and G. Cicala, "Bio-based versus traditional polymer composites. a life cycle assessment perspective," *Journal of Cleaner Production*, vol. 74, pp. 135 – 144, 2014.

[59] M. Pervaiz and M. M. Sain, "Carbon storage potential in natural fiber composites," *Resources, Conservation and Recycling*, vol. 39, no. 4, pp. 325 – 340, 2003.

[60] D. A. Jesson and J. F. Watts, "The interface and interphase in polymer matrix composites: Effect on mechanical properties and methods for identification," *Polymer Reviews*, vol. 52, no. 3, pp. 321–354, 2012.

[61] T. Gurunathan, S. Mohanty, and S. K. Nayak, "A review of the recent developments in biocomposites based on natural fibres and their application perspectives," *Composites Part A: Applied Science and Manufacturing*, vol. 77, pp. 1 – 25, 2015.

[62] C. Baley, "Analysis of the flax fibres tensile behaviour and analysis of the tensile stiffness increase," *Composites Part A: Applied Science and Manufacturing*, vol. 33, no. 7, pp. 939 – 948, 2002.

[63] K. Oksman, M. Skrifvars, and J.-F. Selin, "Natural fibres as reinforcement in polylactic acid (pla) composites," *Composites Science and Technology*, vol. 63, no. 9, pp. 1317 – 1324, 2003, eco-Composites.

[64] H. Dhakal, Z. Zhang, and M. Richardson, "Effect of water absorption on the mechanical properties of hemp fibre reinforced unsaturated polyester composites," *Composites Science and Technology*, vol. 67, no. 7, pp. 1674 – 1683, 2007.

[65] L. Y. Mwaikambo and M. P. Ansell, "Chemical modification of hemp, sisal, jute, and kapok fibers by alkalization," *Journal of Applied Polymer Science*, vol. 84, no. 12, pp. 2222–2234, 2002.

[66] J. Gassan and A. K. Bledzki, "Possibilities for improving the mechanical properties of jute/epoxy composites by alkali treatment of fibres," *Composites Science and Technology*, vol. 59, no. 9, pp. 1303 – 1309, 1999.

[67] N. Cordeiro, C. Gouveia, A. Moraes, and S. Amico, "Natural fibers characterization by inverse gas chromatography," *Carbohydrate Polymers*, vol. 84, no. 1, pp. 110 – 117, 2011.

[68] U. O. Costa, L. F. C. Nascimento, J. M. Garcia, W. B. A. Bezerra, G. F. Fabio da Costa, F. S. da Luz, W. A. Pinheiro, and S. N. Monteiro, "Mechanical properties of composites with graphene oxide functionalization of either epoxy matrix or curaua fiber reinforcement," *Journal of Materials Research and Technology*, vol. 9, no. 6, pp. 13 390–13 401, 2020.

[69] T. Nishino, K. Hirao, M. Kotera, K. Nakamae, and H. Inagaki, "Kenaf reinforced biodegradable composite," *Composites Science and Technology*, vol. 63, no. 9, pp. 1281 – 1286, 2003, eco-Composites.

[70] S. Ochi, "Mechanical properties of kenaf fibers and kenaf/pla composites," *Mechanics of Materials*, vol. 40, no. 4, pp. 446 – 452, 2008.

[71] Y. Li, Y.-W. Mai, and L. Ye, "Sisal fibre and its composites: a review of recent developments," *Composites Science and Technology*, vol. 60, no. 11, pp. 2037 – 2055, 2000.

[72] K. Charlet, "Chapter 3 natural fibres as composite reinforcement materials: Description and new sources," in *Natural Polymers: Volume 1: Composites*. The Royal Society of Chemistry, 2012, vol. 1, pp. 37–62.

[73] M. Ramesh, "9 - hemp, jute, banana, kenaf, ramie, sisal fibers," in *Handbook of Properties of Textile and Technical Fibres (Second Edition)*, ser. The Textile Institute Book Series, A. R. Bunsell, Ed. Woodhead Publishing, 2018, pp. 301 – 325.

[74] F. M. AL-Oqla and S. Sapuan, "Natural fiber reinforced polymer composites in industrial applications: feasibility of date palm fibers for sustainable automotive industry," *Journal of Cleaner Production*, vol. 66, pp. 347 – 354, 2014.

[75] T. Väisänen, A. Haapala, R. Lappalainen, and L. Tomppo, "Utilization of agricultural and forest industry waste and residues in natural fiber-polymer composites: A review," *Waste Management*, vol. 54, pp. 62–73, 2016.

[76] M. po Ho, H. Wang, J.-H. Lee, C. kit Ho, K. tak Lau, J. Leng, and D. Hui, "Critical factors on manufacturing processes of natural fibre composites," *Composites Part B: Engineering*, vol. 43, no. 8, pp. 3549 – 3562, 2012.

[77] C. Baillie, *Green composites: polymer composites and the environment*. CRC Press, 2005.

[78] J. Chard, G. Creech, D. Jesson, and P. Smith, "Coupling agent for natural fibre composites utilising thermosetting resin systems," in *Proceedings of the 15th European Conference on Composite Materials ESCM, Venice, Italy*, 2012, pp. 24–28.

[79] J. Chard, G. Creech, D. Jesson, and P. Smith, "A potential addition to the technical fibres family?" in *ICCM20 Conference Proceedings*, 2015.

[80] L. Yan, N. Chouw, and K. Jayaraman, “Flax fibre and its composites – a review,” *Composites Part B: Engineering*, vol. 56, pp. 296–317, 2014.

[81] D. Shah, “Developing plant fibre composites for structural applications by optimising composite parameters: a critical review,” *Journal of Materials Sc*, vol. 48, pp. 6083–6107, 2013.

[82] B. Dewilde, “eeuwen vlas in vlaanderen,” *Tielt, Bussum, Lannoo*, 1983.

[83] C. Bergfjord, S. Karg, A. Rast-Eicher, M.-L. Nosch, U. Mannering, R. G. Allaby, B. M. Murphy, and B. Holst, “Comment on "30,000-year-old wild flax fibers",” *Science*, vol. 328, no. 5986, pp. 1634–1634, 2010.

[84] CELC, “European linen,” http://news.europeanflax.com/en/lin/, 2022, accessed: 2022-08-10.

[85] C. Baley, A. Bourmaud, and P. Davies, “Eighty years of composites reinforced by flax fibres: A historical review,” *Composites Part A: Applied Science and Manufacturing*, vol. 144, p. 106333, 2021.

[86] D. Pantaloni, A. L. Rudolph, D. U. Shah, C. Baley, and A. Bourmaud, “Interfacial and mechanical characterisation of biodegradable polymer-flax fibre composites,” *Composites Science and Technology*, vol. 201, p. 108529, 2021.

[87] A. Barouni, C. Lupton, C. Jiang, A. Saifullah, K. Giasin, Z. Zhang, and H. N. Dhakal, “Investigation into the fatigue properties of flax fibre epoxy composites and hybrid composites based on flax and glass fibres,” *Composite Structures*, vol. 281, p. 115046, 2022.

[88] A. Kandemir, M. L. Longana, I. Hamerton, and S. J. Eichhorn, “Developing aligned discontinuous flax fibre composites: Sustainable matrix selection and repair performance of vitrimers,” *Composites Part B: Engineering*, p. 110139, 2022.

[89] BMW, “Bmw i ventures invests in high-performance composites made from natural fibres,” https://www.nccuk.com/news/ncc-finds-sustainable-cost-effective-composites-alternative-for-innovative-sme/, 2022, accessed: 2022-08-10.

[90] ClimateColab, “Jute (corchorus capsularis & c. olitorius),” https://www.climatecolab.org/contests/2016/materials-matter/c/proposal/1330505, 2016, accessed: 2022-08-10.

[91] M. R. Rahman, M. M. Huque, M. N. Islam, and M. Hasan, “Improvement of physico-mechanical properties of jute fiber reinforced polypropylene composites by post-treatment,” *Composites Part A: Applied Science and Manufacturing*, vol. 39, no. 11, pp. 1739–1747, 2008.

[92] Worldjute.com, “History of jute,” http://www.worldjute.com/about_jute/juthist.html, 2002, accessed: 2022-08-10.

[93] Jute.com, “Jute related faq,” https://www.jute.com/about-us/faq, 2022, accessed: 2022-08-10.

[94] H. Singh, J. Inder Preet Singh, S. Singh, V. Dhawan, and S. Kumar Tiwari, “A brief review of jute fibre and its composites,” *Materials Today: Proceedings*, vol. 5, no. 14, Part 2, pp. 28 427–28 437, 2018, international Conference on Composite Materials: Manufacturing, Experimental Techniques, Modeling and Simulation, March 1-3, 2018.

[95] M. A. Fuqua, S. Huo, and C. A. Ulven, “Natural fiber reinforced composites,” *Polymer Reviews*, vol. 52, no. 3, pp. 259–320, 2012.

[96] M. H. Islam, M. R. Islam, M. Dulal, S. Afroj, and N. Karim, “The effect of surface treatments and graphene-based modifications on mechanical properties of natural jute fiber composites: A review,” *iScience*, vol. 25, no. 1, p. 103597, 2022.

[97] R. Silva and E. Aquino, “Curaua fiber: A new alternative to polymeric composites,” *Journal of Reinforced Plastics and Composites*, vol. 27, no. 1, pp. 103–112, 2008.

[98] F. Tomczak, K. G. Satyanarayana, and T. H. D. Sydenstricker, “Studies on lignocellulosic fibers of brazil: Part iii – morphology and properties of brazilian curauá fibers,” *Composites Part A: Applied Science and Manufacturing*, vol. 38, no. 10, pp. 2227–2236, 2007.

[99] S. Souza, M. Ferreira, M. Sain, M. Ferreira, H. Pupo, B. Cherian, and A. Leão, “22 - the use of curaua fibers as reinforcements in composites,” in *Biofiber Reinforcements in Composite Materials*, O. Faruk and M. Sain, Eds. Woodhead Publishing, 2015, pp. 700–720.

[100] A. L. Leao, R. Rowell, and N. Tavares, *Applications of Natural Fibers in Automotive Industry in Brazil — Thermoforming Process*. Boston, MA: Springer US, 1998, pp. 755–761.

[101] R. Zah, R. Hischier, A. Leão, and I. Braun, “Curauá fibers in the automobile industry – a sustainability assessment,” *Journal of Cleaner Production*, vol. 15, no. 11, pp. 1032–1040, 2007, the Automobile Industry & Sustainability.

[102] U. O. Costa, L. F. C. Nascimento, J. M. Garcia, W. B. A. Bezerra, G. F. Fabio da Costa, F. S. da Luz, W. A. Pinheiro, and S. N. Monteiro, “Mechanical properties of composites with graphene oxide functionalization of either epoxy matrix or curaua fiber reinforcement,” *Journal of Materials Research and Technology*, vol. 9, no. 6, pp. 13 390–13 401, 2020.

[103] N. de Oliveira Roque Maciel, J. B. Ferreira, J. da Silva Vieira, C. G. D. Ribeiro, F. P. D. Lopes, F. M. Margem, S. N. Monteiro, C. M. F. Vieira, and L. C. da Silva, “Comparative

tensile strength analysis between epoxy composites reinforced with curaua fiber and glass fiber," *Journal of Materials Research and Technology*, vol. 7, no. 4, pp. 561–565, 2018.

[104] G. Garcia del Pino, A. C. Kieling, A. Bezazi, H. Boumediri, J. F. Rolim de Souza, F. Valenzuela Diaz, J. L. Valin Rivera, J. Dehaini, and T. H. Panzera, "Hybrid polyester composites reinforced with curauá fibres and nanoclays," *Fibers and Polymers*, vol. 21, no. 2, pp. 399–406, 2020.

[105] S. Członka, E. Fischer Kerche, R. Motta Neves, A. Strąkowska, and K. Strzelec, "Bio-based rigid polyurethane foam composites reinforced with bleached curauá fiber," *International Journal of Molecular Sciences*, vol. 22, no. 20, 2021.

[106] "Sources of the images taken from web for the figure, respectively (accessed by 05.08.2022)," http://www.geograph.org.uk/photo/499918, https://www.pinterest.com/pin/447897125415204924/, https://commons.wikimedia.org/wiki/File:Scanning_Electron_Microscope_image_of_contents_of_pendant,_showing_unprocessed_flax_fibres_(FindID_256636-385397).jpg, https://correiodaamazonia.com/pesquisas-pretendem-potencializar-uso-da-fibra-de-curaua-no-amazonas/, https://www.flickr.com/photos/celcoimbra/9122028480, https://www.mdpi.com/2073-4360/11/8/1356/htm, https://img.etimg.com/thumb/width-1200,height-900,imgsize-150603,resizemode-1,msid-71688658/markets/commodities/news/cotton-prices-likely-to-fall-further-ind-ra.jpg, https://textile-craft.blogspot.com/2013/12/cotton-fibre-physical-properties-and.html, https://www.pinterest.com/pin/246572148332714393/, https://medium.com/@diegoschmunis/be-like-bamboo-in-a-storm-509f4efb850c, https://sourcingjournal.com/topics/raw-materials/eco-friendly-bamboo-fiber-development-ll-19163/, https://tinyurl.com/bamboopicture2018April04, https://inchemistry.acs.org/content/inchemistry/en/atomic-news/spider-webs.html, https://www.theverge.com/2013/6/6/4401184/mit-media-lab-silk-pavilion, https://curiositykilledthecation.wordpress.com/2019/01/16/unraveling-the-secrets-of-spider-silk-1/, https://www.solidwool.com/material, https://shepherdsdream.com/blog/wonders-of-wool/understanding-wool-processing-5/, https://www.scienceimage.csiro.au/tag/microscopy/i/2487/electron-microscope-image-of-merino-wool-fibre/, https://www.sandatlas.org/basalt/, https://www.mdpi.com/2076-3417/10/5/1561/htm.

[107] G. Bhat and D. Parikh, "3 - biodegradable materials for nonwovens," in *Applications of Nonwovens in Technical Textiles*, ser. Woodhead Publishing Series in Textiles, R. Chapman, Ed. Woodhead Publishing, 2010, pp. 46 – 62.

[108] "A new way of working with wool," https://www.solidwool.com/material, accessed: 2020-08-12.

[109] J. M. Gosline, M. DeMont, and M. W. Denny, "The structure and properties of spider silk," *Endeavour*, vol. 10, no. 1, pp. 37 – 43, 1986.

[110] D. Kaplan, W. W. Adams, B. Farmer, and C. Viney, *Silk: Biology, Structure, Properties, and Genetics*. ACS Symposium Series, 1993, vol. 544, ch. 1, pp. 2–16.

[111] M. Heim, D. Keerl, and T. Scheibel, "Spider silk: From soluble protein to extraordinary fiber," *Angewandte Chemie International Edition*, vol. 48, no. 20, pp. 3584–3596, 2009.

[112] F. Vollrath and D. P. Knight, "Liquid crystalline spinning of spider silk," *Nature*, vol. 410, no. 6828, pp. 541–548, 2001.

[113] Y. Dou, Z.-P. Wang, W. He, T. Jia, Z. Liu, P. Sun, K. Wen, E. Gao, X. Zhou, X. Hu *et al.*, "Artificial spider silk from ion-doped and twisted core-sheath hydrogel fibres," *Nature communications*, vol. 10, no. 1, pp. 1–10, 2019.

[114] V. Dhand, G. Mittal, K. Y. Rhee, S.-J. Park, and D. Hui, "A short review on basalt fiber reinforced polymer composites," *Composites Part B: Engineering*, vol. 73, pp. 166 – 180, 2015.

[115] J. Militký, R. Mishra, and H. Jamshaid, "20 - basalt fibers," in *Handbook of Properties of Textile and Technical Fibres (Second Edition)*, ser. The Textile Institute Book Series, A. R. Bunsell, Ed. Woodhead Publishing, 2018, pp. 805 – 840.

[116] H. Jamshaid, R. Mishra, J. Militky, M. Pechociakova, and M. T. Noman, "Mechanical, thermal and interfacial properties of green composites from basalt and hybrid woven fabrics," *Fibers and Polymers*, vol. 17, no. 10, pp. 1675–1686, 2016.

[117] M. T. L. Hanusa, "Basalt composite panel," US Patent, US2011/0136401A1.

[118] M. Urbanski, A. Lapko, and A. Garbacz, "Investigation on concrete beams reinforced with basalt rebars as an effective alternative of conventional r/c structures," *Procedia Engineering*, vol. 57, pp. 1183 – 1191, 2013, modern Building Materials, Structures and Techniques.

[119] M. Inman, E. R. Thorhallsson, and K. Azrague, "A mechanical and environmental assessment and comparison of basalt fibre reinforced polymer (bfrp) rebar and steel rebar in concrete beams," *Energy Procedia*, vol. 111, pp. 31 – 40, 2017, 8th International Conference on Sustainability in Energy and Buildings, SEB-16, 11-13 September 2016, Turin, Italy.

[120] "Life cycle assessment (lca) of basalt fibers versus glass fibers, incotelogy.de," https://basaltfiberworld.wordpress.com/scientifical-research/life-cycle-assessment-lca-of-basalt-fibers-versus-glass-fibers/, accessed: 2020-08-21.

[121] A. Kandemir, T. R. Pozegic, I. Hamerton, S. J. Eichhorn, and M. L. Longana, "Characterisation of natural fibres for sustainable discontinuous fibre composite materials," *Materials*, vol. 13, no. 9, 2020.

[122] X.-Q. Dai, "10 - fibers," in *Biomechanical Engineering of Textiles and Clothing*, ser. Woodhead Publishing Series in Textiles, Y. Li and X.-Q. Dai, Eds. Woodhead Publishing, 2006, pp. 163–177.

[123] J. Gosline, P. Guerette, C. Ortlepp, and K. Savage, "The mechanical design of spider silks: from fibroin sequence to mechanical function," *Journal of Experimental Biology*, vol. 202, no. 23, pp. 3295–3303, 1999.

[124] C. P. Brown, A. D. Whaite, J. M. MacLeod, J. Macdonald, and F. Rosei, "With great structure comes great functionality: Understanding and emulating spider silk," *Journal of Materials Research*, vol. 30, no. 1, p. 108–120, 2015.

[125] P. Colomban and V. Jauzein, "5 - silk: Fibers, films, and composites—types, processing, structure, and mechanics," in *Handbook of Properties of Textile and Technical Fibres (Second Edition)*, ser. The Textile Institute Book Series, A. R. Bunsell, Ed. Woodhead Publishing, 2018, pp. 137 – 183.

[126] A. R. Bunsell, "1 - introduction to the science of fibers," in *Handbook of Properties of Textile and Technical Fibres (Second Edition)*, ser. The Textile Institute Book Series, A. R. Bunsell, Ed. Woodhead Publishing, 2018, pp. 1 – 20.

[127] M. J. Mochane, T. C. Mokhena, T. H. Mokhothu, A. Mtibe, E. Sadiku, S. Ray, I. Ibrahim, and O. Daramola, "Recent progress on natural fiber hybrid composites for advanced applications: A review," *Express Polymer Letters*, vol. 13, no. 2, pp. 159–198, 2019.

[128] S. Pimenta and S. T. Pinho, "Recycling carbon fibre reinforced polymers for structural applications: Technology review and market outlook," *Waste Management*, vol. 31, no. 2, pp. 378 – 392, 2011, environmental Implications of Alternative Materials in Construction and Treatment of Waste.

[129] G. Oliveux, L. O. Dandy, and G. A. Leeke, "Current status of recycling of fibre reinforced polymers: Review of technologies, reuse and resulting properties," *Progress in Materials Science*, vol. 72, pp. 61 – 99, 2015.

[130] A. Conroy, S. Halliwell, T. Reynolds, and A. Waterman, "Recycling fibre reinforced polymers in construction: a guide to best practicable environmental option building research establishment," *ISBN*, vol. 1, no. 86081, p. 689, 2004.

[131] A. Dotan, "Biobased thermosets," in *Handbook of thermoset plastics*. Elsevier, 2014, pp. 577–622.

[132] J.-M. Raquez, M. Deléglise, M.-F. Lacrampe, and P. Krawczak, "Thermosetting (bio)materials derived from renewable resources: A critical review," *Progress in Polymer Science*, vol. 35, no. 4, pp. 487 – 509, 2010, topical Issue on Biomaterials.

[133] A. Gandini, T. M. Lacerda, A. J. Carvalho, and E. Trovatti, "Progress of polymers from renewable resources: furans, vegetable oils, and polysaccharides," *Chemical reviews*, vol. 116, no. 3, pp. 1637–1669, 2016.

[134] R. Auvergne, S. Caillol, G. David, B. Boutevin, and J.-P. Pascault, "Biobased thermosetting epoxy: present and future," *Chemical reviews*, vol. 114, no. 2, pp. 1082–1115, 2014.

[135] Y. Zhu, C. Romain, and C. K. Williams, "Sustainable polymers from renewable resources," *Nature*, vol. 540, no. 7633, pp. 354–362, 2016.

[136] G. Mashouf Roudsari, A. K. Mohanty, and M. Misra, "Green approaches to engineer tough biobased epoxies: A review," *ACS Sustainable Chemistry & Engineering*, vol. 5, no. 11, pp. 9528–9541, 2017.

[137] S. Pilla, *Handbook of bioplastics and biocomposites engineering applications*. John Wiley & Sons, 2011, vol. 81.

[138] "Cnsl technology, cardolite corporation," https://www.cardolite.com/technology/, accessed: 2020-08-20.

[139] Europa.eu, "Understanding reach," https://echa.europa.eu/regulations/reach/understanding-reach, 2022, accessed: 2022-03-30.

[140] Bitrez.com, "Furacure (pfa)," https://www.bitrez.com/products/furacure-pfa/, 2022, accessed: 2022-03-30.

[141] M. E. Otheguy, A. G. Gibson, E. Findon, R. M. Cripps, A. O. Mendoza, and M. T. A. Castro, "Recycling of end-of-life thermoplastic composite boats," *Plastics, Rubber and Composites*, vol. 38, no. 9-10, pp. 406–411, 2009.

[142] T. Y. Gowda, M. Sanjay, K. S. Bhat, P. Madhu, P. Senthamaraikannan, and B. Yogesha, "Polymer matrix-natural fiber composites: An overview," *Cogent Engineering*, vol. 5, no. 1, p. 1446667, 2018.

[143] M. Li, Y. Pu, V. M. Thomas, C. G. Yoo, S. Ozcan, Y. Deng, K. Nelson, and A. J. Ragauskas, "Recent advancements of plant-based natural fiber–reinforced composites and their applications," *Composites Part B: Engineering*, p. 108254, 2020.

[144] M. Kabir, H. Wang, K. Lau, and F. Cardona, "Chemical treatments on plant-based natural fibre reinforced polymer composites: An overview," *Composites Part B: Engineering*, vol. 43, no. 7, pp. 2883 – 2892, 2012, natural Materials in Composites Engineering.

[145] F. Sarasini, "Thermoplastic biopolymer matrices for biocomposites," in *Biocomposites for High-Performance Applications*. Elsevier, 2017, pp. 81–123.

[146] A. Bourmaud, D. U. Shah, J. Beaugrand, and H. N. Dhakal, "Property changes in plant fibres during the processing of bio-based composites," *Industrial Crops and Products*, vol. 154, p. 112705, 2020.

[147] K. Ramakrishnan, N. Le Moigne, O. De Almeida, A. Regazzi, and S. Corn, "Optimized manufacturing of thermoplastic biocomposites by fast induction-heated compression moulding: Influence of processing parameters on microstructure development and mechanical behaviour," *Composites Part A: Applied Science and Manufacturing*, vol. 124, p. 105493, 2019.

[148] K. Sudesh, H. Abe, and Y. Doi, "Synthesis, structure and properties of polyhydroxyalkanoates: biological polyesters," *Progress in Polymer Science*, vol. 25, no. 10, pp. 1503 – 1555, 2000.

[149] Sicomin.com, "Sr infugreen 810," Sicomin Epoxy Systems, Tech. Rep., 2018.

[150] M. A. Lucherelli, A. Duval, and L. Avérous, "Biobased vitrimers: Towards sustainable and adaptable performing polymer materials," *Progress in Polymer Science*, vol. 127, p. 101515, 2022.

[151] E. Enriquez, A. K. Mohanty, and M. Misra, "Biobased polymer blends of poly(trimethylene terephthalate) and high density polyethylene," *Materials & Design*, vol. 90, pp. 984 – 990, 2016.

[152] A. J. Carvalho, "Starch: major sources, properties and applications as thermoplastic materials," in *Monomers, polymers and composites from renewable resources*. Elsevier, 2008, pp. 321–342.

[153] S. Farah, D. G. Anderson, and R. Langer, "Physical and mechanical properties of pla, and their functions in widespread applications — a comprehensive review," *Advanced Drug Delivery Reviews*, vol. 107, pp. 367–392, 2016, pLA biodegradable polymers.

[154] K. Budak, O. Sogut, and U. Sezer, "A review on synthesis and biomedical applications of polyglycolic acid," *Journal of Polymer Research*, vol. 27, no. 208, 2020.

[155] F. Pavan, T. Junqueira, M. Watanabe, A. Bonomi, L. Quines, W. Schmidell, and G. de Aragao, "Economic analysis of polyhydroxybutyrate production bycupriavidusnecatorusing different routes for product recovery," *Biomechanical Engineering Journal*, vol. 146, pp. 97–104, 2019.

[156] J. Sahari and S. Sapuan, "The development and properties of biodegradable and sustainable polymers," *Journal of Polymer Materials*, vol. 29, no. 1, pp. 153–165, 2012.

[157] D. Gay, *Composite Materials: Design and Applications*, B. Raton, Ed. CRC Press, 2015.

[158] S. Bader, "Crystic®ve679-03pa," Scott Bader, Tech. Rep., 2014.

[159] Vitrimat.eu, "Vitrimat," https://www.vitrimat.eu/, 2020, accessed: 2022-08-12.

[160] D. Chukov, S. Nematulloev, M. Zadorozhnyy, V. Tcherdyntsev, A. Stepashkin, and D. Zherebtsov, "Structure, mechanical and thermal properties of polyphenylene sulfide and polysulfone impregnated carbon fiber composites," *Polymers*, vol. 11, no. 4, 2019.

[161] Arkema-S.A., "Elium 188xo," Arkema, Tech. Rep., 2021.

[162] K. Mazur, P. Jakubowska, P. Romańska, and S. Kuciel, "Green high density polyethylene (hdpe) reinforced with basalt fiber and agricultural fillers for technical applications," *Composites Part B: Engineering*, p. 108399, 2020.

[163] Arkema.com, "Elium® resins for composites," https://www.arkema.com/global/en/products/product-finder/product-range/incubator/elium_resins, 2022, accessed: 2022-03-30.

[164] ——, "Elium resin for recyclable composite boats," https://www.arkema.com/global/en/products/product-finder/product/incubator/elium/elium-for-recyclable-composite-boats/, 2022, accessed: 2022-08-11.

[165] A. Mohammadi Nafchi, M. Moradpour, M. Saeidi, and A. K. Alias, "Thermoplastic starches: Properties, challenges, and prospects," *Starch - Stärke*, vol. 65, no. 1-2, pp. 61–72, 2013.

[166] M. Wollerdorfer and H. Bader, "Influence of natural fibres on the mechanical properties of biodegradable polymers," *Industrial Crops and Products*, vol. 8, no. 2, pp. 105 – 112, 1998.

[167] E. Rudnik, "Environmental impact of compostable polymer materials," *Handbook of Biopolymers and Biodegradable Plastics: Properties, Processing and Applications*, p. 189, 2012.

[168] C. A. Cruz-Ramos, "Natural fiber reinforced thermoplastics," in *Mechanical properties of reinforced thermoplastics*. Springer, 1986, pp. 65–81.

[169] D. Montarnal, M. Capelot, F. Tournilhac, and L. Leibler, "Silica-like malleable materials from permanent organic networks," *Science*, vol. 334, no. 6058, pp. 965–968, 2011.

[170] W. Denissen, J. M. Winne, and F. E. Du Prez, "Vitrimers: permanent organic networks with glass-like fluidity," *Chem. Sci.*, vol. 7, pp. 30–38, 2016.

[171] N. J. Van Zee and R. Nicolaÿ, "Vitrimers: Permanently crosslinked polymers with dynamic network topology," *Progress in Polymer Science*, vol. 104, p. 101233, 2020.

[172] C. Xu, R. Cui, L. Fu, and B. Lin, "Recyclable and heat-healable epoxidized natural rubber/bentonite composites," *Composites Science and Technology*, vol. 167, pp. 421 – 430, 2018.

[173] S. Wang, S. Ma, Q. Li, X. Xu, B. Wang, W. Yuan, S. Zhou, S. You, and J. Zhu, "Facile in situ preparation of high-performance epoxy vitrimer from renewable resources and its application in nondestructive recyclable carbon fiber composite," *Green Chem.*, vol. 21, pp. 1484–1497, 2019.

[174] F. Lossada, J. Guo, D. Jiao, S. Groeer, E. Bourgeat-Lami, D. Montarnal, and A. Walther, "Vitrimer chemistry meets cellulose nanofibrils: Bioinspired nanopapers with high water resistance and strong adhesion," *Biomacromolecules*, vol. 20, no. 2, pp. 1045–1055, 2019, pMID: 30589531.

[175] X. Yang, L. Guo, X. Xu, S. Shang, and H. Liu, "A fully bio-based epoxy vitrimer: Self-healing, triple-shape memory and reprocessing triggered by dynamic covalent bond exchange," *Materials & Design*, vol. 186, p. 108248, 2020.

[176] S. Dhers, G. Vantomme, and L. Avérous, "A fully bio-based polyimine vitrimer derived from fructose," *Green Chem.*, vol. 21, pp. 1596–1601, 2019.

[177] H. Memon, Y. Wei, L. Zhang, Q. Jiang, and W. Liu, "An imine-containing epoxy vitrimer with versatile recyclability and its application in fully recyclable carbon fiber reinforced composites," *Composites Science and Technology*, vol. 199, p. 108314, 2020.

[178] L. Yu, C. Zhu, X. Sun, J. Salter, H. Wu, Y. Jin, W. Zhang, and R. Long, "Rapid fabrication of malleable fiber reinforced composites with vitrimer powder," *ACS Applied Polymer Materials*, vol. 1, no. 9, pp. 2535–2542, 2019.

[179] Mallinda.com, "Vitrimax™ product: the technology," https://mallinda.com/product/, 2022, accessed: 2022-03-30.

[180] P. Taynton, K. Yu, R. K. Shoemaker, Y. Jin, H. J. Qi, and W. Zhang, "Heat- or water-driven malleability in a highly recyclable covalent network polymer," *Advanced Materials*, vol. 26, no. 23, pp. 3938–3942, 2014.

[181] P. Taynton, H. Ni, C. Zhu, K. Yu, S. Loob, Y. Jin, H. J. Qi, and W. Zhang, "Repairable woven carbon fiber composites with full recyclability enabled by malleable polyimine networks," *Advanced Materials*, vol. 28, no. 15, pp. 2904–2909, 2016.

[182] O. Adekomaya and T. Majozi, "Sustainability of surface treatment of natural fibre in composite formation: challenges of environment-friendly option," *The International Journal of Advanced Manufacturing Technology*, vol. 105, no. 7-8, pp. 3183–3195, 2019.

[183] K. L. Pickering, Y. Li, R. L. Farrell, and M. Lay, "Interfacial modification of hemp fiber reinforced composites using fungal and alkali treatment," *Journal of Biobased Materials and Bioenergy*, vol. 1, no. 1, pp. 109–117, 2007.

[184] M. MIAO and N. FINN, "Conversion of natural fibres into structural composites," *Journal of Textile Engineering*, vol. 54, no. 6, pp. 165–177, 2008.

[185] M. Ashby, *Materials and the Environment*, M. Ashby, Ed. Butterworth-Heinemann, 2013.

[186] M. Weiss, J. Haufe, M. Carus, M. Brandao, S. Bringezu, B. Hermann, and M. Patel, "A review of the environmental impacts of biobased materials," *Journal of Industri*, vol. 16, no. 1, 2012.

[187] J. P. Correa, J. M. Montalvo-Navarrete, and M. A. Hidalgo-Salazar, "Carbon footprint considerations for biocomposite materials for sustainable products: A review," *Journal of Cleaner Production*, vol. 208, pp. 785 – 794, 2019.

[188] G. Dolci, S. Nessi, L. Rigamonti, and M. Grosso, "Life cycle assessment of waste prevention in the delivery of pasta, breakfast cereals, and rice," *Integrated Environmental Assessment and Management*, vol. 12, no. 3, pp. 445–458, 2016.

[189] N. de Beus and M. Carus, Mand Barth, "Carbon footprint and sustainability of different natural fibres for biocomposites and insulation material," Nova Institute, Tech. Rep., 2015.

[190] H. M. van der Werf and L. Turunen, "The environmental impacts of the production of hemp and flax textile yarn," *Industrial Crops and Products*, vol. 27, no. 1, pp. 1 – 10, 2008.

[191] P. Ougane, L. Bizet, C. Baley, and J. Bread, "Analysis of the film-stacking processing parameters for plla/flax fiber biocomposites," *Journal of Composite Materials*, vol. 44, no. 10, pp. 1201–1215, 2010.

[192] Y. Tokiwa, B. Calabia, C. Ugwu, and S. Aiba, "Biodegradability of plastics," *International Journal of Molecular Sciences*, vol. 10, no. 9, p. 3722–3742, Aug 2009.

[193] "Bio-based plastics: Feedstocks, production and the uk market," https://www.bpf.co.uk/plastipedia/polymers/biobased_plastics_feedstocks_production_and_the_uk_market.aspx, accessed: 2022-08-08.

[194] J. Bachmann, C. Hidalgo, and S. Bricout, "Environmental analysis of innovative sustainable composites with potential use in aviation sector—a life cycle assessment review," *Science China Technological Sciences*, vol. 60, pp. 1301–1317, 2017.

[195] W. Yang and Y. Li, "Sound absorption performance of natural fibers and their composites," *Science China Technological Sciences*, vol. 55, pp. 2278–2283, 2012.

[196] M. Haufe, Jand Carus, "Hemp fibres for green products – an assessment of life cycle studieson hemp fibre applications," European Industrial Hemp Association (EIHA), Hemp Fibres for Green Products – An assessment of life cycle studies on hemp fibre applications, 2011.

[197] F. M. AL-Oqla, S. M. Sapuan, M. R. Ishak, and A. A. Nuraini, "Decision making model for optimal reinforcement condition of natural fiber composites," *Fibers and Polymers*, vol. 16, no. 1, pp. 153–163, 2015.

[198] G. George, K. Joseph, E. Nagarajan, E. Tomlal Jose, and K. George, "Dielectric behaviour of pp/jute yarn commingled composites: Effect of fibre content, chemical treatments, temperature and moisture," *Composites Part A: Applied Science and Manufacturing*, vol. 47, pp. 12 – 21, 2013.

[199] P. Sreekumar, J. M. Saiter, K. Joseph, G. Unnikrishnan, and S. Thomas, "Electrical properties of short sisal fiber reinforced polyester composites fabricated by resin transfer molding," *Composites Part A: Applied Science and Manufacturing*, vol. 43, no. 3, pp. 507 – 511, 2012.

[200] Z. Feng, M. Zeng, D. Meng, J. Chen, W. Zhu, Q. Xu, and J. Wang, "A novel bio-based benzoxazine resin with outstanding thermal and superhigh-frequency dielectric properties," *Journal of Materials Science: Mater*, vol. 31, pp. 4364–4376, 2020.

[201] X. Yang, W. Wang, and M. Miao, "Moisture-responsive natural fiber coil-structured artificial muscles," *ACS Appl Mater Interfaces*, vol. 10, no. 38, pp. 32 256–3226, 2018.

[202] L. Pil, F. Bensadoun, and J. Pariset, "Why are desdesign fascinated by flax annd hemp fibre composites?" *Composites Part A: Applied Science and Manufacturing*, vol. 83, pp. 193–205, 2016.

[203] F. Duc, P. Bourban, C. Plummer, and J. Manson, "Damping of thermoset and thermoplastic flax fibre composite," *Composites Part A: Applied Science and Manufacturing*, vol. 64, pp. 115–123, 2014.

[204] T. Jana, P. Maiti, and T. Dhar, "Development of a novel bio-based hybrid resin system for hygienic coating," *Progress in Organic Coatings*, vol. 137, 2019.

[205] J. Mussig, *Industrial Applications of Natural Fibres: Structure, Properties and Technical Applications*, J. Mussig, Ed. John Wiley and Sons, Ltd, 2010.

[206] P. Davies and W. Verbouwe, "Evaluation of basalt fibre composites for marine applications," *Applied Composite Materials*, vol. 25, no. 2, pp. 299–308, 2018.

[207] "Global hemp clothing market size, share & industry trends analysis report by end user, by type, by distribution channel, by regional outlook and forecast, 2022 – 2028," https://www.reportlinker.com/p06322055/.

[208] R. Chinthapalli, P. Skoczinski, M. Carus, W. Baltus, D. de Guzman, H. Käb, A. Raschka, and J. Ravenstijn, "Biobased building blocks and polymers—global capacities, production and trends, 2018–2023," *Industrial Biotechnology*, vol. 15, no. 4, pp. 237–241, 2019.

[209] A. Constante, S. Pillay, H. Ning, and U. K. Vaidya, "Utilization of algae blooms as a source of natural fibers for biocomposite materials: Study of morphology and mechanical performance of lyngbya fibers," *Algal Research*, vol. 12, pp. 412 – 420, 2015.

[210] U. Arnold, T. Brück, A. De Palmenaer, and K. Kuse, "Carbon capture and sustainable utilization by algal polyacrylonitrile fiber production: Process design, techno-economic analysis, and climate related aspects," *Industrial & Engineering Chemistry Research*, vol. 57, no. 23, pp. 7922–7933, 2018.

[211] A. Constante and S. Pillay, "Compression molding of algae fiber and epoxy composites: Modeling of elastic modulus," *Journal of Reinforced Plastics and Composites*, vol. 37, no. 19, pp. 1202–1216, 2018.

[212] A. Constante and S. Pillay, "Algae fiber polypropylene composites: Modeling of the degradation by solid state kinetics," *Journal of Applied Polymer Science*, vol. 134, no. 12, 2017.

[213] P. Roesle, F. Stempfle, S. K. Hess, J. Zimmerer, C. Río Bártulos, B. Lepetit, A. Eckert, P. G. Kroth, and S. Mecking, "Synthetic polyester from algae oil," *Angewandte Chemie International Edition*, vol. 53, no. 26, pp. 6800–6804, 2014.

[214] J. P. Reis, M. de Moura, and S. Samborski, "Thermoplastic composites and their promising applications in joining and repair composites structures: A review," *Materials*, vol. 13, no. 24, 2020.

[215] M. Hosur, U. Vaidya, D. Myers, and S. Jeelani, "Studies on the repair of ballistic impact damaged s2-glass/vinyl ester laminates," *Composite Structures*, vol. 61, no. 4, pp. 281–290, 2003, selected Papers from the Symposium on Design and Manufacturing of Composites.

[216] C. Soutis, D.-M. Duan, and P. Goutas, "Compressive behaviour of cfrp laminates repaired with adhesively bonded external patches," *Composite Structures*, vol. 45, no. 4, pp. 289–301, 1999.

[217] R. Wool and K. O'connor, "A theory crack healing in polymers," *Journal of applied physics*, vol. 52, no. 10, pp. 5953–5963, 1981.

[218] M. A. Stubblefield, C. Yang, S.-S. Pang, and R. H. Lea, "Development of heat-activated joining technology for composite-to-composite pipe using prepreg fabric," *Polymer Engineering & Science*, vol. 38, no. 1, pp. 143–149, 1998.

[219] N. Lorwanishpaisarn, P. Kasemsiri, N. Srikhao, C. Son, S. Kim, S. Theerakulpisut, and P. Chindaprasirt, "Carbon fiber/epoxy vitrimer composite patch cured with bio-based curing agents for one-step repair metallic sheet and its recyclability," *Journal of Applied Polymer Science*, vol. 138, no. 47, p. 51406, 2021.

[220] J. Pang and I. Bond, "Bleeding composites—damage detection and self-repair using a biomimetic approach," *Composites Part A: Applied Science and Manufacturing*, vol. 36, no. 2, pp. 183–188, 2005.

[221] M. Zako and N. Takano, "Intelligent material systems using epoxy particles to repair microcracks and delamination damage in gfrp," *Journal of Intelligent Material Systems and Structures*, vol. 10, no. 10, pp. 836–841, 1999.

[222] A. Le Duigou, P. Davies, and B. Christophe, "Journal of biobased materials and bioenergy," *Journal of Biobased Materials and Biotechnology*, vol. 5, no. 1, pp. 153–165, 2011.

[223] N. Sakellariou, "Current and potential decommissioning scenarios for end-of-life composite wind blades," *Energy Systems*, vol. 9, pp. 981–1023, 2017.

[224] A. Jacob, "Composites can be recycled," *Reinforced Plastics*, vol. 55, no. 3, pp. 45 – 46, 2011.

[225] E. Council, "Directive 2000/53/ec of the european parliament and of thecouncil," European Council, Tech. Rep., 2000.

[226] F. Vilaplana, E. Strömberg, and S. Karlsson, "Environmental and resource aspects of sustainable biocomposites," *Polymer Degradation and Stability*, vol. 95, no. 11, pp. 2147 – 2161, 2010, 2nd International Conference on Biodegradable Polymers and Sustainable Composites - Alicante 2009.

[227] A. R. de Matos Costa, A. Crocitti, L. Hecker de Carvalho, S. C. Carroccio, P. Cerruti, and G. Santagata, "Properties of biodegradable films based on poly(butylene succinate) (pbs) and poly(butylene adipate-co-terephthalate) (pbat) blends," *Polymers*, vol. 12, no. 10, p. 2317, Oct 2020.

[228] K. M. Brinsko, S. Sparenga, and M. King, "The effects of environmental exposure on the optical, physical, and chemical properties of manufactured fibers of natural origin," *Journal of Forensic Sciences*, vol. 61, no. 5, pp. 1215–1227, 2016.

[229] P. Goswami and T. O'Haire, "3 - developments in the use of green (biodegradable), recycled and biopolymer materials in technical nonwovens," in *Advances in Technical Nonwovens*, ser. Woodhead Publishing Series in Textiles, G. Kellie, Ed. Woodhead Publishing, 2016, pp. 97 – 114.

[230] A. Soroudi and I. Jakubowicz, "Recycling of bioplastics, their blends and biocomposites: A review," *European Polymer Journal*, vol. 49, no. 10, pp. 2839 – 2858, 2013.

[231] A. Le Duigou, I. Pillin, A. Bourmaud, P. Davies, and C. Baley, "Effect of recycling on mechanical behaviour of biocompostable flax/poly(l-lactide) composites," *Composites Part A: Applied Science and Manufacturing*, vol. 39, no. 9, pp. 1471 – 1478, 2008.

[232] C. UK, "End-of-life solutions for frp composites," U.K. Composites, Technical sheet, 2015.

[233] R. J. Tapper, M. L. Longana, A. Norton, K. D. Potter, and I. Hamerton, "An evaluation of life cycle assessment and its application to the closed-loop recycling of carbon fibre reinforced polymers," *Composites Part B: Engineering*, vol. 184, p. 107665, 2020.

[234] J. Summerscales, N. P. Dissanayake, A. S. Virk, and W. Hall, "A review of bast fibres and their composites. part 1 – fibres as reinforcements," *Composites Part A: Applied Science and Manufacturing*, vol. 41, no. 10, pp. 1329 – 1335, 2010.

[235] W. Wang, M. Sain, and P. Cooper, "Study of moisture absorption in natural fiber plastic composites," *Composites Science and Technology*, vol. 66, no. 3, pp. 379 – 386, 2006.

[236] S.-Y. Fu and B. Lauke, "Effects of fiber length and fiber orientation distributions on the tensile strength of short-fiber-reinforced polymers," *Composites Science and Technology*, vol. 56, no. 10, pp. 1179 – 1190, 1996.

[237] L. Drzal and M. Madhukar, "Fibre-matrix adhesion and its relationship to composite mechanical properties," *Journal of Materials Science*, vol. 28, no. 3, pp. 569–610, 1993.

[238] E. Spārniņš, B. Nyström, and J. Andersons, "Interfacial shear strength of flax fibers in thermoset resins evaluated via tensile tests of ud composites," *International Journal of Adhesion and Adhesives*, vol. 36, pp. 39 – 43, 2012.

[239] S. Wong, R. Shanks, and A. Hodzic, "Effect of additives on the interfacial strength of poly(l-lactic acid) and poly(3-hydroxy butyric acid)-flax fibre composites," *Composites Science and Technology*, vol. 67, no. 11, pp. 2478 – 2484, 2007.

[240] A. Arbelaiz, G. Cantero, B. Fernández, I. Mondragon, P. Gañán, and J. Kenny, "Flax fiber surface modifications: Effects on fiber physico mechanical and flax/polypropylene interface properties," *Polymer Composites*, vol. 26, no. 3, pp. 324–332, 2005.

[241] N. Zafeiropoulos, C. Baillie, and J. Hodgkinson, "Engineering and characterisation of the interface in flax fibre/polypropylene composite materials. part ii. the effect of surface treatments on the interface," *Composites Part A: Applied Science and Manufacturing*, vol. 33, no. 9, pp. 1185 – 1190, 2002.

[242] M. Seghini, F. Touchard, F. Sarasini, L. Chocinski-Arnault, D. Mellier, and J. Tirillò, "Interfacial adhesion assessment in flax/epoxy and in flax/vinylester composites by single yarn fragmentation test: Correlation with micro-ct analysis," *Composites Part A: Applied Science and Manufacturing*, vol. 113, pp. 66 – 75, 2018.

[243] R. Joffe, J. Andersons, and L. Wallström, "Interfacial shear strength of flax fiber/thermoset polymers estimated by fiber fragmentation tests," *Journal of Materials Science*, vol. 40, no. 9, pp. 2721–2722, May 2005.

[244] T. Huber and J. Müssig, "Fibre matrix adhesion of natural fibres cotton, flax and hemp in polymeric matrices analyzed with the single fibre fragmentation test," *Composite Interfaces*, vol. 15, no. 2-3, pp. 335–349, 2008.

[245] U. Gaur and B. Miller, "Microbond method for determination of the shear strength of a fiber/resin interface: Evaluation of experimental parameters," *Composites Science and Technology*, vol. 34, no. 1, pp. 35 – 51, 1989.

[246] H. Khalil, H. Ismail, H. Rozman, and M. Ahmad, "The effect of acetylation on interfacial shear strength between plant fibres and various matrices," *European Polymer Journal*, vol. 37, no. 5, pp. 1037 – 1045, 2001.

[247] C. Baley, F. Busnel, Y. Grohens, and O. Sire, "Influence of chemical treatments on surface properties and adhesion of flax fibre–polyester resin," *Composites Part A: Applied Science and Manufacturing*, vol. 37, no. 10, pp. 1626 – 1637, 2006.

[248] F. Wang, M. Lu, S. Zhou, Z. Lu, and S. Ran, "Effect of fiber surface modification on the interfacial adhesion and thermo-mechanical performance of unidirectional epoxy-based composites reinforced with bamboo fibers," *Molecules*, vol. 24, no. 15, 2019.

[249] J. F. V. Vincent, "A unified nomenclature for plant fibres for industrial use," *Applied Composite Materials*, vol. 7, pp. 269 – 271, 2000.

[250] Gurit.com, "Prime™20lv datasheet," https://www.gurit.com/-/media/Gurit/Datasheets/prime-20lv.pdf, Gurit, Technical sheet, 2019.

[251] ASTM.org, "Standard test methods for apparent porosity, liquid absorption, apparent specific gravity, and bulk density of refractory shapes by vacuum pressure," ASTM International, West Conshohocken, PA, Standard, 2016.

[252] M. Truong, W. Zhong, S. Boyko, and M. Alcock, "A comparative study on natural fibre density measurement," *The journal of the Textile Institute*, vol. 100, no. 6, pp. 525–529, 2009.

[253] A. Amiri, Z. Triplett, A. Moreira, N. Brezinka, M. Alcock, and C. A. Ulven, "Standard density measurement method development for flax fiber," *Industrial Crops and Products*, vol. 96, pp. 196 – 202, 2017.

[254] J. G. Cook, *Handbook of Textile Fibres: Vol. 1: Natural Fibres*. Woodhead Publishing, Cambridge, England, 2001.

[255] M. Lewin, *Handbook of fiber chemistry, 3rd edition*. CRC Press, Florida, USA, 2010.

[256] C. Sawsen, K. Fouzia, B. Mohamed, and G. Moussa, "Optimizing the formulation of flax fiber-reinforced cement composites," *Construction and Building Materials*, vol. 54, pp. 659 – 664, 2014.

[257] B. Madsen and H. Lilholt, "Physical and mechanical properties of unidirectional plant fibre composites—an evaluation of the influence of porosity," *Composites Science and Technology*, vol. 63, no. 9, pp. 1265 – 1272, 2003, eco-Composites.

[258] A. Bourmaud, J. Beaugrand, D. U. Shah, V. Placet, and C. Baley, "Towards the design of high-performance plant fibre composites," *Progress in Materials Science*, vol. 97, pp. 347–408, 2018.

[259] A. Bismarck, I. Aranberri-Askargorta, J. Springer, T. Lampke, B. Wielage, A. Stamboulis, I. Shenderovich, and H.-H. Limbach, "Surface characterization of flax, hemp and cellulose fibers; surface properties and the water uptake behavior," *Polymer Composites*, vol. 23, no. 5, pp. 872–894, 2002.

[260] S. P. Wesson, J. J. Vajo, and S. Ross, "Determination of specific surface areas of glass filaments by bet and caedmon methods," *Journal of Colloid and Interface Science*, vol. 94, no. 2, pp. 552 – 563, 1983.

[261] M. A. Spinacé, C. S. Lambert, K. K. Fermoselli, and M.-A. D. Paoli, "Characterization of lignocellulosic curaua fibres," *Carbohydrate Polymers*, vol. 77, no. 1, pp. 47 – 53, 2009.

[262] M. Ramiah, "Thermogravimetric and differential thermal analysis of cellulose, hemicellulose, and lignin," *Journal of Applied Polymer Science*, vol. 14, no. 5, pp. 1323–1337, 1970.

[263] ASTM.org, "Standard test method for tensile strength and young's modulus of fibers," ASTM International, West Conshohocken, PA, Standard, 2014.

[264] D. U. Shah, P. J. Schubel, M. J. Clifford, and P. Licence, "The tensile behavior of off-axis loaded plant fiber composites: An insight on the nonlinear stress–strain response," *Polymer Composites*, vol. 33, no. 9, pp. 1494–1504, 2012.

[265] J. Summerscales, A. S. Virk, and W. Hall, "Fibre area correction factors (facf) for the extended rules-of-mixtures for natural fibre reinforced composites," *Materials Today: Proceedings*, vol. 31, pp. S318–S320, 2020.

[266] A. Komuraiah, N. S. Kumar, and B. D. Prasad, "Chemical composition of natural fibers and its influence on their mechanical properties," *Mechanics of Composite Materials*, vol. 50, no. 3, pp. 359–376, 2014.

[267] S. M. Mortazavi and M. Kamali Moghaddam, "An analysis of structure and properties of a natural cellulosic fiber (leafiran)," *Fibers and Polymers*, vol. 11, no. 6, pp. 877–882, 2010.

[268] S. Ouajai and R. Shanks, "Composition, structure and thermal degradation of hemp cellulose after chemical treatments," *Polymer Degradation and Stability*, vol. 89, no. 2, pp. 327 – 335, 2005.

[269] Y. Swolfs, I. Verpoest, and L. Gorbatikh, "A review of input data and modelling assumptions in longitudinal strength models for unidirectional fibre-reinforced composites," *Composite Structures*, vol. 150, pp. 153 – 172, 2016.

[270] R. Day and J. Rodrigez, "Investigation of the micromechanics of the microbond test," *Composites Science and Technology*, vol. 58, no. 6, pp. 907–914, 1998. [Online]. Available: https://www.sciencedirect.com/science/article/pii/S0266353897001978

[271] S. J. Eichhorn, C. A. Baillie, N. Zafeiropoulos, L. Y. Mwaikambo, M. P. Ansell, A. Dufresne, K. M. Entwistle, P. J. Herrera-Franco, G. C. Escamilla, L. Groom, M. Hughes, C. Hill, T. G. Rials, and P. M. Wild, "Review: Current international research into cellulosic fibres and composites," *Journal of Materials Science*, vol. 36, no. 9, pp. 2107–2131, May 2001.

[272] F. Sarker, N. Karim, S. Afroj, V. Koncherry, K. S. Novoselov, and P. Potluri, "High-performance graphene-based natural fiber composites," *ACS Applied Materials & Interfaces*, vol. 10, no. 40, pp. 34 502–34 512, 2018.

[273] T.-T.-L. Doan, H. Brodowsky, and E. Mäder, "Jute fibre/epoxy composites: Surface properties and interfacial adhesion," *Composites Science and Technology*, vol. 72, no. 10, pp. 1160 – 1166, 2012.

[274] M. J. Pitkethly, J. P. Favre, U. Gaur, J. Jakubowski, S. F. Mudrich, D. L. Caldwell, L. T. Drzal, M. Nardin, H. D. Wagner, L. Di Landro, A. Hampe, J. P. Armistead, M. Desaeger, and I. Verpoest, "A round-robin programme on interfacial test methods," *Composites Science and Technology*, vol. 48, no. 1, pp. 205 – 214, 1993.

[275] D. Bryce, L. Yang, and J. Thomason, "An investigation of fibre sizing on the interfacial strength of glass-fibre epoxy composites," in *ECCM18 - 18th European Conference on Composite Materials ; Conference date: 24-06-2018 Through 28-06-2018*, 2018.

[276] S.-K. Kang, D.-B. Lee, and N.-S. Choi, "Fiber/epoxy interfacial shear strength measured by the microdroplet test," *Composites Science and Technology*, vol. 69, no. 2, pp. 245 – 251, 2009.

[277] Toray.com, "Torayca t300 and toray t700s technical data sheet," https://www.toraycma.com/page.php?id=661, Toray Carbon Fibres, Technical sheet, 2019.

[278] P. Wambua, J. Ivens, and I. Verpoest, "Natural fibres: can they replace glass in fibre reinforced plastics?" *Composites Science and Technology*, vol. 63, no. 9, pp. 1259 – 1264, 2003.

[279] F. Bensadoun, I. Verpoest, J. Baets, J. Müssig, N. Graupner, P. Davies, M. Gomina, A. Kervoelen, and C. Baley, "Impregnated fibre bundle test for natural fibres used in composites," *Journal of Reinforced Plastics and Composites*, vol. 36, no. 13, pp. 942–957, 2017.

[280] H. L. Cox, "The elasticity and strength of paper and other fibrous materials," *British Journal of Applied Physics*, vol. 3, no. 3, pp. 72–79, 1952.

[281] A. Fitzgerald, W. Proud, A. Kandemir, R. J. Murphy, D. A. Jesson, R. S. Trask, I. Hamerton, and M. L. Longana, "A life cycle engineering perspective on biocomposites as a solution for a sustainable recovery," *Sustainability*, vol. 13, no. 3, p. 1160, Jan 2021.

[282] M. Fogorasi and I. Barbu, "The potential of natural fibres for automotive sector -review," *IOP Conference Series: Materials Science and Engineering*, vol. 252, p. 012044, oct 2017.

[283] U. Nirmal, J. Hashim, and M. Megat Ahmad, "A review on tribological performance of natural fibre polymeric composites," *Tribology International*, vol. 83, pp. 77–104, 2015.

[284] Y. Yao, M. Li, M. Lackner, and L. Herfried, "A continuous fiber-reinforced additive manufacturing processing based on pet fiber and pla," *Materials*, vol. 13, no. 14, 2020.

[285] J. Chacón, M. Caminero, P. Núñez, E. García-Plaza, I. García-Moreno, and J. Reverte, "Additive manufacturing of continuous fibre reinforced thermoplastic composites using fused deposition modelling: Effect of process parameters on mechanical properties," *Composites Science and Technology*, vol. 181, p. 107688, 2019.

[286] H. Yu, M. L. Longana, M. Jalalvand, M. R. Wisnom, and K. D. Potter, "Pseudo-ductility in intermingled carbon/glass hybrid composites with highly aligned discontinuous fibres," *Composites Part A: Applied Science and Manufacturing*, vol. 73, pp. 35–44, 2015.

[287] "Skyflex k51 epoxy prepregtechnical data sheet. skchemicals, seoul, republic of korea„" http://www.triplehcomposites.co.uk/userfiles/files/SKR%20K51%20ver1_0(1).pdf, accessed: 2021-02-02.

[288] "3d4makerspla (polylactic acid) filament technical information„" https://www.3d4makers.com/products/pla-filament, accessed: 2021-02-02.

[289] "Hiperdif web page, bristol composites institute, university of bristol," http://www.bristol.ac.uk/composites/research/hiperdif/, accessed: 2022-08-08.

[290] L. Blok, M. Longana, and B. Woods, "Fabrication and characterisation of aligned discontinuous carbon fibre reinforced thermoplastics as feedstock material for fused filament fabrication," *Materials*, vol. 13, no. 20, p. 4671, Oct 2020.

[291] ASTM.org, "Standard test method for tensile properties of polymer matrix composite materials," ASTM International, West Conshohocken, PA, Standard, 2016.

[292] K. Hamad, M. Kaseem, F. Deri *et al.*, "Melt rheology of poly (lactic acid)/low density polyethylene polymer blends," *Advances in Chemical Engineering and Science*, vol. 1, no. 4, pp. 208–214, 2011.

[293] C. de Kergariou, A. Le Duigou, V. Popineau, V. Gager, A. Kervoelen, A. Perriman, H. Saidani-Scott, G. Allegri, T. H. Panzera, and F. Scarpa, "Measure of porosity in flax fibres reinforced polylactic acid biocomposites," *Composites Part A: Applied Science and Manufacturing*, vol. 141, p. 106183, 2021.

[294] V. Piemonte and F. Gironi, "Kinetics of hydrolytic degradation of pla," *Journal of Polymers and the Environment*, vol. 21, no. 2, pp. 313–318, 2013.

[295] U. K. Sanivada, G. Mármol, F. P. Brito, and R. Fangueiro, "Pla composites reinforced with flax and jute fibers—a review of recent trends, processing parameters and mechanical properties," *Polymers*, vol. 12, no. 10, 2020.

[296] "European linen„" http://news.europeanflax.com/lin/, accessed: 2021-01-28.

[297] M. H. Hassan, A. R. Othman, and S. Kamaruddin, "A review on the manufacturing defects of complex-shaped laminate in aircraft composite structures," *The International Journal of Advanced Manufacturing Technology*, vol. 91, no. 9, pp. 4081–4094, 2017.

[298] E. Artetxe, H. González, A. Calleja, A. F. Valdivielso, R. Polvorosa, A. Lamikiz, and L. N. L. D. Lacalle, "Optimised methodology for aircraft engine ibrs five-axis machining process," *International Journal of Mechatronics and Manufacturing Systems*, vol. 9, no. 4, pp. 385–401, 2016.

[299] C. Ward, K. Hazra, and K. Potter, "Development of the manufacture of complex composite panels," *International Journal of Materials and Product Technology*, vol. 42, no. 3-4, pp. 131–155, 2011.

[300] A. Kelly and W. Tyson, "Tensile properties of fibre-reinforced metals: Copper/tungsten and copper/molybdenum," *Journal of the Mechanics and Physics of Solids*, vol. 13, no. 6, pp. 329–350, 1965.

[301] J. Zheng, Z. M. Png, S. H. Ng, G. X. Tham, E. Ye, S. S. Goh, X. J. Loh, and Z. Li, "Vitrimers: Current research trends and their emerging applications," *Materials Today*, vol. 51, pp. 586–625, 2021.

[302] A. Ruiz de Luzuriaga, R. Martin, N. Markaide, A. Rekondo, G. Cabañero, J. Rodríguez, and I. Odriozola, "Epoxy resin with exchangeable disulfide crosslinks to obtain reprocessable, repairable and recyclable fiber-reinforced thermoset composites," *Mater. Horiz.*, vol. 3, pp. 241–247, 2016.

[303] EC-Directive *et al.*, "Directive 2008/98/ec of the european parliament and of the council of 19 november 2008 on waste and repealing certain directives," *Official Journal of the European Union L*, vol. 312, no. 3, 2008.

[304] M. S. Madhukar and L. T. Drzal, "Fiber-matrix adhesion and its effect on composite mechanical properties: Ii. longitudinal (0) and transverse (90) tensile and flexure behavior of graphite/epoxy composites," *Journal of Composite Materials*, vol. 25, no. 8, pp. 958–991, 1991.

[305] R. Petersen, "Discontinuous fiber-reinforced composites above critical length," *Journal of Dental Research*, vol. 84, no. 4, pp. 365–370, 2005.

[306] I. Robinson and J. Robinson, "The effect of fibre aspect ratio on the stiffness of discontinuous fibre-reinforced composites," *Composites*, vol. 25, no. 7, pp. 499–503, 1994, third International Conference on Interfacial Phenomena in Composite Materials.

[307] A. Kandemir, M. L. Longana, T. H. Panzera, G. G. del Pino, I. Hamerton, and S. J. Eichhorn, "Natural fibres as a sustainable reinforcement constituent in aligned discontinuous polymer composites produced by the hiperdif method," *Materials*, vol. 14, no. 8, p. 1885, Apr 2021.

[308] A. Hart and J. Summerscales, "Effect of time at temperature for natural fibres," *Procedia Engineering*, vol. 200, pp. 269–275, 2017.

[309] P. Wu, L. Liu, and Z. Wu, "A transesterification-based epoxy vitrimer synthesis enabled high crack self-healing efficiency to fibrous composites," *Composites Part A: Applied Science and Manufacturing*, vol. 162, p. 107170, 2022.

[310] Y. Zhao, M. Zhao, A. Wang, Z. Chang, Z. Wang, and K. Zhang, "Experimental study on the mode i interlaminar properties of self-healable vitrimeric cfrp with various interfaces," *Composites Part B: Engineering*, vol. 261, p. 110806, 2023.

[311] H. Rijsdijk, M. Contant, and A. Peijs, "Continuous-glass-fibre-reinforced polypropylene composites: I. influence of maleic-anhydride-modified polypropylene on mechanical properties," *Composites Science and Technology*, vol. 48, no. 1, pp. 161–172, 1993.

[312] V. Placet, O. Cissé, and M. Lamine Boubakar, "Nonlinear tensile behaviour of elementary hemp fibres. part i: Investigation of the possible origins using repeated progressive loading with in situ microscopic observations," *Composites Part A: Applied Science and Manufacturing*, vol. 56, pp. 319–327, 2014.

[313] M. Marie, "Lca & sustainability workshop at university of bristol," website:marineshift360.org/, Marineshift360, Oral presentation, 2022.

[314] N. P. Dissanayake, J. Summerscales, S. Grove, and M. Singh, "Infusion of natural vs. synthetic fibre composites with similar reinforcement architecture in the context of a lca," in *The 9th international conference on flow processes in composite materials (FPCM-9), Montréal*, 2008, pp. 8–10.